N° d'ordre : 4388 **ANNÉE 2011**

THÈSE / UNIVERSITÉ DE RENNES 1
sous le sceau de l'Université Européenne de Bretagne

pour le grade de

DOCTEUR DE L'UNIVERSITÉ DE RENNES 1

Mention : Sciences de la Terre

Ecole doctorale Sciences de la Matière

présentée par

Rémi MARSAC

Préparée à l'unité de recherche Géosciences Rennes
(UMR CNRS 6118)
UFR Structure et Propriétés de la Matière

Contrôle de la spéciation des terres rares par les acides humiques : rôle de l'hétérogénéité des sites de complexation et de la compétition entre cations

Thèse soutenue à Rennes le 21 octobre 2011

devant le jury composé de :

Marc Benedetti
Professeur, Université Paris Diderot / *rapporteur*

Karen Johannesson
Professeur, Université Tulane / *rapporteur*

Yoshio Takahashi
Professeur, Université Hiroshima / *examinateur*

Stephen Lofts
Docteur, Center for Ecology & Hydrology / *examinateur*

Aline Dia
Directeur de recherche, CNRS / *invité*

Mélanie Davranche
Maître de Conférences, Université Rennes 1 / *directeur de thèse*

Gérard Gruau
Directeur de recherche, CNRS / *directeur de thèse*

À mes parents,

À mes amis, mes frères,

À Prissou...

"Je ne sais qu'une chose, c'est que je ne sais rien."

Socrate

Avant-Propos

Ce mémoire de thèse est le résultat d'un travail effectué au sein de l'équipe Géochimie des eaux et des interfaces de Géosciences Rennes (UMR CNRS 6118). Cette thèse a été encadrée par Mélanie Davranche et Gérard Gruau, en collaboration avec Aline Dia. Le travail expérimental et analytique a été réalisé au sein de l'atelier de Géochimie Analytique de Géosciences Rennes avec le soutien technique de Martine Bouhnik-Le Coz, Patrice Petitjean et Odile Hénin.

Cette thèse a été financée par le projet ANR Jeunes Chercheuses - Jeunes Chercheurs SURFREE : Rare earth elements partitioning at solid-water interface: Impact on REE geochemical behaviour and tracing properties.

Remerciements

Ce travail n'ayant pu être réalisable sans l'aide et le soutien de nombreuses personnes, je souhaite les remercier sincèrement.

Je tiens tout d'abord à remercier mes deux directeurs de thèse, Mélanie et Gérard, qui m'ont accordé beaucoup de liberté quant à l'orientation de mes recherches, me permettant ainsi de laisser s'exprimer ma curiosité et ma créativité, et qui se sont toujours rendus disponibles lorsque j'ai eu besoin de leurs conseils, critiques ou connaissances. Un jour, Mélanie m'a dit que ma réussite en thèse était une de ses priorités : ce n'était pas des paroles en l'air ! Je les remercie tous deux ainsi qu'Aline pour les nombreuses discussions que nous avons pu avoir sur "l'après thèse" et qui me permettent de réfléchir quant aux stratégies à adopter pour le début de ma carrière.

Un grand merci à Martine, Patrice et Odile pour m'avoir formé sur les instruments analytiques, pour toute l'aide et les conseils apportés au labo et pour leur bonne humeur.

Je remercie les rapporteurs, Marc Benedetti et Karen Johannesson, et les examinateurs de cette thèse, Yoshio Takahashi et Steve Lofts, d'avoir accepté de juger mon travail et pour l'intérêt qu'il y ont porté. Merci à tous d'avoir accepté de vous déplacer pour ma soutenance malgré la distance qui sépare nos laboratoires.

Je remercie Guillaume Morin et Yoshio Takahashi pour leur collaboration sur notre projet de recherche, parallèle à ma thèse, comportant des expériences au synchrotron. J'espère pouvoir travailler encore avec vous durant ma carrière.

Je souhaiterais remercier Corinne Lagrost et Jean-François Bergamini qui m'ont encadré en Licence lors de mon premier stage de recherche. Cette première expérience à leurs côtés a été déterminante car elle a clairement confirmé mon désir de travailler dans la recherche.

Un grand merci à tous les gens qui ont été à mes côtés au laboratoire durant ces trois années, ou au moins durant une partie. Merci d'abord à Thibault et Morgane qui ont dû me supporter dans le même bureau pendant ces longues années. Merci à Mathieu, Mohamad, Gravos, Ange, Anne, Anne-lyse, Michael, Rebecca, Nico... Merci aux autres thésards et stagiaires n'ayant pas "vécu" dans ce bureau 316 : Alex et Nico (nos indiens), Clément, Pietro, Christoff, Eline, Claudine, Alain, Jérémy, Maria, Fabien, Gwen, Romain... J'en oublie évidemment.

Je voudrais également remercier mes parents ainsi que tous mes potes, d'ici et d'ailleurs, qui m'ont toujours soutenu et avec qui nous avons passé des moments formidables : Jotard, loulou, Simon, Bébert, Mazoute, Mutard, Jak, War, Toby, Fab, Flash, Guiche, Cam, Buet, Balloche, Prisca, Milouz, Guy, Yannis, Lol, Sophie, Alice, Alex, Kévin, Hubert, Mélo... Je suis fils unique mais certains d'entre vous sont comme des frères pour moi ! Merci également aux mangeurs de nains poilus pour touts ces moments de rigolade.

Je remercie finalement Prissou qui a toujours su faire de ma vie un vrai bonheur malgré les difficultés que j'ai pu rencontrer au cours cette aventure universitaire !

Sommaire

Résumé

Cette thèse a pour objectif de comprendre les mécanismes de complexation des terres rares par les acides humiques et notamment : (i) d'expliquer la variabilité des spectres de terres rares observée dans les eaux riches en matières organiques ; (ii) d'affiner un modèle de spéciation géochimique afin de mieux décrire les processus de complexation des terres rares par les acides humiques ; (iii) d'évaluer l'influence de cations compétiteurs trivalents (Al et Fe) sur la complexation des terres rares par les acides humiques.

La première partie de ce travail a été consacrée à l'étude expérimentale de la complexation des terres rares par les acides humiques à pH = 3 en fonction de la charge en terres rares (i.e. le rapport entre les concentrations en terre rare et en acide humique). Pour de faibles concentrations en terres rares, l'acide humique a plus d'affinité pour les terres rares lourdes. Pour de fortes concentrations en terres rares, l'acide humique a une plus forte affinité pour les terres rares moyennes. Cette variabilité d'affinité se traduit par une variabilité de la forme de spectre terres rares-acides humiques. Elle s'explique par la grande diversité des sites de complexation présents sur l'acide humique. Les sites forts multidentates sont présents en faible quantité tandis que les sites faibles monodentates sont présents en forte quantité.

La deuxième partie a été consacrée à la création d'un modèle couplé PHREEQC/Model VI. Les équations de "Model VI" ont été modifiées afin de mieux décrire les interactions entre terre rares et acides humiques et introduites dans le modèle plus générique PHREEQC. Les acides humiques présentent deux types de groupements fonctionnels complexants : des acides carboxyliques et des phénols formant des complexes monodentates et multidentates. L'étude des constantes de complexation des terres rares avec des ligands organiques de référence montre que les spectres diffèrent pour les acides carboxyliques, les phénols et les ligands multidentates. Aucun des sites de complexation définis dans Model VI ne présentait de spectre de type phénolique. En définissant des sites présentant des spectres plus cohérents avec des ligands de références, PHREEQC/Model VI a pu reproduire l'ensemble des spectres terres rares-acides humiques expérimentaux obtenus pour différentes conditions expérimentales. PHREEQC/Model VI montre que les terres rares légères et lourdes se lient préférentiellement à différents sites complexants de l'acide humique.

La troisième partie a été consacrée à l'étude expérimentale de la complexation compétitive entre cations trivalents et terres rares pour les acides humiques. L'aluminium et le fer sont de forts compétiteurs des terres rares. Cependant les mécanismes de complexation de ces cations par la matière organique évoluent avec les conditions expérimentales et l'espèce chimique dominante du fer et de l'aluminium en solution (i.e. hydroxylée ou non). Ces différents mécanismes de complexation se traduisent par un spectre de terres rares sur l'acide humique différent. L'aluminium et le fer ont donc une forte influence sur le spectre terres rares-acides humiques. De plus, les terres rares peuvent être utilisées comme traceurs des processus de complexation des cations sur les acides humiques.

Les substances humiques sont de très forts complexants des terres rares. La forte hétérogénéité de sites de complexation induit une variation des spectres de terres rares liées à ces molécules en fonction de la charge en métaux, du pH et de la nature des cations compétiteurs. Cette étude apporte de nouveaux outils d'interprétation des spectres de terres rares dans les eaux riches en matières organiques ainsi qu'une méthode novatrice d'étude des mécanismes de complexation des cations par les acides humiques.

Mots clés : terres rares, acide humique, modélisation, PHREEQC, Model VI, spéciation, complexation, aluminium, fer, compétition.

Abstract

This thesis aimed at understanding rare earth elements complexation mechanisms to humic acids and, especially: (i) explaining rare earth elements pattern variability observed in organic-rich waters; (ii) improving a geochemical speciation model to describe more precisely processes controlling rare earth elements complexation by humic acids; (iii) testing trivalent cations (aluminium and iron) competitive effect on rare earth elements complexation by humic acids.

The first part was dedicated to an experimental study of rare earth elements complexation to humic acids at pH = 3 as a function of rare earth loading (i.e. rare earth element to humic acid concentration ratio). At low loading, humic acids have more affinity for heavy rare earths whereas, at high loading, humic acids have more affinity for middle rare earths. This variable affinity implies a variability of rare earth elements-humic acids complexation pattern and can be explained by humic acids binding sites heterogeneity. Indeed, humic acids present a few amount of strong multidentate sites whereas low affinity sites are present in high concentrations in humic acids molecules.

In the second part, Humic Ion binding model VI (Model VI) was coupled with PHREEQC. Model VI equations were modified in order to describe more precisely rare earth elements interactions with humic acids and were introduced into the more generic model PHREEQC. Humic acids present two major types of binding groups for cations: carboxylic and phenolic groups which can participate in monodentate or multidentate complexes. Comparison between rare earth elements binding behavior with standard ligands shows that complexation patterns differ for carboxylic, phenolic and multidentate ligands. And in Model VI, no binding site presented a phenolic-type pattern. By defining Model VI sites rare earth elements complexation patterns more consistent with standard ligands, PHREEQC/Model VI could simulate the variability of rare earth-humic acids complexation pattern determined experimentally. PHREEQC/Model VI also showed that light and heavy rare earths have different preferential humic acid binding groups.

In the third part, competitive complexation between rare earth elements and trivalent cations for humic acids binding was studied experimentally. Aluminium and iron are strong competitor for rare earth elements. However, these cations binding to humic acids mechanisms evolve with experimental conditions and the major aluminium and iron chemical species in solution (i.e. hydrolyzed or not). These different binding mechanisms imply different rare earth elements-humic acids complexation patterns. Therefore, aluminium and iron have a strong influence on rare earth elements-humic acids complexation patterns. Furthermore, rare earth elements can be used as a probe of competitor cations binding to humic acids mechanisms.

Humic substances can bind strongly rare earth elements. Their heterogeneity of binding sites imply a variability of rare earth elements pattern depending on the metal loading, the pH and the nature of competitive cations. The present study provide new tools for the interpretation of rare earth elements patterns in natural organic-rich waters but also a new method to determine cations binding to humic acids mechanisms.

Keywords: rare earth elements, humic acids, modeling, PHREEQC, Model VI, speciation, complexation, aluminium, iron, competition.

I. Introduction

Les terres rares (REE), ou lanthanides, forment une famille de 15 éléments chimiques (du La au Lu) appartenant au groupe IIIA dans la classification périodique des éléments, du numéro atomique 57 au numéro atomique 71. Le Pm (numéro atomique 61) n'étant pas présent naturellement, seules 14 REE sont généralement étudiées. Les REE sont fréquemment subdivisées en deux groupes, opposant les terres rares légères (du La à l'Eu) aux REE lourdes (du Gd au Lu). La notion de terres rares intermédiaires (du Sm au Tb) est parfois introduite, réduisant les REE légères et lourdes respectivement aux ensembles La-Nd et Dy-Lu. La chimie des REE est caractérisée par la prédominance du degré d'oxydation +III. Les cations REE ont une structure électronique de type $[Xe]4f^n$ avec $[0(La) < n < 14(Lu)]$. Comme les électrons de la couche électronique 4f sont des électrons de couche interne, les REE forment des composés présentant des liaisons à caractère ionique dominant. Le remplissage progressif de la couche électronique 4f s'accompagne par ailleurs d'une diminution faible mais progressive des rayons ioniques et atomiques le long de la série, connue sous le terme de 'contraction des lanthanides'. Cette 'contraction' reste cependant faible et explique les propriétés chimiques très voisines des lanthanides. Ainsi, du fait de son plus faible rayon ionique et considérant une liaison purement ionique, on pourrait s'attendre à ce que le Lu présente de plus fortes constantes de stabilité que toutes les autres REE et ce, quel que soit le type de ligand considéré. Or, les études réalisées jusqu'ici sur la complexation des lanthanides par les ligands en solution montrent que ce phénomène de 'contraction des lanthanides' ne régit pas systématiquement l'évolution des constantes de stabilité des lanthanides avec un ligand, que celui-ci soit inorganique (Byrne and Sholkovitz, 1996) ou organique (Byrne and Li, 1995).

Les REE sont naturellement présentes dans les eaux où leurs abondances sont le plus souvent visualisées sous la forme de spectres, spectres dans lesquels les abondances normalisées en REE sont présentées en ordonnées, les REE étant 'rangées' en abscisse par numéro atomique croissant. Les abondances normalisées sont obtenues en divisant les concentrations absolues mesurées dans les eaux par les concentrations mesurées dans un réservoir de référence. Cette procédure de normalisation est utilisée pour éliminer les variations d'abondances observées entre les terres rares de numéro atomique pair et impair. Les REE des eaux provenant de l'altération des enveloppes superficielles de la Terre, la coutume veut que le réservoir de référence utilisés dans le cas des eaux soit un réservoir "rocheux" de surface. Deux types de réservoirs sont classiquement utilisés: (i) la composition moyenne de la croûte continentale supérieure et (ii) la composition moyenne des schistes argileux ou "shales" (Haskin et al., 1968; Taylor et McLennan, 1985; McLennan, 1989).

Les REE dans les eaux superficielles se distribuent entre deux composantes principales traditionnellement séparées par filtration à 0,2 ou 0,45 µm. La composante de granulométrie >0.2 µm correspond à la fraction particulaire, tandis que la composante de granulométrie <0.2 µm, dite dissoute, regroupe en fait les fractions colloïdales (organiques et minérales) et le "dissous vrai" (Sholkovitz, 1995; Viers et al., 1997; Braun et al., 1998). Le partage des terres rares entre chacune des deux fractions est fortement influencé par des processus de sorption sur les particules et les colloïdes ainsi que par la complexation des REE par les différents ligands organiques et inorganiques présents dans la solution. Les différences de propriétés chimiques existant entre les différentes REE, même si celles-ci sont faibles, créent des différences dans la répartition des différentes REE entre solution et particules, et entre des solutions de composition différentes. Il en résulte une grande variabilité de spectres due aux différences de composition chimique des eaux naturelles et de natures des phases solides avec lesquelles les eaux naturelles sont en équilibre. Cette propriété confère aux REE un puissant pouvoir de traçage des circulations d'eau ou de traçage des processus biogéochimiques contrôlant la composition des eaux naturelles (complexation des solutés par des ligands en solution, adsorptions sur des particules en suspension, précipitation/dissolutions de minéraux, conditions redox…) qu'il s'agisse des eaux souterraines (Smedley, 1991; Johannesson et al., 1995; 1996b; 1997; Viers et al., 1997; Braun et al., 1998; Johannesson et al., 1999; Dia et al., 2000; Johannesson et Hendry, 2000; Johannesson et al., 2000; Aubert et al., 2001; Janssen et Verweij, 2003; Duncan et Shaw, 2004; Gruau et al., 2004; Johannesson et al., 2004; Nelson et al., 2004), des lacs (Fee et al., 1992; Möller et Bau, 1993; Johannesson et Lyons, 1994; 1995; Johannesson et Zhou, 1999; De Carlo et Green, 2002; Gammons et al., 2003; Shacat et al., 2004), des rivières et des fleuves (Goldstein et Jacobsen, 1988; Elderfield et al., 1990; Sholkovitz, 1993; Sholkovitz, 1995; Bau et Dulski, 1996; Dupré et al., 1996; Gaillardet et al., 1997; Viers et al., 1997; Dupré et al., 1999; Elbaz-Poulichet et Dupuy, 1999; Tricca et al., 1999; Ingri et al., 2000; Deberdt et al., 2002; Shiller et al., 2002; Gerard et al., 2003; Gaillardet et al., 2004; Andersson et al., 2006), ou des océans et des mers (Goldberg et al., 1963; Martin et al., 1976; Elderfield et Greaves, 1982; De Baar et al., 1983; Hoyle et al., 1984; De Baar et al., 1985; De Baar et al., 1988; Elderfield, 1988; Byrne et Kim, 1990; German et al., 1991; German et al., 1995; Bau et al., 1996; Byrne et Sholkovitz, 1996; Bau et al., 1997; Duncan et Shaw, 2004; Lawrence et Kamber, 2006).

Cependant, afin de pouvoir utiliser de manière précise les spectres de REE en tant que traceur, une solide connaissance théorique des différents processus pouvant induire des

différences de répartition entre REE est nécessaire. Ainsi, depuis ces vingt dernières années, de nombreuses études expérimentales ont eu pour but d'identifier le comportement et le partage des REE entre différents types de solution et différents types de surface minérale telles que les oxydes de fer et de manganèse (Ohta and Kawabe, 2000 ; 2001; Quinn and Byrne, 2004; 2006) ou certaines argiles (Takahashi et al., 2000 ; Coppin et al., 2002), la capacité des terres rares à se lier avec des ligands en solution (Byrne and Lee, 1995; Byrne and Sholkovitz, 1996; Luo and Byrne 2004), ou des cellules bactériennes (Takahashi et al., 2005; 2007), ou encore le comportement des REE dans le cas de la présence simultanée de matière organique et d'oxydes métalliques (Davranche et al. 2004; Davranche et al., 2005; Davranche et al., 2008). Les constantes thermodynamiques obtenues lors de ces études permettent la mise au point de modèles permettant de prédire la spéciation des REE en solution et leur partage entre les phases dissoutes, colloïdales et particulaires et de révéler, par là même, les principaux mécanismes mis en jeu dans la régulation de la composition chimique des eaux naturelles.

Une caractéristique des REE est d'être très fortement complexée par les matières organiques en solution. Ainsi, dans les eaux riches en matière organique (teneur en Carbone Organique Dissous ou COD >5mg/L) des études par ultrafiltration montrent que les REE sont majoritairement associées à la phase colloïdale (Tanizaki et al., 1992; Dupré et al., 1996; 1999; Viers et al., 1997; Ingri et al., 2000; Dia et al, 2000; Gruau et al., 2004; Pokrovsky et al., 2005; 2006). Cependant, deux types de spectre de REE sont rencontrés dans ces eaux (Elderfield et al., 1990). Le premier est généralement observé dans des eaux acides (pH < 6) et présente un enrichissement relatif en REE intermédiaires (figure I.1a). Ce comportement est attribué au contrôle de la spéciation des REE par les substances humiques présentes dans ces eaux, lesquelles ont, d'après certains auteurs, une plus forte affinité pour les REE intermédiaires (Goldstein et Jacobsen 1988; Tang et Johannesson, 2003 ; Pourret et al., 2007b). Le second type est généralement observé dans des eaux neutres à basiques et présente un enrichissement relatif en REE lourdes (figure I.1b). Ce comportement a été attribué historiquement au contrôle de la spéciation des REE dans ces eaux par les carbonates, lesquels présentent des constantes de complexation croissantes du La au Lu (Luo and Byrne, 2004).

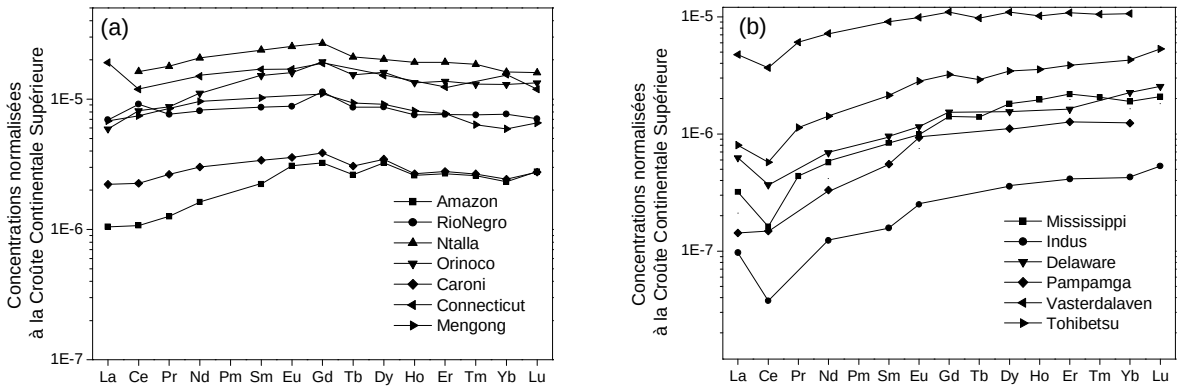

Figure I.1. Spectres de terres rares normalisés à la Croûte Continentale Supérieure d'eaux de rivières montrant (a) un enrichissement en terres rares légères à intermédiaires et (b) un enrichissement en terres rares lourdes (Goldstein et Jacobsen, 1988; Elderfield et al., 1990; Sholkovitz, 1995; Deberdt et al., 2002).

Cependant, des études récentes contredisent cette hypothèse. Ainsi, Pourret et al. (2007b) ont démontré expérimentalement que les REE restaient majoritairement complexés aux substances humiques (>90%) pour des valeurs de pH aussi élevées que 7.5, avec toujours la même plus forte complexation relative des REE intermédiaires (figure I.2a). Le rôle des carbonates dans la genèse des spectres enrichis en REE lourdes observés dans certaines eaux organiques semblent donc exclu. Reste une hypothèse alternative, qui est celle d'une mauvaise appréciation des constantes de complexation des REE par les substances humiques. Cette hypothèse a pris corps suite aux travaux réalisés par Sonke and Salters (2006) qui ont déterminé des constantes de complexation entre REE et acides humiques pour des pH de 6 à 9, en utilisant l'EDTA comme ligand compétiteur des acides humiques. Ces auteurs ont en effet observé une augmentation régulière de la complexation du La au Lu (figure I.2b). Ces résultats remettent donc en cause la complexation préférentielle des REE intermédiaires par les substances humiques telle qu'établit jusqu'ici. Cependant, à la différence des expériences réalisées par Pourret et al. (2007b), les expériences effectuées par Sonke and Salters (2006) l'ont été a un très faible rapport REE/acides humiques. Se pose alors la question du rôle de ce rapport sur la détermination des constantes de complexation des REE par les acides humiques. Ainsi, ces résultats montrent le besoin de connaître plus précisément les mécanismes par lesquels les REE se lient aux substances humiques et l'effet du rapport REE/acides humiques sur ces mécanismes. Cette question renvoie également à la structure des substances humiques et à la nature des sites par lesquels les REE se lient à ces substances.

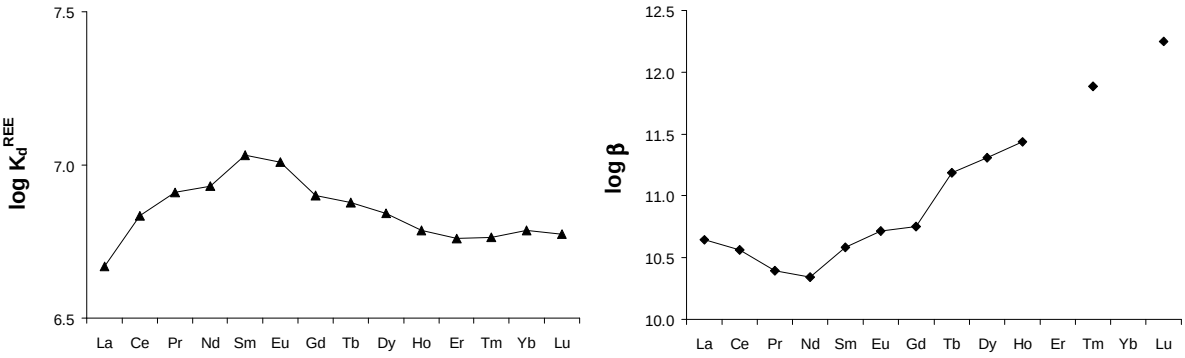

Figure I.2. (a) Coefficient de distribution des terres rares entre acides humiques et solution à pH = 6 (Pourret et al., 2007b). (b) Constantes de stabilité conditionnelles entre les terres rares et les acides humiques à pH = 6 (Sonke et Salters, 2006).

Les acides humiques sont des colloïdes organiques de poids moléculaire compris entre 3 et 1000 kDa (Sparks, 1995) et sont constitués principalement de carbone, d'hydrogène, d'oxygène et, dans de moindre proportions, d'azote, de phosphore et de souffre. Plusieurs classes de composés constituent ces colloïdes parmi lesquels on trouve des acides carboxyliques, des phénols, des acides aminés, des saccarides et des hydrocarbures (Thurman, 1985). Ces colloïdes jouent un rôle majeur dans la spéciation et le transport non seulement des REE mais aussi de la plupart des cations métalliques (e.g. Al, Fe, Cu, Th,..) dans l'environnement car ils possèdent une grande quantité de groupements fonctionnels complexants. La complexation des cations métalliques par les acides humiques étant fortement dépendante du pH, il est largement admis que les groupements fonctionnels impliqués sont principalement des groupements acido-basiques de type carboxyliques et/ou phénoliques (e.g. Tipping, 1998). L'absence de points d'inflexion distincts sur la courbe de titration d'une solution d'acide humique montre que les groupements acido-basiques portées par les substances humiques couvrent une large gamme de constantes d'acidité (e.g. Ritchie et Perdue, 2003). L'environnement atomique d'un groupement acido-basique influence la stabilité de la liaison entre oxygène et hydrogène. Etant donné la complexité de la structure moléculaire des substances humiques, des groupements de même nature peuvent se retrouver dans des environnements chimiques très différents, expliquant ainsi la gamme étendue des constantes d'acidité observées expérimentalement.

Beaucoup de métaux ont été étudiés du point de vue de leur capacité à former des complexes avec les substances humiques. C'est le cas par exemple de Al (Mota et al., 1996; Sutheimer and Cabaniss, 1997), Fe (Liu and Millero, 1999; Weber et al., 2006), Ca, Cd, Cu (Benedetti et al., 1995), Am (Peters et al., 2001), As (Buschmann et al., 2004), Sb (Buschmann and Sigg, 2006), Pb, Cd (Abate and Masini, 2002) et Eu (Lead et al. 1998, Glaus

et al., 2000). Des études de compétition entre cations métalliques montrent que la compétition a lieu pour les mêmes types de sites des acides humiques (Kinniburgh et al. 1999; Mandal et al., 1999; Pinheiro et al. 2000; Tipping et al., 2002; Tipping 2005; Marang et al., 2008). La figure I.3 présente une isotherme de complexation du Cu à la surface d'acides humiques à pH 4 (Benedetti et al., 1995). Elle présente l'évolution de la concentration en Cu complexé par gramme de ligand en fonction de la concentration en Cu libre en solution. Les isothermes de complexation du Cu avec deux ligands hypothétiques dont les constantes sont égales à 10^4 et 10^6 sont également comparées pour une concentration en ligand total de 1 mmol g^{-1}. La pente de l'isotherme pour les ligands hypothétique tend vers 1 lorsque la concentration en cuivre dissous diminue. On parle alors d'isotherme de complexation linéaire. L'isotherme de complexation du Cu avec les acides humiques est non linéaire, elle présente une pente égale à 0.43. Cette différence illustre l'hétérogénéité des groupements complexants des acides humiques et leur influence sur la complexation du Cu. En effet, pour de fortes concentrations en Cu dissous, les acides humiques se comportent globalement comme des ligands plus faibles que lorsque la concentration en Cu dissous est faible. Cette observation montre que les acides humiques présentent une grande quantité de ligands faibles et une faible quantité de ligands forts. L'hétérogénéité des acides humiques vis-à-vis de la complexation des cations peut s'expliquer par trois mécanismes chimiques : (i) tout comme pour H^+, la stabilité de liaison métal-ligand est influencée par l'environnement chimique du groupement fonctionnel complexant, expliquant la gamme de constantes de stabilité mesurées pour les complexes cation-acide humique. (ii) Contrairement au H^+, lorsque plusieurs groupements fonctionnels complexants des acides humiques (notés L) sont proches, un cation métallique peut former une liaison avec chacun de ces groupements. On parle alors de complexe multidentate (notés D). Un ligand multidentate présente une affinité accrue pour un métal par rapport à un même nombre de ligands monodentates de même nature chimique. Cette stabilisation s'appelle « effet de chélation » et est dû à une différence de changement d'entropie lors de la formation des complexes ML_n (où M représente le cation métallique) et MD (Martell et Hancock, 1996). La denticité et 'l'effet de chélation' augmentent également la gamme de constantes de stabilité cation-acide humique. (iii) Les acides humiques sont également composé de N, de P et de S qui peuvent former des ligands de surface complexants de certains cations métalliques, par exemple, des groupements amine, phosphate et thiol, respectivement. C'est le cas, par exemple du Cu qui a une forte affinité pour les groupements amine des acides humiques (Frenkel et al., 2000) ou de Hg qui a une forte affinité pour les groupements thiol (Yoon et al., 2005).

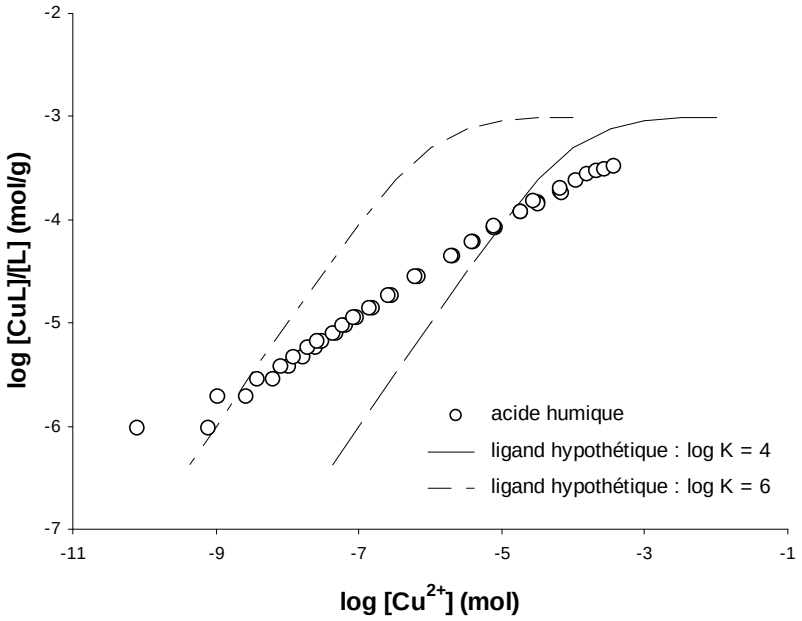

Figure I.3. Isotherme de complexation du Cu par des acides humique à pH = 4. Comparaison entre les acides humiques (Benedetti et al., 1995) et deux ligands hypothétiques dont log K Cu-ligand = 4 et 6.

L'hétérogénéité des groupements complexants les cations métalliques peut être modélisée soit par une distribution continue de constantes de stabilité soit par un grand nombre de constantes de stabilité présentant des valeurs discrètes. Ces deux concepts ont été appliqués dans les modèles spécifique de complexation des cations métalliques par les substances humiques NICA-Donnan (Koopal et al., 1994; Benedetti et al., 1995) et Model VI (Tipping, 1998) qui reproduisent tous deux les résultats obtenus en laboratoire de manière satisfaisante. Le concept de sites de complexation discrets permet de concevoir les acides humiques comme un ensemble de groupements carboxyliques, phénoliques formant des sites de complexation soit monodentates soit multidentates. A l'aide de cette représentation simplifiée des ligands des acides humiques, il est possible de comparer leurs propriétés de complexation des terres rares avec celui de ligands organiques modèles, présentant des structures comparables aux ligands suspectés d'intervenir dans les liaisons cations-substances humiques. Cette approche s'est avérée très utile pour l'interprétation des mécanismes d'adsorption des REE sur des surfaces hétérogènes tels que les cellules de bactéries (Takahashi et al., 2005; 2007; 2010). La figure I.4 compare les constantes de complexation entre les REE et des ligands modèles carboxylique (l'acide acétique; Fig. I.4a), phénolique (le catéchol ; Fig. I.4b) et chélate (l'acide nitrilotriacétique ou NTA; Fig. I.4c) (Byrne and Li, 1995). Le catéchol a été choisi comme ligand modèle phénolique car les constantes de stabilité entre les REE et le phénol ne sont pas connues. Cette figure montre que les REE

présentent un comportement différent en fonction de la nature du ligand. En effet, le ligand modèle faible représenté par l'acide acétique a une plus forte affinité pour les REE intermédiaires, alors que le ligand modèle plus fort représenté par le catéchol montre des constantes de stabilité avec les REE qui augmentent fortement du La au Sm puis légèrement jusqu'aux REE les plus lourdes. Le ligand modèle chélate, représenté par le NTA, montre quant à lui des constantes de stabilité avec les REE qui augmentent très fortement et de manière continue du La au Lu. En fait, la tendance observée d'un accroissement relatif des constantes des REE lourdes, par rapport aux REE légères, avec l'accroissement de la force du ligand est généralisable à l'ensemble des ligands organiques. La figure I.4d présente le rapport des constantes de stabilité entre Lu et La en fonction de la constante de stabilité moyenne du groupe des REE avec 101 ligands organiques (Byrne and Li, 1995). Le rapport Lu/La est utilisé comme indicateur de la différence des constantes de complexation entre REE lourdes et REE légères. Cette figure montre que plus le ligand est fort, plus son affinité relative pour les REE lourdes est grande. De plus, les REE intermédiaires forment systématiquement des complexes plus stables que les REE légères. Les ligands faibles présentent donc une plus forte affinité pour les REE intermédiaires que pour les REE lourdes et légères.

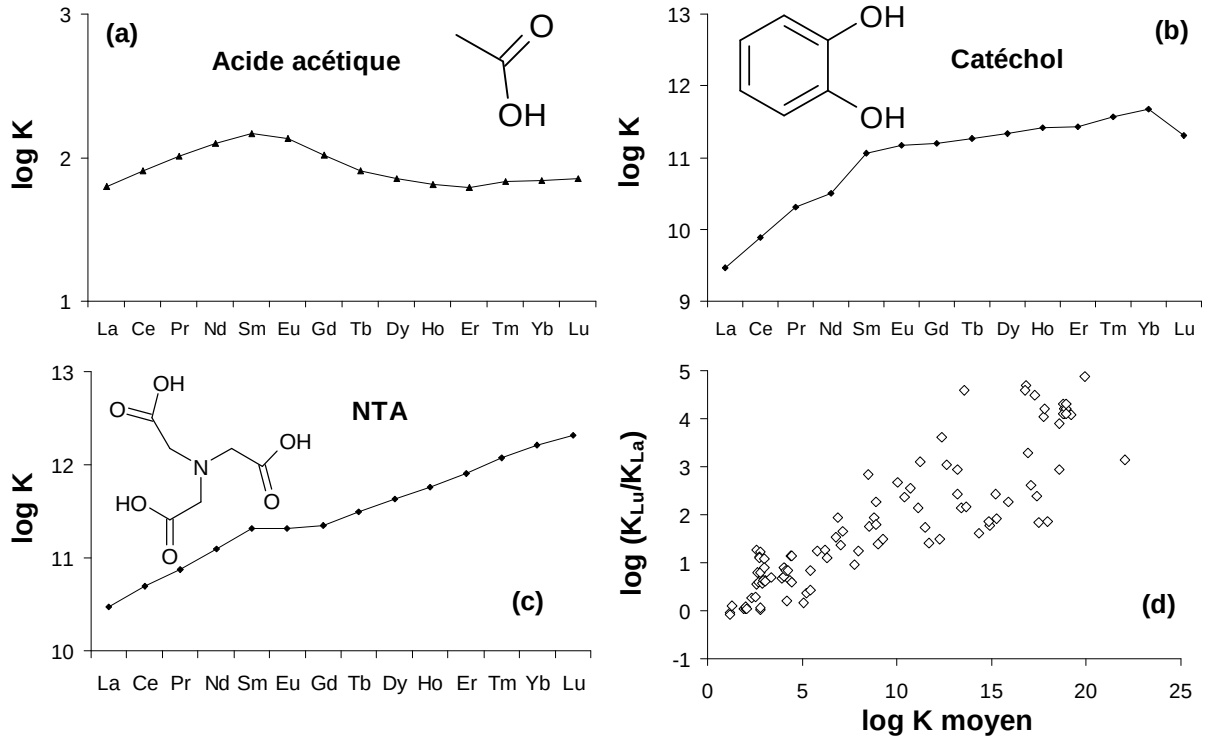

Figure I.4. Constantes de stabilité des terres rares avec (a) l'acide acétique, (b) le catéchol et (c) le NTA. (d) Rapport des constantes de stabilité de Lu et La en fonction de la constante moyenne pour les terres rares pour 101 ligands organiques (Byrne et Li, 1995).

Ainsi, au sein des acides humiques, la présence de sites aux propriétés complexantes et d'abondances différentes fournit une explication potentiellement unificatrice des différences de résultats obtenus par Sonke et Salters (2006) et Pourret et al. (2007b). En effet, les ligands forts des acides humiques étant présents en plus faible quantité que les ligands faibles (cf figure I.3 et les explications associées), on s'attend à ce qu'un faible rapport REE/acides humiques génère une stabilité des complexes croissante depuis le La jusqu'au Lu, comme observé avec le NTA. A l'inverse, on s'attend à ce qu'un rapport REE/acides humiques élevé induise des complexes plus stables pour les REE intermédiaires, comme observé avec l'acide acétique. Les groupements carboxyliques sont des ligands plus faibles mais présentent une plus forte constante d'acidité que les groupements phénoliques. Ainsi, le pH pourrait influer sur la distribution des REE entre les sites carboxyliques et phénoliques des acides humiques. D'après les figures I.4a et I.4b, les groupements carboxyliques et phénoliques des acides humiques pourraient former des complexes plus stables respectivement pour les REE intermédiaires et lourdes, comme c'est le cas pour l'acide acétique et le catéchol. Finalement, l'ensemble de ces hypothèses suggère qu'un cation compétiteur des REE pourrait limiter la complexation des REE légères ou lourdes selon son affinité relative pour les sites carboxyliques, phénoliques et chélates des acides humiques. En fonction de la spéciation des REE au sein des acides humiques et donc des conditions chimique du milieu (i.e. pH, REE/acides humiques, concentration et nature des cations présents), les acides humiques pourraient complexer préférentiellement soit les REE intermédiaires soit les lourdes. La variabilité des spectres de REE dans les eaux riches en matière organique serait alors intimement liée à une augmentation de la solubilité d'un groupe particulier des REE due à leur complexation préférentielle par les colloïdes organiques.

L'objectif de ce travail est d'expliquer la variabilité des spectres de REE observée dans les eaux riches en matière organique où la spéciation des REE est majoritairement contrôlée par les colloïdes organiques. Plus spécifiquement, il s'agit d'étudier (i) l'influence de l'hétérogénéité de composition et d'abondance des groupements fonctionnels sur la complexation des différentes REE par les acides humiques et (ii) les facteurs pouvant influencer la distribution des REE sur ces différents sites de complexation. Pour atteindre ce double objectif, des expériences d'équilibre de complexation des REE par les acides humiques ont été réalisées en conditions contrôlées de laboratoire en fonction du rapport REE/acide humique, du pH, et de la nature et de la concentration de cations compétiteurs. La modélisation des résultats expérimentaux par Model VI a été utilisée afin de tester les hypothèses quant aux mécanismes de complexation des REE et, plus particulièrement, leur

distribution sur les sites carboxyliques, phénoliques et chélates des acides humiques en fonction des facteurs étudiés expérimentalement. Finalement, les résultats obtenus par le couplage expérimentation-modélisation ont été confrontés aux spectres de terres rares mesurés dans les eaux organiques naturelles afin de comprendre l'origine et la signification des variabilités de forme observées.

Ce manuscrit, qui se présente comme une succession d'articles rédigés en anglais publiés ou soumis dans des revues scientifiques internationales, comprend quatre grandes parties : la **première partie** est consacrée à l'influence du rapport REE/acide humique sur la complexation quantitative des différentes REE par les acides humiques afin de vérifier la principale hypothèse émise lors de la comparaison des résultats de Sonke et Salters (2006) et de Pourret et al. (2007b) : le spectre des REE complexées aux acides humiques dépend-il de la nature de la liaison entre terres rares et acide humique ? La **deuxième partie** a pour but de vérifier, par modélisation, si la complexation des REE par les acides humiques peut s'expliquer par la participation simultanée de sites carboxyliques, phénoliques et chélates présentant respectivement un comportement proche de l'acide acétique, du catéchol et du NTA vis-à-vis de la complexation des REE. Des modifications ont été apportées à Model VI qui a été intégré dans PHREEQC afin (i) de réaliser des simulations de complexation des REE par les acides humiques proches des résultats expérimentaux obtenus dans des conditions variées, (ii) de simuler un acide humique dont les sites de complexation présentent des spectres de constante de stabilité avec les REE plus cohérent avec des ligands organiques de référence et (iii) d'étudier la distribution REE sur l'ensemble des sites des acides humiques et ainsi de déterminer les facteurs susceptibles de modifier le spectre des terres rares complexées par les acides humiques. Les **troisième et quatrième parties** sont dédiées à l'étude du comportement des REE lorsqu'elles sont en compétition avec un autre cation trivalent : les autres cations peuvent-ils modifier la distribution relative des REE sur les sites des acides humiques ? Deux études successives ont été menées avec Al et Fe comme compétiteurs des REE. Enfin, les **conclusions** et les **implications** des principaux résultats sont synthétisées et des **perspectives** sont proposées.

II. Chapitre I :

Effet de la charge en métaux sur la complexation des terres rares par les acides humiques

Metal loading effect on rare earth element binding to humic acid: experimental and modelling evidence

Cette partie est extraite de Geochimica et Cosmochimica Acta, Marsac R., Davranche M., Gruau G. and Dia A. (2010) Metal loading effect on rare earth element binding to humic acid: experimental and modelling evidence, 74, 1749-1761.

Résumé- L'effet de la charge en métaux sur la complexation des terres rares (REE) par les acides humiques (HA) a été étudié en combinant des techniques d'ultrafiltration et ICP-MS. Les expériences de complexation REE-HA ont été effectuées à pH 3 pour des rapports molaires REE/C allant de $4{,}10^{-4}$ à $2{,}7.10^{-2}$. Les résultats montrent que la quantité relative de REE liées aux HA augmente fortement lorsque le rapport REE/C diminue. Le spectre des coefficients ($\log K_d^{REE}$) de partages augmente pour les REE intermédiaires (MREE) pour un rapport REE/C élevé tandis qu'il augmente de manière régulière du La au Lu pour un rapport REE/C faible. La modélisation avec Model VI peut reproduire cette variation à condition que (i) le paramètre ΔLK_2 (i.e. le paramètre de Model VI qui permet de tenir compte de l'existence de sites forts présent à de faibles teneurs) croît du La au Lu et (ii) les valeurs de $\log K_{MA}$, précédemment publiée, sont légèrement modifiées, plus particulièrement pour les REE lourdes (HREE). Le modèle démontre que les variations des spectres de $\log K_d^{REE}$ avec la charge en métaux sont dues à la complexation des REE par deux types de sites de HA présents dans des proportions différentes : (i) une faible quantité de sites forts, complexant préférentiellement les HREE, contrôlent le spectre de $\log K_d^{REE}$ à de faibles rapport REE/C tandis que (ii) une grande quantité de sites faibles de HA, complexant préférentiellement les MREE, contrôlent le spectre de $\log K_d^{REE}$ à de forts rapport REE/C. La charge en métaux a donc un effet majeur sur la complexation des REE par HA et pourrait expliquer la diversité des spectres de complexation des REE par HA précédemment publiés. Une étude approfondie de la littérature suggère que les sites forts, activés à de faible rapport REE/C, pourraient être des ligands carboxyliques multidentates avec, potentiellement, la participation de ligands contenant des atomes d'azote ou de phosphore. Finalement, l'examen de données publiées de terrain suggère que la charge en métaux, décrite dans cette étude, pourrait expliquer la variabilité des spectres de REE observées dans les eaux riches en matière organique dissoute ($DOC>5mg\ L^{-1}$ and $4\leq pH\leq 7$).

Abstract- The effect of metal loading on the binding of rare earth elements (REE) to humic acid (HA) was studied by combining ultrafiltration and Inductively Coupled Plasma Mass Spectrometry techniques. REE-HA complexation experiments were performed at pH 3 for REE/C molar ratios ranging from ca $4x10^{-4}$ to $2.7x10^{-2}$. Results show that the relative amount of REE bound to HA strongly increases with decreasing REE/C. A middle-REE (MREE) downward concavity is shown by $\log K_d^{REE}$ patterns at high metal loading, whereas patterns at

low metal loading display a regular increase from La to Lu. Humic Ion Model VI modelling are close to the experimental data variations, provided that (i) the ΔLK_2 parameter (i.e. the Model VI parameter taken into account the presence of strong but low density binding sites) is allowed to increase regularly from La to Lu (from 1.1 to 2.1) and (ii) the published log K_{MA} values (i.e. the REE-HA binding constants specific to Model VI) are slightly modified, in particular with respect to heavy REE. The modelling approach provided evidence that $\log K_d^{REE}$ patterns with varying REE/C likely arises because REE binding to HA occurs through two types of binding sites in different density: (i) a few strong sites that preferentially complex the heavy REE and thus control the $\log K_d^{REE}$ patterns at low REE/C; (ii) a larger amount of weaker binding sites that preferentially complex the middle REE and thus control the $\log K_d^{REE}$ pattern at high REE/C. Hence, metal loading exerts a major effect on HA-mediated REE binding, which could explain the diversity of published conditional constants for REE binding with HA. A literature survey suggests that the few strong sites activated at low REE/C could be multidentate carboxylic sites, or perhaps N- or P-containing functional groups. Finally, an examination of the literature field data proposed that the described loading effect could account for much of the variation in REE patterns observed in natural organic-rich waters (DOC>5mg L^{-1} and $4 \leq pH \leq 7$).

1. Introduction

There is now widespread evidence that rare earth elements (REE) in natural organic waters occur as organic complexes (Bidoglio et al., 1991; Glaus et al., 1995; Takahashi et al., 1997; Viers et al., 1997; Dia et al., 2000; Tang and Johannesson, 2003; Gruau et al., 2004; Pourret et al., 2007a, b; Glaus et al., 2000; Yamamoto et al., 2005; Sonke and Salters, 2006; Stern et al., 2007; Pédrot et al., 2008; Yamamoto et al., 2010). This explains why the determination of conditional binding constants of the REE by humic acids (HA) has recently become a major issue of REE hydrochemical studies (Tang and Johannesson, 2003; Yamamoto et al., 2005; Sonke and Salters, 2006; Pourret et al., 2007a, b; Stern et al., 2007; and Yamamoto et al., 2010). Several recent studies showed that determining such constants is not an easy task because of the presence of a possible metal loading effect, leading to variations in the $\log K_d^{REE}$ patterns with variations in REE/HA ratio. Thus, Yamamoto et al. (2005 and 2006) and Pourret et al. (2007b) reported a middle REE (MREE) downward concavity in the $\log K_d^{REE}$ patterns from complexation experiments conducted at high metal

loading (i.e. REE/C molar ratio ranging from 10^{-3} to $1.5x10^{-2}$, with C corresponding to the amount of organic carbon). By contrast, Sonke and Salters (2006) and Stern et al. (2007) reported an overall increase of the $\log K_d^{REE}$ values from La to Lu (so-called lanthanide contraction effect) from experiments at much lower REE/C (10^{-4}). One possible explanation for this discrepancy is that the binding of the REE with HA occurs through the heterogeneity of the HA binding sites, having different stability constants and occurring in markedly distinct density. More specifically, the "lanthanide contraction effect" observed in low metal loading experiments could be due to the dominant binding of the REE to high affinity sites which, although occurring in the range of a few percent, would determine the $\log K_d^{REE}$ pattern under such low REE/C conditions. These sites, whose binding strength regularly increases with the REE atomic number, could be multidendate carboxylic sites, or phenolic, or aminocarboxylic sites as suggested by Stern et al. (2007) and Pourret and Martinez (2009). Alternatively, the MREE downward concavity observed at high metal loading could be due to the binding characteristics of high density but weak sites, which would determine the HA binding under high REE/C conditions. These sites would complex the MREE much more efficiently than the LREE and the HREE, and could be attributed to carboxylic sites, which are known to be the main binding sites of REE in HA as demonstrated by NEXAFS analysis (C 1s-near edge X-ray absorption fine structure) of Eu-HA complexes at high Eu/C ratio (Plaschke et al., 2004).
The binding characteristics of different trace metals with HA were previously studied by adsorption isotherm experiments. These studies focused on the binding of Al (Kinniburg et al. 1999), Ca, Cd, Cu (Benedetti et al. 1995), Am (Peters et al., 2001), As (Buschmann et al., 2004), Sb (Buschmann and Sigg, 2006), Pb and Cd (Abate and Masini, 2002) to humic substances (HS), evidenced an increase in the binding strength following the metal loading decrease, that can be related to HS surface site heterogeneity. Such non-linear binding was also observed by Hummel et al. (2000) for Eu complexation to HA. These studies agree with the hypothesis of a variation of the apparent $\log K_d^{REE}$ patterns with REE/C due to the heterogeneity of the HA binding sites occurring at different density. More recently, Yamamoto et al. (2010) demonstrated a regular and progressive evolution of the $\log K_d^{REE}$ patterns with decreasing metal loading, from a downward concave MREE distribution to a pattern showing the lanthanide contraction effect. However, this hypothesis still lacks corroboration from a comprehensive study involving experimental and modelling approaches.

In the present study, REE-HA binding experiments were performed simultaneously on the 14 naturally occurring REE over a wide range of REE/C molar ratio (ranging from $4x10^{-4}$

to $2.7x10^{-2}$). Whereas the Sonke and Salters study used CE-ICPMS at low REE/C and the Pourret et al. (2007) study used ultrafiltration combined with ICP-MS, at high metal loading, all the here below presented data were obtained using the same combined ultrafiltration and ICP-MS techniques. The experimental data are analysed to assess the variation in binding sites with changing REE/C using Humic Ion binding Model VI (hereafter denoted as Model VI), developed by Tipping (1998). Finally, a compilation of 350 samples of organic-rich, river-, and soil-waters were pooled to show whether variations in REE pattern displayed by natural organic-rich waters could be due to a metal loading effect.

2. Materials and methods

All chemicals used in this study were of analytical grade, with all experimental solutions being prepared with doubly-deionised water (Milli-Q system, Millipore™). Synthetic REE solutions were prepared from a nitrate REE standard (10 mg L^{-1}, Accu Trace™ Reference Standard). Polyethylene containers used to attain REE-HA complexation equilibrium were all previously soaked in 10% Ultrapure HNO_3 for 48h at 60°C, then rinsed with deionised water for 24h at 60°C to remove all REE contamination sources. All experiments were performed at room temperature, i.e. 20°C ± 2.

2.1. Humic acid

Purified humic acid (HA) was obtained from synthetic Aldrich humic acid (Aldrich™, H1, 675-2). The purification was performed with the protocol of Vermeer et al. (1998), except that a tangential ultrafiltration step was added to remove any possible HA molecules <10 kDa using a Labscale TFF system equipped with a Pellicon XL membrane (PLCGC10, Millipore™). Humic acid was freeze-dried and stored in a glass container. Prior to use, purified HA was solubilized overnight in a solution of 0.01 M NaCl at pH = 10 to ensure complete dissolution (Vermeer et al., 1998).

2.2. Experimental set-up of the REE binding with HA

A standard batch equilibrium technique was used to study REE complexation with HA. The fourteen REE were added simultaneously to a solution of 5 to 40 mg L^{-1} of HA and 10^{-2} M NaCl. The REE/C (metal loading) varied from $4x10^{-4}$ to $2.7x10^{-2}$. REE-HA binding experiments were carried out at pH = 3. This acidic pH was chosen to avoid total complexation of the REE with HA, and to prevent complexation of the REE inorganic

fraction by OH^- and CO_3^{2-}. Owing to their low stability constants ($-0.66<\log \beta<-0.41$ at 0.7 M ionic strength and 25°C) (Byrne and Sholkovitz, 1996), REE-Cl complexes were neglected. All inorganic REE can thus be confidently assumed to occur as free aqueous REE^{3+} species in all the experiments, and are modelled accordingly (Tang and Johannesson, 2003; Pourret et al., 2007a). According to Yamamoto et al. (2009), Al and Fe form stable complexes with carboxylic sites within humic substances and cannot be excluded completely by purification of HA. Although humic acid was here purified with an acidic cation-exchange resin (Dionex 50) at pH 1, some Al and Fe could effectively remain in HA. Therefore, HA sites strongly bound with residual Fe and Al may be considered as not available for cation binding. Moreover, HA site density is generally evaluated by potentiometric titration carried out between pH 2 and 11 (e.g. Ritchie and Perdue, 2003). Considering the titration pH, titrations do not allow removal of residual Fe and Al from the HA surface. In consequence, the HA sites strongly bound with Fe and Al do not account for surface site density. Therefore, the potential effect of residual Al and Fe on REE binding was not taken into account in this study. Prior to REE addition, the pH was adjusted directly to a value of 3 in the HA suspensions, which were then filtered to remove any potential precipitate. The dissolved organic carbon (DOC) concentration was then measured to assess the true HA concentration of the filtrate. Immediately following REE addition, a solution aliquot was systematically analysed to determine the exact REE concentration and thus the true REE/C of each experimental suspension.

Experimental suspensions were stirred for 48 h to reach equilibrium according to the protocol defined by Pourret et al. (2007b). The pH was monitored regularly with a combined Radiometer Red Rod electrode, calibrated with WTW standard solutions (pH 4 and 7). The accuracy of pH measurements was ± 0.05 pH units. At equilibrium (48 h), 10 mL of the suspension were sampled and ultra-filtered at 5 kDa to separate the REE-HA complexes from the remaining inorganic REE. Ultrafiltrations were carried out by centrifuging the suspension aliquots through 15 mL centrifugal tubes equipped with permeable membranes of 5 kDa pore size (Vivaspin 15RH12, Sartorius). All the membranes used were first washed with 0.15 mol L^{-1} HCl, then rinsed twice with MilliQ water to minimise contamination. Centrifugations were performed using a Jouan G4.12 centrifuge with swinging bucket rotor at 3000 g for 30 min.

Dissolved organic carbon concentrations measured in the ultrafiltrates were systematically lower than or equal to 0.1 mg L^{-1}, a concentration corresponding to the blank value currently observed in our laboratory (e.g. Pourret et al., 2007b). The 10 kDa

ultrafiltration step added in the HA purification protocol ensures that no organic molecules pass through the 5 kDa ultrafiltration cells. Previously, Pourret et al. (2007b) showed from mass balance calculations, that more than 98% of REE were recovered and that REE adsorption onto the membrane and the cell device was insignificant. Hence, the concentrations of REE complexed to HA correspond strictly to the difference between the initial REE concentration and the REE concentration in the <5 kDa ultrafiltrate.

The REE complexation with HA is described using the apparent partition coefficient K_d, as follows:

$$K_d(Ln_i) = \frac{\mu g Ln_i \text{ adsorbed } L^{-1}/g DOC\, L^{-1}}{\mu g Ln_i^{3+}\, mL^{-1}} \quad \text{(II.1)}$$

where Ln_i = La to Lu.

2.3. Solution analysis

Rare earth element concentrations were determined at Rennes I University with an Agilent Technologies™ HP4500 ICP-MS instrument. All sample solutions were injected directly, except the initial suspensions, which were analysed to determine precisely the REE/C ratios for each experiment. The suspensions were first digested with sub-boiled nitric acid (HNO_3 14 N) at 100°C, then resolubilized in HNO_3 0.37 N after complete evaporation to avoid interferences with organic matter during mass analysis by ICP-MS. Quantitative analyses were performed using a conventional external calibration procedure. Three external standard solutions with REE concentrations similar to the analysed samples were prepared from a multi-REE standard solution (Accu Trace™ Reference, 10 mg L^{-1}, USA). Indium was added to all samples as an internal standard at a concentration of 0.87 µmol L^{-1} (100 ppb) to correct for instrumental drift and possible matrix effects. Indium was also added to the external standard solutions. Calibration curves were calculated from measured REE/indium intensity ratios. As established from repeated analyses of multi-REE standard solution (Accu Trace™ Reference, USA) and the SLRS-4 water standard, the instrumental error on REE analysis is below 3 %. Chemical blanks of all individual REE were all lower than detection limit (1ng L^{-1}), and are thus negligible.

Dissolved organic carbon concentrations were determined using a Shimadzu 5000 TOC analyzer. The accuracy of DOC concentration measurements is estimated at ± 5%, as determined by repeated analysis of freshly prepared standard solutions (potassium biphtalate).

2.4. Humic Ion binding Model VI

The Humic Ion binding Model VI (Model VI) has been precisely described by Tipping (1998). This model is a discrete binding site model which takes into account electrostatic interactions. Eight sites are considered, divided into an equal number of Type A sites (the weak acidic group, commonly associated with carboxylic functional groups) and Type B sites (the strong acidic group, commonly associated with phenolic functional groups). There are n_A (mol g^{-1}) Type A sites and $n_A/2$ (mol g^{-1}) Type B sites. The thermodynamic properties of each site are described by intrinsic proton-binding constants (pK_A or pK_B) and the spread of the values (ΔpK_A or ΔpK_B). Cation binding is described by the intrinsic binding constant of a given cation with each type of site (namely, log K_{MA} and log K_{MB}), together with a parameter (ΔLK_1) describing the spread of values around the median. By considering results from many datasets, a universal average value of ΔLK_1 was obtained for all cations, and a correlation established between log K_{MB} and log K_{MA} (Tipping, 1998). Model VI parameters used for REE binding to humic acid modelling (Tipping, 1998) are presented in Table II.1.

Model VI also takes into account the formation of bidentate and tridentate complexes by a proximity factor, which quantifies whether the binding sites are close enough to form multidentate sites[1]. The occurrence of bidendate and tridendate sites is calculated probalistically. A fraction of multidentate sites can be considered as equivalent to strong sites, and may be compared to other strong sites formed by atoms such as N, P or S (Tipping, 2007). The binding constant of the bidendate and tridendate sites are calculated by increasing the logarithms of monodendate site constants by N ΔLK_2, where N=1 and 2 for 9 and 0.9% of the bidentate sites, respectively, and N= 1.5 and 3 for 9 and 0.9% of the tridentate sites, respectively (Tipping, 2002). Thus, the ΔLK_2 parameter (so-called "the strong binding site term") introduced in Model VI, can be used to model cation binding by the few strong sites.

[1] Text modified from the published article.

Parameter	Description	Values
n_A	Amount of type A sites (mol g^{-1})	$3.3\ 10^{-3}$
n_B	Amount of type B sites (mol g^{-1})	0.5 x n_A
pK_A	Intrinsic proton dissociation constant for type A sites	4.1
pK_B	Intrinsic proton dissociation constant for type B sites	8.8
ΔpK_A	Distribution terms that modifies pK_A	2.1
ΔpK_B	Distribution terms that modifies pK_B	3.6
$\log K_{MA}$	Intrinsic equilibrium constant for metal binding at type A sites	Fitted from experimental data
$\log K_{MB}$	Intrinsic equilibrium constant for metal binding at type B sites	3.39 $\log K_{MA}$ -1.15
ΔLK_1	Distribution term that modifies $\log K_{MA}$	2.8
ΔLK_2	Distribution term that modifies the strengths of bidentate and tridentate sites	Fitted from experimental data
P	Electrostatic parameter	-330
K_{sel}	Selectivity coefficient for counterion accumulation	1
M	Molecular weight	15000 Da
r	Molecular radius	1.72 nm

Table II.1. Model VI parameters used for REE binding to humic acid (Tipping, 1998).

3. Results

(All experimental data can be found in the supplementary file)

3.1. Experimental data

The influence of metal loading on REE complexation with HA is examined by considering the variation of the REE distribution coefficient ($\log K_d^{REE}$) patterns as a function of the REE/C (Fig. II.1). Firstly, a variation in the $\log K_d^{REE}$ value is observed from 4.8 to 6.6 for La, and from 4.8 to 7.3 for Lu over the range of tested REE/C (from $4x10^{-4}$ to $2.7x10^{-2}$). Secondly, and more importantly, the suggested variation of the $\log K_d^{REE}$ patterns with changing REE/C is confirmed (see discussions in Pourret et al., 2007b and Stern at al., 2007). More specifically, $\log K_d^{REE}$ patterns at low REE/C display a continuous enrichment from La to Lu, a feature already reported by Sonke and Salters (2006) and Stern et al. (2007) for patterns obtained at similarly low REE/C. Conversely, $\log K_d^{REE}$ patterns at high REE/C show the typical downward concavity of the MREE earlier reported by Davranche et al. (2005), Yamamoto et al., (2005) and Pourret et al., (2007b) from high metal loading experiments. This $\log K_d^{REE}$ pattern variation can be quantified by means of the $\log (K_d^{La} / K_d^{Sm})$ and $\log (K_d^{Gd} / K_d^{Yb})$ (denoted below as log(La/Sm) and log(Gd/Yb), respectively). Indeed, the $\log K_d^{REE}$ patterns from low REE/C experiments - displaying the typical increase from La to Lu - are characterized by log (La/Sm) and log (Gd/Yb) values <0, whereas patterns from high REE/C experiments - showing the characteristic downward concavity of the MREE - have log

(La/Sm) and log (Gd/Yb) ratios <0 and >0, respectively. As a whole, the log (Gd/Yb) decreases more strongly with decreasing REE/C (from 0.11 for REE/C = $2.7x10^{-2}$ to -0.35 for REE/C = $4x10^{-4}$) than the log (La/Sm) (from -0.24 for REE/C = $2.7x10^{-2}$ to -0.41 for REE/C = $4x10^{-4}$).

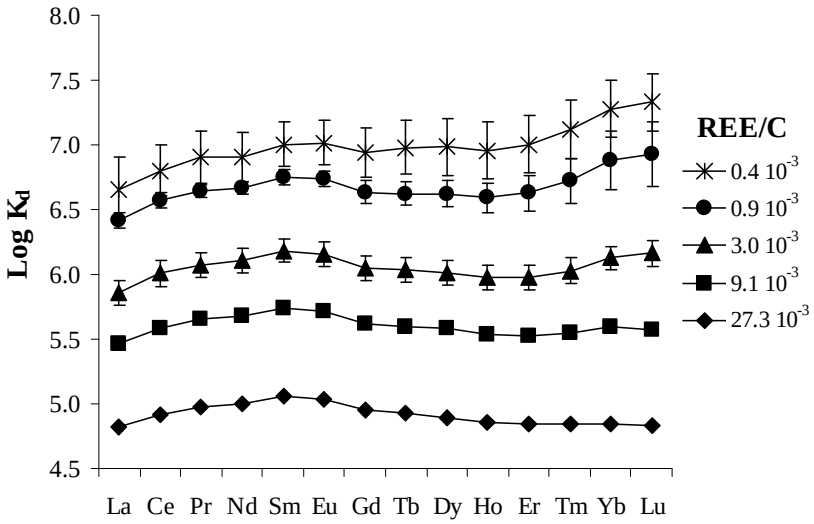

Figure II.1. Variation of log K_d^{REE} as a function of REE/C. Error bars correspond to standard deviation of triplicates.

Log K_d and log (REE/C) display negative linear correlations (R^2>0.99) when reported together (e.g., La, Lu; Fig. II.2) within the tested REE/C range. The $\log K_d^{REE}$ increase with the decreasing metal loading demonstrates the non-linearity of the REE-HA binding involved by the HA binding site heterogeneity. Slopes of $\log K_d^{REE}$ versus log REE/C noted a_i (i = La to Lu), which corresponds to the non linearity coefficient of the REE-HA binding increase regularly along the REE series, suggesting that HREE binding to HA is strongly influenced by the HA site heterogeneity (Fig. II.3). Our results demonstrate that REE-HA binding occurs through high density but weak HA sites at high metal loading, implying a concave $\log K_d^{REE}$ pattern. By contrast, at low metal loading, REE and notably HREE are preferentially bound to strong affinity but low density HA sites, which involves a regular $\log K_d^{REE}$ increase from La to Lu.

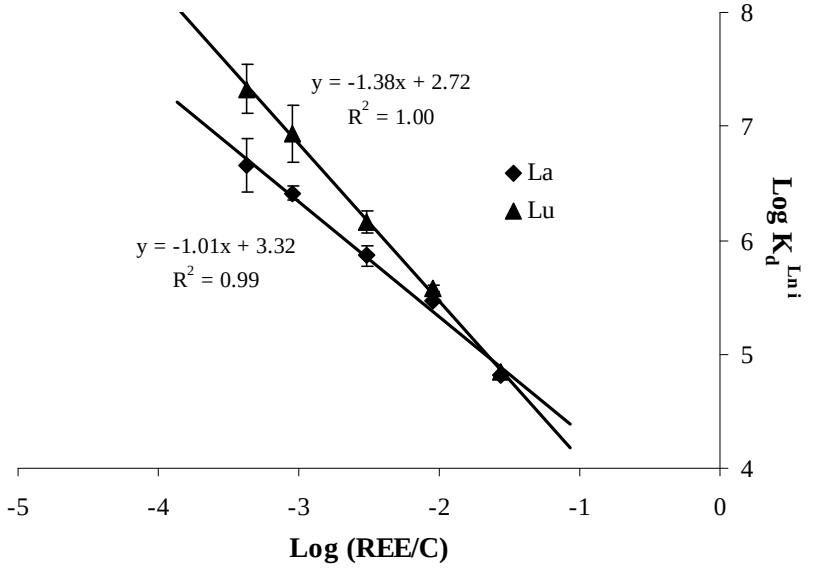

Figure II.2. Diagram illustrating negative linear correlations between log Kd and log (REE/C) for La and Lu. Error bars correspond to standard deviation of triplicates.

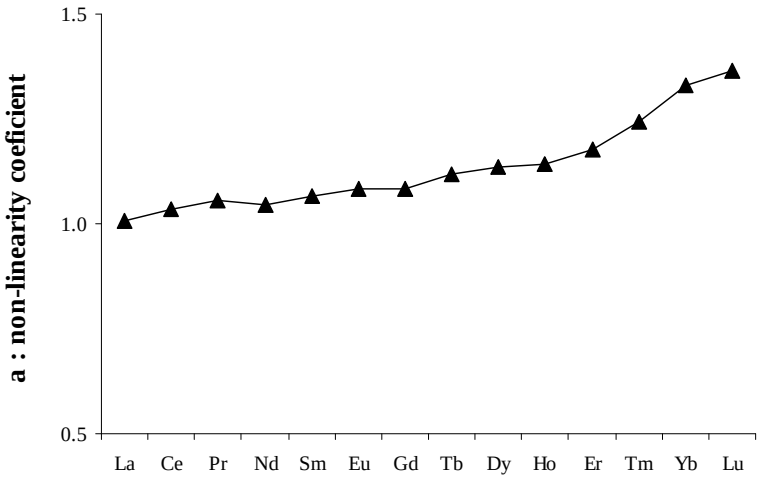

Figure II.3. Variation of "a" coefficient through the REE series. "a" is a measure of the non-linearity of the REE-HA binding isotherms, determined by the slope of log K_d^{REE} versus log (REE/C).

3.2. Calculating log K_{MA} and ΔLK2 values

Calculations are performed using the computer program WHAM 6 (Version 6.0.13), which includes Model VI. We used a classic strategy that consists of adjusting the intrinsic parameters of the model to each REE simultaneously until the minimization of the root mean square error (rmse). We not only adjust log K_{MA} (i.e. the parameter that quantifies REE complexation via the high-density, low-affinity sites), but also the ΔLK_2 values. ΔLK_2 is the parameter that addresses the non-linearity of the cation-HA binding in Model VI and is used

to increase HA strong site influence on the binding. Tipping (2002) designate ΔLK_2 as "the strong binding site term". This procedure is a unique feature of the present study, as all previous workers have considered this parameter as constant and equal to 0.29 for each individual REE (e.g. Pourret et al., 2007b). Pourret et al.'s (2007b) log K_{MA} dataset was used as initial log K_{MA} values. Considering that ΔLK_2 and $|a_i|$ coefficient represent both the non linearity of the REE-HA binding and the subsequent HA site heterogeneity, ΔLK_2 values were optimised assuming a linear correlation with a_i. ($\Delta LK_2 = 2.98 * a_i - 1.88$).

REE	log $K_{MA}^{(1)}$	log $K_{MA}^{(2)}$	$\Delta LK_2^{(2)}$	$rmse^{(2)}$
La	2.58	2.70	1.10	0.02
Ce	2.60	2.72	1.15	0.02
Pr	2.61	2.73	1.20	0.02
Nd	2.63	2.74	1.20	0.01
Sm	2.65	2.75	1.30	0.01
Eu	2.65	2.74	1.35	0.01
Gd	2.63	2.72	1.35	0.01
Tb	2.62	2.71	1.50	0.01
Dy	2.61	2.70	1.60	0.02
Ho	2.60	2.69	1.65	0.02
Er	2.60	2.69	1.70	0.01
Tm	2.59	2.67	1.90	0.01
Yb	2.60	2.65	2.05	0.02
Lu	2.60	2.64	2.10	0.02

(1) Pourret et al. (2007b)
(2) This study

Table II.2. Log KMA and ΔLK2 values fitted from the experimental data using Model VI. The quality of the fit is determined by the rmse, calculated as $\sqrt{mean(\log \nu_{exp} - \log \nu_{calc})^2}$, where ν is the amount of REE bound to HA per gram of DOC for experimental and modelled data, respectively. The log KMA data published by Pourret et al. (2007b) are shown for comparison.

Table II.2 reports the two sets of optimized log K_{MA} and ΔLK_2 values thus obtained for the 14 analysed REE. As indicated, by rmse values (<0.03), the fits can be considered of good quality. The optimized ΔLK_2 values are intermediate between the values for trivalent Al and Fe (0.46 and 2.20, respectively) determined by Tipping et al. (2002). The new set of optimized log K_{MA} values is compared with the earlier dataset published by Pourret et al. (2007b) (Table II.2). The new values are higher than the previous results by ca. 0.1 log unit. They are also distinguished by the presence of a slight but continuous decrease of Log K_{MA} from Dy to Lu. The optimized log K_{MA} and ΔLK_2 values reported in Table II.2 are used to draw the calculated La and Lu adsorption isotherm (Fig. II.4a) as well as log (La/Sm) and log (Gd/Yb) variations vs. log (REE/C) (Fig. II.4b). The comparison between calculated and

experimental data shows a reasonably good fit which demonstrates the ability of Model VI to predict the REE-HA binding at high and low REE/C. In particular, calculated log (La/Sm) and log (Gd/Yb) decrease with decreasing log (REE/C), in the same way as the experimental values (Fig. II.4b).

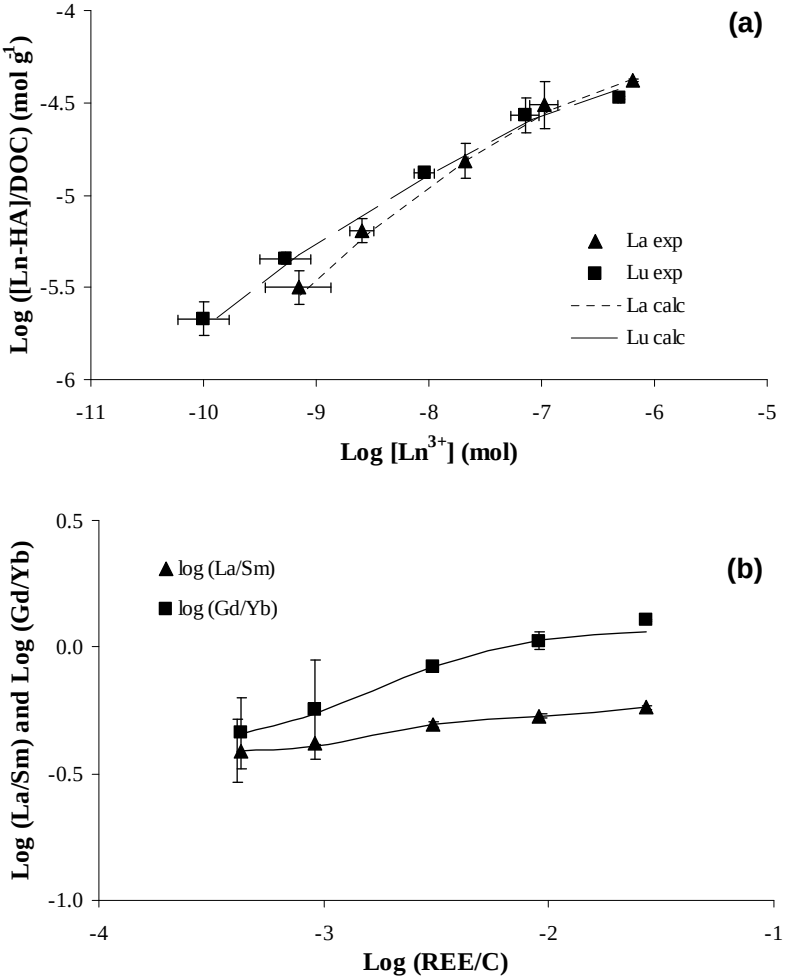

Figure II.4. Binding of REE by HA. (a) La-HA and Lu-HA binding isotherm, presented for La and Lu, and (b) Variation of log (La/Sm) and log (Gd/Yb) versus log (REE/C). Closed symbols and lines correspond to experimental data and best fits, respectively. Error bars correspond to standard deviation of triplicates.

4. Discussion

4.1. Comparison with the literature

In Model VI, the log K_{MA} values may be regarded as representing the binding characteristics of weak sites controlling REE complexation with HA at high REE/C.

Although, these values do not represent stability constants, the relative variation of log K_{MA} through the REE series likely reflects the ability of the weak sites to bind REE. Thus, the weak sites may be considered as preferentially complexing the MREE whereas the strong sites, whose complexation constant depend on ΔLK_2, may be regarded as preferentially complexing HREE rather than MREE or LREE.

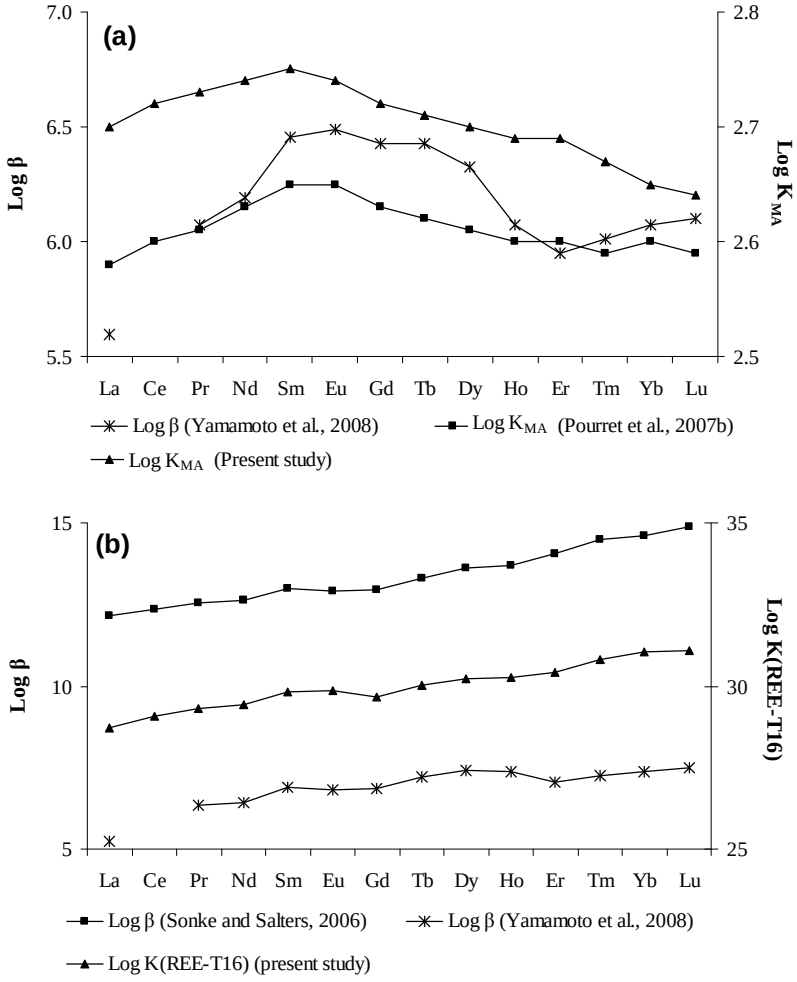

Figure II.5. REE patterns for apparent REE-HA binding constant obtained from (a) high REE/C experiments (weak sites) and (b) low REE/C experiments (strong sites). Data source: this study for log K_{MA} and log K(REE-T16) (log K Model VI strongest site: 0.9% of T16 site); Sonke and Salters (2006) (Leonardite coal HA; pH = 7); Pourret et al. (2007b) (Aldrich HA); Yamamoto et al. (2010) (Suwannee River HA; pH = 4.7).

In Figure II.5a, the optimized log K_{MA} values were compared with the log K_{MA} values reported earlier by Pourret et al. (2007b), as well as with the conditional stability constants (log β) published by Yamamoto et al. (2010). Both published datasets were computed from high metal loading experiments ($3x10^{-3}$<REE/C<$3x10^{-2}$) in which the REE behaviour should be determined by the weak sites. This comparison is interesting since the three datasets were

obtained using different experimental techniques, namely: ultrafiltration in the present study and Pourret et al.'s datasets (2007b), as against solvent extraction for the dataset reported by Yamamoto et al. (2010). Quite clearly, the three data sets exhibit similar patterns, characterized by a strong MREE downward concavity. The apparent decrease of the optimized log K_{MA} from Dy to Lu is a consequence of the high ΔLK_2 values introduced into Model VI to accurately describe REE binding by HA. Optimized ΔLK_2 values computed from the new experimental data are not only different for each REE (varying from 1.1 to 2.1), but also much higher than the common value of 0.29 adopted by users of Model VI (i.e. Pourret et al., 2007b; Yamamoto et al., 2010).

In Figure II.5b, log K pattern of the REE-HA strongest, but less abundant, site occurring in Model VI (i.e. 0.9% of T16 site, whose log K is increased by 3 x ΔLK_2 in Tipping, 1998), noted log K(REE-T16), is compared to that of log β reported by Sonke and Salters (2006) and Yamamoto et al. (2010) for low metal loading experiments. All patterns are characterized by a continuous increase from La to Lu. This similarity is considered as confirming that the ΔLK_2 values computed here can be used to model the role of strong sites controlling REE binding at low REE/C.

4.2. Impact of ΔLK_2 values on modelling results at high to low REE/C

To obtain further insight into the influence of the ΔLK_2 parameter in calculating REE complexation by HA using Model VI, modelling calculations were performed at REE/C lower than present experimental ratios, using (i) the low and common ΔLK_2 value of 0.29 proposed by Tipping (1998) for each REE (simulation 1), and (ii) the optimized ΔLK_2 (simulation 2). In these simulations, the HA concentration, the pH and the ionic strength of the solution are kept constant and equal to 10 mg L^{-1}, 3, and 10^{-2} M NaCl, respectively. Rare earth element concentration ranges from 10^{-5} to 10^{-12} M. These simulations were carried out to determine quantitatively the bias introduced under low REE/C ratio conditions by using the ΔLK_2 value of 0.29. Moreover, this approach is also a way of emphasizing and quantifying the role of strong binding sites in controlling REE binding with HA at low to high REE/C ratio. The common use of the ΔLK_2 value of 0.29 leads to a large underestimation of REE bound to HA when the REE/C becomes lower than ca. 10^{-4}, as compared to the predictions performed with the optimized ΔLK_2 values. For La, the underestimation ranges from ca. 0.4 log units for REE/C of ca. 10^{-4} up to ca 1.5 for REE/C of ca. 10^{-7}. The underestimation is even higher for Lu: from ca. 1 log unit for REE/C of ca. 10^{-4} up to ca. 3.5 for REE/C of ca. 10^{-7}. The higher

underestimation obtained for Lu is consistent with the fact that the optimized ΔLK_2 values, which must be introduced in Model VI to account for the strong REE-binding sites, are much higher for Lu (2.1) than for La (1.1). In agreement with this behaviour, and as illustrated in Figure II.6, the use of a low and constant ΔLK_2 value of 0.29 as proposed by Tipping (1998) would lead to an underestimation of the fraction of the REE bound to HA under low REE/C conditions. More importantly, ΔLK_2 values of 0.29 would also produce a biased $\log K_d^{REE}$ pattern that remains concave whatever the metal loading.

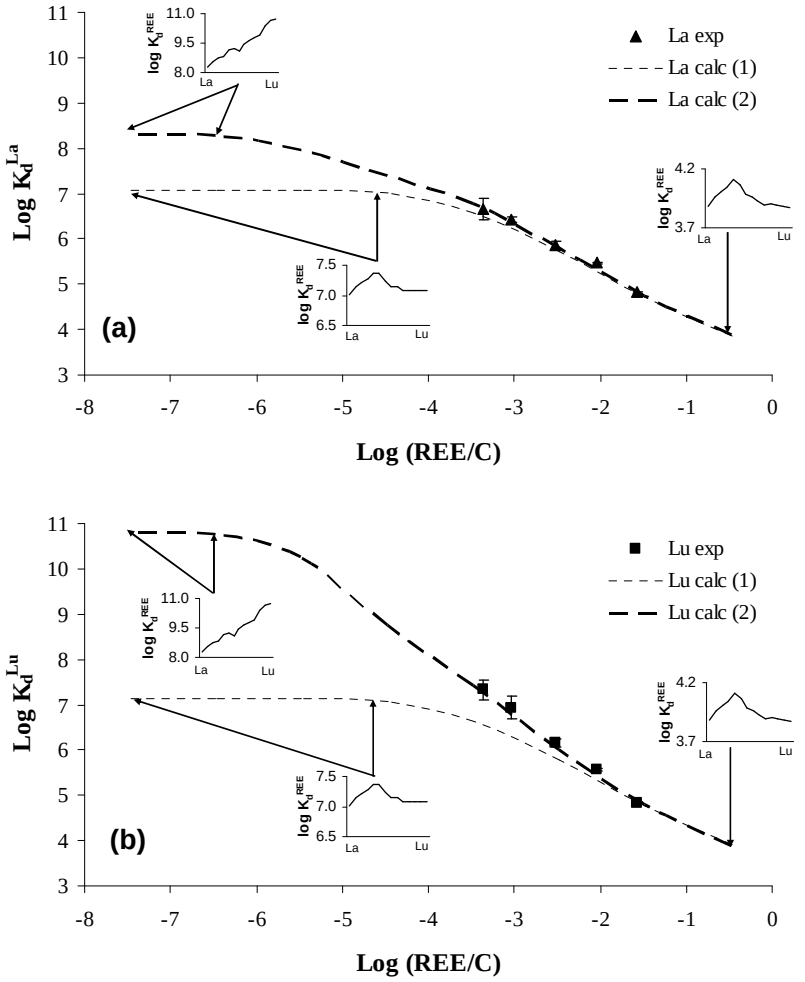

Figure II.6. Variation of (a) log K_d^{La} and (b) log K_d^{Lu} relative to the log (REE/C), on a large range of metal loading. Comparison of Model VI prediction with (1) ΔLK_2 = 0.29 (dashed line) and (2) with the optimized ΔLK_2 (bold dashed line). Symbols represent experimental data. Error bars correspond to standard deviation of triplicates.

4.3. Nature of the binding sites

Previous studies have shown that the downward concavity of log K_{MA} or/and log K_d^{REE} patterns obtained from high REE/C experiments is also apparent in the patterns for

simple organic compounds possessing carboxylic functional groups such as acetic acid (Fig. II.7a; Yamamoto et al., 2005, and Pourret et al., 2007b). As stated above, the weak sites that control the binding of REE to humic substances at high REE/C are likely to be carboxylic functional groups, a hypothesis supported by the C 1s-NEXAFS analyses of saturated Eu-HA complexes published by Plaschke et al. (2004). This implies that simple organic compounds having carboxylic functional groups such as acetate (e.g. Byrne and Li, 1995) can be regarded as analogues of these weak sites.

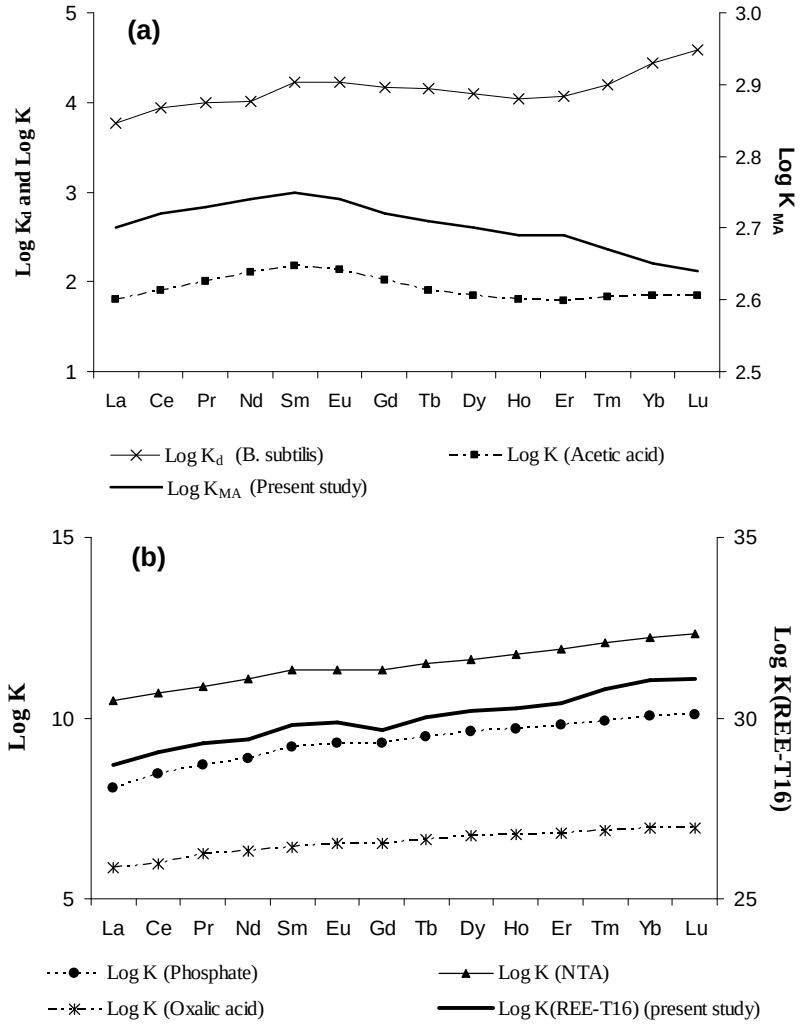

Figure II.7. REE patterns comparing the Log K_{MA} obtained in this study and log K published for acetic acid and bacteria cells (*Bacillus Subtillis*) (a), as well log K(REE-T16), log K Model VI strongest site (0.9% of T16 site);(this study) and log K of NTA, oxalic acid and phosphate complexes (b). Data source: this study, Byrne and Li (1995); Schijf and Byrne (2001); Takahashi et al. (2007).

A similar comparative approach may provide information about the nature of the strong sites. High-affinity sites in HA are generally thought to comprise phenolic functions

and/or multi-dentate carboxylic (Takahashi et al., 1997; Stern et al., 2007; Pourret and Martinez, 2009). Amine sites are known to be involved in the complexation of Am (III) and Cu (II) by HA (Peters et al., 2001; Wu and Tanoue, 2001), so they could be also involved in strong binding sites. Due to the high pKa of HA phenolic sites (around 9; Ritchie and Perdue, 2003), it is unlikely that strong sites correspond to phenolic sites given the low pH value (pH = 3) of the present experiments. Stability constant patterns of REE-phosphate, REE-oxalic acid and REE-NTA complexes exhibit the same lanthanide contraction effect as the log K of the REE-HA strongest sites occurring in Model VI (REE-T16) complexes (Byrne and Sholkovitz, 1996; Schijf and Byrne, 2001; Takahashi et al., 2007; Fig. II.7b). Rare earth element binding to oxalic acid and NTA occurs either through multicarboxylic sites or multicarboxylic N-containing sites. Given the similarity of the stability constant patterns, the strong sites that control REE binding at low REE/C might be similar to simple multicarboxylic sites, or multicarboxylic sites containing amino or, possibly, phosphate binding groups.

Finally, the new log K_{MA} and log K (REE-T16) patterns were also compared with patterns of REE binding to bacteria cells (*B. Subtilis*; Takahashi et al., 2007; see Fig. II.7a). These patterns are interesting because they combine the binding features of the strong and weak sites of HA, namely a relative enrichment of the HREE and a middle downward concavity of the MREE. As observed in the present study, Takahashi et al. (2007) found that, with decreased metal loading, the log K_d^{REE} between the bacteria suspension and the experimental solution increased more strongly than the log K_d^{REE} (Fig. II.1, and Fig. 2 in Takahashi et al., 2007). More recently, Takahashi et al. (2008) demonstrated that the binding of the LREE and of the HREE at the surface of bacteria involved two types of sites: monodentate phosphate sites for the LREE and multidentate phosphate sites (alkylphosphates) for the HREE. Although bacteria cells cannot be compared to HA, it is a striking observation that similar variations in metal loading led to similar changes in REE binding capacity and a similar fractionation of REE distribution patterns.

To conclude, this literature review suggests that the few strong sites activated at low REE/C in REE binding with HA could be multidentate carboxylic sites, or perhaps N-, or P-functional groups. The identification of the exact nature of these sites clearly remains a challenging issue. To solve this problem, further detailed high-resolution spectroscopic investigations of REE-HA complexes involving, for example, EXAFS studies are required.

4.4. Is there any evidence for a metal loading effect in natural organic-rich waters?

There is now ample evidence that humic substances (HS) control REE speciation in natural organic-rich waters (Bidoglio et al., 1991; Takahashi et al., 1997; Glaus et al., 1995; Viers et al., 1997; Dia et al., 2000; Glaus et al., 2000; Gruau et al., 2004; Johannesson et al., 2004; Davranche et al., 2005; Yamamoto et al., 2005; 2006; 2010; Sonke and Salters, 2006; Pourret et al., 2007a, b; Stern et al., 2007; Davranche et al., 2008; Pédrot et al., 2008; Yamamoto et al., 2010). Speciation studies show that nearly 100% of the REE occur as organic complexes in such waters (Viers et al. 1997, Dia et al., 2000; Tang and Johannesson, 2003; Gruau et al., 2004; Johannesson et al., 2004; Pourret et al., 2007b; Pédrot et al., 2008). Yet, REE patterns are highly variable in these waters. As shown on Figure II.8, which presents a compilation of REE data for <0.2µm filtered organic-rich waters, log $(La/Sm)_{UCC}$ and log $(Gd/Yb)_{UCC}$ values vary by ca. 0.5 and 0.8 log units in such waters, respectively, reflecting strong fractionation of the REE patterns. All the waters compiled in Figure II.8 have DOC concentrations >5 mg L^{-1}, and pH values in the range 4 to 7. This implies that the REE pattern in these waters must be controlled, at least in part, by the binding affinities of the organic molecules REE binding sites. Given the results presented in this study, we are led to pose the following question: could the variation in REE pattern displayed by natural organic-rich waters be due to the metal loading effect?

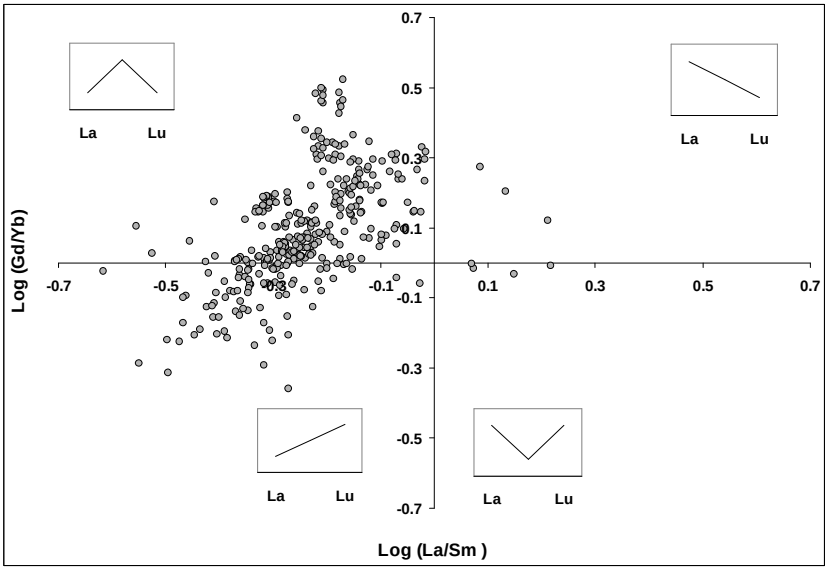

Figure II.8. Literature compilation of log $(Gd/Yb)_{UCC}$ versus log $(La/Sm)_{UCC}$, illustrating coherent variations of REE pattern, in natural organic-rich river- and soil-waters. The REE patterns indicate the types of REE pattern specific to each corner of the diagram. Data sources: Dia et al. (2000), Viers et al. (2000), Gaillardet et al. (2004), Gruau et al. (2004), Tosiani et al. (2004), Auterives (2007).

Addressing this question is not a trivial task because of the pH dependence of the metal loading effect, and the chemical composition variability of these waters. Nevertheless, we can note the following two features which allow us to consider this possibility. Figure II.8 presents a compilation of 350 samples of organic-rich, river-, and soil-waters. Besides the strong variability of the REE pattern, Figure II.8 shows that organic-rich waters are not randomly distributed when plotted in a log $(La/Sm)_{UCC}$ versus log $(Gd/Yb)_{UCC}$ diagram. Indeed, the data points are almost entirely restricted to the upper and lower left-hand corners of the diagram, illustrating that REE patterns in organic-rich waters range from patterns showing a MREE downward concavity to patterns showing a continuous enrichment from La to Lu. Only a very small number of waters (7 out of a total of 350) display patterns exhibiting a continuous enrichment from Lu to La, or showing a MREE upward concavity. This non-random distribution of REE patterns in organic-rich waters was already pointed out by Pourret et al. (2007b), although based on a compilation pooling a far more limited number of waters (Fig. 6 in Pourret et al., 2007b). Figures II.9a and II.9b plotting log $(La/Sm)_{UCC}$ and log $(Gd/Yb)_{UCC}$ against log (REE/C), respectively, display both log $(La/Sm)_{UCC}$ and log $(Gd/Yb)_{UCC}$ decrease with decreasing metal loading, which is consistent with the present experimental results, HREE-HS and MREE-HS binding being favoured at low and high metal loading, respectively. Therefore, natural waters with low REE/C should exhibit an HREE-enriched REE pattern, by contrast to high REE/C waters which should display a MREE-

enriched REE pattern. The dispersion of data observed in Figures II.8 and II.9 may be attributed to two major uncertainties. (i) The metal loading should be expressed as log (M/C) where M represents the sum of the dissolved cations that compete with REE for HS surface sites. However, because metallic nano-oxides (Fe or Al) may be included in the <0.2 μm water fraction, (e.g. Pokrovsky et al. 2006; Pédrot et al., 2009), log (M/C) could be overestimated. By contrast, published chemical water compositions often lack the entire cation content, which consequence could be an underestimation of the log (M/C). (ii) REE distribution may also be strongly influenced by the surface functional group heterogeneity and density of the different HS types. Although these uncertainties, REE distributions in Figures II.8 and II.9 do correspond to the expected distributions if the REE pattern shape prevailing in organic-rich waters is controlled by a metal loading effect.

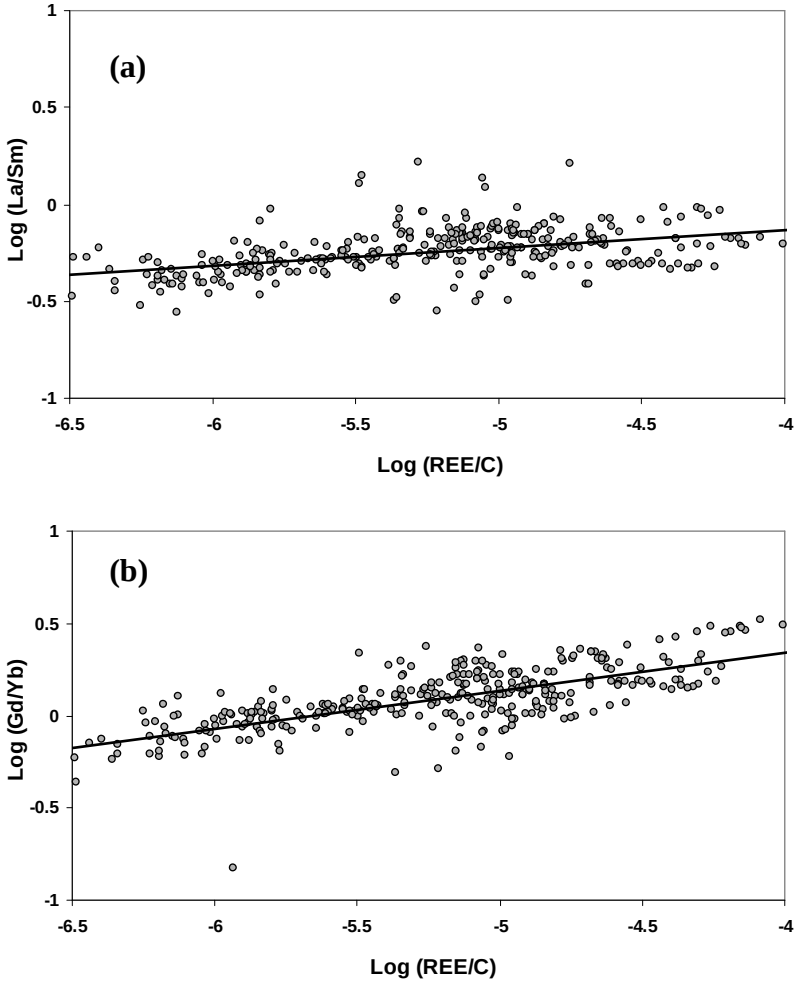

Figure II.9. (a) Log $(La/Sm)_{UCC}$ and (b) log $(Gd/Yb)_{UCC}$ versus log REE/C for the data compiled in Figure II.8. Solid line represents the linear relationship.

Thus, the special fractionation of REE patterns in natural organic-rich waters suggests that the metal loading effect could be the cause of the marked variability of REE patterns that characterize these systems. As a whole, the present investigation, when combined with results from previous studies by Yamamoto et al. (2005; 2010), Sonke and Salters (2006), Stern et al. (2007) and Pourret et al. (2007b) demonstrates that: (i) HA binding site heterogeneity (strong and weak sites) directly influences the REE complexation patterns, and (ii) this latter point may be explained by a loading effect: at low metal loading, stronger sites are favoured yielding HREE-enriched REE patterns, whereas, at high metal loading, the more abundant weaker sites dominate complexation leading to REE patterns with MREE downward concavity.

5. Summary

The effect of metal loading on the binding of the rare earth elements (REE) to humic acid (HA) was studied by combining ultrafiltration and Inductively Coupled Plasma Mass Spectrometry techniques. REE-HA binding experiments were performed at pH 3 for REE/C ranging from ca $4x10^{-4}$ to $2.7x10^{-2}$, using a standard batch equilibration method. Results show that the relative amount of REE bound to HA strongly increases with decreasing REE/C. Moreover, a middle-REE (MREE) downward concavity is displayed by $\log K_d^{REE}$ patterns at high metal loading, whereas patterns at low metal loading exhibit a regular increase from La to Lu. These results demonstrate that the variability of REE-HA binding patterns published so far (Yamamoto et al., 2005; 2006; 2010; Sonke and Salters, 2006; Pourret et al., 2007b; Stern et al., 2007) is not an artefact resulting from the use of different analytical procedures. The variability of patterns is real, reflecting the presence of two types of sites in HA surface, each occurring in markedly distinct proportions and each having different binding affinities for the REE. The resulting metal loading effect explains the variation of $\log K_d^{REE}$ patterns with changing REE/C.

Calculations performed using Model VI show that the two types of sites involved in the binding of REE with HA can be defined by the Model VI intrinsic log K_{MA} and ΔLK_2 parameters, ΔLK_2 parameter being free to vary among the REE series. Optimization of both parameters provides evidence that high density but weak sites determine the distribution of REE to HA at high REE/C, favouring the complexation of the MREE. By contrast, the few strong sites determine the distribution of REE to HA at low REE/C, favouring the HREE complexation. A literature review suggests that the few strong sites activated at low REE/C

could be multidentate carboxylic sites, or perhaps N-, or P-functional groups, whereas the weak sites involved at high metal loading are likely to be monodendate carboxylic sites. Application of Model VI to the experimental data shows that this model closely reproduces the observed variations. Hence, this model is a very powerful tool for studying and taking into account the loading effect that controls REE binding by HA.

Finally, confronting the variability of REE patterns in natural organic-rich waters and their metal loading level, expressed as REE/C, shows that the loading effect discussed here could explain part of the shape variability of REE patterns observed in these waters. Overall, our results suggest that further factors, such as competitive cations and/or colloidal nano-oxides, should be considered to improve the metal loading effect accuracy. Also the variability of humic substances chemical composition should be considered to explain the diversity of the binding sites that may be involved in REE complexation mediated by organic matter. These other factors should be taken into account to model and thus better understand REE cycling and transport in natural systems. Once again, Model VI may provide a reliable and powerful tool for this purpose.

III. Chapitre II :

Modélisation des interactions entre terres rares et acides humiques

An improved description of the interactions between rare earth elements and humic acids by modeling: PHREEQC-Model VI coupling

Cette partie est extraite de Geochimica et Cosmochimica Acta, Marsac R., Davranche M., Gruau G., Bouhnik-Le Coz M. and Dia A. (2011) An improved description of the interactions between rare earth elements and humic acids by modeling: PHREEQC-Model VI coupling (In press).

Résumé- Le modèle de complexation des ions par les substances humiques Model VI - utilisé précédemment pour modéliser les équilibre de complexation des terres rares (REE) par les acides humiques (HA) - a été modifié afin de tenir compte des différences de spectres de complexation des REE entre les groupements carboxyliques et phénoliques des HA. Les modifications apportées améliorent significativement les résultats de modélisation. Elles permettent, pour la première fois, de reproduire de manière satisfaisante un large jeu de données expérimentales de complexation de l'ensemble des REE par HA avec les mêmes paramètres et équations. L'utilisation de PHREEQC montre que les REE légères (LREE) et lourdes (HREE) ne se complexent pas aux mêmes groupements fonctionnels des HA. Les LREE se lient préférentiellement à des groupements carboxyliques tandis que les HREE se lient préférentiellement à des groupements carboxy-phénoliques et phénoliques. Cette différence de comportement entre LREE et HREE pourrait induire un fractionnement des REE lorsqu'elles sont en compétition avec d'autres cations pour la complexation par les sites des HA. L'étude des données disponibles de complexation entre cations et ligands organiques suggère que Al^{3+} pourrait limiter la complexation des HREE par les HA. Ce nouveau modèle devrait améliorer la modélisation hydrochimique des REE puisque PHREEQC tient compte d'un grand nombre de réactions chimiques telles que les équilibres de dissolution/précipitation de minéraux et les réactions d'oxydo-réduction mais peut aussi modéliser les cinétiques de réaction et du transport à une dimension.

Abstract- The Humic Ion Binding Model VI (Model VI) - previously used to model the equilibrium binding of rare earth elements (REE) by humic acid (HA) - was modified to account for differences in the REE constant patterns of the HA carboxylic and phenolic groups, and introduced into PHREEQC to calculate the REE speciation on the HA binding sites. The modifications were shown to greatly improve the modeling. They allow for the first time to both satisfactorily and simultaneously model a large set of multi-REE experimental data with the same set of equations and parameters. The use of PHREEQC shows that the light rare earth elements (LREE) and heavy rare earth elements (HREE) do not bind to HA by the same functional groups. The LREE are preferentially bound to carboxylic groups, whereas the HREE are preferentially bound to carboxy-phenolic and phenolic groups. This binding differentiation might lead to a fractionation of REE-HA patterns when competition between REE and other metals occur during complexation. A survey of the available data shows that competition with Al^{3+} could lead to the development of HREE-depleted HA patterns. This new model should improve the hydrochemical modeling of the REE since PHREEQC takes

into account chemical reactions such as mineral dissolution/precipitation equilibrium and redox reactions, but also models kinetically controlled reactions and one-dimensional transport.

1. Introduction

Dissolved humic acids (HA) are complex macro-molecules that contain a large variety of functional groups giving rise to strong binding capacities with cations. Because of HA ubiquity, a lot of effort has been made in the past 20 years to set up thermodynamic models that are suitable for predicting cation complexation by HA in natural waters (Marinsky and Ephraim, 1986; Tipping and Hurley, 1992; Koopal et al., 1994; Kim and Czerwinski, 1996; Tipping, 1998; Sasaki et al., 2008). The two major types of HA-cation binding surface groups are the carboxylic and phenolic groups. Each type covers a large range of cation stability constants (log K). The two most used cation-HA binding models are Model VI (Tipping, 1998), in which both the carboxylic and phenolic groups are discrete entities displaying specific stability constants, and NICA-Donnan (Kinniburgh et al., 1996), in which continuous distributions of log K are considered. In both models, the variety of the HA binding sites is taken into account, as the log K distribution is calculated from the cation-carboxylic and cation-phenolic specific binding parameters. By fitting the datasets for each of these two models, Tipping (1998) and Milne et al. (2003) were able to determine the generic HA binding parameters for a wide variety of cations. They found that cation-phenolic model parameters can be mathematically correlated to cation-carboxylic parameters. These mathematical correlations are very useful to estimate phenolic binding parameters from carboxylic binding parameters, notably when experimental data are limited or non-existent. For Model VI, Tipping (1998) chose to impose a linear relationship between the carboxylic and phenolic cation binding parameters (log K_{MA} and log K_{MB}, respectively). Thus, only one parameter has to be adjusted in order to describe the interaction of cations with humic acids using Model VI, i.e. Log K_{MA}.

Rare earth elements (REE) are a highly coherent series of elements, whose chemical properties vary regularly along the series. Their relative affinity for ligands can be visualized in the plot of the intrinsic stability constants (log K) or the partition coefficient between two phases (log K_d) versus the REE atomic number. Different and specific shapes of log K patterns are therefore displayed depending on the ligands (Byrne and Li, 1995). Moreover, the REE are particularly suitable to study cation-HA interactions. Experimental and field studies showed that when HAs are present in natural waters, most of the REE occur as REE-HA

complexes (Bidoglio et al., 1991; Takahashi et al., 1997; Viers et al., 1997; Dia et al., 2000; Tang and Johannesson, 2003; Johannesson et al., 2004; Gruau et al., 2004; Davranche et al., 2005; Sonke and Salters 2006; Pourret et al., 2007a, b; Pédrot et al., 2008). Recent experimental studies on REE-HA binding have shown that the metal loading (REE/HA) can modify the REE partitioning between an aqueous solution and HA (Marsac et al., 2010; Yamamoto et al., 2010). At high loading, a middle-REE (MREE) downward concavity, typical of REE binding to low affinity carboxylic sites, was observed. However, under low REE/HA conditions, the log K_d pattern exhibited a regular increase from La to Lu, which is typical of REE binding to strong affinity multidentate sites (Marsac et al., 2010; Yamamoto et al., 2010). These two types of log K_d patterns correspond to the log K patterns obtained for the corresponding simple organic ligands (namely acetic acid for the carboxylic sites, and EDTA for the multidentate sites). Their successive occurrence is plausible since the site density of the HA high affinity sites is much lower than the density of the low affinity sites. Marsac et al. (2010) showed that in order to properly model this data with Model VI, it was necessary to let the parameter accounting for the high affinity sites, ΔLK_2, vary among the REE series instead of keeping it constant, as commonly assumed. However, although there is a good agreement between the experimental and modeled data, the HA sites defined in Model VI are still not fully satisfactory for the REE series. The assumption of a similar log K pattern shape for the carboxylic and phenolic sites, imposed by the Log K_{MA}-Log K_{MB} linear relationship, is not consistent with the log K pattern observed for the REE-catechol complex - an analog of phenol - which exhibits a regular increase in heavy-REE (HREE) log K values (IUPAC, Stability Constants Database). Because phenolic sites have a lower acidic constant (K_a) than carboxylic sites and occur in lower density (Ritchie and Perdue, 2003), their log K pattern could theoretically be directly determined by performing REE-HA binding experiments at pH > 7 and low REE/HA ratios. However, these kinds of experiments are technically hard to perform with regard to the low aqueous REE concentration imposed by the pH values. Marsac et al. (2010) and Yamamoto et al. (2010) therefore carried out their experimental studies at a low pH (3 and 4.7, respectively) in order to be able to measure the REE aqueous concentration at low REE/HA ratios. Pourret et al. (2007b) explored higher pH values (up to 10.5), but the high imposed REE/HA ratio prevented the study of the phenolic log K patterns. This problem might be circumvented by studying REE-HA binding through competition ligand experiments with EDTA, as previously done by Sonke and Salters (2006). However, as stated by Yamamoto et al. (2010), the increasing log K(REE-EDTA) values from La to Lu implies that each REE binding is not studied at the same metal loading, thereby

preventing the comparison of the log K patterns with the patterns for the conditional stability constants.

In this study, a modeling approach was used to evaluate whether the HA phenolic sites differ from the HA carboxylic sites in their ability to complex REE. The stability constants of the REE-HA phenolic sites were thus independently estimated. For this purpose, Model VI equations were introduced into PHREEQC (Parkhurst and Appelo, 1999), following Liu et al. (2008). The PHREEQC/Model VI model was then used to fit the HA-REE binding datasets published by Sonke and Salters (2006), Pourret et al. (2007b) and Marsac et al. (2010).

2. Materials and methods

2.1. Humic Ion binding Model VI

The humic-ion binding Model VI was developed by Tipping (1998) and introduced into the WHAM 6 program. A thorough description of Model VI can be found in Tipping (1998). The model is a discrete binding site model which takes electrostatic interactions into account. Eight sites are considered and divided into an equal number of type A sites (the weak acidic sites, commonly associated with carboxylic functional groups) and type B sites (the strong acidic sites, commonly associated with phenolic functional groups). There are n_A (mol g^{-1}) type A sites and $n_A/2$ type B sites. Proton binding is described by the two median intrinsic constants (pK_A or pK_B) and two parameters defining the spread of the equilibrium constants around the median (ΔpK_A or ΔpK_B). The intrinsic equilibrium constants for cation binding are defined by two median constants (log K_{MA} and log K_{MB}), together with parameters (ΔLK_{1A} and ΔLK_{1B}) that define the spread of the values around the medians. By considering the results from many datasets, a universal average value of ΔLK_1 was obtained for all cations (2.8) and a linear relationship was established between the log K_{MB} and log K_{MA} parameters (Tipping, 1998):

$$\log K_{MB} = 3.39 \times \log K_{MA} - 1.15 \qquad \text{(III.1)}$$

Therefore, only one single adjustable parameter (log K_{MA}) is necessary to describe metal complexation by HA in Model VI. In Model VI, cations first hydrolysis products (e.g. $LaOH^{2+}$) are also considered to bind to HA with the same parameters than the corresponding aquo ions.

Some of the type A and type B monodentate sites can form bi- and tridentate sites. The stability constants of these bi- and tridentate sites are defined by the sum of the log K values

of the monodentate sites of which they are constituted. Cation-HA binding can occur through carboxylic groups (CG), carboxy-phenolic groups (CPG) or phenolic groups (PG). A small part of the stability constants of multidentate groups are increased by the ΔLK_2 parameter, the so-called "strong binding site term" (Tipping, 1998). ΔLK_2 is attributed to both favorable spatial arrangements of the ligands, which stabilizes the complex, and to the chelate effect or participation of ligands, such as the nitrogen-containing groups. ΔLK_2 is the parameter of the HA site heterogeneity. An elevation of ΔLK_2 increases the range of the stability constants covered by the HA sites, thus increasing the heterogeneity of the HA sites. The total heterogeneity of the HA surface sites in Model VI is defined by 80 different sites.

An electrical double layer, where only counter-ions can accumulate, is defined. The double layer thickness is set by the Debye-Hückel parameter κ. The distribution of ions between the diffuse layer and the bulk solution is calculated by a simple Donnan model. The Donnan volume (V_D) is the volume adjacent to the surface. The electrostatic correction is represented by an empirical equation which mimics the Boltzmann factor:

$$\text{Exp}\ (-zF\psi/RT) = \exp\ (-2PzZ\ \log_{10}I) \qquad \text{(III.2)}$$

where P is an adjustable parameter, z is the ion charge, Z is the net humic acid charge (eq/g), I is the ionic strength (mol L^{-1}), ψ is the surface potential (V), T is the temperature (K), F is the Faraday constant and R is the gas constant. The Model VI parameters used in the present study are summarized in Table III.1.

Parameter	Description	Values
n_A	Amount of type A sites (mol g^{-1})	3.3 10-3
n_B	Amount of type B sites (mol g^{-1})	0.5 x n_A
pK_A	Intrinsic proton dissociation constant for type A sites	4.1
pK_B	Intrinsic proton dissociation constant for type B sites	8.8
ΔpK_A	Distribution term that modifies pK_A	2.1
ΔpK_B	Distribution term that modifies pK_B	3.6
log K_{MA}	Intrinsic equilibrium constant for metal binding at type A sites	Fitted from experimental data
log K_{MB}	Intrinsic equilibrium constant for metal binding at type B sites	Fitted from experimental data
ΔLK_1	Distribution term that modifies log K_{MA} and log K_{MB}	2.8
ΔLK_2	Distribution term that modifies the strengths of bidentate and tridentate sites	Fitted from experimental data
SA	HA surface area ($m^2\ g^{-1}$)	Fitted from WHAM 6/Model VI simulations
κ	Debye-Hückel parameter (m)	$(3.29 \times 109 \times I^{1/2})^{-1}$

Table III.1. Parameters used in this study to model REE binding by humic acid.

2.2. PHREEQC/Model VI coupling

PHREEQC is based on an ion-association aqueous model and was designed to perform speciation and saturation-index calculations (Parkhurst and Appelo 1999). The cation-HA binding reaction with the 80 types of HA sites defined in Model VI was written and introduced into the PHREEQC "minteq.v4" database. Before removing the constraint imposed by the linear relationship between log K_{MA} and log K_{MB}, a first version of PHREEQC/Model VI using the equations defined in WHAM 6/Model VI was tested for its ability to give identical results to WHAM 6/Model VI. Humic acid was defined as the SOLUTION_MASTER_SPECIES, SOLUTION_SPECIES and PHASES in the "minteq.v4" database. The 80 types of sites considered by Model VI were defined as the SURFACE_MASTER_SPECIES, and their respective stability constants as the SURFACE_SPECIES in the "minteq.v4" database. This procedure is similar to that used previously by Liu et al. (2008) to model the binding of Eu by HA in clay pore water using the same PHREEQC-Model VI combination, except that in this study, we used ΔLK_2 values $\neq 0$. Therefore, the 80 binding sites defined by Tipping (1998) are taken into account versus only 32 sites in Liu et al. (2008). In order to model similar REE binding by each specific HA sites with WHAM 6/Model VI and PHREEQC/Model VI, REE-HA binding simulations were compared with the corresponding REE-simple ligands complexes in solution. The results obtained differed between both models. The ΔLK_1 parameter (=2.8) should actually be defined as $\Delta pK_A - \Delta LK_{1A}$, for carboxylic groups, and as $\Delta pK_B - \Delta LK_{1B}$, for phenolic groups (i.e. $\Delta LK_{1A} = -0.7$ and $\Delta LK_{1B} = 0.8$). In order to model the non-specific binding in a similar fashion (i.e. ions accumulated around HA molecules by electrostatic attraction) as well as the electrostatic correction in WHAM 6/Model VI and PHREEQC/Model VI, the Gouy-Chapman type double layer defined in PHREEQC was coupled with a Donnan phase, excluding the presence of co-ions. The Debye-Hückel parameter κ was calculated from the relationship: $\kappa = (3.29 \times 10^9 \times I^{1/2})^{-1}$ (Appelo and Postma, 2005). In PHREEQC, the surface area (SA), upon which the Boltzmann factor depends, is an adjustable parameter. Marsac et al. (2010) determined Model VI REE-HA specific binding parameter with P = -330. To satisfy equation III.2, the PHREEQC SA was simply determined by fitting the HA surface charge (Q_{WHAM} in eq g^{-1}) generated by WHAM 6/Model VI as a function of pH, at varied NaCl concentrations and 10 mg of HA. The best fit was obtained for a SA equal to 40000, 19000 and 13000 $m^2\ g^{-1}$ at an ionic strength 0.001, 0.01 and 0.1, respectively. By this method we found $Q_{PHREEQC} = 0.92 \times Q_{WHAM} + 3\ 10^{-4}$ ($R^2 = 1$). Since SA decreases with P, our results are consistent with

those of Liu et al. (2008) who determined SA = 30000 m^2 g^{-1} at an ionic strength of 0.015 mol L^{-1} and P = -120.

2.3. Experimental data

Three datasets were used to calibrate the PHREEQC/Model VI parameters for REE binding to HA (Sonke and Salters, 2006; Pourret et al., 2007b; Marsac et al., 2010). These datasets were preferentially chosen because they provide data for the entire REE group and they covered a large range of pHs, metal loading and organic ligand competition. The experimental conditions of the three datasets used are given below.

2.3.1. Pourret et al's. dataset (2007b)

Pourret et al. (2007b) performed REE-HA binding experiments for the 14 REE simultaneously over pHs ranging from 2 to 10.5 at an ionic strength (IS) of 10^{-3} M. The HA used was purified Aldrich Humic Acid. The experiments were performed with 50 ppb of each REE at three HA concentrations: 5, 10 and 20 mg L^{-1} ($5\ 10^{-3}$<REE/HA<$2\ 10^{-2}$ mol REE/mol C). The separation of HA from the inorganic complexes was performed by ultrafiltration. The REE concentrations were measured by Inductively Coupled Plasma Mass Spectrometry (ICP-MS). The results showed an increase in the REE-HA binding with increasing pH and increasing HA concentrations. The log K REE-HA pattern is marked by a downward, MREE concavity. These data therefore provide a dataset for REE-HA binding at high metal loading and over a large pH range where the REE are bound to HA by carboxylic or phenolic sites, depending on the pH. Note however, that the data at pH > 7 were not considered in the model calibration, since 100% of the REE were bound to HA in Pourret et al. (2007b), making the data useless for the calibration of the model.

2.3.2. Marsac et al.'s dataset (2010)

Marsac et al. (2010) used Pourret et al.'s method (2007b) to study the metal loading effect on REE binding to HA ($4\ 10^{-4}$<REE/HA<$2.7\ 10^{-2}$ mol REE/mol C). In order to obtain measurable REE concentrations in the solution, Marsac et al. (2010) performed all their experiments under acidic conditions (pH = 3). The ionic strength was fixed at 10^{-2} M. Marsac et al. (2010) observed an increase in the REE-HA binding and a change in the log K REE-HA pattern with decreasing metal loading. At high metal loading, the log K REE-HA pattern exhibited a MREE-downward concavity and at low metal loading, a regular increase from La to Lu was observed. These data therefore provide an REE-HA complexation dataset at

variable metal loading under acidic pH conditions. At pH 3 and low metal loading, the REE are bound to HA by low density strong multidentate sites, whereas at high loading, the REE are primarily bound to high density weak sites.

2.3.3. Sonke and Salters' dataset (2006)

Sonke and Salters (2006) performed REE-HA binding experiments for each REE separately. The HA used was purified Leonardite HA. These authors used EDTA as a competitive ligand of HA for the REE. The experiments were carried out at low metal loading ($2\ 10^{-4}$ mol REE/mol C), slightly acidic to basic pH (6 to 9) and an IS = 0.1 M. The separation and measurement of the EDTA-REE and HA-REE complexes were done by capillary electrophoresis coupled with ICP-MS. This study provides single REE-HA binding data for high pH and low metal loading, two conditions that cannot be obtained by the methods developed by Pourret et al. (2007b) and Marsac et al. (2010). To simulate Sonke and Salters' experiments (2006), EDTA was introduced into the PHREEQC “minteq.v4” database as the SOLUTION_MASTER_SPECIES and SOLUTION_SPECIES. The four EDTA protonation constants and the fourteen REE-EDTA stability constants for IS = 0 given in Sonke and Salters (2006) were also introduced as the SOLUTION_SPECIES.

2.4. Modeling strategy

Linear free energy relationships (LFER) are commonly used to determine the cation-HA binding parameters (Tipping, 1998). This method was used by several authors to estimate the log K_{MA} parameter in Model VI (or the previous version, Model V) in order to describe the REE-HA binding (Tang and Johannesson, 2003; Sonke, 2006; Pourret et al., 2007b). In particular, Tang and Johannesson (2003) and Pourret et al. (2007b) demonstrated that REE-HA binding could be reasonably well modeled by using the existing LFER between log K_{MA} (pK_{MA} in Model V) and log K for metal complexation by acetic acid. However, Marsac et al. (2010) demonstrated that log K_{MA} for the HREE are lower than those estimated by LFER when log K_{MA} and ΔLK_2 were optimized simultaneously. The decrease in log K_{MA} compensates for the high ΔLK_2 values obtained for the HREE. Here, the new REE log K_{MA} were optimized, thus keeping a linear relationship with log K_{MA} reported in Marsac et al. (2010). This method allows preserving the same pattern. Log $K_{MA,}$ the REE-HA carboxylic binding parameter, mainly influences the calculation of REE-HA binding at acidic to neutral pHs since the carboxylic groups have high proton dissociation constants. Therefore, the log

K_{MA} values were first optimized by fitting the "acidic" experimental data from Pourret et al. (2007b) and Marsac et al. (2010).

Log K_{MB} represents the binding parameter for the HA phenolic groups. However, no stability constants are currently available for REE complexation by phenol. Therefore, catechol was used as an analog. A linear relationship was applied between the log K values for REE-catechol (IUPAC stability constant database) and log K_{MB} in order to impose a phenolic-type pattern onto log K_{MB}. Because phenolic groups have low acidic constants (Ka), the influence of log K_{MB} on REE-HA binding is mainly observed at neutral to basic pHs. Therefore, log K_{MB} was optimized by fitting the data of Sonke and Salters (2006).

As already stated, ΔLK_2 represents the HA heterogeneity parameter or the strong binding site term of Model VI. ΔLK_2 indicates the presence of multidentate sites, whose affinity for REE increases from La to Lu (Byrne and Li, 1995; Sonke and Salters, 2006; Pourret et al., 2007b; Marsac et al., 2010). Tipping (1998) suggests that the ΔLK_2 parameter is similar for the carboxylic and phenolic multidentate sites. However, preliminary experimental data fitting, carried out during the course of this study, showed that the three datasets used to optimize the HA binding parameters could not be satisfactorily modeled, except when using different ΔLK_2 values for the carboxylic and phenolic sites. In the same way that PHREEQC/Model VI allows independent log K_{MA} and log K_{MB} optimization, it also allows different ΔLK_2 values to be ascribed to the multidentate sites depending on their composition in carboxylic (ΔLK_{2C}) or phenolic (ΔLK_{2P}) sites. Note that the strong binding site terms of the carboxylic-phenolic multidentate sites are calculated as the ΔLK_{2C} and ΔLK_{2P} weighted average, depending on the chemical composition of the sites. Because the density of the multidentate sites is low at the surface of HA, their control on REE binding occurs mainly under low metal loading conditions, and under low and high pH conditions for the carboxylic and phenolic sites, respectively. Consequently, ΔLK_{2C} optimization was first performed with Marsac et al.'s data (2010) and ΔLK_{2P} optimization with Sonke and Salters' data (2006). Both ΔLK_{2C} and ΔLK_{2P} were constrained to increase progressively from La to Lu due to a linear correlation between the new ΔLK_{2C} and ΔLK_{2P} and the ΔLK_2 previously reported by Marsac et al. (2010).

Errors between the experimental data and the calculations were quantified by the root mean square error of the regression (rmse), i.e. the sum of the squares of the differences between the observed and calculated log υ, where υ is the amount of REE bound to HA per gram of dissolved organic carbon (DOC). The fit was considered as being good when the total

rmse calculated from the whole REE and experimental conditions was low and when the rmse values for each REE were close to each other. The modeling strategy here above described shows that some of WHAM 6/Model VI constrains on parameters were suppressed only to introduce other comparable constrains. Therefore, WHAM 6/Model VI and PHREEQC/Model VI fit goodness can be compared directly with rmse since the degree of freedom does not significantly varies from a model to another.

3. Results

3.1. Modeling parameters

The new REE-HA binding parameters were obtained from the combination of PHREEQC/Model VI and the assumptions and strategy described above. They were adjusted until a reasonable fit - quantified by the rmse - was reached. The results are presented in Table III.2. In Figure III.1, they are compared with the REE-HA binding parameters obtained by Marsac et al. (2010) with WHAM 6/Model VI and the corresponding model ligands (i.e. acetic acid for log K_{MA} and catechol for log K_{MB}). The following equations for the linear relationships were used to determine the REE-HA specific binding parameters with PHREEQC/Model VI:

$$\log K_{MA} = 2.12 \times \log K_{MA}(1) - 2.44 \quad (R^2 = 0.98) \quad \text{(III.3)}$$

$$\log K_{MB} = 0.37 \times \log K(\text{REE-catechol}) + 0.86 \quad (R^2 = 0.95) \quad \text{(III.4)}$$

$$\Delta LK_{2C} = 0.26 \times \Delta LK_2(1) + 1.74 \quad (R^2 = 0.97) \quad \text{(III.5)}$$

$$\Delta LK_{2P} = 0.72 \times \Delta LK_2(1) + 3.60 \quad (R^2 = 1) \quad \text{(III.6)}$$

where log $K_{MA}(1)$ and $\Delta LK_2(1)$ refer to the log K_{MA} and ΔLK_2 values determined by Marsac et al. (2010).

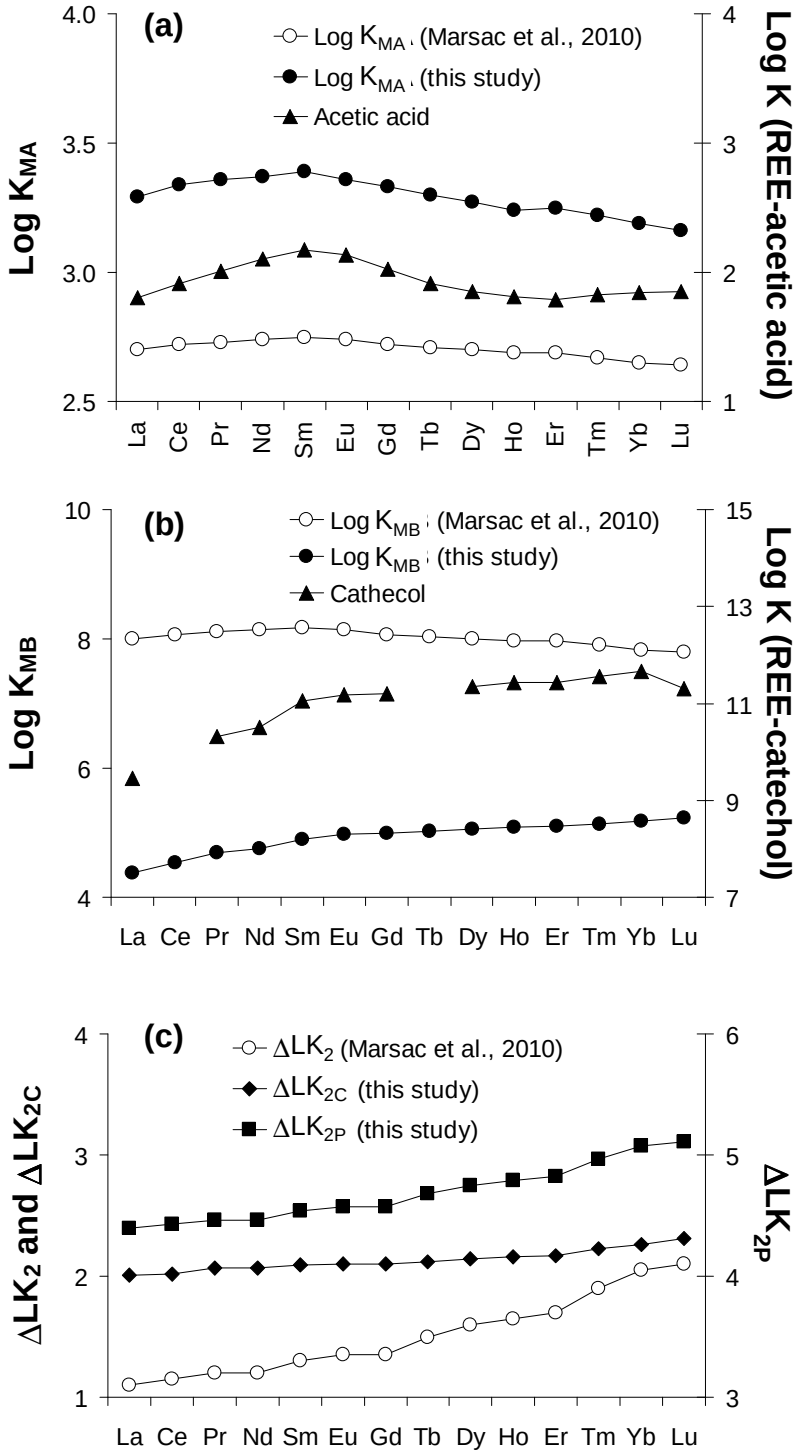

Figure III.1. Comparison of the REE patterns for the HA binding parameters obtained by Marsac et al. (2010) with WHAM 6/Model VI and the patterns obtained with PHREEQC/Model VI: (a) log K_{MA} compared with log K (REE-acetic acid), (b) log K_{MB} compared with log K(REE-catechol) and (c) ΔLK_{2C} and ΔLK_{2P} (this study) compared with ΔLK_2 (Marsac et al., 2010; $\Delta LK_2 = \Delta LK_{2C} = \Delta LK_{2P}$).

REE	log $K_{MA}^{(1)}$	log $K_{MA}^{(2)}$	log $K_{MB}^{(1)}$	log $K_{MB}^{(2)}$	$\Delta LK_2^{(1)}$	$\Delta LK_{2C}^{(2)}$	$\Delta LK_{2P}^{(2)}$	$rmse^{(1)}$	$rmse^{(2)}$
La	2.70	3.29	8.00	4.39	1.10	2.01	4.39	0.09	0.07
Ce	2.72	3.34	8.07	4.54	1.15	2.02	4.43	0.08	0.06
Pr	2.73	3.36	8.10	4.69	1.20	2.06	4.46	0.07	0.05
Nd	2.74	3.37	8.14	4.76	1.20	2.06	4.46	0.08	0.05
Sm	2.75	3.39	8.17	4.90	1.30	2.09	4.54	0.08	0.05
Eu	2.74	3.36	8.14	4.98	1.35	2.10	4.57	0.08	0.05
Gd	2.72	3.33	8.07	4.99	1.35	2.10	4.57	0.10	0.06
Tb	2.71	3.30	8.04	5.03	1.50	2.12	4.68	0.11	0.06
Dy	2.70	3.27	8.00	5.06	1.60	2.14	4.75	0.12	0.07
Ho	2.69	3.24	7.97	5.09	1.65	2.16	4.79	0.14	0.08
Er	2.69	3.25	7.97	5.09	1.70	2.17	4.82	0.15	0.09
Tm	2.67	3.22	7.90	5.14	1.90	2.22	4.97	0.15	0.09
Yb	2.65	3.19	7.83	5.18	2.05	2.26	5.08	0.15	0.10
Lu	2.64	3.16	7.80	5.23	2.10	2.31	5.11	0.16	0.10
Mean	2.70	3.29	8.02	4.93	1.51	2.13	4.69	0.11	0.07

(1) Marsac et al. (2010)
(2) This study

Table III.2. Log K_{MA}, log K_{MB}, ΔLK_{2C} and ΔLK_{2P} values fitted from the experimental data using PHREEQC/Model VI. The quality of the fit is determined by the rmse, calculated as $\sqrt{mean(\log\nu_{exp} - \log\nu_{calc})^2}$, where ν is the amount of REE bound to HA per gram of DOC for the experimental and modeled data, respectively. The log K_{MA}, log K_{MB}, ΔLK_2 (where $\Delta LK_2 = \Delta LK_{2C} = \Delta LK_{2P}$) data published by Marsac et al. (2010) using WHAM 6/Model VI are shown for comparison.

The removal of the constraint imposed by the linear relationship between log K_{MA} and log K_{MB} in WHAM6/Model VI and the use of REE-catechol binding parameters results in a significant increase of the log K_{MA} values (3.29 versus 2.7, on average, in Marsac et al. 2010). By contrast, the log K_{MB} values are greatly reduced: from 8.02 to 4.93, on average, in Marsac et al. (2010) and as reported in this study, respectively. The log K_{MB} values produced independently with PHREEQC/Model VI are very different from the log K_{MB} values calculated with the log K_{MB}-log K_{MA} linear correlation established by Tipping (1998) in WHAM6/Model VI (Eq. III.1). The present log K_{MA} and log K_{MB} are not related to each other by a linear correlation, but their relative order of magnitude order is preserved, log K_{MB} > log K_{MA}. Tipping (1998) obtained values of log K_{MA}(Eu) = 3.09 and log K_{MB}(Eu) = 5.33, when they independently optimized the log K_{MA} and log K_{MB} values for Eu during the construction of Model VI. These values are close to the values obtained here in this study: log K_{MA}(Eu) = 3.36 and log K_{MB}(Eu) = 4.98; (Table III.2). The ΔLK_{2C} and ΔLK_{2P} values obtained here are higher than the ΔLK_2 values reported in Marsac et al. (2010) (denoted as ΔLK_2(1) in Table III.2) for all REE. Hence, HA appears more heterogeneous with respect to REE binding when the constraint of a single ΔLK_2 value is deleted. The ΔLK_{2C} and ΔLK_{2P} patterns also differ

from the ΔLK_2 patterns given in Marsac et al. (2010). The major change concerns the ΔLK_{2C} pattern which presents a lower increase for HREE than Marsac et al. (2010) ΔLK_2 (Fig. III.1c). This lower increase for HREE is the consequence of both the introduction of REE-phenolic site binding constants that increase from La to Lu, and the propagation of this increase to the phenolic containing-multidentate site binding constants. As a result, the strong multi-phenolic sites, which depend on ΔLK_{2P}, are no longer constrained to accommodate so much HREE, which explains why the increase in ΔLK_{2P} for HREE is less pronounced as compared to ΔLK_2 presented in Marsac et al. (2010) (Fig. III.2c).

In Model VI, the ΔLK_2 are thought to depend on either the geometry of the carboxylic and phenolic multidentate sites (ΔLK_2 accounts for favorable arrangement of the spatial ligands that stabilize REE complexes), or the involvement of additional groups, notably nitrogen-containing groups (Tipping, 1998). Tipping (1998) suggested that ΔLK_2 could be estimated from the metal stability constants with NH_3. Therefore, ΔLK_2 is linearly correlated with the stability constant of metal-NH_3 complexes in WHAM 6/Model VI. The ΔLK_2 values obtained for the REE using this linear relationship are very low (e.g. 0.29 for Eu), and much lower than the ΔLK_2 values calculated in Marsac et al. (2010), and the ΔLK_{2C} and ΔLK_{2P} values obtained in the present study. This may suggest that the participation of N-containing groups only plays a small role in the strong, bi- and tridentate binding sites. The strength of these sites has to be mainly due to the development of favorable spatial arrangements of carboxylic and phenolic ligands as well as the effect of chelation. It is interesting to note that the high ΔLK_{2P} values stemming from the new simulations compensate for the decrease in the log K_{MB} values generated by this simulation. Because phenolic groups have high pKa (Ritchie and Perdue, 2003), only a small fraction of the REE is able to bind to monodentate phenolic ligands, as the majority remain bound to specific multidentate, phenol-containing groups.

3.2. Experimental data fit

The three experimental datasets used to optimize the Model VI parameters were modeled separately. The results of the simulations with WHAM 6/Model VI and PHREEQC/Model VI are compared in Figure III.2 for (i) Eu binding by HA at pH 2 to 7 and under high metal loading conditions (Pourret et al.'s experimental dataset (2007b); Fig. III.2a), (ii) La and Lu binding by HA at pH = 3 under variable metal loading conditions (Marsac et al.'s dataset (2010); Fig. III.2b), and (iii) Eu binding by HA at pH 6 to 9 with EDTA, and under low metal loading conditions (Sonke and Salters's dataset (2006); Fig. III.2c). The

quality of the fits can also be evaluated by comparing the measured and simulated REE distribution patterns (log K_d) for the data of Pourret et al. (2007b) and Marsac et al. (2010) (Figs. III.2d and III.2e, respectively), or the measured and simulated patterns of the conditional REE-HA stability constants (log β_{HS}) for Sonke and Salters' data (2006) (Fig. III.2f). The log β_{HS} values were corrected from the REE-EDTA interaction (Sonke and Salters 2006). The new hypotheses in PHREEQC/Model VI model significantly improve the quality of the fits as the total rmse (i.e. calculated for the whole REE and conditions studied) decreased from 0.10 to 0.07 (Table III.2). There is a moderate improvement in the fit for Pourret et al.'s results (2007b) (from 0.10 to 0.07), which is primarily seen in high pH conditions at low metal loading (Figs. III.2a and III.2d). By contrast, the improvement of the fit is very significant for Sonke and Salters' data (2006), as the rmse is divided by a factor of around 2: 0.10 in the new calculations versus 0.26 in WHAM 6/Model VI. This improvement is particularly significant for the LREE at high pH (e.g. at pH 9 in Fig. III.2f). The strong overestimation of the log β_{HS} values obtained for the LREE under this pH condition with WHAM 6/Model VI is no longer apparent. At a high pH and low REE/HA ratio, the REE are strongly bound to the HA phenolic groups. The LREE overestimation of the latter with WHAM 6/Model VI is the consequence of the Log K_{MA}-Log K_{MB} linear relationship, the HA phenolic sites present high stability constants with LREE. Rmse increases slightly for Marsac et al.'s results (2010), from 0.02 with WHAM 6/Model VI to 0.04 with the new parameters, but remains very low.

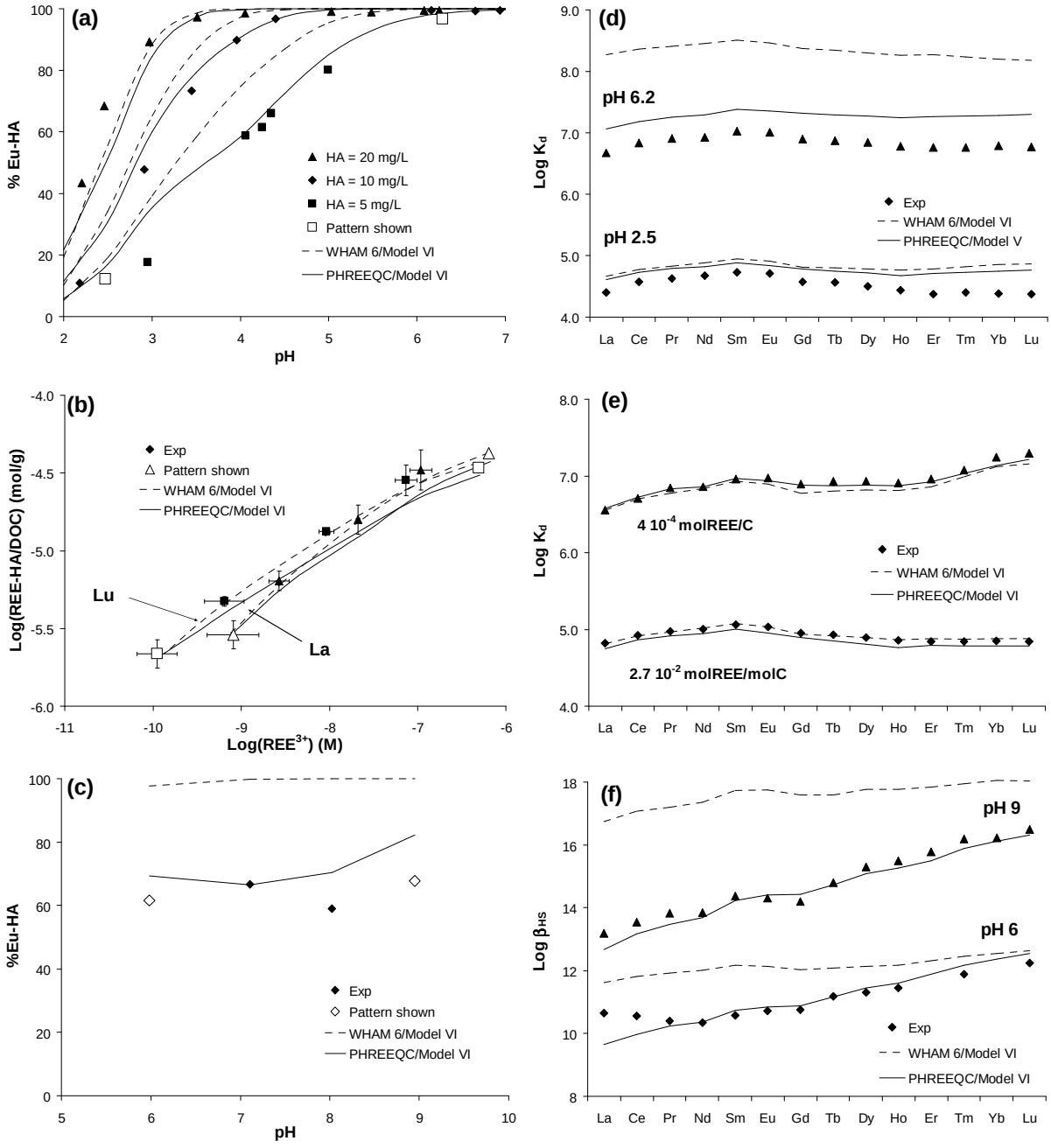

Figure III.2. Comparison between published experimental data for REE binding with HA and the results of simulations of the same data using WHAM 6/Model VI and PHREEQC/Model VI, respectively. The experimental data are from Pourret et al. (2007b) (a), Marsac et al. (2010) (b) and Sonke and Salters (2006) (c). The "patterns shown" correspond to the REE-HA patterns, presented for the experiments demarcated with an open symbol, in (d), (e) and (f).

4. Discussion

The independent optimization of the HA carboxylic and phenolic binding parameters (i.e. removal of the log K_{MA}-log K_{MB} linear relationship and ΔLK_2 dissociation for the carboxylic and phenolic groups) allowed for the first time to satisfactorily and simultaneously model a large set of multi-REE experimental data with the same set of equations and parameters. The following discussion will show that these parameter modifications not only improve the fit of the data, but that the 80 HA sites present REE log K patterns that are more consistent with the data available for simple organic ligands (Byrne and Li, 1995). We will also discuss the implications of these parameter modifications on REE speciation of the different HA sites. This was possible for the first time by the introduction of Model VI into PHREEQC.

4.1. Assessing the consistency of the new modeling parameters

Figure III.3 presents a plot comparing the log K_{Lu}/K_{La} ratio, which represent the fractionation of the REE Log K pattern with the average REE stability constants determined for (i) 101 organic ligands studied independently (Byrne and Li, 1995) and (ii) the 80 HA sites defined in WHAM 6/Model VI and PHREEQC/Model VI. Since the REE-ligand log K values were available at IS = 0.1M, the REE-HA log K values were calculated at IS = 0.1M using the Davies equation. The log K_{Lu}/K_{La} ratio shows a positive correlation when reported against the average REE log K value (R^2=0.77). This correlation indicates that the LREE and MREE have more affinity for weak carboxylic ligands, such as acetic acid, than the HREE whereas HREE have more affinity for strong multidentate ligands, such as EDTA, than LREE and MREE. This general increase in the log K_{Lu}/K_{La} ratio with increasing stability constants can be used to assess the consistency and accuracy of the new optimized parameters obtained for the 80 HA sites. It is remarkable that the REE-HA log K values defined by the new optimized parameters show a similar positive correlation (R^2=0.75) as do the data for the 101 ligands, whereas the parameters obtained in WHAM 6/Model VI lead to a dispersion of the log (K_{Lu}/K_{La}) versus the average stability constants in Figure III.3 (no observed correlation). More particularly, because of the log K_{MA}-Log K_{MB} linear relationship in WHAM 6/Model VI, strong HA sites (i.e. average REE log K > 15) present $K_{La} > K_{Lu}$, which is not observed among either the 101 organic ligands or the HA sites defined with the new PHREEQC/Model

VI parameters. Consequently, PHREEQC/Model VI appears to be more realistic than WHAM 6/Model VI.

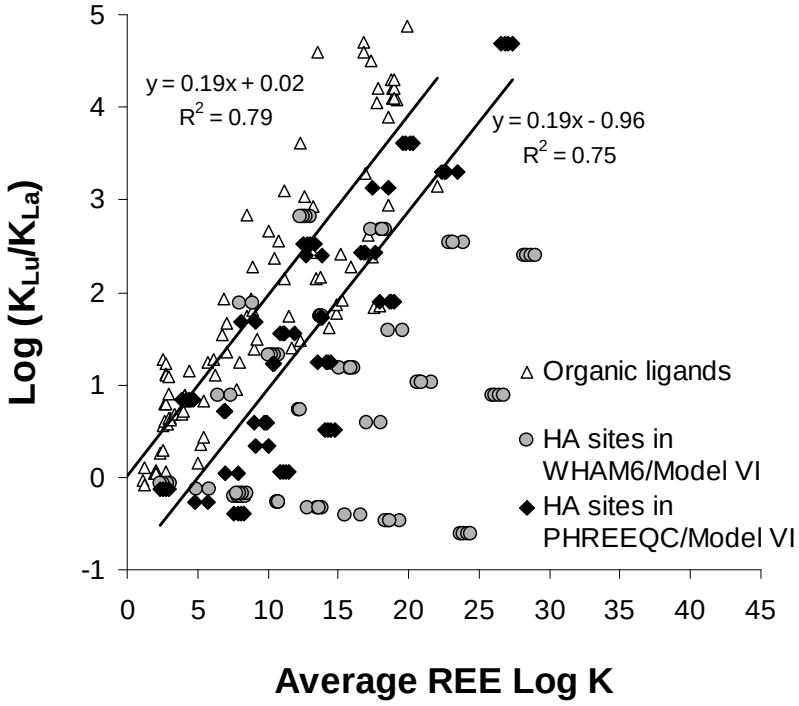

Figure III.3. Log (K_{Lu}/K_{La}) versus the average REE Log K_{REE} values obtained for 101 organic ligands (Byrne and Li, 1995) and for the 80 ligands defined in WHAM 6/Model VI and PHREEQC/Model VI. Log (K_{Lu}/K_{La}) is used as an indicator of the REE-ligand pattern. The linear regression for the 101 organic ligands (Byrne and Li, 1995) and for the 80 HA sites obtained here with PHREEQC/Model VI are also presented.

4.2. REE distribution on HA sites

This section compares the REE speciation on the HA surface obtained using the WHAM 6/Model VI hypotheses (i.e. using the log K_{MA}-log K_{MB} linear relationship and a single and constant ΔLK_2 value for all REE; Tipping, 1998) and the new hypotheses stemming from this study and involved in PHREEQC/Model VI. In Model VI, 80 different sites are expected to participate in the cation-HA binding. To simplify the REE speciation on the HA surface, these 80 sites can be gathered in several groups based on two main characteristics: the chemical nature of the ligands (i.e. carboxylic groups: CG, phenolic groups: PG and carboxy-phenolic groups: CPG) and their denticity (i.e. mono-, bi- and tridentate sites).

Figure III.4 displays the calculations performed at high metal loading using Pourret et al.'s experimental conditions (2007b), namely HA = 5mg L^{-1}, and over a wide pH range for

La, Eu and Lu, respectively. At high metal loading, the few strong binding sites play a subordinate role in HA-REE complexation. The criterion that primarily differentiates the two simulations is the chemical nature of the binding sites (i.e. whether they are CG, CPG or PG sites). The WHAM 6/Model VI complexation hypotheses yield very similar speciation results for all of the REE. The complexation is dominated by CPG in each case (La_{CPG} = 50-80%; Lu_{CPG} = 50-60%). The situation is clearly different if the new hypotheses and new modeling parameters are used. The speciation of La and Lu is no longer similar. The dominant REE-HA species for La is CG (80 to 100% vs. pH) instead of CPG when using the equations and parameters of WHAM 6/Model VI. The LREE speciation generated by the new equations and parameters (dominant role of the carboxylic groups) is consistent with the C 1s-NEXAFS analysis of Eu-HA complexes at high metal loading and low pH (pH = 5.1), which showed that Eu was bound to HA carboxylic sites (Plaschke et al., 2004; Naber et al., 2006). Note that the new equations and parameters do not induce significant changes in Lu-HA speciation.

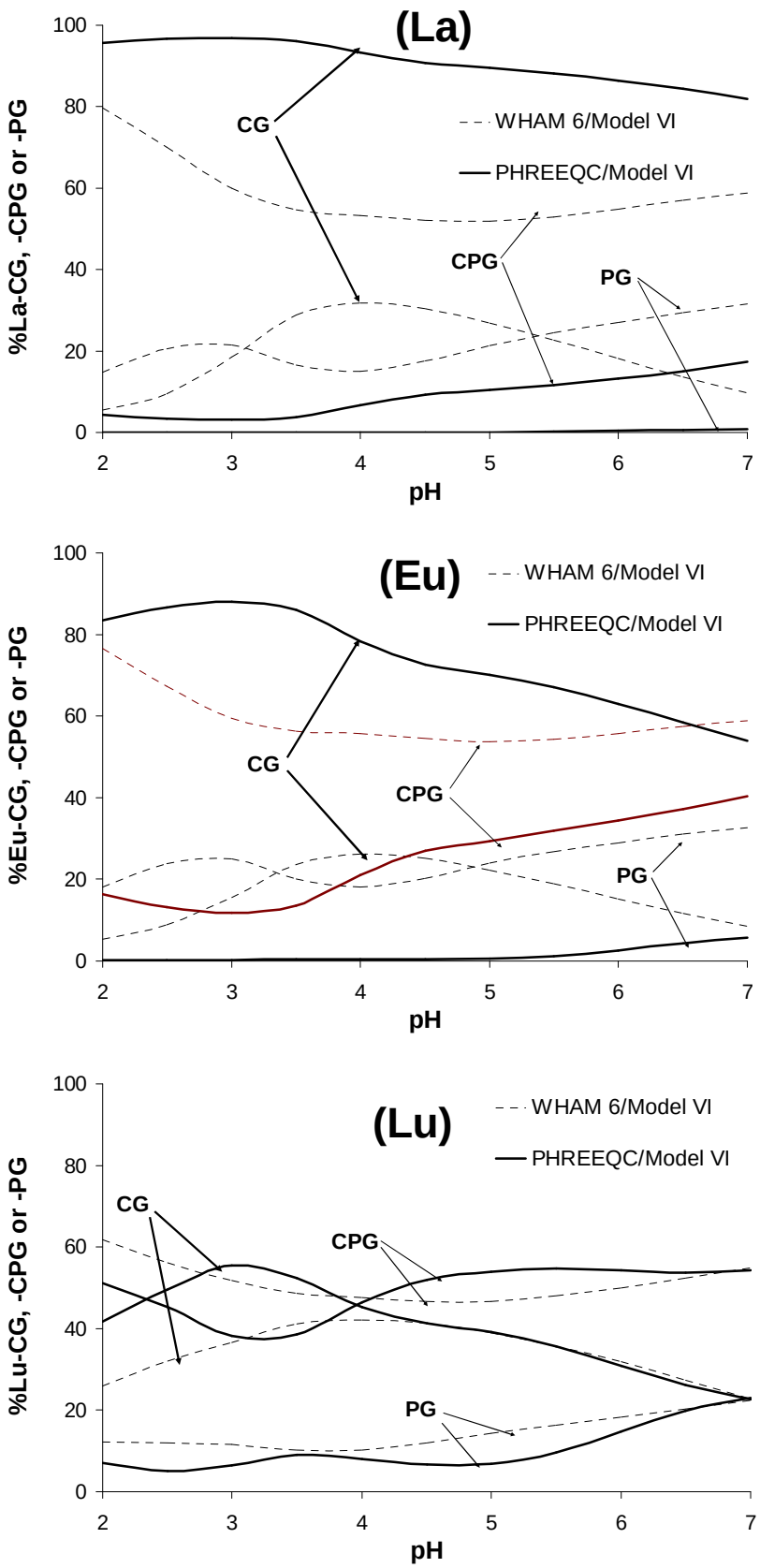

Figure III.4. Speciation calculation results for La (a), Eu (b) and Lu (c) depending on the complexation hypotheses used. The simulated experimental data are those from Pourret et al. (2007b). CG: carboxylic groups; CPG: carboxy-phenolic groups; PG: phenolic groups.

With regards to the effects of site denticity under high metal loading and varying pH conditions (data not shown), the main consequence of the new equations and parameters is to reduce the relative amount of the REE bound to monodentate sites to almost 0%, whereas it could reach 15% at pH = 7 with the WHAM 6/Model VI parameters. REE-HA binding occurs mainly through bidentate sites (80-90%) under high metal loading conditions, regardless of the REE and pH. Only a small proportion (10 to 20%, depending on the REE) is bound to the tridentate sites. Another consequence of the new equations and parameters is a drastic decrease of the REE bound to tridentate sites at low metal loading (Marsac et al. 2010; experimental conditions). The WHAM 6/Model VI equations and parameters led to a (i) large increase of the REE bound to HA tridentate sites with decreasing metal loading at pH = 3 (20% at 2 10^{-2} metal loading to 60% at 4 10^{-4} metal loading for La) (Fig. III.5) and (ii) fractionation between La and Lu: the relative amount of La bound to tridentate sites increased much more strongly than that of Lu with decreasing metal loading. The new equations and parameters clearly modify the REE speciation on HA sites. Firstly, the increase of the REE bound to tridentate sites with decreasing metal loading is less pronounced. Secondly, the amount of La bound to tridentate sites always remains lower than that of Lu even under very low metal loading. This effect is clearly a consequence of the disappearance of multidentate sites combining REE log K >15 and log K_{La} > log K_{Lu} in the new modeling strategy, a combination that is totally unrealistic based on Figure III.3.

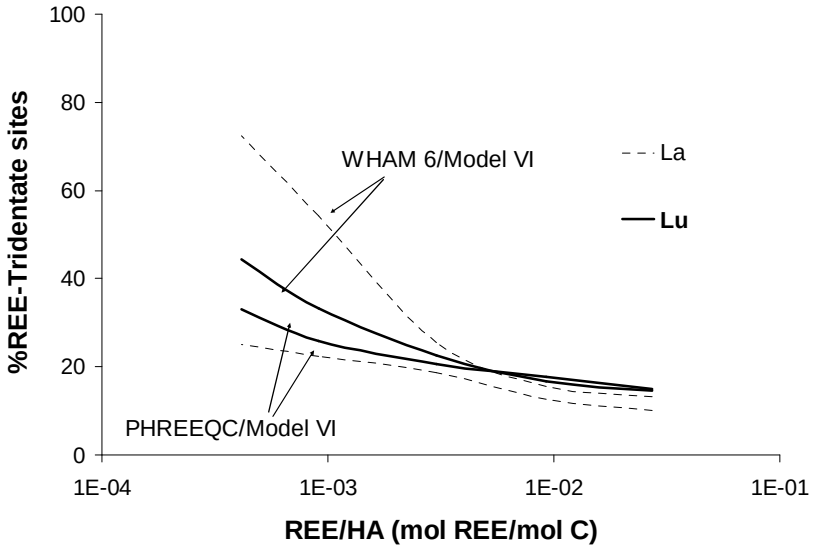

Figure III.5. The proportion of La and Lu bound to tridentate sites versus the REE/HA ratios. The displayed evolutions depend on whether the new equations and parameters or those formerly installed in WHAM6/ModelVI are used. The simulated experimental data are from Marsac et al. (2010).

4.3. Consequences for cation competition

In natural waters, the REE compete with many other dissolved cations during HA complexation. Among the cations present in natural waters, several cations, such as Fe^{3+} and Al^{3+}, are known to complex strongly with HA (Tanizaki et al., 1992; Takahashi et al., 1997; Dupré et al., 1999; Olivié-Lauquet et al., 1999; Allard at al., 2004; Tipping et al., 2002; Tipping, 2005; Lofts et al., 2008), and are therefore a strong potential competitor of REE for HA binding. Experimental studies of a single REE (Lippold et al., 2005; 2007) and a modeling study of the whole REE series (Tang and Johannesson, 2003) showed that Al and Fe could significantly reduce the amount of the REE bound to HA. Therefore, the question to be asked is if metal competition could modify the REE-HA pattern. This cation-REE competition can be accessed through WHAM 6/Model VI simulations. Although the log K_{MA}-log K_{MB} linear relationship used in WHAM 6/Model VI implies that all cations will exhibit the same carboxylic to phenolic HA site affinity, the competitive metal tendency to form strong multidentate complexes (simulated by the ΔLK_2 parameter) can modify the REE-HA pattern. For instance, the ΔLK_2 value is equal to 0.46 for Al^{3+} and 2.2 for Fe^{3+} (Tipping, 1998). Therefore, according to WHAM 6/Model VI's definition of HA, Al^{3+} and Fe^{3+} will compete more efficiently for the LREE and HREE, respectively, since the ΔLK_2 parameter increases from La to Lu. However, the results obtained here demonstrate that the LREE and HREE are not complexed to the same sites. The LREE are preferentially complexed to carboxylic sites, whereas the HREE are preferably bound to carboxy-phenolic sites (Fig. III.4). Therefore, a metal will compete with the REE in different ways depending on whether it complexes itself preferentially with the carboxylic or phenolic sites. This unequal competition will produce REE-HA fractionation patterns that are different from the WHAM 6/Model VI simulations. The occurrence of competing metals with strong affinities for phenolic sites will lead to a release of part of the HREE bound to HA. As part of the HA phenolic groups are unavailable for REE binding, the resulting REE-HA pattern will present the specific feature of carboxylic ligands such as acetic acid (Fig. III.1a). Given that competing metals have strong affinities for carboxylic sites, this will lead to a relative decrease in the LREE bound to HA. The resulting REE-HA pattern will present the specific feature of phenolic ligands such as catechol (Fig. III.1b).

To evaluate the expected effects of metal competition on the REE-HA binding patterns, the stability constants of the potential competing metals with acetic acid and catechol were compiled and compared both between them and with the stability constants of the REE

(IUPAC, Stability Constants Database). Metals such as Al^{3+} and Cu^{2+}, with regards to their high affinity for phenol-bearing sites, should preferentially compete with the HREE (Fig. III.6). The resulting REE pattern should exhibit a lower increase for HREE than that expected without any competition. Cadmium competition should result in a relative LREE depletion in the REE-HA pattern, as Cd^{2+} has more affinity for carboxylic groups (assumed to be analogous with acetic acid) than for phenolic groups (assumed to be analogous with catechol) when compared with the average REE. By contrast, Fe^{3+} competition should not result in a fractionation of the REE-HA pattern since Fe^{3+} presents a relative affinity for carboxylic and phenolic groups, equal to that of the average REE. Note that the effect of Al^{3+} and Fe^{3+} on the REE-HA pattern with regards to their affinity for carboxylic and phenolic ligands is opposed to what is expected with WHAM 6/Model VI. These presumed impacts, though plausible, must nevertheless be viewed with caution: only the affinity for carboxylic and phenolic ligands is discussed here. The metal affinity for multidentate ligands is also a binding mechanism thereby affecting the REE-HA pattern. As compared to the light rare earth elements, heavy rare earth elements are indeed more bound to the HA multidentate sites. Experimental studies should be conducted to confirm if this statement is both true and accurate. The present improvements in the modeling of REE-HA binding will therefore provide a valuable and powerful tool for the interpretation of future experimental results.

These expected effects of metal competition on the REE-HA pattern have two important implications. (i) The change in the REE pattern could provide a way to highlight the occurrence of competing processes. It might even help to clarify the affinity of a given metal for the different HA sites. Several studies have shown the difficulty of calibrating cation-HA binding parameters, especially in cation competition experiments. An example of this is Al with the NICA-Donnan model (Kinniburgh et al., 1996). Because Al is a possible competitor to Pb, Kinniburgh et al. (1999) considered that Al was only bound to phenolic groups. However, since Al is able to compete with Cd and Pb, Pinheiro et al. (2000) considered that Al and Pb were only assigned to be bound with carboxylic groups. Our results suggest that the REE-HA pattern could be used as a probe of the metal affinity for HA binding sites in further REE-metal competition experiments, depending on whether the metal competes with LREE (i.e. a higher affinity for HA carboxylic sites), HREE (i.e. a higher affinity for HA phenolic sites) or every REE. (ii) The REE pattern variability in natural organic-rich waters is generally attributed to the competition between dissolved organic matter (DOM) and carbonate (Elderfield et al., 1990; Tang and Johannesson, 2010). A MREE-enrich pattern is observed when REE binding by DOM dominates, whereas a HREE-

enrich pattern is observed (a REE-carbonate log K increase from LREE to HREE; Luo and Byrne, 2004) when REE binding by carbonate dominates. However, the LREE and HREE affinity for HA can also vary with regards to the considered metal loading (cation/DOM concentration ratio). Therefore, the present study suggests that not only the metal loading could account for the diversity of the REE patterns in organic-rich waters (Marsac et al., 2010), but also the "phenolic" and "carboxylic" competing cations, especially Al^{3+} and Fe^{3+}.

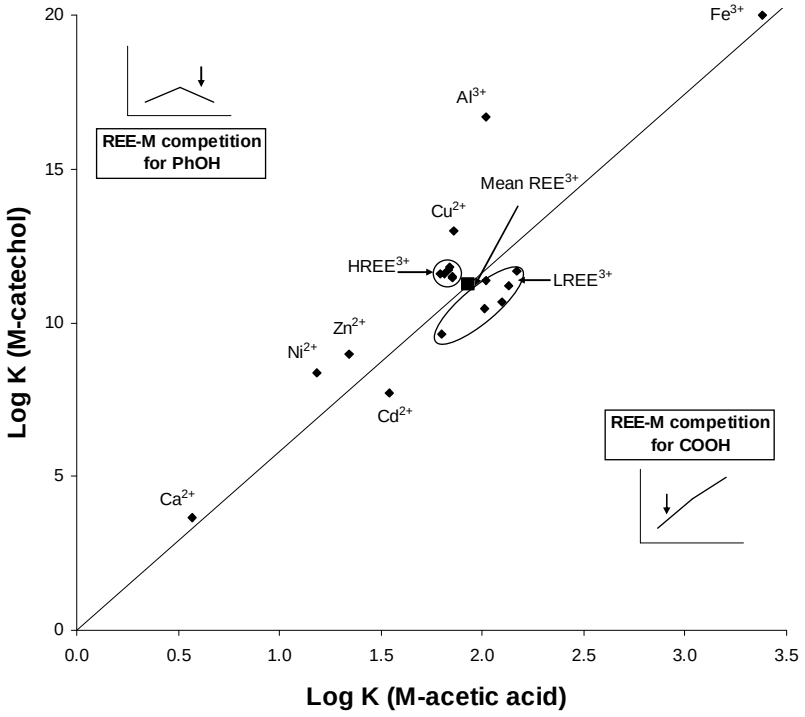

Figure III.6. Literature compilation of metal-acetic acid or -catechol binding constants. The straight line passing through the mean REE value indicates metals that should not compete differently with the LREE and MREE. Conversely, metals below this line, such as Cd^{2+}, should compete primarily with the LREE, whereas those above this line, such as Al^{3+}, should be mainly in competition with the HREE. Data sources: IUPAC Stability constants database.

5. Summary

The results show that removal of the log KMA-log KMB linear relationship existing in Model VI, coupled with the introduction of two independent ΔLK2 sets to describe the REE equilibrium complexation with HA low density strong sites, resulted in a strong improvement of REE-HA interaction modeling. This new modeling approach allows, for the first time, to simultaneously and satisfactorily model a large set of multi-REE binding to HA experimental data. The increase for HREE in the log KMB pattern, obtained by removing the linear

relationship, is consistent with the phenolic nature of type B sites and REE-catechol binding constants, as catechol is considered as analogous with phenolic ligands. REE log K with the 80 HA sites defined in Model VI, calculated from the newly optimized REE-HA Model VI parameters, are consistent with the REE stability constants for the 101 simple organic ligands, in contrast with the previous data. The introduction of the new Model VI equations and parameters into PHREEQC allows for the first time to highlight the speciation of the REE at the HA surface. The modeling data show that the LREE and HREE are not bound to similar HA sites. The LREE are preferentially bound to carboxylic groups, whereas HREE are preferentially complexed to carboxy-phenolic and phenolic groups. As a consequence, a different REE-HA pattern could arise from competition between cations and REE for HA binding, depending on the cation affinity for these different groups. A survey of available data shows that competition with Al^{3+} should result in a release of part of the HREE bound to HA, whereas competition with Fe^{3+} should not have any effect on the REE-HA pattern. Competing cations for phenolic and carboxylic HA sites may therefore account for the diversity of the REE patterns observed in natural organic-rich waters.

Further experimental studies have to be conducted to confirm the accuracy of these predictions, which should largely benefit from the performed improvements in the modeling of REE-HA interactions. The PHREEQC/Model VI model set-up provides a valuable and powerful tool for the interpretation of complex REE-competitor metal-HA interactions. The PHREEQC/Model VI coupling should also improve the hydrochemical modeling of the REE since PHREEQC/Model VI accounts for chemical reactions such as mineral dissolution/precipitation, redox reactions, and the modeling of kinetically-controlled reactions and one-dimensional transport. Finally, it should be highlighted that the new modeling results argue for the development of fine spectroscopic measurements to confirm the exact nature of the HA sites involved in the complexation of the REE by HA.

IV.Chapitre III :

Compétition entre terres rares et aluminium pour la complexation par les acides humiques

Aluminium competitive effect on Rare Earth Elements binding to humic acid

Cette partie est extraite d'un article soumis à Geochimica et Cosmochimica Acta, Marsac R., Davranche M., Gruau G, Dia A. and Bouhnik-Le Coz M. (2011) Aluminium competitive effect on Rare Earth Elements binding to humic acid.

Résumé- Les mécanismes de compétition entre terres rares (REE) et aluminium (Al) pour la complexation par les acides humiques (HA) ont été étudiés en combinant des expériences de laboratoire et la modélisation afin de déterminer l'effet de Al sur la complexation des REE par les HA. Les résultats montrent que Al^{3+} est un plus fort compétiteur pour les REE lourdes (HREE) à pH acide (pH = 3) et à un faible rapport de concentration REE/HA. Ces résultats démontrent que Al a une forte affinité pour les sites multidentates des HA, présents à de faibles teneurs. A des pH plus élevés, entre 5 et 6, et à un rapport REE/HA plus élevé, Al est un plus fort compétiteur pour les REE légères (LREE) suggérant que Al se lie aux groupements carboxyliques des HA plutôt qu'aux groupements phénoliques. Les paramètre de complexation entre Al et HA de PHREEQC/Model VI ont été optimisés afin de décrire simultanément la complexation de Al par HA et son effet de compétition sur la complexation des REE par HA. L'interaction entre Al et HA à pH > 5 a été simulée par une très forte complexation de $Al(OH)_2^+$ par les groupements carboxyliques de HA suggérant que d'autres espèces hydrolysées de Al sont impliquées dans la complexation de Al par HA. Ces espèces seraient probablement des poly-hydroxy-cations. La complexation des espèces polynucléaires de Al n'a pas pu être introduite dans le modèle puisqu'elle devrait impliquer des sites d'une denticité supérieure à ceux définis dans le modèle. Cette étude fournit des connaissances fondamentales quant aux mécanismes de compétition entre REE et Al pour la complexation par HA : l'effet de compétition de Al dépend de son affinité relative pour les ligands carboxyliques, phénoliques et chélates et peut donc modifier le spectre de complexation des REE par HA. Les eaux naturelles neutres et riches en matière organique devraient être appauvries en LREE puisque, dans ces conditions de pH, Al ne se lie probablement pas ni aux groupements phénoliques ni aux groupements forts multidentates de HA. Par extrapolation des résultats obtenus avec Al, d'autres cations compétiteurs potentiels tels que le fer (Fe) pourraient avoir leur propre effet de compétition sur la complexation des REE par HA. Par conséquent, pour pourvoir comprendre et modéliser la variabilité des spectres des REE dans les eaux, une connaissance précise des mécanismes de complexation des différents cations compétiteurs des REE par HA est requise. Finalement, démontre la puissance des REE lorsqu'elles sont utilisées comme « sonde de spéciation » dans le but de décrire les mécanismes de complexation des cations par HA comme démontré, dans le cas présent, pour les différentes espèces chimiques de Al.

Abstract- Competitive mechanism between rare earth elements (REE) and aluminium for humic acid (HA) binding were investigated by combining laboratory experiments and

modeling to study the effect of Al on REE-HA complexation. Results indicates that Al^{3+} competes dominantly with heavy REE (HREE) in acidic (pH=3) and low REE/HA concentration ratio conditions assessing the Al high affinity for the few HA multidentate sites. Under higher pH - 5 to 6 - and high REE/HA conditions, Al is more competitive for light REE (LREE) suggesting that Al is bound to HA carboxylic rather than phenolic sites. PHREEQC/Model VI Al-HA binding parameters were optimized to simulate precisely both Al binding to HA and Al competitive effect on REE binding to HA. Al-HA interaction at pH >5 was simulated by a strong complexation of $Al(OH)_2^+$ by HA carboxylic groups suggesting that hydrolyzed species other than $Al(OH)_2^+$ were involved in the complexation. Polynuclear hydroxy-Al-HA complexes are expected. This mechanism could not be introduced into the model since it should involve HA sites with higher denticity than those defined in the model. The present study provides fundamental knowledge on Al-REE competitive mechanisms for HA binding: Al competitive effect depends on the relative affinity of the different Al species for carboxylic, phenolic or chelate ligands and therefore can modify REE-HA pattern. Under circumneutral pH conditions in natural waters, Al should lead to LREE-depleted patterns since Al is not expected to bind efficiently neither to HA phenolic groups nor to strong HA multidentate groups. As deduced from the behavior of Al species, other potential competitor cations such as iron are expected to have their own competitive effect on REE-HA binding. Therefore, in order to reliably understand and model REE-HA pattern variations in natural waters, a precise knowledge of the exact behavior of the different REE competitor cations is required. Finally, this study highlights the ability of the REE to be used as a "speciation probe" to precisely describe cation interactions with HA as here evidenced with the different Al species.

1. Introduction

Rare earth elements (REE) are a group of 14 elements that are strongly bound with natural dissolved organic matter (DOM) (Takahashi et al., 1997; Viers et al., 1997; Dia et al., 2000; Tang and Johannesson, 2003; Johannesson et al., 2004; Gruau et al., 2004; Davranche et al., 2005; Sonke and Salters, 2006; Pourret et al., 2007a; Pédrot et al., 2008; Marsac et al., 2010; Yamamoto et al., 2010). The unique property of REE is to consist of a chemically coherent series of elements. The regular variations along the series can generate DOM/solution partition coefficient (K_d) patterns showing specific shapes depending on the binding conditions (i.e. the nature of the functional group involved). REE binding by humic acid (HA) experiments conducted under variable REE/HA ratios (defined as the REE to

carbon molar ratio) and pH conditions exhibit changes in K_d^{REE} pattern demonstrated to occur through HA binding sites heterogeneity (Marsac et al., 2011). More precisely, REE-HA binding experiments under acidic and low REE/HA conditions yielded K_d^{REE} patterns showing an increase of heavy REE (HREE) as compared to light REE (LREE). This feature is involved by the REE binding to HA few strong sites that are similar to chelate ligands such as EDTA and have more affinity for HREE than LREE (Sonke and Salters, 2006; Marsac et al., 2010; Yamamoto et al., 2010). Experiments conducted at high REE/HA conditions showed K_d^{REE} pattern with an increase for the middle REE (MREE) specific of REE binding with carboxylic ligands such as acetic acid (Tang and Johannesson, 2003; Pourret et al., 2007b). This downward MREE concavity was suggested to be developed through the REE binding with abundant and weak HA carboxylic sites. This K_d^{REE} pattern dependence to REE/HA and involved HA binding site was successfully modeled by Marsac et al. (2011) using the specific humic-ion binding model (Model VI) developed by Tipping (1998). The modeling approach suggest that at high REE/HA conditions, although LREE are dominantly (>80%) bound to carboxylic sites, a majority of HREE (>80%) are bound to phenolic and carboxy-phenolic sites (Marsac et al., 2011). The experimental and modeling results raise therefore the possibility that REE could be used as a tool to determine which of the carboxylic, phenolic or chelate functional groups are implicated in the binding of a given cation by HA. All cations able to compete with REE for HA binding could not only involve a quantitative decrease of the complexed REE bound to HA but also modify the REE-HA K_d pattern depending on their respective affinity for carboxylic, phenolic or chelate HA sites. Conversely, variations of the REE-HA K_d pattern patterns observed in the presence of a competitive cation could provide additional clues to explain why REE pattern variations occur in natural, organic-rich waters (Marsac et al., 2010, and references therein).

In this respect, aluminum (Al) is of particular interest. Aluminium is abundant in natural, organic-rich waters, specifically acidic water, with Al^{3+} activity up to around 10^{-3} mol L^{-1} (Tipping, 2005). Moreover, Al has strong affinity for HA and is thus a strong competitor for cations-HA binding including REE (Bidoglio et al., 1991; Tanizaki et al., 1992; Takahashi et al., 1997; Dupré et al., 1999; Kinniburgh et al., 1999; Pinheiro et al., 2000; Tipping et al., 2002; Lippold et al., 2005). The competitive binding of Al with the whole REE group has not been experimentally studied. A common belief is that Al is preferentially bound to strong HA sites and is therefore a stronger competitor for HREE than for LREE. As a consequence, Al should induce a relative decrease of HREE in the K_d^{REE} pattern (Yamamoto et al., 2010; Tang and Johannesson, 2010; Marsac et al., 2011). However, this stronger competition of Al for

HREE is opposite to the current parameters of Model VI describing Al and REE binding to HA. The ΔLK_2 parameter that defines the strength of HA multidentate sites are $\Delta LK_2(Al) < \Delta LK_2(LREE) < \Delta LK_2(HREE)$. Therefore, Model VI currently predicts a stronger competitive effect of Al on LREE than on HREE.

In the present study, REE-Al-HA binding experiments were performed simultaneously on the 14 naturally occurring REE over a range of metal loading and pH conditions. The aim of this work is threefold: i) to experimentally investigate the competitive effects of Al on REE complexation by HA in conditions that highlight the competition with the few strong multidentate and phenolic groups, respectively; ii) to evaluate the ability of PHREEQC/Model VI to predict the experimental data and to improve the quality of the modeling and iii) to test the ability of the REE to be used as a fingerprint of the mechanisms of Al binding to HA.

2. Materials and methods

All chemicals used were of analytical grade, with all experimental solutions being prepared with doubly-deionised water (Milli-Q system, Millipore™). Synthetic REE solutions were prepared from a nitrate REE standard (10 mg L^{-1}, Accu Trace™ Reference Standard). Polyethylene containers used to study REE-HA complexation equilibrium were all previously soaked in 10% Ultrapure HNO_3 for 48h at 60°C, then rinsed with deionised water for 24h at 60°C to remove all REE contamination sources. All experiments were performed at room temperature, i.e. 20°C ± 2.

2.1. Humic acid

Purified humic acid (HA) was obtained from synthetic Aldrich humic acid (Aldrich™, H1, 675-2). The purification was performed with the protocol of Vermeer et al. (1998), except that a tangential ultrafiltration step was added to remove any possible HA molecules <10 kDa using a Labscale TFF system equipped with a Pellicon XL membrane (PLCGC10, Millipore™). Humic acid was freeze-dried and stored in a glass container. Prior to use, purified HA was solubilized overnight in a solution of 0.01 M NaCl at pH = 10 to ensure complete dissolution (Vermeer et al., 1998). The pH was adjusted to 3 in the HA suspensions, which were then filtered at 0.2µm to remove any potential precipitate and therefore to ensure studying the same HA fraction in any experiments performed even at higher pH. The dissolved organic carbon (DOC) concentration of the filtrates was then measured to assess the true HA concentration of the experimental suspensions.

2.2. Experimental set-up of the REE and Al binding to HA

A standard batch equilibrium technique was used to study the competitive effect of Al on REE binding by HA. The fourteen REE and Al were simultaneously added to HA suspension set in a 10^{-2} M (NaCl) electrolyte solution. Experimental suspensions were stirred for 48 h to reach equilibrium according to the protocol defined by Pourret et al. (2007b). The pH was monitored regularly with a combined Radiometer Red Rod electrode, calibrated with WTW standard solutions (pH 4 and 7). The accuracy of pH measurements was ±0.05 pH units. At equilibrium (48 h), 10 mL of the suspension were sampled and ultra-filtered at 5 kDa to separate the REE-HA and Al-HA complexes from the remaining inorganic REE and Al. Ultrafiltrations were carried out by centrifuging the suspension aliquots through 15 mL centrifugal tubes equipped with permeable membranes of 5 kDa pore size (Vivaspin 15RH12, Sartorius). All the membranes used were first washed with 0.15 mol L^{-1} HCl, then rinsed twice with ultrapure water to minimize contamination. Centrifugations were performed using a Jouan G4.12 centrifuge with swinging bucket rotor at 3000g for 30 min. Removing of HA fractions <10 kDa in the HA mother solution ensures that no organic molecules pass through the 5 kDa membrane at this stage of the experiments. All experiments were performed in triplicate.

Two types of REE-Al competition experiments were performed. The first type was performed at pH 3, under low REE/HA ($\sum$[REE] = 1 µM; DOC = 9 mg L^{-1}; REE/HA = 1.2 10^{-3} molREE/molC) and variable Al concentration (0 to 20 µM) conditions. Under these conditions, REE should be preferentially bound to HA by means of the few strong multidentate sites occurring on them. The competition with Al for these sites, if occurring, should result in a relative HREE depletion of the log K_d^{REE} pattern (see above). This first series of experiments was limited to pH 3 because higher pH values do not allow keeping measurable amounts of REE in solution, due to the low REE/HA effect. The second series of experiments was performed at variable pH ranging from 3 to 6, using higher REE/HA ($\sum$[REE] = 10 µM; DOC = 6.7 mg L^{-1}; REE/HA = 2 10^{-2} molREE/molC) and equal REE-Al concentrations ($\sum$[REE] = [Al] = 10 µM). Reference experiments without Al were performed for comparison. Due to higher REE/HA, REE are expected to be preferentially complexed by carboxylic and phenolic functional groups in this second series of experiments, with an expected increase of the phenolic/carboxylic ratio with increasing pH due to the higher proton dissociation constant of phenolic groups (Marsac et al., 2011). Thus, this second series of experiments was designed to provide information about the ability of Al to compete with REE

for binding with HA phenolic sites. Speciation calculations carried out with PHREEQC showed that all inorganic REE could be confidently assumed to occur as free aqueous REE^{3+} species in the two series of experiments, and the REE behavior was therefore modeled, accordingly (Tang and Johannesson, 2003; Pourret et al., 2007a; Marsac et al., 2010). The Al speciation in 0.01 NaCl aqueous solution was simulated with PHREEQC. Stability constants between Al and hydroxides from the minteq.v4 database were used and the precipitation of amorphous Al hydroxides was assumed (Figure IV.1). Aluminium activity was controlled by the precipitation of $Al(OH)_3$, following the reaction:

$$Al(OH)_3 + 3H^+ = Al^{3+} + 3H_2O \quad K_{SO} \qquad \text{(IV.1)}$$

And,

$$\log a_{Al3+} = \log K_{SO} - 3\ pH \qquad \text{(IV.2)}$$

The $\log K_{SO}$ was set equal to 10.8 (IUPAC, Stability Constants Database). At pH 3, all the inorganic Al species occur as free aqueous Al^{3+} species. At high pH, Al occurs as $Al(OH)_n^{(3-n)}$, especially between pH 5 and 6. At pH > 5, Al hydroxides could precipitate and would be removed from the solution as Al-HA complexes by ultrafiltration at 5 kDa.

The REE complexation with HA is described using the apparent partition coefficient K_d, as follows:

$$K_d(Ln_i) = \frac{\mu g Ln_i \text{ adsorbed } L^{-1}/g \text{ DOC } L^{-1}}{\mu g Ln_i^{3+}\ mL^{-1}} \qquad \text{(IV.3)}$$

where Ln_i = La to Lu.

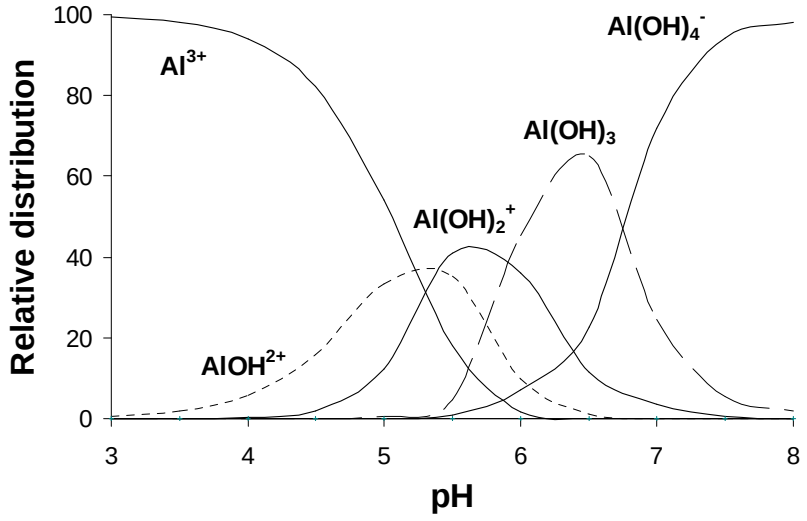

Figure IV.1. Al speciation calculated with PHREEQC for [Al] = 10 µM, IS = 0.01 M (NaCl) and pH ranging from 3 to 8.

2.3. Solution analysis

Rare earth elements and Al concentrations were determined with an Agilent Technologies™ HP4500 ICP-MS instrument. Ultrafiltrate, containing Al and REE inorganic species, were injected directly after adding HNO_3 to a concentration of 0.37 N. The initial suspensions were also analyzed to determine precisely total cation concentrations for each experiment. The suspensions were first digested with sub-boiled nitric acid (HNO_3 14 N) at 100°C, and then resolubilized in HNO_3 0.37 N after complete evaporation, to avoid interferences with organic carbon during mass analysis by ICP-MS. Quantitative analyses were performed using a conventional external calibration procedure. Three external standard solutions with REE and Al concentrations similar to the analyzed samples were prepared from a multi-REE and an Al standard solution (Accu Trace™ Reference, 10 mg L^{-1}, USA). Indium (In) was added to all samples as an internal standard at a concentration of 0.87 μmol L^{-1} (100 ppb) to correct for instrumental drift and possible matrix effects. Indium was also added to the external standard solutions. Calibration curves were calculated from measured REE/In and Al/In intensity ratios. As established from repeated analyses of multi-REE standard solution (Accu Trace™ Reference, USA) and the SLRS-4 water standard, the instrumental error on REE and Al analysis were below 3 and 5 %, respectively.

Dissolved organic carbon concentrations were determined using a Shimadzu 5000 TOC analyzer. The accuracy of DOC concentration measurements is estimated at ± 5%, as determined by repeated analysis of freshly prepared standard solutions (potassium biphtalate).

2.4. PHREEQC/Model VI

Humic ion-Binding Model VI (hereafter referred to as Model VI) is a model developed by Tipping (1998), which is implemented in the geochemical code WHAM 6. The equations of this model were recently introduced into the PHREEQC (version 2) developed by Parkhurst and Appelo (1999) for the entire REE series to improve REE-HA binding description, in particular by removing the linear relationship between log K_{MA} and log K_{MB} (Marsac et al., 2011). PHREEQC (version 2) is a computer code based on an ion-association aqueous model, which was designed to perform speciation and saturation-index calculations in waters.

In Model VI, HA is defined by discrete acido-basic chemical groups (carboxylic and phenolic) which can bind aqueous metal ions (e.g. La^{3+} or Al^{3+}) and their first hydrolysis product (e.g. $LaOH^{2+}$ or $AlOH^{2+}$), forming either monodentate, bidentate or tridentate

complexes. In practice, thanks to Tipping's (1998) work, cation stability constants are adjusted using two parameters, log K_{MA} and log K_{MB}, respectively for carboxylic and phenolic groups. Another parameter (ΔLK_2) is introduced to increase cation stability constants with a fraction of the multidentate sites, considering them as chelate ligands or simulating the participation in these multidentate sites of additional chemical groups, such as nitrogen containing groups. Marsac et al. (2011) showed that to accurately simulate REE-HA binding, ΔLK_2 parameter had to be optimized independently for carboxylic (ΔLK_{2C}) and phenolic groups (ΔLK_{2P}). An electrical double layer, where only counter-ions can accumulate, is also defined in the model. The double layer thickness is set by the Debye-Hückel parameter $\kappa = (3.29 \times 10^9 \times I^{1/2})^{-1}$ (Appelo and Postma, 2005). The distribution of ions between the diffuse layer and the bulk solution is calculated by a simple Donnan model. Intrinsic equilibrium constants are corrected by the Boltzmann factor that depends on HA surface area which was determined to be equal to 19000 m²/g at ionic strength of 0.01 (Marsac et al., 2011). In this study, HA was defined as the SOLUTION_MASTER_SPECIES, SOLUTION_SPECIES and PHASES in the PHREEQC database. The 80 types of site considered by Model VI to bind REE, Al and their respective first hydrolysis products were defined as SURFACE_MASTER_SPECIES, and their respective stability constants as SURFACE_SPECIES in the PHREEQC database. Al hydroxide precipitation was also taken into account by defining $Al(OH)_3$(ha) - noted "ha" for the experiments carried out in the presence of HA - in the PHASES block of PHREEQC database. Aluminium activity was controlled by the precipitation of $Al(OH)_3$, following eq. IV.1 and IV.2. With ultrafiltration at 5 kDa, Al-HA amount and precipitated as hydroxides cannot be separately measured. The calculated amount of Al present in the fraction > 5kDa is defined therefore by:

$$Al > 5\ kDa = Al(OH)_{3(s)} + Al\text{-}HA \qquad (IV.4)$$

Errors between experiments and simulations were quantified by the root mean square error of the regression (rmse), i.e. the sum of the squares of the differences between observed and calculated log υ, where υ is the amount of REE bound to HA per gram of dissolved organic carbon (DOC). To consider a fit to be of good quality, two conditions had to be fulfilled, namely: i) that the total rmse calculated from the whole experimental conditions and REE were low, and ii) that the rmse values calculated for the fourteen REE were sufficiently close to each other.

3. Results

3.1. Experimental Al competitive effect on REE-HA binding

Figure IV.2 illustrates Al influence on log K_d^{REE} patterns at pH = 3 and low REE/HA (= 1.2 10^{-3}). For [Al] = 0, REE-HA pattern increases from La to Lu occurring through preferential binding of REE to the low density strong multidentate sites with higher affinity for HREE than for LREE (Yamamoto et al., 2010; Marsac et al., 2010). The presence of 5 µM of Al strongly decreases the amount of REE bound to HA, changing the log K_d^{REE} patterns, which increases for MREE (MREE downward concavity). The Al concentration rise from 5 to 20 µM decreases the amount of REE bound to HA, but does not influence the log K_d^{REE} pattern which remains essentially identical to that of the [Al] = 5 µM experiment. These data indicate that Al competes more strongly with HREE than LREE in these experiments promoting the REE complexation by strong multidentate sites, suggesting in turn that Al has a stronger affinity for these sites. Low concentration of Al (1 µM, in the present study) can suppress the metal loading effect developed for REE-HA binding since these sites are in low density on HA surface. Because fewer strong sites are available for REE, they can only bind to HA weak sites present in higher surface density. At pH 3, the main REE-HA binding sites are thus carboxylic ligands whose stability constants increase for MREE.

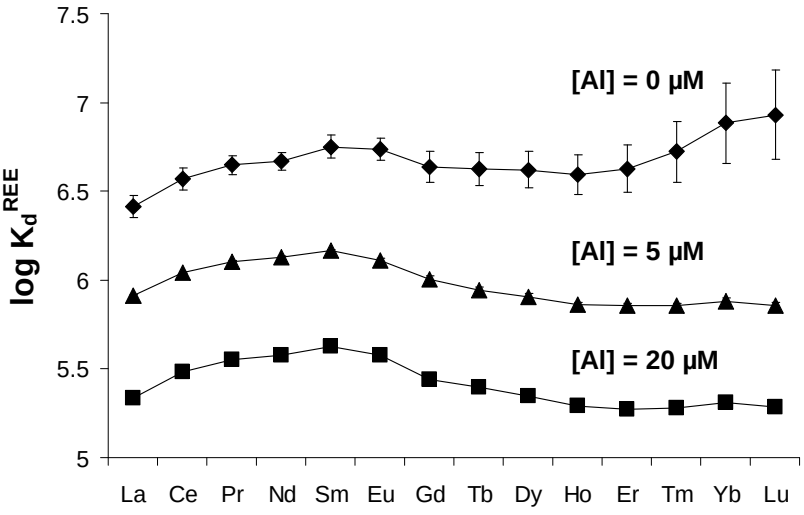

Figure IV.2. log K_d^{REE} patterns for REE, Al competitive binding to HA experiments at pH 3 and low REE/HA ratios (1.2 10^{-3} molREE/molC) as a function of Al concentration. Error bars represent standard deviation from triplicates (can be hidden by symbols).

Figure IV.3a presents the percentage of REE bound to HA for [Al] = 0 and 10 µM for the experiments conducted at high REE/HA ($2\ 10^{-2}$) and variable pH (3 to 6). Without Al, around 30% of REE are bound to HA at pH = 3, a value that reaches 95% at pH = 6. The presence of Al in equal amount to REE decreases the proportion of REE bound to HA. This decrease is not uniform as revealed by an inflection in the REE-HA sorption-edge, by contrast to experiment with Al which presents a sigmoid shape. This rupture of the sorption-edge in the REE-Al-HA experiment illustrates an apparent decrease of the Al competitive effect. Aluminium is hydrolyzed from pH< 6 and $Al(OH)_3$ precipitation might occur, decreasing dissolved Al concentration and hence the competition effect of Al on REE binding to HA.

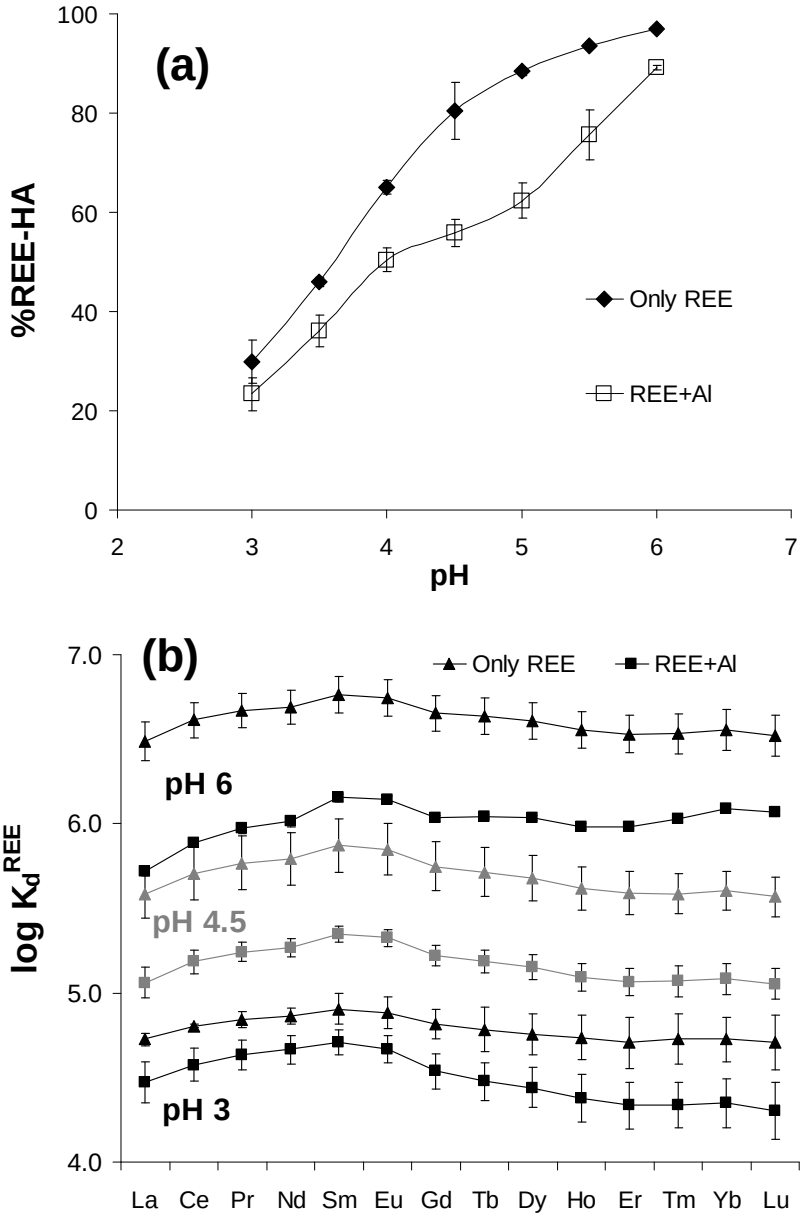

Figure IV.3. REE-HA binding for high REE/HA experiments: (a) effect of Al concentration on the % of REE bound to HA relative to pH. (b) log K_d^{REE} patterns with and without Al relative to pH.

Figure IV.3b compares the log K_d^{REE} patterns at pH = 3, 4.5 and 6 for the REE-HA and REE-Al-HA experiments. As previously observed at high REE/HA and any pH studied here, REE-HA experiments result in log K_d^{REE} patterns with a MREE downward concavity, specific of the predominant binding of REE with weak, high density carboxylic HA sites (Tang and Johannesson 2003; Pourret et al., 2007b; Marsac et al., 2010, and references therein). With Al, the LREE/HREE balance is progressively modified with increasing pH. At pH = 3, the competitive effect of Al is more pronounced for the HREE than for the LREE, and at pH = 6, Al displaces more strongly LREE than HREE (Fig. IV.3b). The corresponding change of the log K_d^{REE} pattern from a log K_d^{REE} pattern presenting a MREE downward concavity at pH = 3 to a log K_d^{REE} pattern slightly increasing for HREE at pH = 6 might be indicative of the type of HA sites that bind to Al and REE. At pH=3 with Al, the HREE depletion suggests the preferential binding of Al to the few strong multidentate HA sites as for low REE/HA. Conversely, the LREE depletion or HREE enrichment at pH = 6 points to the inability of Al to bind to HA phenolic sites. Marsac et al. (2011) showed that about 80% of HREE are bound to HA phenolic and carboxy-phenolic groups (i.e. phenol-containing groups) at pH=6. Conversely, at pH = 6, 80% LREE are bound to HA carboxylic groups. Therefore, Al appears to be a strong competitor of REE bound to COOH groups (i.e. mainly the LREE) than REE bound to phenol-containing groups (i.e. mainly the HREE). In turn, $Al(OH)_n^{(3-n)}$ species - which are the dominant Al species at pH = 6 - present stronger affinity for carboxylic groups than for phenolic groups.

3.2. Al and REE speciation modeling with PHREEQC/Model VI

The first step of the modeling strategy consists in the optimization of the $Al(OH)_3$ K_{SO} as $Al(OH)_3$ is expected to precipitate at the highest pH studied. The activity of Al^{3+} were calculated using PHREEQC from the dissolved Al concentration measured in solution (i.e. Al present in the ultrafiltrate (< 5 kDa), and plotted against pH (Fig. IV.4). According to eq. IV.2, the activity of Al^{3+} reaches a solubility limit corresponding to log K_{SO} = 9. This value is consistent with Al aqueous solutions equilibrated during 48h (IUPAC Stability Constants Database). Therefore, $Al(OH)_3$ solubility product was set equal to 9. As shown by Quinn et al. (2004), REE can bind to $Al(OH)_3$. However, the log K_d^{REE} on $Al(OH)_3$ are very low. From the experimental results of Quinn et al. (2004), the amount of REE adsorbed on $Al(OH)_3$ was

estimated to be lower than 1% in the present experimental conditions (Σ[REE] = [Al]), even if 100% of Al is considered to precipitate.

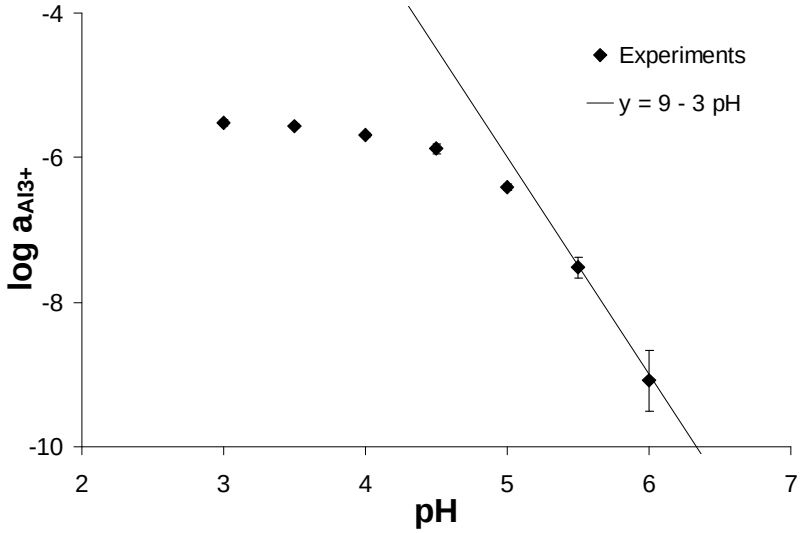

Figure IV.4. Log a_{Al3+} for Al-HA binding experiments at Σ[REE] = [Al] = 10µM and [DOC] = 6.7 mg L^{-1}. Log a_{Al3+} data were calculated from measured, dissolved (< 5 kDa) Al concentrations. The line (y = 9 - 3 pH) illustrates the control of Al activity by a $Al(OH)_{3(s)}$ phase with log K_{SO} = 9.

The above experimental results were first modeled using the Al-HA and REE-HA parameters determined by Tipping et al. (2002) and Marsac et al. (2011). In a second step, Al-HA binding parameters were optimized taking benefit of the constraints-set provided by the Al-REE competition experimental dataset. Figure IV.5 presents experimental and modeling pattern of the percentage of REE bound to HA in pH 3 experiments at low REE/HA and [Al] = 20 µM (Fig. IV.5a) and pH 6 and Σ[REE] = [Al] = 10 µM (Fig. IV.5b). The modeled results were obtained from Tipping et al. (2002) and Marsac et al. (2011) HA binding parameters for Al and REE, respectively. At low REE/HA, the experimental percentages of REE-HA present MREE downward concavity by contrast to the simulated pattern, which also exhibits a strong increase for HREE (Fig. IV.5a). At pH 6, Al competitive effect on REE and more particularly on LREE is underestimated: the simulated REE-HA percentage pattern presents MREE downward concavity, whereas the experimental percentages of MREE- and HREE-HA were similar (Fig. IV.5b). Calculated concentrations of REE bound to HA are plotted versus experimental results (log-log plot) for the whole studied conditions (Fig. IV.5c). The distance from the 1:1 line indicates a poorer fit. Therefore, Al competitive effect on REE-HA binding is not satisfactorily simulated. This discrepancy might be induced by the Al binding parameters used by Tipping et al. (2002) which are not appropriate to describe the Al

competitive effect on REE-HA binding. Model VI REE-HA binding parameters were determined by Marsac et al. (2011) from a large REE-HA binding dataset in a large range of pH and REE/HA conditions. By contrast, Al-HA parameters were determined from a more limited range of pH (<4.5) since Al-HA experimental datasets are limited (Tipping et al., 2002). Therefore, Al-HA binding parameters were optimized with PHREEQC/Model VI.

PHREEQC/Model VI requires the simultaneous adjustment of four parameters to describe Al binding by HA, namely: log K_{MA}, log K_{MB}, ΔLK_{2C} and ΔLK_{2P} which can generate a high degree of uncertainty on each parameter when individually taken. The Al-HA binding parameters cannot be directly fitted from the Al-HA concentration since the possible presence of $Al(OH)_3$ in the >5 kDa fraction prevents the quantification of the experimental Al-HA concentration. However, the Al competitive effects on REE-HA binding and REE-HA concentration provide two independent constraints namely: (i) Al^{+3} has strong affinity for HA -COOH, -PhOH and their corresponding multidentate groups (i.e. in competition mainly with HREE) and (ii) $Al(OH)_n^{(3-n)}$ have more affinity for HA -COOH than for -PhOH groups (i.e. mainly in competition with LREE).

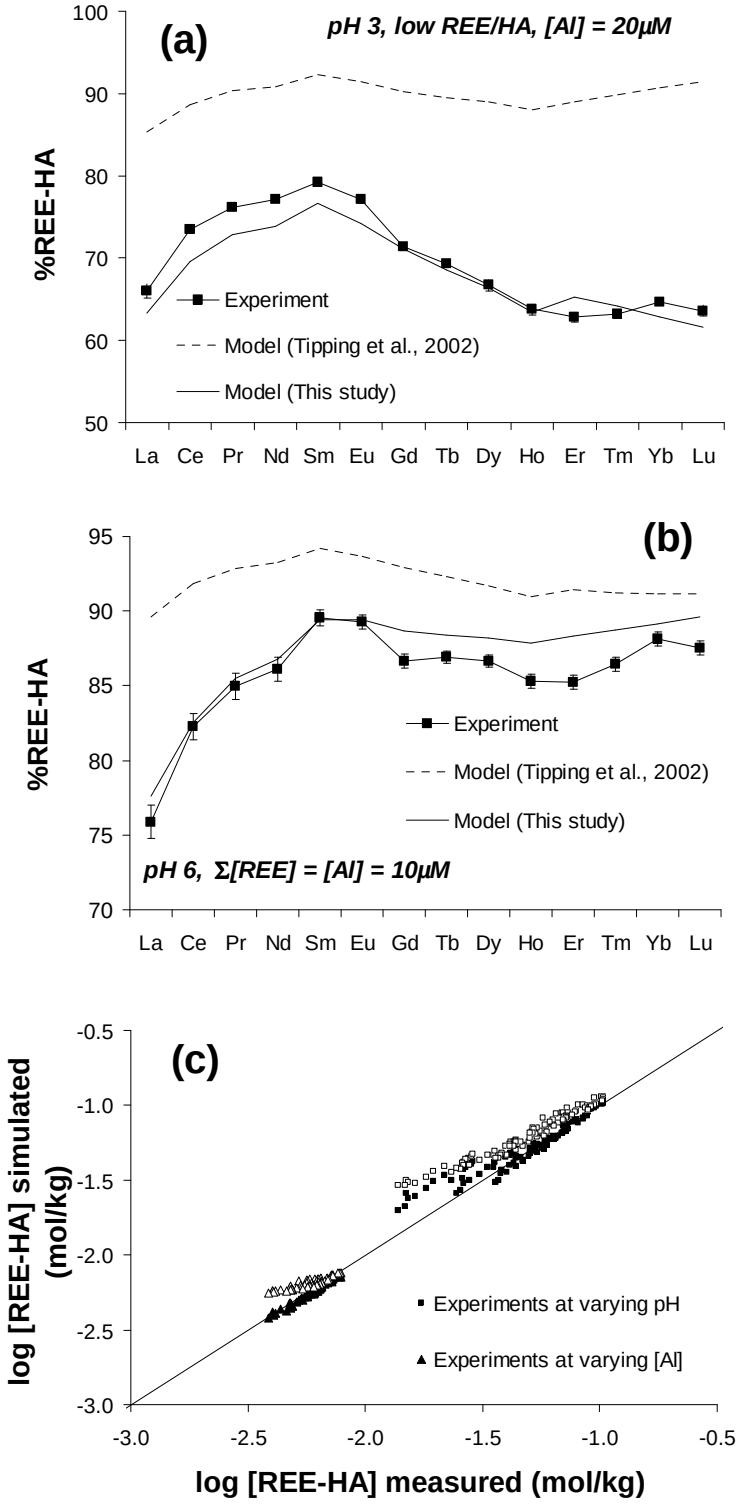

Figure IV.5. REE percentage bound to HA from experimental data and simulation using PHREEQC/Model VI, either in using Tipping et al. (2002) parameters (dotted line) or the optimized parameters determined in this study (plain line). (a) refers to the experiment conducted at pH 3, low REE/HA and [Al] = 20 µM, whereas (b) refers to the experiment performed at pH = 6, high REE/HA and with Σ[REE] = [Al] = 10 µM. (c) Diagram showing the correspondence between the measured and simulated amount of REE bound to HA (log-log plot) using Tipping et al. (2002) Al-HA parameters (open symbols) and optimized parameters (full symbols).

The new PHREEQC/Model VI HA binding parameters for Al were obtained by fitting experimental data recovered from the present study for REE-HA and Al>5kDa. The Al-HA binding datasets from Kinniburgh et al. (1999) and Weng et al. (2002) were also considered in our modeling study. The new PHREEQC/Model VI Al-HA binding parameters are reported in Table IV.1. To define Al^{3+} as a stronger competitor for HREE, log $K_{MB}(Al^{3+})$ and $\Delta LK_{2P}(Al^{3+})$ (6.20 and 6.00, respectively) were set higher than for Lu (5.23 and 5.11, respectively) since Lu presents the highest log K_{MB} and ΔLK_{2P}. The log $K_{MA}(Al^{3+})$ was set equal to 3 close to log K_{MA}(Lu) (3.16), which is the lowest log K_{MA} in the REE series. The REE ΔLK_{2C} are similar and range from 2.01 and 2.31 for La and Lu, respectively. $\Delta LK_{2C}(Al^{3+})$ was set equal to 1 to limit Al^{3+} competitive effect on LREE at low pH. The optimization of the Al-HA binding parameters improves the REE data fits at low REE/HA, pH = 3 and with [Al] = 20 µM. The underestimations of the Al competitive effect on REE-HA binding obtained with the initial Tipping et al. (2002) binding parameter are deleted. The calculated percentages of REE bound to HA present a MREE downward concavity as experimentally observed (Fig. IV.5a). At pH = 6 and high REE/HA, the fit improvement occurs through the introduction of the $Al(OH)_2^+$ species, which was not yet taken into account in Model VI (Tipping, 1998; Tipping et al., 2002). At pH = 5 to 6, $Al(OH)_2^+$ is the dominant Al species in solution (Fig. IV.1). The log K_{MA} for $Al(OH)_2^+$ was adjusted to 4.2, whereas log K_{MB} and strong binding site terms (ΔLK_2) were set equal to zero to limit $Al(OH)_2^+$ competition with HREE. The binding of $AlOH^{2+}$ was not taken into account in order to keep the same degree of freedom in both simulations. This optimization allows for the simulate of a stronger Al competitive effect at pH > 5 and high REE/HA (Table IV.1). Moreover, a better simulation is obtained as compared to simulations using Tipping et al. (2002) Al-HA binding parameters, rmse for REE being equal to 0.04 and 0.09, respectively, for these simulations. The fit improvement is illustrated on figure IV.5c, where simulated versus experimental log [REE-HA] are closer to the 1:1 line with the optimized parameters.

Parameter	Al^{3+}	$Al(OH)_2^+$	Al^{3+} / $AlOH^{2+}$
Log K_{MA}	3.00	4.20	2.6
Log K_{MB}	6.20	0.00	7.66
ΔLK_{2C}	1.00	0.00	0.46
ΔLK_{2P}	6.00	0.00	0.46

Table IV.1. log K_{MA}, log K_{MB}, ΔLK_{2C} and ΔLK_{2P} for Al^{3+} and $Al(OH)_2^+$ fitted from the experimental data using PHREEQC/Model VI. The log K_{MA}, log K_{MB}, ΔLK_2 (where $\Delta LK_2 = \Delta LK_{2C} = \Delta LK_{2P}$) data published by Tipping et al. (2002) using WHAM 6/Model VI, are shown for comparison (Al^{3+}/$AlOH^{2+}$).

The log K_{MA} of 4.2 required to take into account the $Al(OH)_2^+$ species is higher than log $K_{MA}(Al^{3+})$ (Table IV.1). This result is not entirely satisfactory since the successive hydrolysis constants of Al^{3+} decrease from 9 to 7.3 with the increasing number of OH, i.e. from $AlOH^{2+}$ to $Al(OH)_{3(aq)}$. Therefore, $Al(OH)_2^+$ should exhibit a binding constant with HA COOH groups lower than that of Al^{3+}. We tried to modify Marsac et al. (2011) Model VI parameters for REE: theoretically, by decreasing log K_{MA} for REE, $Al(OH)_2^+$ could have the same competitive effect for LREE with a lower, and therefore, more consistent log K_{MA}. However, this attempt led to a poor description of REE patterns in the REE-HA systems. Consequently, log K_{MA} value for $Al(OH)_2^+$ artificially equal to 4.2 was adopted to implicitly take into account the occurrence of other Al-HA binding mechanisms, which will be discussed in the following section.

Figure IV.6 compares experimental and simulated results for Al-HA binding. Figure IV.6a compared simulated log [Al-HA] obtained with the optimized Al-HA binding parameters versus experimental results for experiments at low REE/HA at pH 3 (the present study) and from Kinniburgh et al. (1999) and Weng et al. (2002). Fit are of good quality since the rmse for Al is equal to 0.03 and experimental and calculated Al-HA amount were similar in any conditions (Fig. IV.6a). The optimized Al-HA binding parameters did not improve the fit as compared with Tipping et al (2002) Al-HA binding parameters (rmse = 0.04). Figure IV.6b compares experimental and modeled results for the evolution of the percentage of Al > 5 kDa versus pH (i.e. the sum of Al bound to HA and of Al occurring as $Al(OH)_3$ precipitates). Modeling results using the parameters of Al Tipping et al. (2002) agree reasonably well with experimental data from pH 3 to 4.5 and 5.5-6.5, but not at pH 5, where Al > 5 kDa is underestimated of 20%. However, the optimized Al-HA binding parameters and the introduction of $Al(OH)^{2+}$ binding to HA limits this underestimation. Therefore, if the optimized Al-HA binding parameters do not strongly improve the Al-HA binding (except at pH 5 and high REE/HA), they strongly improve the modeling of Al competitive effect on REE-HA binding.

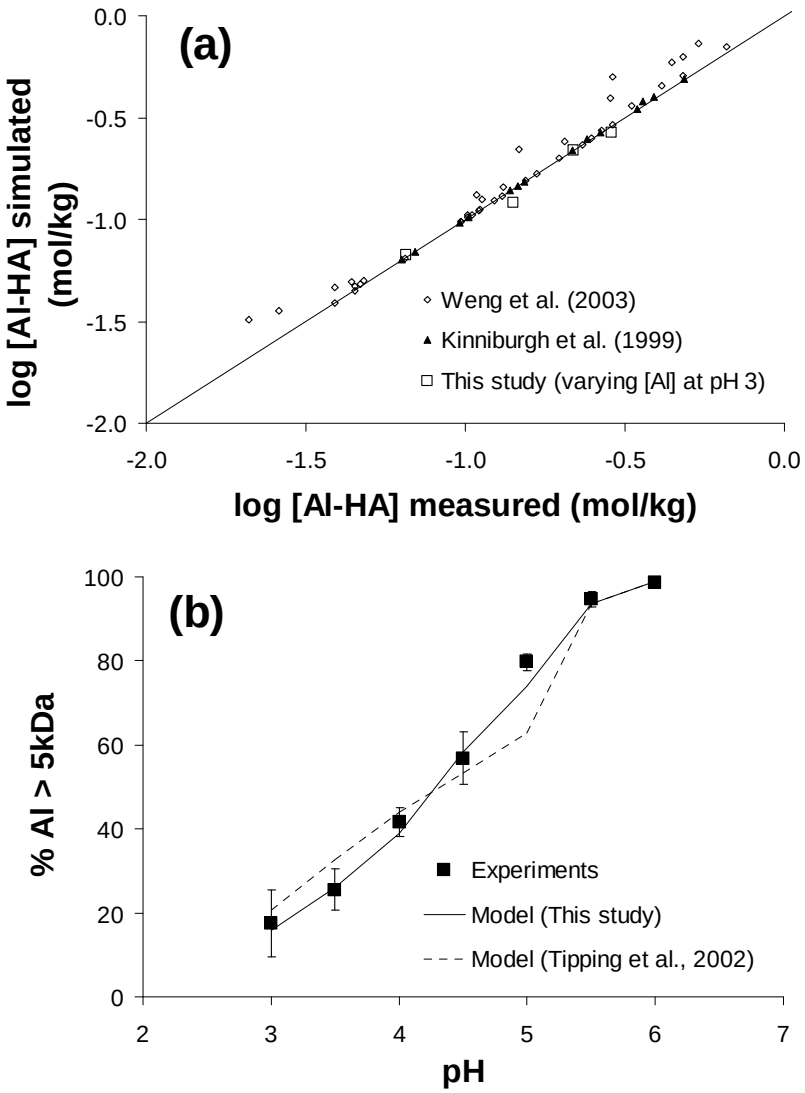

Figure IV.6. (a) Goodness of fit between experimental and simulated Al-HA amount using optimized PHREEQC/Model VI Al-HA parameters for literature data and the present study data at pH 3 and low REE/HA. (b) Percentage of Al present in the > 5 kDa fraction for experiments at Σ[REE] = [Al] = 10µM, [DOC] = 6.7 mg L^{-1} and pH 3-6. Lines represent results simulated with Tipping et al. (2002) parameters (dotted line) and optimized binding parameters (plain line) for Al.

4. Discussion

4.1. Al-HA interaction at pH > 5

The need of high $Al(OH)_2^+$ log K_{MA} raises the question of the nature of the involved Al species. One possibility is the existence of polynuclear Al-hydroxide species. Several authors suggested that polynuclear hydroxy-Al species could bind to fulvic acids (FA) especially at pH>5 (Browne and Discoll, 1993; Sutheimer and Cabaniss, 1997). Light Al polycations (i.e. dimers or trimers) are usually not stable in solution because they tend to

condense to form more stable Al tridecamer or gibbsite (Masion et al., 1994). However, Al dimers or trimers can be stabilized by organic acids (Casey et al., 2001), which prevents the formation of tridecamer species, particularly if the organic ligand is HA (Hiradate and Yamaguchi, 2003). Browne and Discoll (1993) suggested that fulvate could stabilize the formation of hydroxide-bridge bonds between two Al atoms. A possible formation reaction for these dimeric-Al hydroxides in the presence of HA could be as follows:

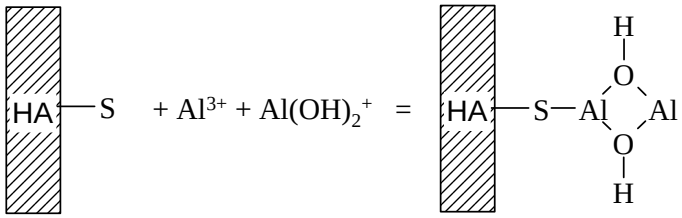

(IV.4)

where HA-S represents a HA binding site, which could be either mono- or multidentate (electric charges of HA sites and H_2O ligands have been omitted for simplicity). Introducing the reaction (IV.4) in PHREEQC/Model VI is however unlikely to result in higher competitive effect on REE-HA binding because the Al-dimer occupies only one HA site. One way to achieve this competitive effect would be to consider a reaction in which both Al atoms of the Al-hydroxide dimer would be bound to two HA sites. Such a reaction could be as follows:

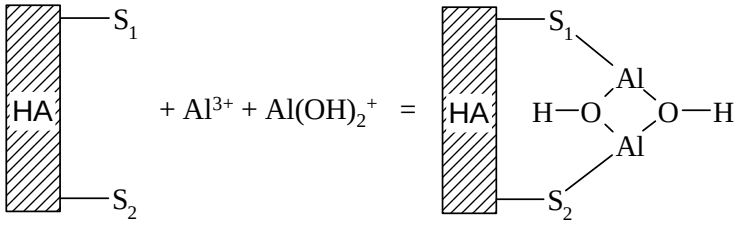

(IV.5)

Where HA-S_1 and -S_2 represent two different HA sites. This mechanism cannot be introduced easily in PREEQC/Model VI because of the description of HA sites as discrete groups. Therefore, we suggest that the artificially high log K_{MA} for $Al(OH)_2^+$ implicitly take into account the stabilization of hydroxy-bridge bonding between Al by HA. The simulation, in doing so, is clearly not realistic from a mechanistic point of view, but the implementation of this artificial value is able to reproduce satisfactorily the effects of reaction (IV.5) on the Al-REE competition (Fig. IV.5b). Tipping et al. (2002) chose to neglect the role of Al-hydroxide dimers in their description of Al-HA interactions because the consideration of these dimers did not improve significantly the fit, as it is observed in the present study (Fig. IV.6). The situation is different when the point is to evaluate the competition between Al and other cations for HA binding. The results obtained here for Al-REE competition demonstrate that the competitive effect of Al is considerably strengthened by the presence of Al-dimers. To

date, this competitive effect of Al-dimers was not revealed because Al competitive effect on cation-humic binding was generally studied at pH < 5 (Mota et al., 1996, Kinniburgh et al., 1999; Pinheiro et al., 2000). The present experimental results and the artificially high log K_{MA} $Al(OH)_2^+$-HA clearly show that Al-HA interactions occur mainly by carboxylic HA sites rather than by phenolic HA sites. Thus, under the circumneutral pH conditions characteristic of most natural waters, Al is therefore expected to be a significant competitor of trace metals and radionuclides presenting a high binding affinity for HA carboxylic groups as compared to phenolic groups such as LREE.

4.2. Al-competition effect on the REE pattern shape of natural organic-rich waters

Numerous studies established that dissolved organic matter (DOM) controls the REE speciation in natural, organic-rich waters (Bidoglio et al., 1991; Takahashi et al., 1997; Viers et al., 1997; Dia et al., 2000; Johannesson et al., 2004; Gruau et al., 2004; Davranche et al., 2005; Pourret et al., 2007a; Pédrot et al., 2008). Laboratory experiments here performed as well as previous studies meanwhile established that HA binding has the potential of fractionating REE depending on the involved HA binding sites and REE/HA ratio (Sonke and Salters, 2006, Pourret et al., 2007b; Yamamoto et al., 2010; Marsac et al., 2010; 2011). For low REE/HA, when REE-HA binding occurs mainly through strong multidentate sites, REE patterns of natural, organic-rich waters are expected to show a progressive increase from La to Lu. By contrast, when REE-HA binding is dominated by weak carboxylic sites (i.e. for high REE/HA), patterns are expected to exhibit a MREE downward concavity (Yamamoto et al., 2010; Marsac et al. 2010). By compiling data from natural, organic-rich waters, Marsac et al. (2010) recently showed that REE patterns effectively displayed variations that could be partly due to the REE/HA (or metal loading) effect. The true occurrence of this effect is however challenged by other mechanisms able to potentially fractionate REE. The competitive effect generated by other cations such as Al and Fe is one possible mechanism (Tang and Johannesson, 2010). Yamamoto et al. (2010) suggested that even low concentrations of Al and Fe could delete the above “low REE/HA” fractionation process. The experiments at pH 3 and low REE/HA reported in the present study show that Al competition has effectively the potential of limiting the higher HREE-HA binding confirming this suggestion. However, at pH > 5, the contrary is observed. Aluminium occurrence decreases LREE binding to HA. Therefore, these results show that the Al binding to HA in circumneutral waters could promote HREE enrichment in the dissolved fraction (i.e. < 0.2 µM) due to HREE higher

affinity for HA binding as compared to that of LREE. In another words, Al competition with REE at circumneutral pH enhances the metal loading effect on REE-HA pattern.

A loss of REE signatures specific of HA binding may be also observed in waters where carbonate ligands compete with HA for REE binding (Elderfield et al., 1990; Tang and Johannesson 2010). REE affinity follows HA > carbonate > FA. When REE binding with HA dominates the REE speciation (i.e. at high HA concentration), MREE-increased patterns are expected due to the dominant role of carboxylic sites. By contrast, when REE binding by carbonate dominates (at low HA concentration), HREE-enriched patterns is expected as log K(REE-carbonate) increase from LREE to HREE (Luo and Byrne, 2004). This competitive effect of carbonate is however highly pH-dependent. Pourret et al. (2007b) showed that carbonate could bind significantly REE (> 10%) only at pH > 7.5 in organic-rich waters. This limited effect was highlighted by Marsac et al. (2010) who reported marked variations of REE patterns for selected natural organic-rich waters with pH < 7, in which REE binding by carbonates is anticipated to be insignificant. Results both reported by Yamamoto et al. (2010) and Marsac et al. (2010), and presented in this study show that HA can act as a preferential carrier either for MREE or HREE, depending on the REE/HA conditions. However, we will not try here to evaluate precisely the relationship between REE pattern and Al concentrations in natural waters because the amount of Al that truly competes with REE cannot be easily determined. Concentrations of competitive Al are strongly pH-dependent because of Al hydroxides solubility. Furthermore, a fraction of the Al measured in the dissolved fraction (< 0.2 or 0.45µm) of natural waters can be present as Al hydroxides associated with organic matter (Pokrovsky et al., 2006), thereby distorting the evaluation of the Al amount available for competition with REE. As a consequence, the amount of competitive Al can only be assessed from geochemical models, making this assessment complicated and sometimes questionable. Another problem is that other cations are expected to be able to compete with REE for HA binding in natural waters. Among these cations, Fe could be a strong competitor of REE (Lippold et al., 2007), with effects on REE pattern not yet experimentally evaluated. Accordingly, without more information on the role of other cations including Fe, any attempt to determine precisely how and to what extent the competition with Al affect the REE pattern of natural, organic-rich waters is a difficult exercise that appears to us more reasonable to postpone before getting more experimental data and modeling as well.

The present study confirms that the REE-HA pattern depends on the REE speciation on HA and can be used as a fingerprint of the dominant HA binding sites in given pH or REE/HA conditions. Modification of REE speciation on HA - and thus in REE-HA pattern -

is expected to occur not only in response to variations of REE/HA ratio but, to the occupation of HA sites by competitor cations, such as Al. Marsac et al. (2011) suggested that different effects on REE-HA pattern are anticipated depending on the affinity of competitor cations for carboxylic and phenolic sites. At pH > 5, the competitive effect of Al, occurring mainly for LREE, confirms this hypothesis. Up to now, predictions of REE speciation in natural, organic-rich waters were performed using Model VI (or the previous version Model V), using generic parameters for other cations (Tang and Johannesson, 2003; Pourret et al., 2007b). These predictions could only give information about the total amount of REE displaced by the competitor cation but, not on the competition effect on the 14 REE taken individually. Generic cation-HA binding parameters commonly used in Model VI are those determined initially by Tipping (1998) applying a linear relationship between carboxylic and phenolic parameters. The cations present therefore the same relative affinity for HA carboxylic and phenolic functional groups. Even if this assumption gives satisfactory modeling results for competitive experiments between two cations (Tipping, 1998; Peters et al., 2001; Tipping et al., 2002), the present REE-Al competition study shows that these generic parameters are not mechanistically sufficient to describe the effects of cation competition on REE pattern. To use geochemical models as a reliable tool to describe REE patterns in natural, organic rich-waters, a more accurate description of the different competitor cations binding behavior with HA is clearly required. In this perspective, further experimental studies of cation-REE competitive binding to HA are required, which might in turn take benefit of the “REE fingerprint” set up in this and previous studies to further highlight the complex mechanisms involved in cation binding to HA.

5. Summary

The competition experiments between REE and Al show different Al competition effects depending on the pH and the REE/HA ratio. Under acidic (pH = 3) and low REE/HA conditions, Al^{3+} as the dominant Al species compete more strongly with HREE than with LREE. Therefore, Al^{3+} has high affinity for the low concentration of HA strong multidentate sites. Under higher pH ranging from 5 to 6 and higher REE/HA conditions, the competition is higher for LREE than for HREE, suggesting a strong interaction of Al with HA carboxylic groups. PHREEQC/Model VI Al-HA binding parameters were optimized to simulate precisely both Al binding to HA and its competitive effect on REE. Al-HA interaction at pH >5 was simulated by the strong binding of $Al(OH)_2^+$ to HA carboxylic groups. The requirement of high binding log K_{MA} between HA carboxylic groups and $Al(OH)_2^+$ indicated

that hydrolyzed species other than $Al(OH)_2^+$ were involved in the complexation. Polynuclear hydroxy-Al complexes are expected to be bound to HA. The polynuclear Al species binding reactions could not be introduced in PHREEQC/Model VI because they should involve higher denticity sites than those defined in the model. The present study provides fundamental knowledge on Al-REE competitive mechanisms for HA binding. Aluminium competitive effect depends clearly on the affinity of the different Al species for carboxylic, phenolic or chelate ligands and therefore can modify the REE-HA pattern. From our experimental results, we can conclude that, the presence of Al should enhance the metal loading effect on REE-HA pattern (i.e. an increase from LREE to HREE) since Al is not expected to bind efficiently neither to HA phenolic groups nor to the low amount of HA strong multidentate groups. As deduced from the different behavior depicted by the different Al species, other potential competitor cations such as Fe are expected to have their own competitive effect on REE-HA binding. Therefore, a precise knowledge of the exact behavior of the different REE competitor cations is required in order to reliably understand and model REE-HA pattern variations in natural waters. Finally, the REE-HA patterns resulting from Al competition were used as a probe to evaluate the ability of the different Al species to bind with the different sites - carboxylic, phenolic or chelate ligands. This ability of the REE to be used as a “speciation probe” could be applied to other cations in order to precisely describe their interactions with HA.

V. Chapitre IV :

Compétition entre terres rares et fer pour la complexation par les acides humiques

Iron competitive effect on REE binding to organic matter: implications with regards to REE patterns in waters

Cette partie est extraite d'un article en préparation pour Geochimica et Cosmochimica Acta, Marsac R., Davranche M., Gruau G, Dia A., Pédrot M., Bouhnik-Le Coz M. and Briant N. Iron competitive effect on REE binding to organic matter: implications with regards to REE patterns in waters.

Résumé- Les mécanismes de compétition entre terres rares (REE) et fer (Fe) pour la complexation par les acides humiques (HA) ont été étudiés expérimentalement, entre pH 3 et 6, et par modélisation avec PHREEQC/Model VI. Cette étude a pour but de déterminer l'effet de compétition de Fe sur la complexation des REE par HA et, réciproquement, d'utiliser le spectre de REE résultant en tant que témoin des mécanismes de complexation de Fe par HA. Cette étude apporte donc de nouvelles informations quant aux processus de complexation de Fe par la matière organique dans l'environnement. Les expériences montrent qu'à pH = 3, Fe^{3+} est un plus fort compétiteur pour les REE lourdes (HREE) et, par conséquent, se complexe préférentiellement aux sites forts multidentates de HA, présents en faible quantité. A des pH plus élevés (e.g. pH = 6), même si des hydroxydes de Fe précipitent, Fe devient compétiteur de manière équivalente pour l'ensemble des REE et, réciproquement, a une forte affinité que ce soit pour les groupements carboxyliques ou phénoliques de HA. Ce comportement a été attribué à la complexation de trimères de Fe par HA. La complexation de $Fe_3O_2^{5+}$ a été définie par la complexation $Fe_{1.5}O^{2.5+}$, permettant de simuler la complexation d'un trimère de Fe par deux sites discrets de l'HA définis dans PHREEQC/Modèle VI (mono-, bi- ou tridentates). Bien que PHREEQC/Model VI tienne compte de la formation de complexes Fe-HA mononucléaires et polynucléaires, la spéciation de Fe n'est pas totalement cohérente avec les observations faites lors de précédentes études par spectroscopie. D'autres espèces telles que $FeOH^{2+}$ pourraient également se complexer aux HA mais n'ont cependant pas pu être pris en compte. Cette étude suggère que la variabilité des spectres de REE observée dans les eaux riches en matière organique – où la spéciation des REE est contrôlée par la matière organique dissoute – pourrait être due (i) à la charge en métaux sur HA, (ii) aux cations compétiteurs des REE pour la complexation par HA et (iii) au pH.

Abstract- Competitive mechanisms between rare earth elements (REE) and iron (Fe) for humic acid (HA) binding were experimentally investigated between pH 3 and 6 and by modeling using PHREEQC/Model VI. This study aimed at determining Fe competitive effect on the REE-HA complexation pattern and, in turn, to use the resulting pattern as a probe of Fe-HA binding mechanisms investigation. This could therefore provide new insights in Fe-organic matter binding process understanding within the environment. At pH = 3, Fe^{3+} appears to be a strong competitor for heavy REE (HREE) and, therefore, has strong affinity for the few HA strong multidentate complexing sites. At higher pH (e.g. pH = 6), even when Fe (hydr)oxides are expected to precipitate, Fe competes equally for every REE and, therefore, has high affinity for both HA carboxylic and phenolic sites. Such Fe behavior was

attributed to the binding of Fe trimer to HA. The binding of $Fe_3O_2^{5+}$ to HA was defined by the binding of $Fe_{1.5}O^{2.5+}$, which assumes the binding of the Fe trimer to two PHREEQC/Model VI HA types of discrete sites (mono-, bi- or tridentate). Although, PHREEQC/Model VI simulation takes into account the formation of monomeric and polymeric Fe-HA complexes, calculated Fe speciation and spectroscopic observations show that the model is not entirely consistent. Additional Fe species, such as $FeOH^{2+}$, may bind to HA but could not here be taken into account. This study suggests that REE pattern variability in organic-rich waters - where dissolved organic matter controls the REE speciation - may be due to (i) HA metal loading, (ii) REE competitor cations for HA binding and (iii) pH.

1. Introduction

Organic colloids such as humic acids (HA) are ubiquitous in natural environment and present a high binding capacity for dissolved metals. Remarkable effort has been made for more than two decades to elucidate processes involved in cation binding by HA, through experimental and modeling approaches (e.g. Tipping, 1998; Milne et al., 2003 and references therein). However, mechanisms controlling cation complexation to HA are not fully understood because of the complex structure of HA as assessed by a large heterogeneity of occurring binding sites. Rare earth elements are a group of fourteen elements whose unique chemical properties make them highly sensitive to HA site heterogeneity. Patterns of REE partition coefficient between HA and aqueous solution (K_d^{REE}) exhibit specific shapes depending on the binding conditions. In turn, the K_d^{REE} pattern can be interpreted as the fingerprint of the major type of HA site, which binds REE in given conditions. In experiments performed at low REE/HA concentration ratio, K_d^{REE} increases from light REE (LREE) to heavy REE (HREE) and is specific to REE binding by strong multidentate ligands, which are present in low concentration in HA molecules (Sonke and Salters, 2006; Marsac et al., 2010; Yamamoto et al., 2010). At high REE/HA and pH 3, K_d^{REE} pattern exhibit an increase for middle REE (MREE) which is specific to REE binding by the abundant and weak HA carboxylic sites (Tang and Johannesson 2003; Pourret et al., 2007b). At high REE/HA for pH 6, K_d^{REE} pattern displays also an increase for middle REE (MREE). However, Marsac et al. (2011a) demonstrated that HA carboxylic sites control LREE-HA binding, whereas HA phenolic groups control HREE-HA binding. This result was obtained by both introducing the specific humic-ion binding Model VI, developed by Tipping (1998) in the geochemical speciation program PHREEQC, as well as new hypotheses proposed for REE-HA binding (Marsac et al., 2011a). LREE and HREE are therefore bound to different preferential HA sites

depending on the prevailing conditions. Thereby, these results suggest that REE competitor cations may variously influence the LREE- or HREE binding with HA depending on their own affinity for carboxylic, phenolic or strong multidentate HA sites. In turn, the resulting K_d^{REE} pattern might be used as a tool to identify the preferential HA binding sites of the considered cations. This hypothesis was recently tested by Marsac et al. (2011b) in a study dedicated to REE-Al competitive binding to HA. At low REE/HA and pH = 3, Al^{3+} appeared to be a stronger competitor for HREE than LREE because Al^{3+} presents a high affinity for HA strong multidentate sites. At high REE/HA and pH = 6, Al is more competitive for LREE than HREE. A stabilization of hydroxy-Al polymers (typically dimers) by HA carboxylic sites may explain such results. Both HA heterogeneity of binding sites and REE competitor cations might account for the variability of REE patterns observed in organic-rich waters, wherein REE speciation is controlled by humic substances (Viers et al., 1997; Dupré et al., 1999; Dia et al., 2000; Johannesson et al., 2004; Gruau et al., 2004; Pédrot et al., 2008).

Iron is one of the most abundant elements on earth and the importance of studying its biogeochemistry is well established. Despite the low solubility of Fe (hydr)oxides, high concentrations can be found in organic-rich waters, associated with organic colloids (Olivié-Lauquet et al. 1999; Allard et al. 2004; Pokrovsky et al., 2005; Pédrot et al., 2011). Indeed, Dissolved Organic Matter (DOM) inhibits the formation of crystalline Fe (hydr)oxides to form instead both Fe nano-(hydr)oxides coated with DOM and Fe(III)-DOM complexes. Therefore, Fe plays a major role in trace metals and radionuclide speciation because of its strong competitive effect on cations binding to HA (Tipping et al., 2002) and especially REE (Tanizaki et al., 1992; Tang and Johannesson, 2003; Lippold et al., 2007). However, Fe competitive effect on the whole REE group binding to HA has not been yet studied. Recent spectroscopic studies demonstrated that, at high Fe/HA ratio, Fe polynuclear species are bound to HA (dimers or trimers) whereas, at low Fe/HA, monomeric Fe-HA complexes are formed (Karlsson and Persson, 2010). Using the Stockholm Humic Model (SHM), Gustafsson et al. (2007) simulated satisfactorily Fe binding and its competitive effect on various cations binding to organic soils. They only took into account the Fe dimers binding to organic matter tridentate sites. Model VI considers Fe^{3+} and $FeOH^{2+}$ binding to HA but not the binding of Fe polymers. Therefore, no currently available humic-ion binding model takes into account the formation of both monomeric and polymeric Fe-HA complexes.

This study aimed at assessing the competitive effect of Fe on REE binding to HA and in turn at identifying the HA surface sites and mechanisms involved in the Fe-HA binding. REE-Fe-HA binding experiments were thus performed over a pH range (3 to 6),

simultaneously for the fourteen REE and Fe. The binding of Fe to HA was simulated using PHREEQC/Model VI and Fe speciation was compared with previous spectroscopic studies in order to verify the consistency of the model. Finally, a large dataset of REE patterns in natural organic-rich waters were compiled to determine whether Fe and Al might effectively affect REE patterns through their competitive effect on REE-HA binding.

2. Materials and methods

2.1. PHREEQC/Model VI

Humic ion-Binding Model VI (hereafter referred to as Model VI) is a model developed by Tipping (1998), which is implemented in the geochemical program WHAM 6. Model VI equations were recently introduced into the PHREEQC (version 2) developed by Parkhurst and Appelo (1999) for the whole REE group. PHREEQC (version 2) is a computer code based on an ion-association aqueous model, which was designed to perform speciation and saturation-index calculations in waters. PHREEQC/Model VI coupling allowed improving REE-HA binding description notably by removing the linear relationship between Model VI carboxylic- and phenolic-cation binding parameters (Marsac et al., 2011).

In Model VI, HA are described as discrete acido-basic chemical functional groups (carboxylic and phenolic) able to bind aqueous metal ions (e.g. La^{3+} or Fe^{3+}) and their first hydrolysis product (e.g. $LaOH^{2+}$ or $FeOH^{2+}$), forming either monodentate, bidentate or tridentate complexes. In the present study, the $FeOH^{2+}$ binding to HA was replaced by a Fe polymer binding which limits the number of adjustable parameters. In practice, thanks to Tipping's (1998) work, cation stability constants are adjusted using 2 parameters, log K_{MA} and log K_{MB}, respectively for carboxylic and phenolic groups. Another parameter (ΔLK_2) is introduced to increase cation stability constants with a fraction of the multidentate sites, considering them as chelate ligands or involving additional chemical groups, such as nitrogen containing groups. To accurately simulate REE-HA binding, Marsac et al. (2011a) demonstrated that the ΔLK_2 parameter had to be optimized independently for carboxylic (ΔLK_{2C}) and phenolic groups (ΔLK_{2P}). An electrical double layer, where only counter-ions can accumulate, is also defined in the model. The double layer thickness is set by the Debye-Hückel parameter $\kappa = (3.29 \times 10^9 \times I^{1/2})^{-1}$ (Appelo and Postma, 2005). The distribution of ions between the diffuse layer and the bulk solution is calculated by a simple Donnan model. Intrinsic equilibrium constants are corrected by the Boltzmann factor that depends to HA

surface area, which was determined to be equal to 19000 and 15000 m²/g at ionic strength of 0.01 and 0.7M, respectively (Marsac et al., 2011). In the present study, HA was defined as the SOLUTION_MASTER_SPECIES, SOLUTION_SPECIES and PHASES in the PHREEQC database. The 80 types of sites considered by Model VI to bind REE, Fe and their respective first hydrolysis products were defined as SURFACE_MASTER_SPECIES, and their respective stability constants as SURFACE_SPECIES in the PHREEQC database. Fe hydroxide precipitation was also taken into account by defining $Fe(OH)_3$(ha) - noted "ha" for the experiments carried out in the presence of HA - in the PHASES block of PHREEQC database. The control of Fe^{3+} activity by the precipitation of $Fe(OH)_3$ was described following the reaction:

$$Fe(OH)_3 + 3H^+ = Fe^{3+} + 3H_2O \qquad K_{SO} \qquad (V.1)$$

Errors between experiments and simulations were quantified by the root mean square error of the regression (rmse), i.e. the sum of the squares of the differences between observed and calculated log υ, where υ is the amount of REE bound to HA per gram of dissolved organic carbon (DOC). The fit goodness was considered of quality if two conditions are fulfilled, (i) the total rmse calculated from the whole experimental conditions and REE must be low, and (ii) the rmse values calculated for the fourteen REE must be sufficiently close to each other.

2.2. Reagents

All chemicals used were of analytical grade. All experimental solutions were prepared with doubly-deionised water (Milli-Q system, Millipore™). Synthetic REE solutions were prepared from a nitrate REE standard (10 mg L^{-1}, Accu Trace™ Reference Standard). Polyethylene containers used to reach REE-HA complexation equilibrium were all previously soaked in 10% Ultrapure HNO_3 for 48h at 60°C, then rinsed with deionised water for 24h at 60°C to remove all REE contamination sources. All experiments were performed at room temperature, i.e. 20°C ± 2.

Purified humic acid (HA) was obtained from synthetic Aldrich humic acid (Aldrich™, H1, 675-2). The purification was performed with the protocol of Vermeer et al. (1998), except that a tangential ultrafiltration step was added to remove any possible HA molecules <10 kDa using a Labscale TFF system equipped with a Pellicon XL membrane (PLCGC10, Millipore™). Humic acid was freeze-dried and stored in a glass container. Prior to use, purified HA was solubilized overnight in a solution of 0.01 M NaCl at pH = 10 to ensure

complete dissolution (Vermeer et al., 1998). The pH was adjusted to 3 in the HA suspensions, which were then filtered at 0.2µm to remove any potential precipitate and therefore to ensure studying the same HA fraction in any experiments performed even at high pH. The dissolved organic carbon (DOC) concentration of the filtrates was then measured to assess the true HA concentration of the experimental suspensions.

2.3. Experimental set-up of REE and Fe competitive binding by HA

The experimental set-up for Fe-REE competitive binding to HA described in the following paragraph, was based on calculated REE distribution on HA functional groups using PHREEQC/Model VI. Calculations were performed for Σ[REE] = 10 µM, [HA] = 6.7 mg L^{-1} of carbon, an ionic strength equal to 0.01 M (NaCl) and for pH = 3 and 6. These conditions correspond to those used by Marsac et al. (2011b) for REE-HA binding. At pH 3, REE are mainly distributed between HA carboxylic and strong multidentate sites because phenolic sites are highly protonated. At pH = 6, HA sites can be divided into two groups: the carboxylic HA sites and the phenol-containing sites. This latter group merges carboxy-phenolic and phenolic HA sites. Figure V.1 represents the relative distribution of REE on the various HA sites. At pH 3, REE are mainly bound to carboxylic groups, except for HREE which are bound up to 50% with strong multidentate sites (i.e. for Lu). At pH 6, more simple phenol-containing sites are deprotoned and thereby bind REE. HREE speciation on HA sites is dominated by phenol-containing sites (70% for Lu), whereas LREE remain mainly bound to HA through carboxylic sites (80% for La). Thereby, according to PHREEQC/Model VI, the potential Fe competitive effect should involve (i) a decrease of LREE-HA binding under any pH conditions when REE are bound to HA carboxylic sites, (ii) a decrease of HREE-HA binding at pH 6 when REE are bound to phenol-containing sites and (iii) a decrease of HREE-HA binding at pH 3 when REE are bound to strong multidentate sites. Experiments of REE-Fe-HA competitive binding were therefore performed at pH ranging from 3 to 6 at high REE/HA ratio (∑[REE] = 10 µM; DOC = 6.7 mg L^{-1}; REE/HA = 2 10^{-2} molREE/molC) and ∑[REE] = [Fe] = 10 µM. A standard batch equilibrium technique was used. The fourteen REE and Fe were simultaneously added to HA solution set in a 10^{-2} M (NaCl) electrolyte solution. Experimental solutions were stirred for 48 h to reach equilibrium according to the protocol defined by Pourret et al. (2007b). The pH was regularly monitored with a combined Radiometer Red Rod electrode, calibrated with WTW standard solutions (pH 4 and 7). The accuracy of pH measurements was ±0.05 pH units. At equilibrium (48 h), 10 mL of the

suspension were sampled and ultra-filtered at 5 kDa to separate the REE-HA and Fe-HA complexes from the remaining inorganic REE and Fe. Ultrafiltrations were carried out by centrifuging the solution aliquots through 15 mL centrifugal tubes equipped with permeable membranes of 5 kDa pore size (Vivaspin 15RH12, Sartorius). All the membranes used were first washed with 0.15 mol L^{-1} HCl, then rinsed twice with ultrapure water to minimize contamination. Centrifugations were performed using a Jouan G4.12 centrifuge with swinging bucket rotor at 3000g for 30 minutes. Removing of HA fractions <10 kDa in the HA pristine solution ensures that no organic molecules pass through the 5 kDa membrane at this stage of the experiments. All experiments were performed in triplicate.

For comparison, experimental results of REE-HA binding without Fe were obtained from Marsac et al. (2011b). Speciation calculations carried out with PHREEQC demonstrated that all inorganic REE could be confidently assumed to occur as free aqueous REE^{3+} species in the two series of experiments. The REE inorganic speciation was modeled accordingly (Tang and Johannesson, 2003; Pourret et al., 2007b; Marsac et al., 2010). Conversely, Fe may be distributed as Fe^{3+}, $FeOH^{2+}$ and $Fe(OH)_2^{+}$ species and may precipitate as $Fe(OH)_3$ depending on pH. Hydrolysis constants for Fe were taken from Milne et al. (2003).

The REE complexation with HA is described using the apparent partition coefficient K_d, as follows:

$$K_d(Ln_i) = \frac{\mu g Ln_i \text{ adsorbed } L^{-1}/g \text{ DOC } L^{-1}}{\mu g Ln_i^{3+} mL^{-1}} \quad (V.2)$$

where Ln_i = La to Lu.

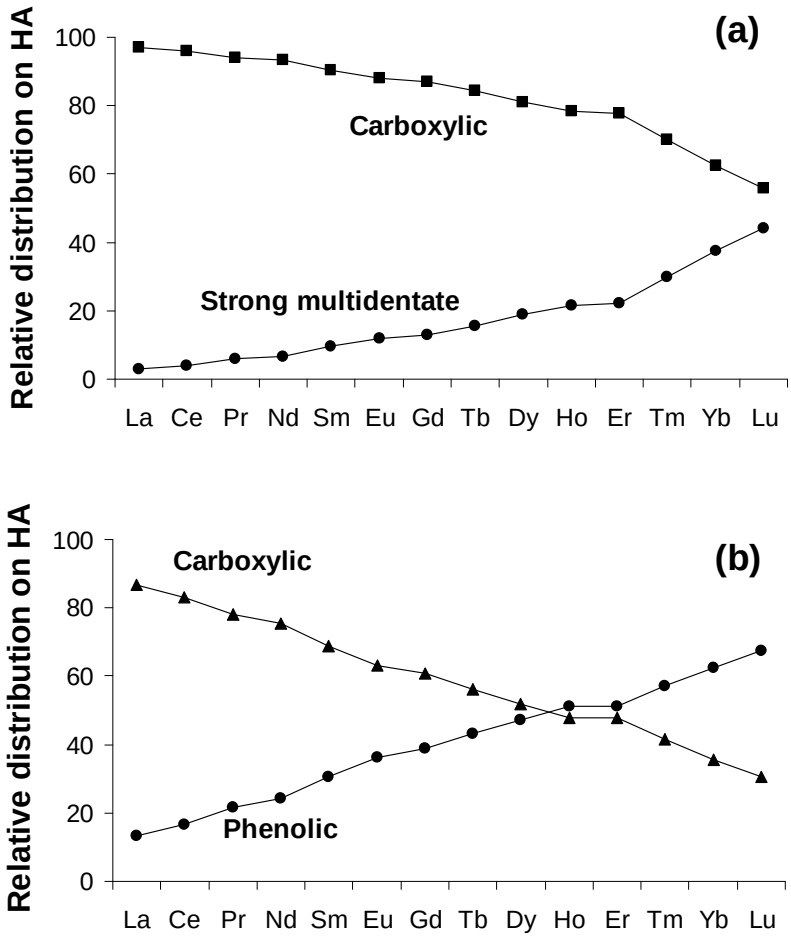

Figure V.1. Relative distribution of REE between the three major HA sites binding REE, at high REE/HA concentration ratio (Σ[REE] = 10 µM, [DOC] = 6.7 mg L^{-1}). The dominant sites are (a) carboxylic and strong multidentate sites at pH=3 and (b) carboxylic and phenolic sites at pH=6.

2.4. Solution analysis

Rare earth elements and Fe concentrations (>30 µg.L^{-1}) were determined with an Agilent Technologies™ HP4500 ICP-MS instrument. Ultrafiltrate, containing Fe and REE inorganic species, were directly injected after adding HNO_3 to a concentration of 0.37 N. The initial suspensions were also analyzed to precisely determine the total REE and Fe concentrations for each experiment. The suspensions were first digested with sub-boiled nitric acid (HNO_3 14 N) at 100°C, and then resolubilized in HNO_3 0.37 N after complete evaporation, to avoid interferences with organic carbon during mass analysis by ICP-MS. Quantitative analyses were performed using a conventional external calibration procedure. Three external standard solutions with REE and Fe concentrations similar to the analyzed samples were prepared from a multi-REE and a Fe standard solution (Accu Trace™

Reference, 10 mg L^{-1}, USA). Indium was added to all samples as an internal standard at a concentration of 0.87 µmol L^{-1} (100 ppb) to correct instrumental drift and possible matrix effects. Indium was also added to the external standard solutions. Calibration curves were calculated from measured REE/indium and Fe/indium intensity ratios. As established from repeated analyses of multi-REE standard solution (Accu Trace™ Reference, USA) and SLRS-4 water standard, the instrumental error on REE and Fe analysis are below 3 and 5 %, respectively. Iron concentrations < 30 $\mu g.L^{-1}$ were analyzed using a furnace atomic adsorption spectrometer (SOLAAR M6, THERMO).

Dissolved organic carbon concentrations were determined using a Shimadzu 5000 TOC analyzer. The accuracy of DOC concentration measurements is estimated at ± 5%, as determined by repeated analysis of freshly prepared standard solutions (potassium biphtalate).

3. Results

3.1. Experimental Fe competitive effect on REE binding to HA

The percentage of REE bound to HA at [Fe] = 0 and 10 µM are displayed in Figure V.2. Without Fe, around 30% of REE are bound to HA at pH 3 and 95% is reached at pH = 6. The presence of Fe in equal amount to REE decreases strongly REE-HA binding because less than 10% of REE are bound to HA at pH 3 whereas 90% are bound at pH 6. Iron competitive effect is more pronounced at low pH because Fe hydroxide may precipitate at circumneutral pH. The decrease of REE binding to HA in the presence of the competitive Fe suggests that a substantial amount of Fe might be complexed to HA even at pH conditions where Fe hydroxides are expected to precipitate.

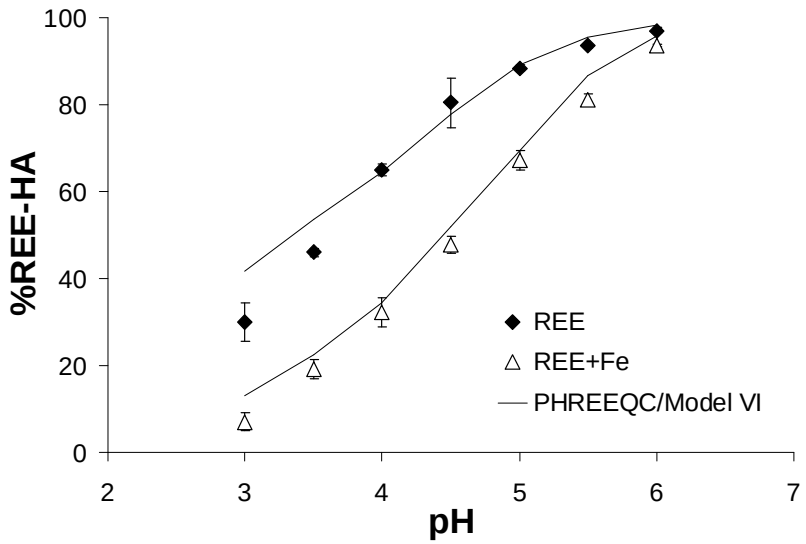

Figure V.2. Percentage of REE bound to HA versus pH without Fe and in the presence of an equal amount of Fe than Σ[REE] (10µM). Error bars represent standard deviation from triplicates. Symbols correspond to experimental data, whereas lines correspond to PHREEQC/Model VI modeling.

The corresponding log K_d^{REE} patterns are plotted in Figure V.3 for REE-HA and REE-Fe-HA systems at pH 3, 4.5 and 6. As observed in previous studies (Tang and Johannesson 2003; Pourret et al., 2007b) at high REE/HA ratio, at any pH studied, REE-HA patterns exhibit a MREE downward concavity. Marsac et al. (2011a) provided evidence that this pattern is developed at pH 3 through the binding of the majority of REE with abundant carboxylic HA sites. However, under such conditions, a substantial proportion of HREE is also bound to the low amount of strong multidentate HA sites, even at high REE/HA (Fig. V.1a). At pH 3, Fe seems to compete with every REE but more with HREE than with LREE. Not only is Fe therefore a strong competitor for REE that are bound to carboxylic HA sites but also for REE that are bound to HA strong multidentate sites. Such behavior were also observed - to a lesser extent - in REE-Al competitive binding to HA experiments recently conducted by Marsac et al. (2011b). Therefore, under acidic conditions, Fe appears to more strongly complex to HA than Al for each type of HA site. At pH = 6, the REE pattern is similar in the presence and abscence of Fe suggesting that Fe competes equally with every REE. Therefore, in such conditions, Fe is bound to both HA carboxylic and phenolic groups by contrast with Al which is mainly bound to HA through carboxylic sites (Marsac et al., 2011b).

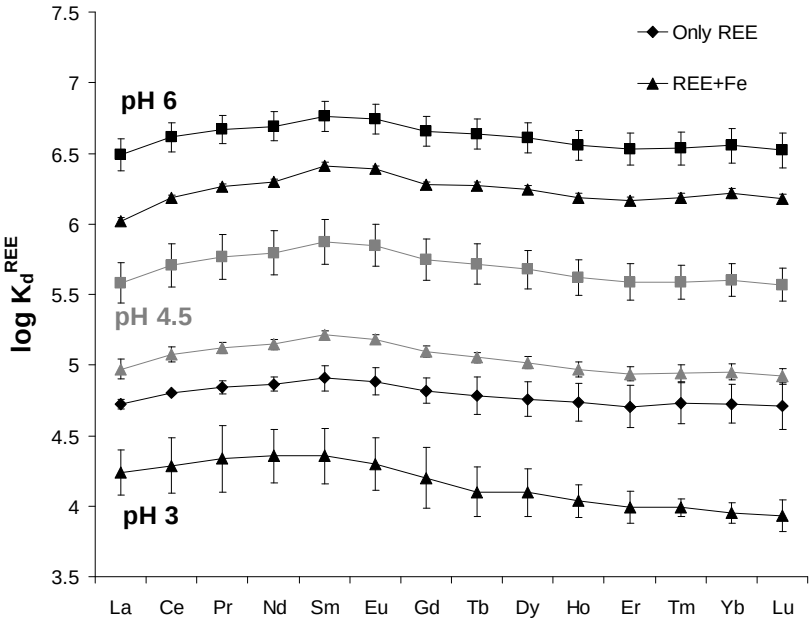

Figure V.3. Log K_d^{REE} between HA and the inorganic solution with and without Fe at three different pH (pH = 3, 4.5 and 6). Error bars represent standard deviation from triplicates.

3.2. Modeling with PHREEQC/Model VI

Recent spectroscopic studies of Fe interactions with HA evidenced the formation Fe polycations-HA complexes (Fe/HA = 50 mg/g, pH = 4.2 to 6.9) constitutive of a mixture of Fe dimer and trimer (Karlsson and Persson 2010). By contrast, these researchers did not detect such complexes at lower Fe concentrations (i.e. 5 mg/gHA). Vilgé-Ritter et al. (1999) by coagulating natural organic matter with Fe, showed that the Fe trimer was dominant and that each Fe atom is complexed with organic matter by two or three bonds. Because the present experimental study was performed in comparable high Fe/HA conditions (40 mg/g), the present modeling study integrates the binding of Fe polymers to HA.

Parameter	Fe^{3+}	$Fe_{1.5}O^{2.5+}$
Log K_{MA}	3.80	2.20
Log K_{MB}	7.50	6.30
ΔLK_{2C}	4.00	0.00
ΔLK_{2P}	4.00	0.00

Table V.1. Log K_{MA}, log K_{MB}, ΔLK_{2C} and ΔLK_{2P} for Fe^{3+} and $Fe_{1.5}O^{2.5+}$ fitted from the experimental data from the present study and Liu and Millero (1999) using PHREEQC/Model VI.

In Model VI, Tipping (1998) described Fe-HA binding by the binding of both Fe^{3+} and $FeOH^{2+}$ species. The complexation of Fe polymers was therefore not taken into account. Gustafsson et al. (2007) modeled Fe binding to soil organic matter with the Stockholm Humic Model (SHM) using only Fe_2O^{4+}. Thereby, Fe monomer complexes were not taken into account in SHM. In the present study, Fe-HA interaction was described with PHREEQC/Model VI using two Fe chemical species such as in Tipping's (1998) definition of Model VI: Fe^{3+} and a Fe polymer. The degree of freedom of PHREEQC/Model VI is therefore as low as possible and similar to those of WHAM 6/Model VI. Specific HA binding parameters for both Fe^{3+} and Fe polymer and K_{SO} of $Fe(OH)_3$ were simultaneously adjusted by minimizing the rmse. The chemical formula of the Fe polymer was also determined by fitting and minimization of the rmse. Here, PHREEQC/Model VI was constrained to simulate both the Fe amount retained by the 5 kDa ultrafiltration (Fe>5kDa) and the Fe competitive effect on REE-HA binding. Data from Liu and Millero (1999) who studied Fe solubility in 0.7 M NaCl solution in the presence of HA relative to pH (with [HA] = 0.6 mg L^{-1}) and HA concentration (with pH = 8) were also taken into account. Fe hydrolysis constants and log K_{SO} = 3.7 of Milne et al. (2003) were used for Liu and Millero (1999) experiments.

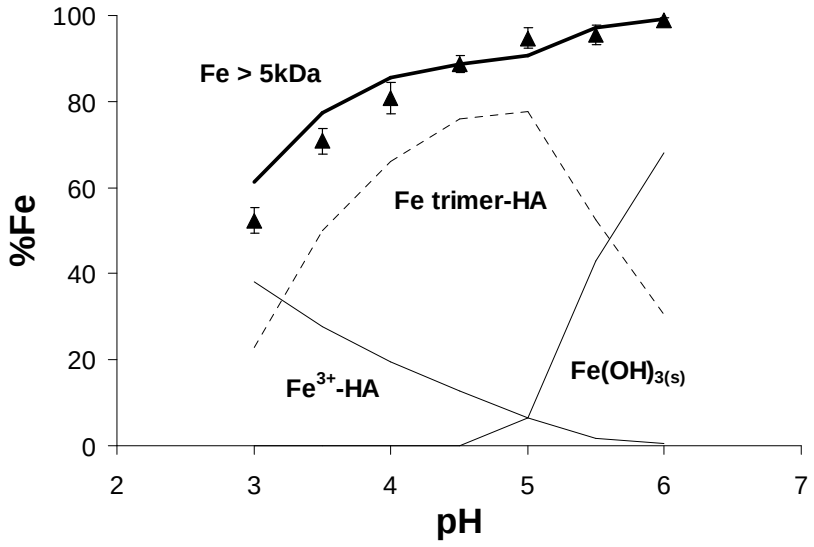

Figure V.4. Percentage of Fe present in the fraction > 5 kDa in competition with REE for HA binding versus pH. Symbols correspond to experimental data, whereas lines represent Fe-HA binding as simulated through PHREEQC/Model VI modeling.

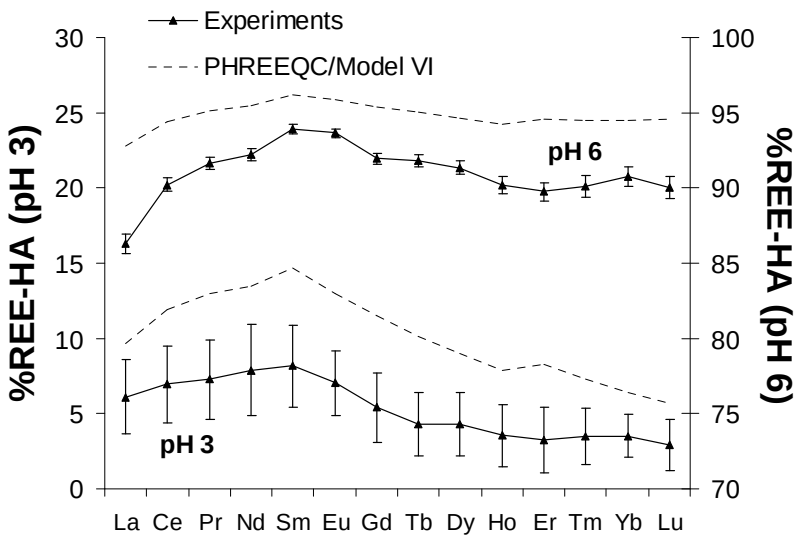

Figure V.5. REE percentage bound to HA in the presence of Fe from experimental data and simulation using PHREEQC/Model VI at two pH (pH = 3 and 6).

PHREEQC/Model VI Fe-HA binding parameters that provided the best fit for both REE-Fe competitive experiments (this study) and the Fe-HA binding data from Liu and Millero (1999) are presented in Table V.1. At low pH, Fe^{3+} appears to be a strong REE competitor for any kind of HA sites because log $K_{MA}(Fe^{3+}) = 3.7 >$ log $K_{MA}(Sm^{3+}) = 3.39$, log $K_{MB}(Fe^{3+}) = 7.5 >$ log $K_{MB}(Lu^{3+}) = 5.23$ and $\Delta LK_{2C}(Fe^{3+}) = 4 > \Delta LK_{2C}(Lu^{3+}) = 2.31$ (cited REE have the highest binding parameters within the REE group). Only $\Delta LK_{2P}(Fe^{3+})$ (= 4) was lower than REE ΔLK_{2P} ($\Delta LK_{2P}(La^{3+}) = 4.39$). Using a larger $\Delta LK_{2P}(Fe^{3+})$ value in the model led to an overestimation of Fe solubility for Liu and Millero (1999) dataset (data not shown). The average values of $\Delta LK_{2C}(Fe^{3+})$ and $\Delta LK_{2P}(Fe^{3+})$ were however higher than that of REE. For higher pH, preliminary tests revealed that the best fit for Fe was obtained by introducing the $Fe_3O_2^{5+}$ binding to HA:

$$HA\text{-}S^{n-} + Fe_3O_2^{5+} = HA\text{-}S\text{-}Fe_3O_2^{(5-n)+} \quad (V.3)$$

Where $HA\text{-}S^{n-}$ represent a HA complexing site (mono-, bi- or tridentate). However, the Fe competitive effect on REE was impossible to simulate through PHREEQC/Model VI modeling. Equation V.3 implies indeed that the Fe trimer binds to HA only through one discrete site. The competitive effect of the Fe trimer on REE is therefore lower than experimental data even if Fe>5kDa was satisfactorily modeled. The definition of discrete HA sites in PHREEQC/Model VI does not allow easily such poly-cations to bind to several HA sites. To simulate HA-Fe trimer complexation with an efficient competitive effect on REE, the binding of half a trimer ($Fe_{1.5}O^{2.5+}$) to HA sites was instead introduced. This allows

simulating Fe trimer binding to HA by two discrete sites without further consideration of spatial site arrangement. The $Fe_{1.5}O^{2.5+}$ log K_{MA} and log K_{MB} were set to 2.2 and 6.3, respectively. The Fe trimer ΔLK_{2C} and ΔLK_{2P} were set equal to 0 because Fe trimer competitive effect on HREE was not observed in the present experiments. The $Fe(OH)_3$ log K_{SO} was set to 5.4 for our dataset suggesting a poorly ordered precipitated Fe hydroxide. This high value of $Fe(OH)_3$ log K_{SO} was already calculated in the presence of HA (Weber et al., 2006). The new optimized set of Fe-HA binding parameters allows the fit to be considered of good quality because rmse is equal to 0.02 for Fe and 0.05 for the whole REE group (Fig. V.4). The simulated speciation of Fe on HA is also reported in Figure V.4. As observed by Tipping et al. (2002), Fe^{3+} is dominant only at low pH (pH = 3 in our simulation). The iron trimer becomes dominant with the increasing pH, but is limited by the precipitation of hydroxides at pH > 4.5. Experimental and modeled patterns of REE bound to HA at pH 3 and 6 are plotted in Figure V.5. At pH = 3, modeled data indicate that Fe^{3+} is the dominant Fe species bound to HA sites, and especially to strong multidentate sites. Iron competitive effect is therefore higher for HREE. At pH = 6, where the Fe trimer dominates, modeled Fe competitive effect is similar for all REE. The Fe trimer competes similarly with LREE for HA carboxylic sites and HREE for HA phenolic sites. Modeled data for Liu and Millero (1999) experimental conditions are plotted in Figure V.6 for pH = 8 and varying HA concentrations (Fig. V.6a) and varying pH at [HA] = 0.6 mg L^{-1} (Fig. V.6b). PHREEQC/Model VI could not satisfactorily simulate present and Liu and Millero (1999) experimental data with the same set of Fe-HA binding parameters. When a reasonably good fit is achieved for the present experimental results, Fe solubility in the presence of HA is overestimated for the data from Liu and Millero (1999) especially at pH = 8 (Figure V.6). Such discrepancy was already encountered in studies aiming at calibrating model binding parameters for Fe-HA binding (Tipping et al., 2002; Gustafsson et al., 2007). In these previous studies, the authors calculated lower Fe-HA stability constants using the data from Liu and Millero (1999) than for other experimental Fe-HA binding datasets. Liu and Millero (1998) successfully studied the Fe solubility in the presence of HA by filtering the Fe/HA suspension at 0.02µm. However, DOC was not monitored and a substantial amount of HA may therefore have been retained during the filtration at 0.02 µm because of the potential HA coagulation involved by Fe or HA coating on precipitated Fe hydroxides. Such HA retention would induce an underestimation of Fe-HA stability constants calculated from experimental data of Liu and Millero (1999). However, by simply decreasing log K_{MA} for $Fe_{1.5}O^{2.5+}$ from 6 to 5.5, the model could satisfactorily simulate Liu and Millero (1999) (see dotted lines in Figure V.6).

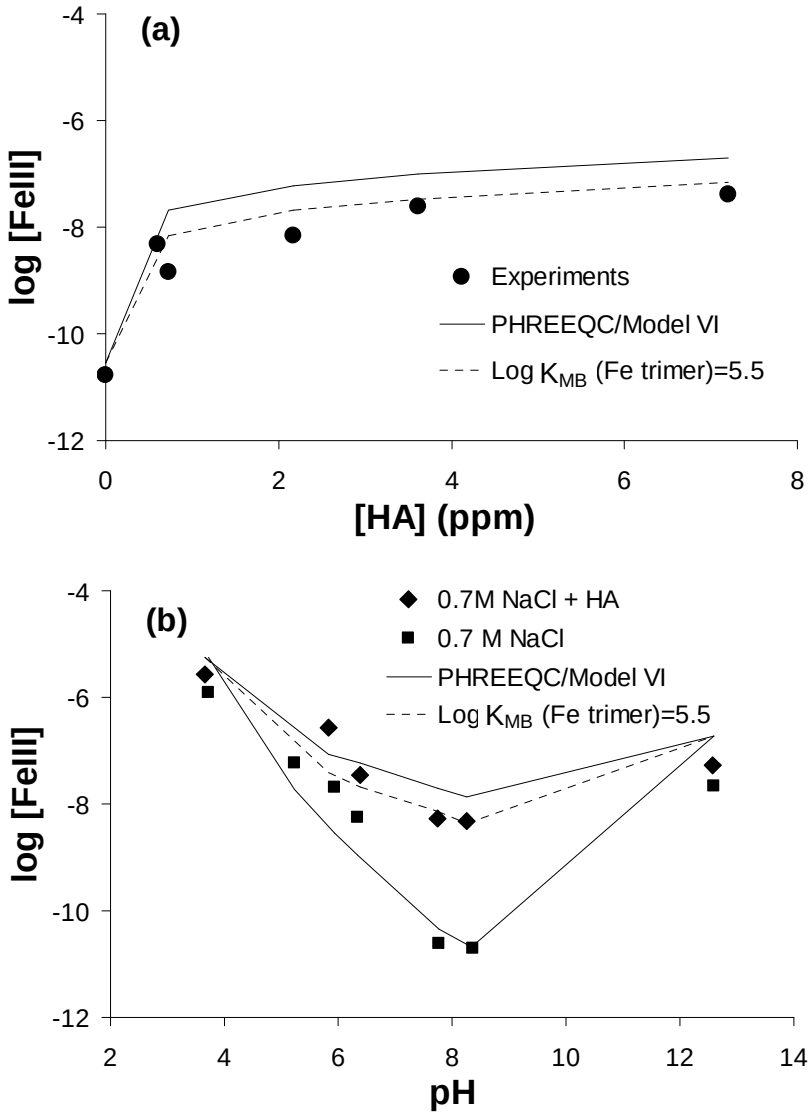

Figure V.6. Experimental results, from Liu and Millero (1998), of Fe(III) solubility in 0.7M NaCl solution (a) at pH 8 versus HA concentration and (b) with HA = 0 and 0.6 mg L^{-1} versus pH. Solid lines represent modeled results with PHREEQC/Model VI Fe-HA binding parameters in Table V.1. Dotted lines correspond to results with log K_{MB} = 5.5 for $Fe_{1.5}O^{2.5+}$.

4. Discussion

4.1. Simulated Fe speciation and spectroscopic data

The consideration of Fe^{3+} and Fe trimer binding to HA allowed modeling satisfactorily both Fe-HA binding and the Fe competitive effect on REE. The Fe competitive effect on REE-HA binding provides unique information about both Fe monomer and Fe trimer binding to HA mechanisms. Such poly-Fe-HA complexes were observed through spectroscopic

analysis in similar experimental conditions to those used in the present work (Fe/HA = 50mg/g) (Karlsson and Persson, 2010). Furthermore, these authors estimated that the proportion of Fe polymer represented 10% at pH 4.2 and 35% at pH 6.9 of total complexed Fe to HA. By contrast, they did not detect such complexes at lower Fe concentrations (i.e. 5mg/gHA). To compare modeling and spectroscopic data, Fe-HA binding were simulated with the Karlsson and Persson (2010) experimental conditions. At Fe/HA = 50mg/g, PHREEQC/model VI predicts that the Fe polymer represented 69% at pH = 4.2 and 42% at pH = 6.9. The lower contribution of the Fe trimer at pH 6.9 is explained by $Fe(OH)_3$ precipitation. PHREEQC/model VI overestimates Fe trimer binding to HA at pH = 4.2 but is close to the percentage determined by Karlsson and Persson (2010) at pH = 6.9. At Fe/HA = 5mg/g and pH 3 to 5, 100% of Fe is bound to HA as Fe mononuclear complexes. At pH = 5.5, 10% of Fe is bound to HA as polynuclear species and reaches 60% at pH 7. These calculated proportions are not consistent with the spectroscopic observations suggesting that Fe-HA binding may be more complex than the hypotheses stated in PHREEQC/model VI. In the present modeling study, only Fe^{3+} was considered able to bind to HA by forming mononuclear complexes. At low Fe/HA, Fe^{3+} dominates Fe speciation on HA sites but its occurrence is limited when pH increases. Other Fe mononuclear species such as $FeOH^{2+}$ may also bind to HA. Such species, if taken into account, would dominate Fe-HA binding at higher pH than Fe^{3+}. Therefore, the introduction of $FeOH^{2+}$ in PHREEQC/Model VI would limit the formation of the Fe trimer (i) at pH = 4.2 and Fe/HA = 50mg/g and (ii) at pH > 5 and Fe/HA = 5mg/g. Unfortunately, this Fe-HA binding mechanism could not be taken into account in the model because its influence could not be quantified in our experiments. However, even if simulated Fe speciation is not entirely satisfactory as compared to the knowledge gained through spectroscopic data, the Fe-HA PHREEQC/Model VI binding parameters provide a consistent description of both Fe speciation with HA and Fe competitive effect on REE.

4.2. Impact of cation competition on REE patterns in natural organic-rich waters

In natural organic-rich waters REE speciation is mainly controlled by humic substances (Bidoglio et al., 1991; Takahashi et al., 1997; Viers et al., 1997; Dia et al., 2000; Johannesson et al., 2004; Gruau et al., 2004; Davranche et al., 2005; Pourret et al., 2007a; Pédrot et al., 2008). Coupling experimentation and modeling allowed identifying the controlling factors of REE distribution on HA sites. These factors are (i) *the metal loading* (Yamamoto et al., 2010; Marsac et al. 2010): at low REE/HA, REE binding occurs mainly

through HA strong multidentate sites, whereas at high REE/HA, REE binding is dominated by HA weak carboxylic sites. This modification of REE speciation on HA sites directly controls the REE-HA pattern which increases from La to Lu at low REE/HA and exhibits a MREE downward concavity at high REE/HA. By contrast to laboratory experiments, REE/HA ratio are very low ranging from 10^{-6} to 10^{-4} mol REE/mol C in natural waters (Tang and Johannesson, 2010). The HA metal loading is therefore imposed by other cations that potentially compete with REE. (ii) *The competitive trivalent cations*: Al and Fe competition with REE for HA binding can control the REE distribution on HA sites (Marsac et al., 2011b; the present study). This Al and Fe competitive effect depends itself on the organic matter metal loading and the pH conditions prevailing in solution. (iii) *Finally the pH*: the pH appears to be the major factor controlling the REE-HA complexation pattern through indirect effects on both HA metal loading and Fe and Al competitive behavior on REE-HA binding. Aluminium and Fe activities are strongly pH dependent because of the relatively low solubility of their (hydr)oxides. Therefore, because Al and Fe aqueous concentrations decrease with increasing pH, HA metal loading is higher at acidic pH than at circumneutral pH.

Because experimental conditions could remain far from natural conditions, simulations were also performed with the World Average River Water (see Table 11 in Tang and Johannesson, 2003) to illustrate which could be the REE-HA log K_d pattern developed in conditions relevant to natural waters. We also followed their assumption that 80% of the active DOM (= 5 mg L^{-1}) is present as fulvic acid (FA) and 20% as HA. However, because REE-FA binding parameters for PHREEQC/Model VI were not yet determined, only the amount of HA (= 1 mg L^{-1}) was introduced in the model. The binding of Ca^{2+} and Mg^{2+} to HA were introduced in PHREEQC/Model VI database and their HA binding parameters were taken from Tipping (1998). Log K_{SO} for $Al(OH)_3$ and $Fe(OH)_3$ were set equal to 9 and 5, respectively, which correspond to poorly crystalline (oxy)hydroxide. REE-HA log K_d patterns were normalized to La and are plotted from pH = 4 to 8 in Figure V.7. REE-HA log K_d patterns regularly evolve from a MREE increasing pattern to a pattern displaying a strong increase from La to Lu. At low pH, Al and Fe are stronger competitors for HREE. Middle REE present the highest log K_d with HA among the REE group. At circumneutral pH, Fe competes similarly for all REE although Al competes more efficiently with LREE. Furthermore, $Al(OH)_3$ solubility is higher than $Fe(OH)_3$. Therefore, Al is the major REE competitor for HA binding under circumneutral conditions involving that HREE present the highest log K_d with HA among the REE group. In figure V.7 are also presented stability

constants patterns of $REECO_3^+$ and $REE(CO_3)_2^-$ normalized to La (Luo and Byrne, 2004). At pH = 7 and 8, REE-HA pattern present a comparable increase from La to Lu to the patterns with carbonate.

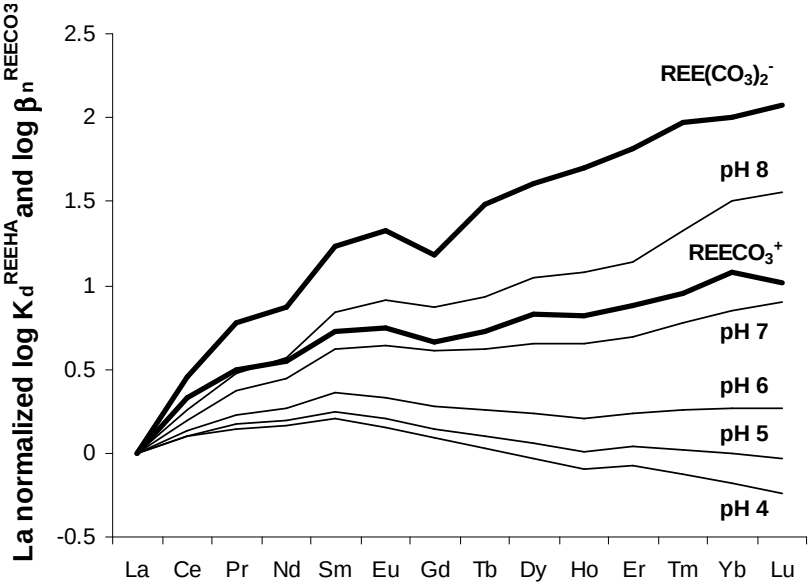

Figure V.7. REE-HA log K_d normalized to La and determined for the World Average River Water between pH 4 to 8. Patterns of REE stability constants with $REECO_3^+$ and $REE(CO_3)_2^-$ (log β_n^{REECO3}) are presented for comparison (Liu and Byrne, 2004).

Organic-rich waters are generally classified into two groups, depending on their Upper Continental Crust (UCC)-normalized REE pattern (Elderfield et al., 1990; Tang and Johannesson, 2010): (i) acidic waters enriched in MREE, with $(La/Yb)_{UCC}$ close to 1 and (ii) alkaline waters enriched in HREE, with $(La/Yb)_{UCC} < 1$. This REE distribution is commonly interpreted as follows: the MREE enriched pattern is generated by the REE binding with dissolved organic matter (DOM), whereas the HREE enriched pattern is generated by the REE complexation by carbonate whose affinity is higher for HREE than for LREE (Luo and Byrne, 2004). In organic-rich waters (DOC>5 mg L^{-1}), $(La/Yb)_{UCC}$ globally decreases with the increasing pH, as shown in Figure V.8 for data compiled in Marsac et al., (2010) (Dia et al., 2000, Viers et al., 1997; Gaillardet et al., 2004; Gruau et al., 2004; Tosiani et al., 2004; Pokrovsky et al., 2006 ; Auterives, 2007), which supports the previous hypothesis concerning the REE pattern variability. However, such $(La/Yb)_{UCC}$ decrease is also observed in organic-rich waters where pH is below 7.5. Moreover, in such pH conditions, DOM was shown to control the REE speciation (Pourret et al., 2007b). Therefore REE-carbonate binding cannot explain the HREE enrichment observed in organic-circumneutral waters. The recent

assessment that REE affinity for HA can vary with the prevailing physico-chemical conditions offers a new tool to explain the REE pattern variability in natural organic-rich waters. Acidic waters are enriched in MREE by the preferential MREE binding with DOM. In circumneutral waters, Al and Fe concentrations are low because of their precipitation as (hydr)oxides. Dissolved organic matter is therefore carrying less cations. Because Fe (hydr)oxides are less soluble than Al (hydr)oxides, Al is the major REE competitor for their binding to DOM. Moreover, Al is more competitive for LREE than HREE. The combination of both low DOM loading and Al competition for LREE-DOM binding involve a stronger HREE binding by DOM and explain the HREE enrichment observed in circumneutral organic-rich waters.

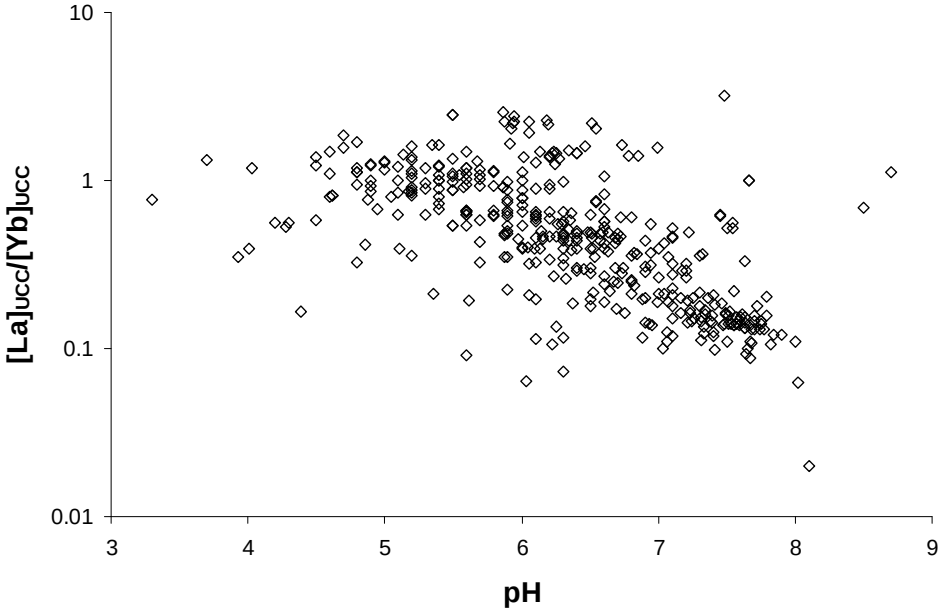

Figure V.8. Upper Continental Crust normalized (La/Yb) ratio $(La/Yb)_{UCC}$ versus pH from organic-rich waters (DOC > 5 mg L^{-1}) (Dia et al., 2000, Viers et al., 2000; Gaillardet et al., 2004; Gruau et al., 2004; Tosiani et al., 2004; Pokrovsky et al., 2006 ; Auterives, 2007).

5. Summary

REE-Fe competitive binding to HA experiments were performed to investigate the competitive effect of Fe on REE binding to HA and in turn to identify the HA surface sites and mechanisms involved in the Fe-HA binding. Iron seems to compete differently with REE for HA binding depending on pH. Under acidic (pH = 3) conditions and high metal loading, Fe^{3+} - as the dominant Fe species - competes more strongly with HREE than with LREE.

Therefore, Fe^{3+} has high affinity for the few amount of available HA strong multidentate sites. Under higher pH conditions (e.g. at pH = 6), Fe competes indifferently for LREE and HREE, suggesting that Fe can bind to both HA carboxylic and phenolic groups. PHREEQC/Model VI Fe-HA binding parameters were optimized and simulate both Fe binding to HA and its competitive effect on REE. Consistently with spectroscopic studies both the formation of monomeric and polymeric Fe-HA complexes were taken into account. Modeling showed that Fe trimer ($Fe_3O_2^{5+}$) was the most competitive species for REE. The binding of $Fe_3O_2^{5+}$ to HA was defined by the binding of $Fe_{1.5}O^{2.5+}$, which simulates the binding of the trimer to two Model VI HA discrete sites (mono-, bi- or tridentate) without any further assumption of binding site spatial arrangement. Comparison between simulated Fe speciation on HA sites and spectroscopic results showed that the model was not entirely consistent: modeling Fe-HA binding requires the use of other Fe chemical species which can bind to HA (e.g. $FeOH^{2+}$). However, such species binding parameters could not be determined with the available experimental dataset. The present study provides fundamental knowledge on Fe-REE competition mechanisms for HA binding and shows that Fe can modify the REE-HA complexation pattern. In turn, the ability of the REE to be used as a "speciation probe" to precisely describe cations interactions with HA is again verified, as previously suggested for another competitive cation - Al - (Marsac et al., 2011b). This study shows that REE-HA complexation patterns vary significantly with the HA metal loading, the REE competitor cations for HA binding and the pH. Calculations of the REE speciation of the World Average River Water were performed using the here optimized PHREEQC/Model VI. For acidic waters, pattern of REE-DOM conditional stability constants presents a MREE downward concavity. For circumneutral water, REE-DOM pattern increases from LREE to HREE. The HREE enrichment observed in circumneutral organic-rich waters, generally attributed to REE binding by carbonates, was here shown to be involved by REE-DOM binding.

VI. Conclusions et Perspectives

1. Conclusions

Cette étude a permis de comprendre et de décrire, dans le détail, les mécanismes impliqués dans la complexation des REE par les acides humiques et le rôle de certains facteurs sur la nature de ces mécanismes. Cette compréhension et description permettent d'apporter des éléments de réponse quant à la l'origine et à la signification de la variabilité des spectres de REE observés dans les eaux naturelles riches en matière organique, origine et signification qui étaient jusqu'ici largement inconnues. Plus précisément, ce travail de thèse a montré que le spectre de complexation des REE par les acides humiques n'était pas indépendant des conditions de complexation, mais présentaient des variations reflétant la forte hétérogénéité de groupements fonctionnels au sein des substances humiques. Cette étude a également validé l'utilisation de ligands organiques de référence dans l'interprétation des mécanismes de complexation des REE par les acides humique en (i) comparant les spectres de ces ligands avec ceux obtenus expérimentalement pour la complexation des REE par les acides humiques, et (ii) imposant aux sites de complexation définis dans Model VI des spectres cohérents avec ces mêmes ligands de référence.

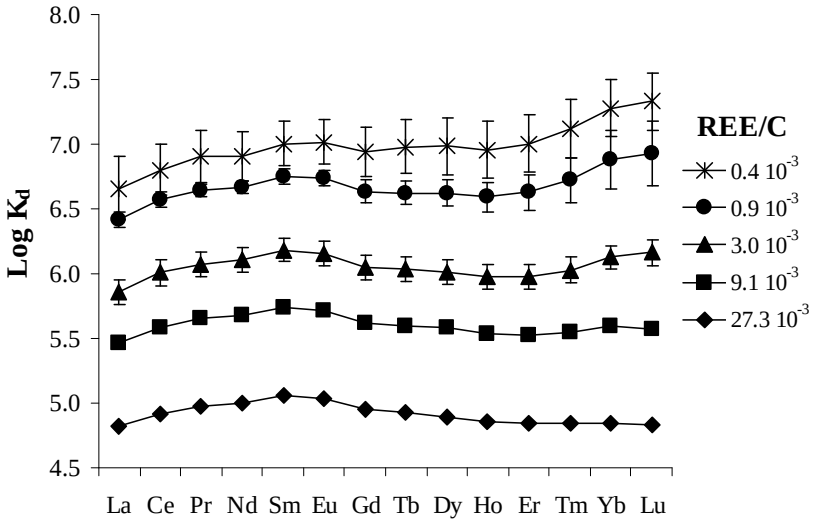

Figure VI.1. Variabilité des spectres des coefficients de distribution des REE entre les acides humiques et la solution à pH = 3 dépendant du rapport REE/acides humiques (mol/molC).

Ainsi, dans la **première partie de la thèse**, il a été démontré qu'à pH = 3 et pour de faibles rapports REE/acides humiques, les REE étaient majoritairement liées à des sites forts multidentates (potentiellement chélates) complexant principalement les REE lourdes, alors

qu'à de plus forts rapports REE/acides humiques les REE étaient principalement liées à des ligands faibles carboxyliques complexant majoritairement les REE intermédiaires (Figure VI.1).

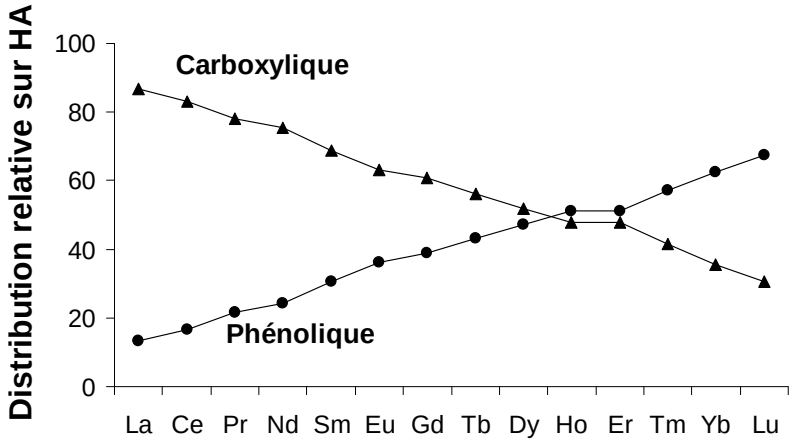

Figure VI.2. Distribution relative des REE sur les sites carboxyliques et phénoliques des acides humiques à pH = 6 et pour un rapport REE/acides humiques élevé.

La **seconde partie la thèse** représente une avancée majeure dans le domaine de la modélisation des interactions entre REE et acides humiques. En effet, la contrainte de linéarité des constantes entre sites carboxyliques et sites phénoliques présentes dans la version originale de Model VI a été supprimée en introduisant ce modèle dans PHREEQC et un spectre de type « catéchol » a été imposé aux groupements phénoliques, différent en forme de celui des groupements carboxyliques. Ainsi, les modifications apportées à Model VI ont permis de reproduire précisément l'ensemble de la variabilité des spectres de complexation des REE par les acides humiques obtenu expérimentalement. De plus, l'introduction de Model VI dans PHREEQC a permis pour la première fois de quantifier la répartition des REE sur chacun des différents sites impliqués dans la complexation. Ainsi, la modélisation a permis de démontrer qu'à pH = 6 et pour un fort rapport REE/Acides humiques, les REE légères étaient majoritairement liées à des sites carboxyliques tandis que les REE lourdes étaient, elles, majoritairement liées à des sites présentant des groupements phénoliques (Figure VI.2). A partir de cette approche de modélisation, une nouvelle hypothèse a été émise. En effet, des cations compétiteurs pourraient modifier le spectre de complexation des REE par les acides humiques, en fonction de leur affinité relative pour les différents types de ligands impliqués dans la complexation. Réciproquement, il en a été déduit que les variations engendrées dans la

forme du spectre de complexation des REE par les acides humides, lors de l'ajout d'un cation compétiteur, devraient pouvoir permettre de "sonder" la nature du ou des sites avec lequel ce cation compétiteur se lie préférentiellement.

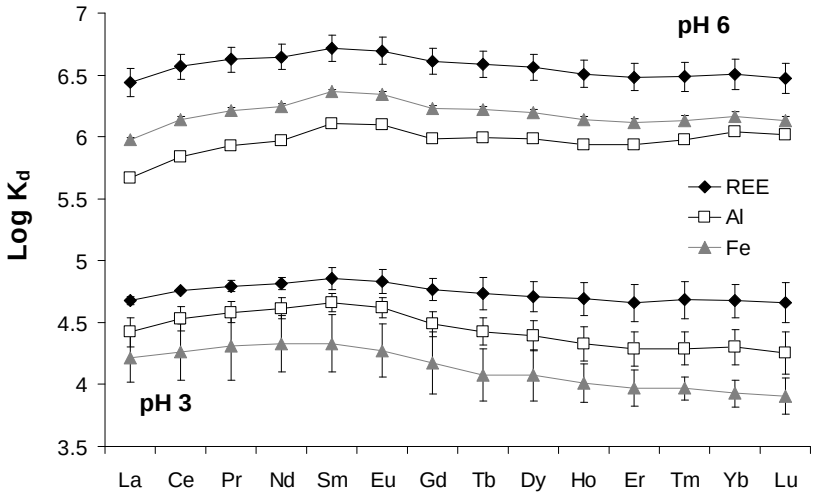

Figure VI.3. Comparaison des spectres des coefficients de distribution des REE entre les acides humiques et la solution obtenus pour des pH de 3 et de 6, avec ou sans présence de Al ou Fe et pour un rapport REE/acide humique (mol/molC) élevé.

Les **troisième et quatrième parties de la thèse** ont permis de vérifier expérimentalement ce rôle de sonde de complexation des REE en réalisant des expériences de compétition entre REE et aluminium, d'une part, et entre REE et fer, d'autre part. A pH = 3, Al et Fe apparaissent plus compétiteurs pour les REE lourdes que pour les REE légères. Par conséquent, ces deux cations qui, à ce pH, se présentent sous la forme de cations aqueux 3+ sont démontrés avoir une très forte affinité pour les sites forts multidentates des acides humiques, plus forte que celle des REE lourdes pour ces mêmes sites (Figure VI.3). Les résultats sont différents à pH 6. A cette valeur de pH, Al apparaît être un plus fort compétiteur pour les REE légères que pour les REE lourdes, contrairement au Fe qui apparaît être un compétiteur pour l'ensemble des REE, indifféremment. Ainsi, à pH=6, Al apparaît se lier majoritairement aux groupements carboxyliques des acides humiques tandis que Fe apparaît se lier lui aussi bien aux groupements carboxyliques des acides humiques qu'à leurs groupements phénoliques. Les changements dans la complexation de Al et de Fe constatés avec l'augmentation du pH ont été interprétés comme dus à leur complexation sous forme polycationique par les acides humiques à pH = 6. Partant de ces résultats, un jeu de constantes

spécifiques Al-acide humique et Fe-acide humique a été déterminé pour PHREEQC/Model VI en utilisant la contrainte apportée par la compétition avec les REE. Ce nouveau jeu de constantes permet de simuler de manière précise la complexation de Al et Fe par les acides humiques ainsi que l'effet de compétition de ces deux métaux sur la complexation des REE.

Ainsi, et comme le prévoyaient les simulations réalisées dans la deuxième partie de la thèse, l'utilisation du spectre de complexation des REE fournit bel et bien une "sonde" permettant de déterminer les mécanismes de complexation des cations par les acides humiques. Au final, les résultats obtenus montrent que les spectres de complexation des REE par les acides humiques sont fonction à la fois de la charge en métaux (expérimenté ici par la charge en REE), de la nature et de la spéciation des cations compétiteurs des REE et, majoritairement mais indirectement, du pH. La figure VI.4 résume l'ensemble des facteurs et mécanismes chimiques influençant la forme du spectre de complexation des REE par les acides humiques.

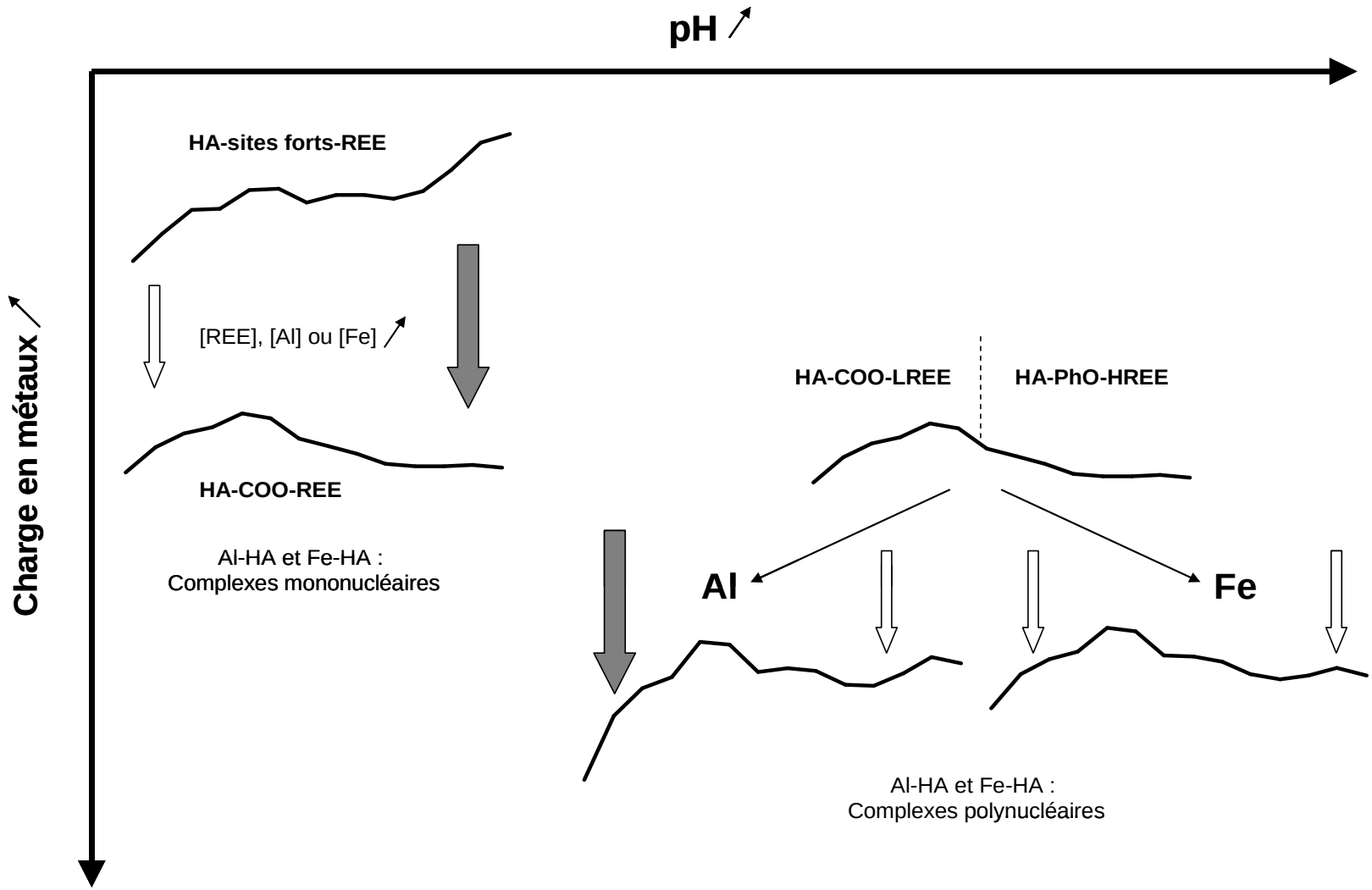

Figure VI.4. Schema récapitulatif des facteurs influençant les mécanismes de complexation des REE par les acides humiques (HA) et des différentes formes de spectre de complexation des REE par les HA. REE légères et lourdes sont notés LREE et HREE, respectivement.

2. Implications

2.1. Origine de la variabilité des spectres de REE observée dans les eaux riches en matière organique

Les études par ultrafiltration ont depuis longtemps établi que dans les eaux riches en matière organique les REE sont majoritairement associées à la fraction organique colloïdale représentée par les substances humiques (Tanizaki et al., 1992; Dupré et al., 1996; 1999; Viers et al., 1997; Ingri et al., 2000; Dia et al, 2000; Gruau et al., 2004 ; Pokrovsky et al., 2005; 2006). Cependant, toutes les eaux ne présentent pas les mêmes formes de spectres, avec deux types le plus souvent observés (Elderfield et al., 1990). Ce travail suggère que, dans ces eaux, la variabilité de forme des spectres de REE est la conséquence directe de l'hétérogénéité des sites de complexation présents au sein des substances humiques et des différences de spectres des constantes de complexation entre les REE et ces sites. Le premier type, caractéristique des eaux acides, se distingue par la présence d'un enrichissement en REE intermédiaires. Les résultats obtenus dans cette thèse démontrent qu'à pH acide (4<pH<6) les colloïdes organiques peuvent enrichir la solution (< 0.2µm) en REE intermédiaires car la complexation des REE par les acides humiques est dominée par les sites carboxyliques. Ce comportement est observé quelque soit le rapport métaux dissous/acides humiques puisque la présence de métaux dissous plus abondants que les REE, comme Al^{3+} et Fe^{3+}, limitent fortement la complexation des REE lourdes par ces mêmes colloïdes (Figure VI.5, 4<pH<6). En revanche, les eaux neutres à basiques présentent un enrichissement en REE lourdes. Pourret et al. (2007b) ont montré que cet enrichissement n'était pas le fait d'une complexation des REE par les carbonates, la présence de matière organique imposant une spéciation organique des REE. Les résultats de cette thèse montrent, premièrement, que les faibles concentrations en Al et Fe dissous en raison de la faible solubilité de leurs hydroxydes à pH neutre, engendrent une faible charge en métaux des colloïdes organiques favorisant ainsi la complexation des REE lourdes par ces colloïdes. De plus, dans ces conditions de pH, les espèces polycationiques de Al limitent la complexation des REE légères tandis que les polycations de Fe ne créent pas de différenciation entre REE. L'ensemble de ces raisons fait que les colloïdes organiques ont, dans ces eaux, une plus forte affinité pour les REE lourdes et en enrichissent la solution (< 0.2µm) par rapport aux REE légères. Le spectre de

complexation des REE par les acides humiques présente alors une forme comparable à celle des carbonates (Figure VI.5, 6<pH<8).

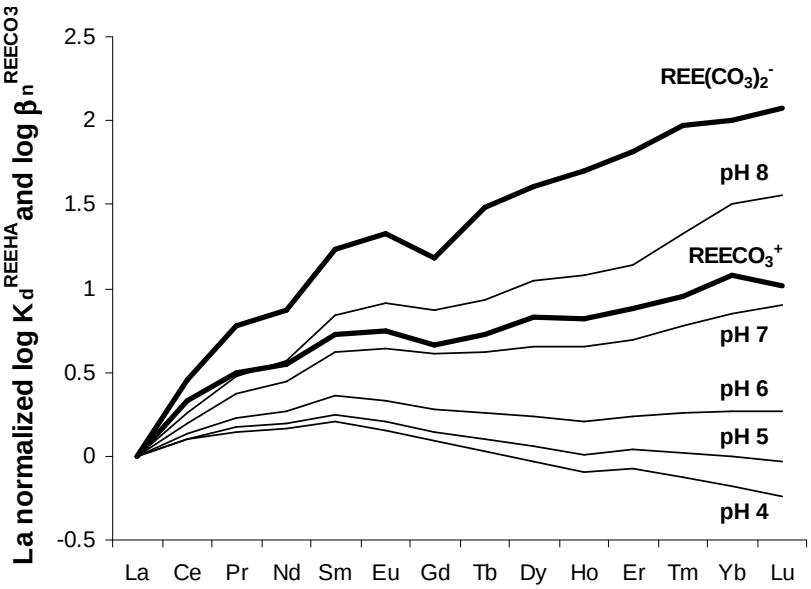

Figure VI.5. Evolution des spectres des coefficients de distribution des REE normalisés au La entre les acides humiques et une solution modèle correspondant en composition à la moyenne des rivières mondiales (Tang et Johannesson, 2003), pour des pH variant de 4 à 8. Les spectres des constantes de stabilité des complexes $REECO_3^+$ et $REE(CO_3)_2^-$ (log β_n^{REECO3}) sont présentés en comparaison.

La variabilité des spectres de REE dans les eaux naturelles contenant des colloïdes organiques peut donc être expliquée par l'évolution des propriétés de complexation des colloïdes organiques en fonction de la charge en métaux, de la nature et de l'abondance des cations compétiteurs et du pH. Cette conclusion démontre une fois de plus l'importance de la prise en compte des colloïdes organiques dans les modèles de spéciation des REE (Tang et Johannesson, 2003 ; Pourret et al., 2007). Le modèle combiné PHREEQC/Model VI développé dans le cadre de cette thèse est actuellement le seul capable de modéliser précisément la variabilité des spectres de complexation des REE par les colloïdes organiques et ainsi de comprendre la spéciation des REE dans les eaux riches en matière organique.

2.2. Spéciation des cations métalliques dans les eaux riches en matière organique

Une autre conséquence majeure de cette thèse est de démontrer l'importance de la prise en compte des complexes polynucléaires d'Al et Fe avec les acides humiques, complexes qui pourraient fortement augmenter la solubilité de ces deux métaux en présence

de matière organique. La prise en compte de ces complexes dans PHREEQC/Model VI permet une meilleure prédiction de la spéciation de Al et de Fe dans les eaux riches en matière organique.

Al et Fe jouent également un rôle majeur dans la spéciation en solution des éléments traces métalliques et des radionucléides par leur effet de compétition avec les autres cations vis-à-vis des groupements fonctionnels complexants des acides humiques (Kinniburgh et al., 1999; Pinheiro et al., 2000; Tipping et al., 2002). On doit s'attendre à ce que ces effets de compétition soient différents suivant le pH du fait de la formation de complexes polynucléaires de Al et de Fe à pH neutre et de complexes mononucléaires à pH acide. De plus, on doit s'attendre à ce que les effets diffèrent entre Al et Fe à pH neutre, les polycations de Al étant stabilisés principalement par les groupements carboxyliques des acides humiques, alors que les polycations de Fe sont stabilisés, à la fois par les groupements carboxyliques et phénoliques. Model VI, dans sa version originale, établit une relation linéaire entre les paramètres régissant la complexation des cations par les groupements carboxyliques et phénoliques des acides humiques. Ainsi, tous les cations présentent systématiquement la même affinité relative pour ces groupements fonctionnels. Une description plus précise des mécanismes de complexation des cations par les différents types de groupements des acides humiques du type de celle générée ici par le couplage PHREEQC/Model VI et l'abandon de cette relation linéaire systématique, entraînera une meilleure compréhension des mécanismes de compétition entre cations vis-à-vis des substances humiques et ainsi, une détermination plus précise de la spéciation des métaux dissous dans les eaux naturelles.

3. Perspectives

3.1. Perspectives à court terme

La compétition entre les REE et des cations à forte affinité pour les acides humiques, tels que Al et Fe, s'est avérée être un facteur majeur de contrôle de la forme des spectres de complexation des REE par les acides humiques. Réciproquement, l'utilisation de l'outil "sonde de spéciation" que représentent les changements de forme des spectres de REE en présence d'un cation compétiteur, a permis de mieux comprendre les mécanismes de complexation de Fe et Al par les substances humiques. Cette "sonde de spéciation" pourrait être utilisée pour d'autres cations présentant une forte affinité pour les substances humiques, notamment des cations divalents comme le cuivre et le plomb. Ces derniers sont présents à

l'état de traces dans les milieux peu anthropisés. Cependant, dans les eaux à pH proche de la neutralité, les teneurs en Al et Fe dissous étant faibles à très faibles du fait de la faible solubilité de leurs hydroxydes, la compétition avec ces cations divalents pourrait devenir prépondérante. Des études de complexation compétitive avec des cations divalents permettraient non seulement de déterminer l'impact de ces cations sur la forme du spectre de complexation des REE par les acides humiques mais aussi de mieux décrire leurs propres mécanismes de complexation.

Une autre perspective est de vérifier les résultats expérimentaux et issus de la modélisation par une analyse directe, in-situ, des interactions entre REE et acides humiques. En effet, les mécanismes locaux d'interaction des REE avec les acides humiques régissent le comportement des REE à l'échelle macroscopique. Une autre façon d'améliorer les modèles de spéciation géochimique, complémentaire des expérimentations macroscopiques conduites dans cette thèse, est de procéder à une analyse de ces interaction à l'échelle moléculaire. Un parallèle peut être fait ici avec l'adsorption des métaux dissous sur des surfaces hétérogènes telles que les oxyhydroxydes de fer dont la compréhension et la modélisation s'appuyent dans à la fois sur des expériences d'adsorption en laboratoire mais aussi sur des résultats de spectroscopie (Venema et al., 1996). De fait, des analyses spectroscopiques telles que l'absorption des rayons X utilisant de la lumière synchrotron (XAFS pour X-ray Absorption Fine Structure) ont montré leur puissance dans l'étude de la nature et de la structure des complexes de REE formés à la surfaces d'oxyde de Fe ou de Mn (Ohta et al., 2009a,b), et de cellules bactériennes (Takahashi et al., 2010). Les techniques XAFS permettent en principe d'étudier des systèmes hétérogènes, tels que les acides humiques, et dilués, tels que des complexes REE-acide humique. PHREEQC/Model VI, permet non seulement de simuler la complexation des REE par les acides humiques mais aussi d'étudier en détail la spéciation des REE sur ses différents types de sites de complexation. Ainsi, la comparaison entre les structures des complexes REE-acides humiques déterminées par XAFS dans différentes conditions expérimentales couplée à la modélisation de la spéciation des REE parles acides humiques par PHREEQC/Model VI devrait permettre de vérifier la cohérence de la modélisation et d'obtenir de nouvelles contraintes pour l'améliorer.

Les REE légères et lourdes possèdent des sites préférentiels de complexation sur les acides humiques. Les spectres de complexation des REE par les acides humiques peuvent ainsi être utilisés comme traceur des processus de complexation des cations compétiteurs (Al ou Fe ; voir ci-dessus). Cette différenciation entre REE légères et REE lourdes peut être également observée sur d'autre types de surfaces hétérogènes. En effet, Ohta et al. (2009a,b)

on montré par analyse EXAFS que les REE légères formaient des complexes monodentates à la surface d'oxyhydroxydes de fer tandis que les REE lourdes formaient des complexes bidentates. Il en est de même à la surface de bactéries, ou Takahashi et al. (2010) ont montré que les REE légères se liaient majoritairement à des groupements carboxyliques à l'inverse des REE lourdes, se liant préférentiellement à des groupements phosphates. Par analogie avec les acides humiques, les REE pourraient être utilisées comme "sonde" des processus impliqués dans la complexation des cations par ces surfaces hétérogènes, dans le but de mieux contraindre et de mieux modéliser leur rôle dans les transferts de métaux en solution et aux interfaces eau-bactéries et eau-oxyhydroxydes de fer.

3.2. Perspectives à moyen et long termes

Les spectres de REE dans les eaux riches en matière organique reflètent les propriétés de complexation de la matière organique et l'hétérogénéité de ces propriétés. Même si ce sont les colloïdes organiques de haut poids moléculaire tels que les acides humiques qui dominent majoritairement la spéciation des REE en solution, une fraction non négligeable de celles-ci semblent liées à des colloïdes organiques plus petits tels que les acides fulviques (e.g. Pokrovsky et al., 2006). Si les propriétés de complexation des acides fulviques devaient s'avérer différentes de celles des acides humiques pour les REE, une variation du rapport humique/fulvique pourrait être à l'origine de variations dans la forme des spectres de REE observée dans les eaux naturelles, fournissant une autre cause possible aux variabilités observées. De plus, les acides fulviques sont plus solubles et donc plus mobiles que les acides humiques. Ces derniers ont tendance à floculer plus facilement dans les estuaires, si bien que les substances humiques marines sont essentiellement composées d'acides fulviques. Ainsi, l'étude de la complexation des REE par les acides fulviques est un champ qu'il conviendrait d'explorer afin de mieux comprendre la géochimie des REE en milieu marin. Finalement, les acides fulviques sont généralement de plus faible poids moléculaire (entre 0,5 et 5 kDa) que les acides humiques (entre 3 et 1000 kDa) (Sparks, 1995). Les techniques d'ultrafiltration, couramment utilisées sur le terrain, ne séparent le plus souvent que partiellement les acides humiques des acides fulviques. Des expériences de compétition entre acides humiques et fulviques pour la complexation des REE, en utilisant des techniques d'ultrafiltration, permettraient d'apporter des informations quant à l'interprétation des données d'ultrafiltration classiquement issues des études de terrain et, ainsi, de mieux comprendre la spéciation des REE dans les eaux.

Au même titre que les particules (>0,2µm), les colloïdes peuvent aussi bien être constituées de phases organiques que minérales, comme des argiles ou des oxydes métalliques. Différentes types de sites de surface sont donc en compétition pour la complexation des REE dans les eaux naturelles ou coexistent différents types de colloïdes organiques et minéraux. Or les spectres des constantes de complexation des REE par les substances humiques (cette thèse), les surfaces d'argile (Coppin et al., 2002), les oxyhydroxydes de fer, de manganèse et d'aluminium (Ohta and Kawabe, 2001; Quinn and Byrne, 2004) présentent différentes formes. Des expériences de compétition entre surfaces devraient donc être réalisées aussi bien à l'échelle particulaire que colloïdale, afin d'être plus proche des conditions prévalant dans les eaux naturelles. L'étude des spectres de REE expérimentaux couplée à la modélisation et à des analyses spectroscopiques permettrait alors de déterminer les mécanismes les plus influents sur la spéciation des REE. L'augmentation de l'hétérogénéité des sites de complexation pour les REE dans ces études de compétition de surfaces par rapport à l'étude d'un seul type de surface est susceptible d'accroître les différences entre la spéciation des différentes REE, comme observé dans cette thèse. Ainsi, ces expériences de compétition de surfaces pour l'adsorption des REE devraient être effectuées également en présence de cations compétiteurs des REE. Les résultats permettraient alors non seulement de mieux comprendre les mécanismes contrôlant la spéciation des REE mais aussi de déterminer ceux contrôlant la spéciation des cations compétiteurs en utilisant le spectre de REE comme traceur, et ce en considérant l'entièreté de la complexité des eaux naturelles.

Annexes

Annexe 1 : Supporting information : Chapitre I

Logarithme des concentrations en REE en solution (mol) et complexées aux acides humiques (mol/kg) à pH = 3 et IS = 0.01 M (NaCl). en fonction de la charge en métaux. Les concentration en carbone organique dissous (DOC) sont présentées en mg L^{-1}.

DOC (mg L^{-1})	4.45	4.28	4.58	3.53	4.82	2.35	3.69	2.96	3.17
pH	3.02	3.03	3.02	3.05	3.03	2.98	3.07	3.00	3.02
REE/C x 10^3	27.3	27.5	27.1	10.3	9.7	7.4	3.1	3.1	2.9
Log [REE^{3+}] (mol) :									
La	-6.193	-6.202	-6.184	-6.920	-6.891	-7.123	-7.677	-7.658	-7.695
Ce	-6.229	-6.237	-6.220	-6.989	-6.973	-7.196	-7.779	-7.767	-7.808
Pr	-6.252	-6.261	-6.243	-7.066	-7.032	-7.245	-7.981	-7.841	-7.885
Nd	-6.266	-6.274	-6.257	-7.072	-7.058	-7.258	-8.001	-7.861	-7.908
Sm	-6.305	-6.313	-6.296	-7.134	-7.116	-7.318	-8.085	-7.943	-7.999
Eu	-6.303	-6.312	-6.294	-7.120	-7.110	-7.306	-8.067	-7.924	-7.973
Gd	-6.291	-6.300	-6.282	-7.071	-7.058	-7.260	-7.985	-7.850	-7.898
Tb	-6.291	-6.300	-6.283	-7.067	-7.054	-7.251	-7.979	-7.845	-7.893
Dy	-6.288	-6.297	-6.280	-7.064	-7.041	-7.240	-7.965	-7.827	-7.878
Ho	-6.290	-6.299	-6.281	-7.053	-7.024	-7.224	-7.944	-7.808	-7.854
Er	-6.289	-6.298	-6.280	-7.048	-7.021	-7.226	-7.949	-7.812	-7.859
Tm	-6.299	-6.307	-6.290	-7.066	-7.038	-7.242	-8.004	-7.852	-7.902
Yb	-6.315	-6.324	-6.306	-7.109	-7.066	-7.284	-8.099	-7.941	-7.992
Lu	-6.312	-6.320	-6.303	-7.096	-7.050	-7.286	-8.134	-7.966	-8.021
Log [REE-HA] (mol/kg):									
La	-1.373	-1.385	-1.371	-1.459	-1.417	-1.658	-1.707	-1.868	-1.868
Ce	-1.306	-1.315	-1.305	-1.406	-1.389	-1.600	-1.663	-1.833	-1.837
Pr	-1.275	-1.282	-1.275	-1.410	-1.376	-1.588	-1.796	-1.838	-1.841
Nd	-1.260	-1.267	-1.264	-1.408	-1.369	-1.577	-1.787	-1.835	-1.834
Sm	-1.246	-1.251	-1.250	-1.404	-1.366	-1.572	-1.799	-1.841	-1.837
Eu	-1.266	-1.272	-1.270	-1.421	-1.377	-1.587	-1.808	-1.846	-1.848
Gd	-1.335	-1.342	-1.339	-1.469	-1.426	-1.642	-1.833	-1.877	-1.881
Tb	-1.362	-1.370	-1.366	-1.485	-1.439	-1.655	-1.843	-1.885	-1.886
Dy	-1.390	-1.399	-1.389	-1.485	-1.452	-1.668	-1.846	-1.895	-1.890
Ho	-1.431	-1.442	-1.435	-1.518	-1.465	-1.697	-1.867	-1.911	-1.906
Er	-1.444	-1.455	-1.443	-1.524	-1.488	-1.705	-1.868	-1.909	-1.910
Tm	-1.453	-1.464	-1.451	-1.520	-1.495	-1.703	-1.866	-1.905	-1.903
Yb	-1.463	-1.474	-1.467	-1.505	-1.498	-1.681	-1.869	-1.891	-1.893
Lu	-1.467	-1.478	-1.471	-1.521	-1.502	-1.680	-1.863	-1.885	-1.885

DOC (mg L^{-1})	4.11	15.32	3.32	4.25	22.61	15.32
pH	3.02	3.02	3.00	2.98	2.98	2.98
REE/C x 10^3	0.9	0.9	0.9	0.5	0.4	0.4
Log [REE^{3+}] (mol) :						
La	-8.479	-8.695	-8.833	-9.101	-9.160	-9.546
Ce	-8.612	-8.854	-9.024	-9.234	-9.305	-9.637
Pr	-8.905	-8.934	-9.197	-9.625	-9.360	-9.783
Nd	-8.915	-8.958	-9.236	-9.615	-9.353	-9.766
Sm	-9.003	-9.073	-9.411	-9.718	-9.433	-9.867
Eu	-9.002	-9.064	-9.431	-9.742	-9.448	-9.888
Gd	-8.895	-9.000	-9.332	-9.637	-9.419	-9.856
Tb	-8.898	-9.010	-9.377	-9.669	-9.457	-9.948
Dy	-8.873	-9.019	-9.389	-9.643	-9.462	-9.966
Ho	-8.853	-9.006	-9.382	-9.631	-9.440	-9.957
Er	-8.857	-9.058	-9.461	-9.655	-9.478	-10.010
Tm	-8.915	-9.189	-9.646	-9.770	-9.567	-10.129
Yb	-9.010	-9.395	-9.879	-9.938	-9.704	-10.264
Lu	-9.029	-9.461	-9.975	-9.982	-9.741	-10.294
Log [REE-HA] (mol/kg):						
La	-2.122	-2.217	-2.465	-2.392	-2.550	-2.597
Ce	-2.100	-2.221	-2.453	-2.385	-2.550	-2.602
Pr	-2.303	-2.232	-2.512	-2.666	-2.567	-2.618
Nd	-2.292	-2.238	-2.509	-2.639	-2.567	-2.623
Sm	-2.315	-2.258	-2.522	-2.668	-2.586	-2.642
Eu	-2.325	-2.261	-2.528	-2.683	-2.590	-2.648
Gd	-2.339	-2.273	-2.543	-2.687	-2.604	-2.659
Tb	-2.346	-2.281	-2.545	-2.708	-2.606	-2.665
Dy	-2.339	-2.286	-2.549	-2.702	-2.611	-2.663
Ho	-2.361	-2.294	-2.557	-2.731	-2.618	-2.677
Er	-2.364	-2.298	-2.556	-2.732	-2.623	-2.680
Tm	-2.369	-2.302	-2.558	-2.757	-2.629	-2.686
Yb	-2.374	-2.311	-2.566	-2.773	-2.638	-2.697
Lu	-2.376	-2.314	-2.564	-2.780	-2.638	-2.699

Annexe 2 : Supporting information : Chapitre II

Eléments à définir dans la base de données de PHREEQC pour y introduire Model VI.

"PHASES" :

Ha

Ha = Ha

log_k 0

"SURFACE_MASTER_SPECIES" :

Ha_a	Ha_aH
Ha_b	Ha_bH
Ha_c	Ha_cH
Ha_d	Ha_dH
Ha_e	Ha_eH
Ha_f	Ha_fH
Ha_g	Ha_gH
Ha_h	Ha_hH
Ha_ab	Ha_abH2
Ha_cd	Ha_cdH2
Ha_ae	Ha_aeH2
Ha_bf	Ha_bfH2
Ha_cg	Ha_cgH2
Ha_dh	Ha_dhH2
Ha_ef	Ha_efH2
Ha_gh	Ha_ghH2
Ha_abx	Ha_abxH2
Ha_cdx	Ha_cdxH2
Ha_aex	Ha_aexH2
Ha_bfx	Ha_bfxH2
Ha_cgx	Ha_cgxH2
Ha_dhx	Ha_dhxH2
Ha_efx	Ha_efxH2
Ha_ghx	Ha_ghxH2
Ha_abxx	Ha_abxxH2
Ha_cdxx	Ha_cdxxH2
Ha_aexx	Ha_aexxH2
Ha_bfxx	Ha_bfxxH2
Ha_cgxx	Ha_cgxxH2
Ha_dhxx	Ha_dhxxH2
Ha_efxx	Ha_efxxH2
Ha_ghxx	Ha_ghxxH2
Ha_abc	Ha_abcH3
Ha_abd	Ha_abdH3
Ha_acd	Ha_acdH3
Ha_bcd	Ha_bcdH3
Ha_abe	Ha_abeH3
Ha_cdf	Ha_cdfH3
Ha_acg	Ha_acgH3
Ha_bdh	Ha_bdhH3
Ha_aef	Ha_aefH3
Ha_bgh	Ha_bghH3
Ha_ceg	Ha_cegH3
Ha_dfh	Ha_dfhH3
Ha_efg	Ha_efgH3
Ha_efh	Ha_efhH3
Ha_egh	Ha_eghH3
Ha_fgh	Ha_fghH3
Ha_abcy	Ha_abcyH3
Ha_abdy	Ha_abdyH3
Ha_acdy	Ha_acdyH3
Ha_bcdy	Ha_bcdyH3
Ha_abey	Ha_abeyH3
Ha_cdfy	Ha_cdfyH3
Ha_acgy	Ha_acgyH3
Ha_bdhy	Ha_bdhyH3
Ha_aefy	Ha_aefyH3
Ha_bghy	Ha_bghyH3
Ha_cegy	Ha_cegyH3
Ha_dfhy	Ha_dfhyH3
Ha_efgy	Ha_efgyH3
Ha_efhy	Ha_efhyH3
Ha_eghy	Ha_eghyH3
Ha_fghy	Ha_fghyH3
Ha_abcyy	Ha_abcyyH3
Ha_abdyy	Ha_abdyyH3
Ha_acdyy	Ha_acdyyH3
Ha_bcdyy	Ha_bcdyyH3
Ha_abeyy	Ha_abeyyH3
Ha_cdfyy	Ha_cdfyyH3
Ha_acgyy	Ha_acgyyH3
Ha_bdhyy	Ha_bdhyyH3
Ha_aefyy	Ha_aefyyH3
Ha_bghyy	Ha_bghyyH3
Ha_cegyy	Ha_cegyyH3
Ha_dfhyy	Ha_dfhyyH3
Ha_efgyy	Ha_efgyyH3
Ha_efhyy	Ha_efhyyH3
Ha_eghyy	Ha_eghyyH3
Ha_fghyy	Ha_fghyyH3

"SURFACE_ SPECIES" :

Ha_aH	=	Ha_aH	;	log_k	0	Ha_aefH3	=	Ha_aefH3	;	log_k	0
Ha_bH	=	Ha_bH	;	log_k	0	Ha_bghH3	=	Ha_bghH3	;	log_k	0
Ha_cH	=	Ha_cH	;	log_k	0	Ha_cegH3	=	Ha_cegH3	;	log_k	0
Ha_dH	=	Ha_dH	;	log_k	0	Ha_dfhH3	=	Ha_dfhH3	;	log_k	0
Ha_eH	=	Ha_eH	;	log_k	0	Ha_efgH3	=	Ha_efgH3	;	log_k	0
Ha_fH	=	Ha_fH	;	log_k	0	Ha_efhH3	=	Ha_efhH3	;	log_k	0
Ha_gH	=	Ha_gH	;	log_k	0	Ha_eghH3	=	Ha_eghH3	;	log_k	0
Ha_hH	=	Ha_hH	;	log_k	0	Ha_fghH3	=	Ha_fghH3	;	log_k	0
Ha_abH2	=	Ha_abH2	;	log_k	0	Ha_abcyH3	=	Ha_abcyH3	;	log_k	0
Ha_cdH2	=	Ha_cdH2	;	log_k	0	Ha_abdyH3	=	Ha_abdyH3	;	log_k	0
Ha_aeH2	=	Ha_aeH2	;	log_k	0	Ha_acdyH3	=	Ha_acdyH3	;	log_k	0
Ha_bfH2	=	Ha_bfH2	;	log_k	0	Ha_bcdyH3	=	Ha_bcdyH3	;	log_k	0
Ha_cgH2	=	Ha_cgH2	;	log_k	0	Ha_abeyH3	=	Ha_abeyH3	;	log_k	0
Ha_dhH2	=	Ha_dhH2	;	log_k	0	Ha_cdfyH3	=	Ha_cdfyH3	;	log_k	0
Ha_efH2	=	Ha_efH2	;	log_k	0	Ha_acgyH3	=	Ha_acgyH3	;	log_k	0
Ha_ghH2	=	Ha_ghH2	;	log_k	0	Ha_bdhyH3	=	Ha_bdhyH3	;	log_k	0
Ha_abxH2	=	Ha_abxH2	;	log_k	0	Ha_aefyH3	=	Ha_aefyH3	;	log_k	0
Ha_cdxH2	=	Ha_cdxH2	;	log_k	0	Ha_bghyH3	=	Ha_bghyH3	;	log_k	0
Ha_aexH2	=	Ha_aexH2	;	log_k	0	Ha_cegyH3	=	Ha_cegyH3	;	log_k	0
Ha_bfxH2	=	Ha_bfxH2	;	log_k	0	Ha_dfhyH3	=	Ha_dfhyH3	;	log_k	0
Ha_cgxH2	=	Ha_cgxH2	;	log_k	0	Ha_efgyH3	=	Ha_efgyH3	;	log_k	0
Ha_dhxH2	=	Ha_dhxH2	;	log_k	0	Ha_efhyH3	=	Ha_efhyH3	;	log_k	0
Ha_efxH2	=	Ha_efxH2	;	log_k	0	Ha_eghyH3	=	Ha_eghyH3	;	log_k	0
Ha_ghxH2	=	Ha_ghxH2	;	log_k	0	Ha_fghyH3	=	Ha_fghyH3	;	log_k	0
Ha_abxxH2	=	Ha_abxxH2	;	log_k	0	Ha_abcyyH3	=	Ha_abcyyH3	;	log_k	0
Ha_cdxxH2	=	Ha_cdxxH2	;	log_k	0	Ha_abdyyH3	=	Ha_abdyyH3	;	log_k	0
Ha_aexxH2	=	Ha_aexxH2	;	log_k	0	Ha_acdyyH3	=	Ha_acdyyH3	;	log_k	0
Ha_bfxxH2	=	Ha_bfxxH2	;	log_k	0	Ha_bcdyyH3	=	Ha_bcdyyH3	;	log_k	0
Ha_cgxxH2	=	Ha_cgxxH2	;	log_k	0	Ha_abeyyH3	=	Ha_abeyyH3	;	log_k	0
Ha_dhxxH2	=	Ha_dhxxH2	;	log_k	0	Ha_cdfyyH3	=	Ha_cdfyyH3	;	log_k	0
Ha_efxxH2	=	Ha_efxxH2	;	log_k	0	Ha_acgyyH3	=	Ha_acgyyH3	;	log_k	0
Ha_ghxxH2	=	Ha_ghxxH2	;	log_k	0	Ha_bdhyyH3	=	Ha_bdhyyH3	;	log_k	0
Ha_abcH3	=	Ha_abcH3	;	log_k	0	Ha_aefyyH3	=	Ha_aefyyH3	;	log_k	0
Ha_abdH3	=	Ha_abdH3	;	log_k	0	Ha_bghyyH3	=	Ha_bghyyH3	;	log_k	0
Ha_acdH3	=	Ha_acdH3	;	log_k	0	Ha_cegyyH3	=	Ha_cegyyH3	;	log_k	0
Ha_bcdH3	=	Ha_bcdH3	;	log_k	0	Ha_dfhyyH3	=	Ha_dfhyyH3	;	log_k	0
Ha_abeH3	=	Ha_abeH3	;	log_k	0	Ha_efgyyH3	=	Ha_efgyyH3	;	log_k	0
Ha_cdfH3	=	Ha_cdfH3	;	log_k	0	Ha_efhyyH3	=	Ha_efhyyH3	;	log_k	0
Ha_acgH3	=	Ha_acgH3	;	log_k	0	Ha_eghyyH3	=	Ha_eghyyH3	;	log_k	0
Ha_bdhH3	=	Ha_bdhH3	;	log_k	0	Ha_fghyyH3	=	Ha_fghyyH3	;	log_k	0

Réactions de première déprotonation des sites mono-, bi- et tridentates de HA :

Ha_aH	=	Ha_a-	+	H+	;	log_k	-3.05		Ha_aefH3	=	Ha_aefH2-	+	H+	;	log_k	-3.05	;
Ha_bH	=	Ha_b-	+	H+	;	log_k	-3.75		Ha_bghH3	=	Ha_bghH2-	+	H+	;	log_k	-3.75	;
Ha_cH	=	Ha_c-	+	H+	;	log_k	-4.45		Ha_cegH3	=	Ha_cegH2-	+	H+	;	log_k	-4.45	;
Ha_dH	=	Ha_d-	+	H+	;	log_k	-5.15		Ha_dfhH3	=	Ha_dfhH2-	+	H+	;	log_k	-5.15	;
Ha_eH	=	Ha_e-	+	H+	;	log_k	-7.00		Ha_efgH3	=	Ha_efgH2-	+	H+	;	log_k	-7.00	;
Ha_fH	=	Ha_f-	+	H+	;	log_k	-8.20		Ha_efhH3	=	Ha_efhH2-	+	H+	;	log_k	-7.00	;
Ha_gH	=	Ha_g-	+	H+	;	log_k	-9.40		Ha_eghH3	=	Ha_eghH2-	+	H+	;	log_k	-7.00	;
Ha_hH	=	Ha_h-	+	H+	;	log_k	-10.60		Ha_fghH3	=	Ha_fghH2-	+	H+	;	log_k	-8.20	;
Ha_abH2	=	Ha_abH-	+	H+	;	log_k	-3.05		Ha_abcyH3	=	Ha_abcyH2-	+	H+	;	log_k	-3.05	;
Ha_cdH2	=	Ha_cdH-	+	H+	;	log_k	-4.45		Ha_abdyH3	=	Ha_abdyH2-	+	H+	;	log_k	-3.05	;
Ha_aeH2	=	Ha_aeH-	+	H+	;	log_k	-3.05		Ha_acdyH3	=	Ha_acdyH2-	+	H+	;	log_k	-3.05	;
Ha_bfH2	=	Ha_bfH-	+	H+	;	log_k	-3.75		Ha_bcdyH3	=	Ha_bcdyH2-	+	H+	;	log_k	-3.75	;
Ha_cgH2	=	Ha_cgH-	+	H+	;	log_k	-4.45		Ha_abeyH3	=	Ha_abeyH2-	+	H+	;	log_k	-3.05	;
Ha_dhH2	=	Ha_dhH-	+	H+	;	log_k	-5.15		Ha_cdfyH3	=	Ha_cdfyH2-	+	H+	;	log_k	-4.45	;
Ha_efH2	=	Ha_efH-	+	H+	;	log_k	-7.00		Ha_acgyH3	=	Ha_acgyH2-	+	H+	;	log_k	-3.05	;
Ha_ghH2	=	Ha_ghH-	+	H+	;	log_k	-9.40		Ha_bdhyH3	=	Ha_bdhyH2-	+	H+	;	log_k	-3.75	;
Ha_abxH2	=	Ha_abxH-	+	H+	;	log_k	-3.05		Ha_aefyH3	=	Ha_aefyH2-	+	H+	;	log_k	-3.05	;
Ha_cdxH2	=	Ha_cdxH-	+	H+	;	log_k	-4.45		Ha_bghyH3	=	Ha_bghyH2-	+	H+	;	log_k	-3.75	;
Ha_aexH2	=	Ha_aexH-	+	H+	;	log_k	-3.05		Ha_cegyH3	=	Ha_cegyH2-	+	H+	;	log_k	-4.45	;
Ha_bfxH2	=	Ha_bfxH-	+	H+	;	log_k	-3.75		Ha_dfhyH3	=	Ha_dfhyH2-	+	H+	;	log_k	-5.15	;
Ha_cgxH2	=	Ha_cgxH-	+	H+	;	log_k	-4.45		Ha_efgyH3	=	Ha_efgyH2-	+	H+	;	log_k	-7.00	;
Ha_dhxH2	=	Ha_dhxH-	+	H+	;	log_k	-5.15		Ha_efhyH3	=	Ha_efhyH2-	+	H+	;	log_k	-7.00	;
Ha_efxH2	=	Ha_efxH-	+	H+	;	log_k	-7.00		Ha_eghyH3	=	Ha_eghyH2-	+	H+	;	log_k	-7.00	;
Ha_ghxH2	=	Ha_ghxH-	+	H+	;	log_k	-9.40		Ha_fghyH3	=	Ha_fghyH2-	+	H+	;	log_k	-8.20	;
Ha_abxxH2	=	Ha_abxxH-	+	H+	;	log_k	-3.05		Ha_abcyyH3	=	Ha_abcyyH2-	+	H+	;	log_k	-3.05	;
Ha_cdxxH2	=	Ha_cdxxH-	+	H+	;	log_k	-4.45		Ha_abdyyH3	=	Ha_abdyyH2-	+	H+	;	log_k	-3.05	;
Ha_aexxH2	=	Ha_aexxH-	+	H+	;	log_k	-3.05		Ha_acdyyH3	=	Ha_acdyyH2-	+	H+	;	log_k	-3.05	;
Ha_bfxxH2	=	Ha_bfxxH-	+	H+	;	log_k	-3.75		Ha_bcdyyH3	=	Ha_bcdyyH2-	+	H+	;	log_k	-3.75	;
Ha_cgxxH2	=	Ha_cgxxH-	+	H+	;	log_k	-4.45		Ha_abeyyH3	=	Ha_abeyyH2-	+	H+	;	log_k	-3.05	;
Ha_dhxxH2	=	Ha_dhxxH-	+	H+	;	log_k	-5.15		Ha_cdfyyH3	=	Ha_cdfyyH2-	+	H+	;	log_k	-4.45	;
Ha_efxxH2	=	Ha_efxxH-	+	H+	;	log_k	-7.00		Ha_acgyyH3	=	Ha_acgyyH2-	+	H+	;	log_k	-3.05	;
Ha_ghxxH2	=	Ha_ghxxH-	+	H+	;	log_k	-9.40		Ha_bdhyyH3	=	Ha_bdhyyH2-	+	H+	;	log_k	-3.75	;
Ha_abcH3	=	Ha_abcH2-	+	H+	;	log_k	-3.05		Ha_aefyyH3	=	Ha_aefyyH2-	+	H+	;	log_k	-3.05	;
Ha_abdH3	=	Ha_abdH2-	+	H+	;	log_k	-3.05		Ha_bghyyH3	=	Ha_bghyyH2-	+	H+	;	log_k	-3.75	;
Ha_acdH3	=	Ha_acdH2-	+	H+	;	log_k	-3.05		Ha_cegyyH3	=	Ha_cegyyH2-	+	H+	;	log_k	-4.45	;
Ha_bcdH3	=	Ha_bcdH2-	+	H+	;	log_k	-3.75		Ha_dfhyyH3	=	Ha_dfhyyH2-	+	H+	;	log_k	-5.15	;
Ha_abeH3	=	Ha_abeH2-	+	H+	;	log_k	-3.05		Ha_efgyyH3	=	Ha_efgyyH2-	+	H+	;	log_k	-7.00	;
Ha_cdfH3	=	Ha_cdfH2-	+	H+	;	log_k	-4.45		Ha_efhyyH3	=	Ha_efhyyH2-	+	H+	;	log_k	-7.00	;
Ha_acgH3	=	Ha_acgH2-	+	H+	;	log_k	-3.05		Ha_eghyyH3	=	Ha_eghyyH2-	+	H+	;	log_k	-7.00	;
Ha_bdhH3	=	Ha_bdhH2-	+	H+	;	log_k	-3.75		Ha_fghyyH3	=	Ha_fghyyH2-	+	H+	;	log_k	-8.20	;

Réactions de deuxième déprotonation des sites bidentates de HA :

Ha_abH-	=	Ha_ab-2	+	H+	;	log_k	-3.75	;	Ha_cgxH-	=	Ha_cgx-2	+	H+	;	log_k	-9.40	;
Ha_cdH-	=	Ha_cd-2	+	H+	;	log_k	-5.15	;	Ha_dhxH-	=	Ha_dhx-2	+	H+	;	log_k	-10.60	;
Ha_aeH-	=	Ha_ae-2	+	H+	;	log_k	-7.00	;	Ha_efxH-	=	Ha_efx-2	+	H+	;	log_k	-8.20	;
Ha_bfH-	=	Ha_bf-2	+	H+	;	log_k	-8.20	;	Ha_ghxH-	=	Ha_ghx-2	+	H+	;	log_k	-10.60	;
Ha_cgH-	=	Ha_cg-2	+	H+	;	log_k	-9.40	;	Ha_abxxH-	=	Ha_abxx-2	+	H+	;	log_k	-3.75	;
Ha_dhH-	=	Ha_dh-2	+	H+	;	log_k	-10.60	;	Ha_cdxxH-	=	Ha_cdxx-2	+	H+	;	log_k	-5.15	;
Ha_efH-	=	Ha_ef-2	+	H+	;	log_k	-8.20	;	Ha_aexxH-	=	Ha_aexx-2	+	H+	;	log_k	-7.00	;
Ha_ghH-	=	Ha_gh-2	+	H+	;	log_k	-10.60	;	Ha_bfxxH-	=	Ha_bfxx-2	+	H+	;	log_k	-8.20	;
Ha_abxH-	=	Ha_abx-2	+	H+	;	log_k	-3.75	;	Ha_cgxxH-	=	Ha_cgxx-2	+	H+	;	log_k	-9.40	;
Ha_cdxH-	=	Ha_cdx-2	+	H+	;	log_k	-5.15	;	Ha_dhxxH-	=	Ha_dhxx-2	+	H+	;	log_k	-10.60	;
Ha_aexH-	=	Ha_aex-2	+	H+	;	log_k	-7.00	;	Ha_efxxH-	=	Ha_efxx-2	+	H+	;	log_k	-8.20	;
Ha_bfxH-	=	Ha_bfx-2	+	H+	;	log_k	-8.20	;	Ha_ghxxH-	=	Ha_ghxx-2	+	H+	;	log_k	-10.60	;

Réactions de deuxième et troisième déprotonation des sites tridentates de HA :

Ha_abcH2-	=	Ha_abcH-2	+	H+	;	log_k	-3.75	;	Ha_abcH-2	=	Ha_abc-3	+	H+	;	log_k	-4.45	;
Ha_abdH2-	=	Ha_abdH-2	+	H+	;	log_k	-3.75	;	Ha_abdH-2	=	Ha_abd-3	+	H+	;	log_k	-5.15	;
Ha_acdH2-	=	Ha_acdH-2	+	H+	;	log_k	-4.45	;	Ha_acdH-2	=	Ha_acd-3	+	H+	;	log_k	-5.15	;
Ha_bcdH2-	=	Ha_bcdH-2	+	H+	;	log_k	-4.45	;	Ha_bcdH-2	=	Ha_bcd-3	+	H+	;	log_k	-5.15	;
Ha_abeH2-	=	Ha_abeH-2	+	H+	;	log_k	-3.75	;	Ha_abeH-2	=	Ha_abe-3	+	H+	;	log_k	-7.00	;
Ha_cdfH2-	=	Ha_cdfH-2	+	H+	;	log_k	-5.15	;	Ha_cdfH-2	=	Ha_cdf-3	+	H+	;	log_k	-8.20	;
Ha_acgH2-	=	Ha_acgH-2	+	H+	;	log_k	-4.45	;	Ha_acgH-2	=	Ha_acg-3	+	H+	;	log_k	-9.40	;
Ha_bdhH2-	=	Ha_bdhH-2	+	H+	;	log_k	-5.15	;	Ha_bdhH-2	=	Ha_bdh-3	+	H+	;	log_k	-10.60	;
Ha_aefH2-	=	Ha_aefH-2	+	H+	;	log_k	-7.00	;	Ha_aefH-2	=	Ha_aef-3	+	H+	;	log_k	-8.20	;
Ha_bghH2-	=	Ha_bghH-2	+	H+	;	log_k	-9.40	;	Ha_bghH-2	=	Ha_bgh-3	+	H+	;	log_k	-10.60	;
Ha_cegH2-	=	Ha_cegH-2	+	H+	;	log_k	-7.00	;	Ha_cegH-2	=	Ha_ceg-3	+	H+	;	log_k	-9.40	;
Ha_dfhH2-	=	Ha_dfhH-2	+	H+	;	log_k	-8.20	;	Ha_dfhH-2	=	Ha_dfh-3	+	H+	;	log_k	-10.60	;
Ha_efgH2-	=	Ha_efgH-2	+	H+	;	log_k	-8.20	;	Ha_efgH-2	=	Ha_efg-3	+	H+	;	log_k	-9.40	;
Ha_efhH2-	=	Ha_efhH-2	+	H+	;	log_k	-8.20	;	Ha_efhH-2	=	Ha_efh-3	+	H+	;	log_k	-10.60	;
Ha_eghH2-	=	Ha_eghH-2	+	H+	;	log_k	-9.40	;	Ha_eghH-2	=	Ha_egh-3	+	H+	;	log_k	-10.60	;
Ha_fghH2-	=	Ha_fghH-2	+	H+	;	log_k	-9.40	;	Ha_fghH-2	=	Ha_fgh-3	+	H+	;	log_k	-10.60	;
Ha_abcyH2-	=	Ha_abcyH-2	+	H+	;	log_k	-3.75	;	Ha_abcyH-2	=	Ha_abcy-3	+	H+	;	log_k	-4.45	;
Ha_abdyH2-	=	Ha_abdyH-2	+	H+	;	log_k	-3.75	;	Ha_abdyH-2	=	Ha_abdy-3	+	H+	;	log_k	-5.15	;
Ha_acdyH2-	=	Ha_acdyH-2	+	H+	;	log_k	-4.45	;	Ha_acdyH-2	=	Ha_acdy-3	+	H+	;	log_k	-5.15	;
Ha_bcdyH2-	=	Ha_bcdyH-2	+	H+	;	log_k	-4.45	;	Ha_bcdyH-2	=	Ha_bcdy-3	+	H+	;	log_k	-5.15	;
Ha_abeyH2-	=	Ha_abeyH-2	+	H+	;	log_k	-3.75	;	Ha_abeyH-2	=	Ha_abey-3	+	H+	;	log_k	-7.00	;
Ha_cdfyH2-	=	Ha_cdfyH-2	+	H+	;	log_k	-5.15	;	Ha_cdfyH-2	=	Ha_cdfy-3	+	H+	;	log_k	-8.20	;
Ha_acgyH2-	=	Ha_acgyH-2	+	H+	;	log_k	-4.45	;	Ha_acgyH-2	=	Ha_acgy-3	+	H+	;	log_k	-9.40	;
Ha_bdhyH2-	=	Ha_bdhyH-2	+	H+	;	log_k	-5.15	;	Ha_bdhyH-2	=	Ha_bdhy-3	+	H+	;	log_k	-10.60	;
Ha_aefyH2-	=	Ha_aefyH-2	+	H+	;	log_k	-7.00	;	Ha_aefyH-2	=	Ha_aefy-3	+	H+	;	log_k	-8.20	;
Ha_bghyH2-	=	Ha_bghyH-2	+	H+	;	log_k	-9.40	;	Ha_bghyH-2	=	Ha_bghy-3	+	H+	;	log_k	-10.60	;
Ha_cegyH2-	=	Ha_cegyH-2	+	H+	;	log_k	-7.00	;	Ha_cegyH-2	=	Ha_cegy-3	+	H+	;	log_k	-9.40	;
Ha_dfhyH2-	=	Ha_dfhyH-2	+	H+	;	log_k	-8.20	;	Ha_dfhyH-2	=	Ha_dfhy-3	+	H+	;	log_k	-10.60	;
Ha_efgyH2-	=	Ha_efgyH-2	+	H+	;	log_k	-8.20	;	Ha_efgyH-2	=	Ha_efgy-3	+	H+	;	log_k	-9.40	;
Ha_efhyH2-	=	Ha_efhyH-2	+	H+	;	log_k	-8.20	;	Ha_efhyH-2	=	Ha_efhy-3	+	H+	;	log_k	-10.60	;
Ha_eghyH2-	=	Ha_eghyH-2	+	H+	;	log_k	-9.40	;	Ha_eghyH-2	=	Ha_eghy-3	+	H+	;	log_k	-10.60	;
Ha_fghyH2-	=	Ha_fghyH-2	+	H+	;	log_k	-9.40	;	Ha_fghyH-2	=	Ha_fghy-3	+	H+	;	log_k	-10.60	;
Ha_abcyyH2-	=	Ha_abcyyH-2	+	H+	;	log_k	-3.75	;	Ha_abcyyH-2	=	Ha_abcyy-3	+	H+	;	log_k	-4.45	;
Ha_abdyyH2-	=	Ha_abdyyH-2	+	H+	;	log_k	-3.75	;	Ha_abdyyH-2	=	Ha_abdyy-3	+	H+	;	log_k	-5.15	;
Ha_acdyyH2-	=	Ha_acdyyH-2	+	H+	;	log_k	-4.45	;	Ha_acdyyH-2	=	Ha_acdyy-3	+	H+	;	log_k	-5.15	;
Ha_bcdyyH2-	=	Ha_bcdyyH-2	+	H+	;	log_k	-4.45	;	Ha_bcdyyH-2	=	Ha_bcdyy-3	+	H+	;	log_k	-5.15	;
Ha_abeyyH2-	=	Ha_abeyyH-2	+	H+	;	log_k	-3.75	;	Ha_abeyyH-2	=	Ha_abeyy-3	+	H+	;	log_k	-7.00	;
Ha_cdfyyH2-	=	Ha_cdfyyH-2	+	H+	;	log_k	-5.15	;	Ha_cdfyyH-2	=	Ha_cdfyy-3	+	H+	;	log_k	-8.20	;
Ha_acgyyH2-	=	Ha_acgyyH-2	+	H+	;	log_k	-4.45	;	Ha_acgyyH-2	=	Ha_acgyy-3	+	H+	;	log_k	-9.40	;
Ha_bdhyyH2-	=	Ha_bdhyyH-2	+	H+	;	log_k	-5.15	;	Ha_bdhyyH-2	=	Ha_bdhyy-3	+	H+	;	log_k	-10.60	;
Ha_aefyyH2-	=	Ha_aefyyH-2	+	H+	;	log_k	-7.00	;	Ha_aefyyH-2	=	Ha_aefyy-3	+	H+	;	log_k	-8.20	;
Ha_bghyyH2-	=	Ha_bghyyH-2	+	H+	;	log_k	-9.40	;	Ha_bghyyH-2	=	Ha_bghyy-3	+	H+	;	log_k	-10.60	;
Ha_cegyyH2-	=	Ha_cegyyH-2	+	H+	;	log_k	-7.00	;	Ha_cegyyH-2	=	Ha_cegyy-3	+	H+	;	log_k	-9.40	;
Ha_dfhyyH2-	=	Ha_dfhyyH-2	+	H+	;	log_k	-8.20	;	Ha_dfhyyH-2	=	Ha_dfhyy-3	+	H+	;	log_k	-10.60	;
Ha_efgyyH2-	=	Ha_efgyyH-2	+	H+	;	log_k	-8.20	;	Ha_efgyyH-2	=	Ha_efgyy-3	+	H+	;	log_k	-9.40	;
Ha_efhyyH2-	=	Ha_efhyyH-2	+	H+	;	log_k	-8.20	;	Ha_efhyyH-2	=	Ha_efhyy-3	+	H+	;	log_k	-10.60	;
Ha_eghyyH2-	=	Ha_eghyyH-2	+	H+	;	log_k	-9.40	;	Ha_eghyyH-2	=	Ha_eghyy-3	+	H+	;	log_k	-10.60	;
Ha_fghyyH2-	=	Ha_fghyyH-2	+	H+	;	log_k	-9.40	;	Ha_fghyyH-2	=	Ha_fghyy-3	+	H+	;	log_k	-10.60	;

Réactions de complexation d'un cation M^{n+} par les sites mono-, bi- et tridentates de HA :

Ha_a-	+	M+n	=	Ha_aM(n-1)	;	log_k	(valeur)	;	Ha_aef-3	+	M+n	=	Ha_aefM(n-3)	;	log_k	(valeur)	;
Ha_b-	+	M+n	=	Ha_bM(n-1)	;	log_k	(valeur)	;	Ha_bgh-3	+	M+n	=	Ha_bghM(n-3)	;	log_k	(valeur)	;
Ha_c-	+	M+n	=	Ha_cM(n-1)	;	log_k	(valeur)	;	Ha_ceg-3	+	M+n	=	Ha_cegM(n-3)	;	log_k	(valeur)	;
Ha_d-	+	M+n	=	Ha_dM(n-1)	;	log_k	(valeur)	;	Ha_dfh-3	+	M+n	=	Ha_dfhM(n-3)	;	log_k	(valeur)	;
Ha_e-	+	M+n	=	Ha_eM(n-1)	;	log_k	(valeur)	;	Ha_efg-3	+	M+n	=	Ha_efgM(n-3)	;	log_k	(valeur)	;
Ha_f-	+	M+n	=	Ha_fM(n-1)	;	log_k	(valeur)	;	Ha_efh-3	+	M+n	=	Ha_efhM(n-3)	;	log_k	(valeur)	;
Ha_g-	+	M+n	=	Ha_gM(n-1)	;	log_k	(valeur)	;	Ha_egh-3	+	M+n	=	Ha_eghM(n-3)	;	log_k	(valeur)	;
Ha_h-	+	M+n	=	Ha_hM(n-1)	;	log_k	(valeur)	;	Ha_fgh-3	+	M+n	=	Ha_fghM(n-3)	;	log_k	(valeur)	;
Ha_ab-2	+	M+n	=	Ha_abM(n-2)	;	log_k	(valeur)	;	Ha_abcy-3	+	M+n	=	Ha_abcyM(n-3)	;	log_k	(valeur)	;
Ha_cd-2	+	M+n	=	Ha_cdM(n-2)	;	log_k	(valeur)	;	Ha_abdy-3	+	M+n	=	Ha_abdyM(n-3)	;	log_k	(valeur)	;
Ha_ae-2	+	M+n	=	Ha_aeM(n-2)	;	log_k	(valeur)	;	Ha_acdy-3	+	M+n	=	Ha_acdyM(n-3)	;	log_k	(valeur)	;
Ha_bf-2	+	M+n	=	Ha_bfM(n-2)	;	log_k	(valeur)	;	Ha_bcdy-3	+	M+n	=	Ha_bcdyM(n-3)	;	log_k	(valeur)	;
Ha_cg-2	+	M+n	=	Ha_cgM(n-2)	;	log_k	(valeur)	;	Ha_abey-3	+	M+n	=	Ha_abeyM(n-3)	;	log_k	(valeur)	;
Ha_dh-2	+	M+n	=	Ha_dhM(n-2)	;	log_k	(valeur)	;	Ha_cdfy-3	+	M+n	=	Ha_cdfyM(n-3)	;	log_k	(valeur)	;
Ha_ef-2	+	M+n	=	Ha_efM(n-2)	;	log_k	(valeur)	;	Ha_acgy-3	+	M+n	=	Ha_acgyM(n-3)	;	log_k	(valeur)	;
Ha_gh-2	+	M+n	=	Ha_ghM(n-2)	;	log_k	(valeur)	;	Ha_bdhy-3	+	M+n	=	Ha_bdhyM(n-3)	;	log_k	(valeur)	;
Ha_abx-2	+	M+n	=	Ha_abxM(n-2)	;	log_k	(valeur)	;	Ha_aefy-3	+	M+n	=	Ha_aefyM(n-3)	;	log_k	(valeur)	;
Ha_cdx-2	+	M+n	=	Ha_cdxM(n-2)	;	log_k	(valeur)	;	Ha_bghy-3	+	M+n	=	Ha_bghyM(n-3)	;	log_k	(valeur)	;
Ha_aex-2	+	M+n	=	Ha_aexM(n-2)	;	log_k	(valeur)	;	Ha_cegy-3	+	M+n	=	Ha_cegyM(n-3)	;	log_k	(valeur)	;
Ha_bfx-2	+	M+n	=	Ha_bfxM(n-2)	;	log_k	(valeur)	;	Ha_dfhy-3	+	M+n	=	Ha_dfhyM(n-3)	;	log_k	(valeur)	;
Ha_cgx-2	+	M+n	=	Ha_cgxM(n-2)	;	log_k	(valeur)	;	Ha_efgy-3	+	M+n	=	Ha_efgyM(n-3)	;	log_k	(valeur)	;
Ha_dhx-2	+	M+n	=	Ha_dhxM(n-2)	;	log_k	(valeur)	;	Ha_efhy-3	+	M+n	=	Ha_efhyM(n-3)	;	log_k	(valeur)	;
Ha_efx-2	+	M+n	=	Ha_efxM(n-2)	;	log_k	(valeur)	;	Ha_eghy-3	+	M+n	=	Ha_eghyM(n-3)	;	log_k	(valeur)	;
Ha_ghx-2	+	M+n	=	Ha_ghxM(n-2)	;	log_k	(valeur)	;	Ha_fghy-3	+	M+n	=	Ha_fghyM(n-3)	;	log_k	(valeur)	;
Ha_abxx-2	+	M+n	=	Ha_abxxM(n-2)	;	log_k	(valeur)	;	Ha_abcyy-3	+	M+n	=	Ha_abcyyM(n-3)	;	log_k	(valeur)	;
Ha_cdxx-2	+	M+n	=	Ha_cdxxM(n-2)	;	log_k	(valeur)	;	Ha_abdyy-3	+	M+n	=	Ha_abdyyM(n-3)	;	log_k	(valeur)	;
Ha_aexx-2	+	M+n	=	Ha_aexxM(n-2)	;	log_k	(valeur)	;	Ha_acdyy-3	+	M+n	=	Ha_acdyyM(n-3)	;	log_k	(valeur)	;
Ha_bfxx-2	+	M+n	=	Ha_bfxxM(n-2)	;	log_k	(valeur)	;	Ha_bcdyy-3	+	M+n	=	Ha_bcdyyM(n-3)	;	log_k	(valeur)	;
Ha_cgxx-2	+	M+n	=	Ha_cgxxM(n-2)	;	log_k	(valeur)	;	Ha_abeyy-3	+	M+n	=	Ha_abeyyM(n-3)	;	log_k	(valeur)	;
Ha_dhxx-2	+	M+n	=	Ha_dhxxM(n-2)	;	log_k	(valeur)	;	Ha_cdfyy-3	+	M+n	=	Ha_cdfyyM(n-3)	;	log_k	(valeur)	;
Ha_efxx-2	+	M+n	=	Ha_efxxM(n-2)	;	log_k	(valeur)	;	Ha_acgyy-3	+	M+n	=	Ha_acgyyM(n-3)	;	log_k	(valeur)	;
Ha_ghxx-2	+	M+n	=	Ha_ghxxM(n-2)	;	log_k	(valeur)	;	Ha_bdhyy-3	+	M+n	=	Ha_bdhyyM(n-3)	;	log_k	(valeur)	;
Ha_abc-3	+	M+n	=	Ha_abcM(n-3)	;	log_k	(valeur)	;	Ha_aefyy-3	+	M+n	=	Ha_aefyyM(n-3)	;	log_k	(valeur)	;
Ha_abd-3	+	M+n	=	Ha_abdM(n-3)	;	log_k	(valeur)	;	Ha_bghyy-3	+	M+n	=	Ha_bghyyM(n-3)	;	log_k	(valeur)	;
Ha_acd-3	+	M+n	=	Ha_acdM(n-3)	;	log_k	(valeur)	;	Ha_cegyy-3	+	M+n	=	Ha_cegyyM(n-3)	;	log_k	(valeur)	;
Ha_bcd-3	+	M+n	=	Ha_bcdM(n-3)	;	log_k	(valeur)	;	Ha_dfhyy-3	+	M+n	=	Ha_dfhyyM(n-3)	;	log_k	(valeur)	;
Ha_abe-3	+	M+n	=	Ha_abeM(n-3)	;	log_k	(valeur)	;	Ha_efgyy-3	+	M+n	=	Ha_efgyyM(n-3)	;	log_k	(valeur)	;
Ha_cdf-3	+	M+n	=	Ha_cdfM(n-3)	;	log_k	(valeur)	;	Ha_efhyy-3	+	M+n	=	Ha_efhyyM(n-3)	;	log_k	(valeur)	;
Ha_acg-3	+	M+n	=	Ha_acgM(n-3)	;	log_k	(valeur)	;	Ha_eghyy-3	+	M+n	=	Ha_eghyyM(n-3)	;	log_k	(valeur)	;
Ha_bdh-3	+	M+n	=	Ha_bdhM(n-3)	;	log_k	(valeur)	;	Ha_fghyy-3	+	M+n	=	Ha_fghyyM(n-3)	;	log_k	(valeur)	;

Réactions de complexation d'un cation $MOH^{(n-1)}$ par les sites mono-, bi- et tridentates de HA :

Ha_a-	+	MOH(n-1)	=	Ha_aMOH(n-2)	;	log_k	(valeur)	Ha_aef-3	+	MOH(n-1)	=	Ha_aefMOH(n-4)	;	log_k	(valeur)	;
Ha_b-	+	MOH(n-1)	=	Ha_bMOH(n-2)	;	log_k	(valeur)	Ha_bgh-3	+	MOH(n-1)	=	Ha_bghMOH(n-4)	;	log_k	(valeur)	;
Ha_c-	+	MOH(n-1)	=	Ha_cMOH(n-2)	;	log_k	(valeur)	Ha_ceg-3	+	MOH(n-1)	=	Ha_cegMOH(n-4)	;	log_k	(valeur)	;
Ha_d-	+	MOH(n-1)	=	Ha_dMOH(n-2)	;	log_k	(valeur)	Ha_dfh-3	+	MOH(n-1)	=	Ha_dfhMOH(n-4)	;	log_k	(valeur)	;
Ha_e-	+	MOH(n-1)	=	Ha_eMOH(n-2)	;	log_k	(valeur)	Ha_efg-3	+	MOH(n-1)	=	Ha_efgMOH(n-4)	;	log_k	(valeur)	;
Ha_f-	+	MOH(n-1)	=	Ha_fMOH(n-2)	;	log_k	(valeur)	Ha_efh-3	+	MOH(n-1)	=	Ha_efhMOH(n-4)	;	log_k	(valeur)	;
Ha_g-	+	MOH(n-1)	=	Ha_gMOH(n-2)	;	log_k	(valeur)	Ha_egh-3	+	MOH(n-1)	=	Ha_eghMOH(n-4)	;	log_k	(valeur)	;
Ha_h-	+	MOH(n-1)	=	Ha_hMOH(n-2)	;	log_k	(valeur)	Ha_fgh-3	+	MOH(n-1)	=	Ha_fghMOH(n-4)	;	log_k	(valeur)	;
Ha_ab-2	+	MOH(n-1)	=	Ha_abMOH(n-3)	;	log_k	(valeur)	Ha_abcy-3	+	MOH(n-1)	=	Ha_abcyMOH(n-4)	;	log_k	(valeur)	;
Ha_cd-2	+	MOH(n-1)	=	Ha_cdMOH(n-3)	;	log_k	(valeur)	Ha_abdy-3	+	MOH(n-1)	=	Ha_abdyMOH(n-4)	;	log_k	(valeur)	;
Ha_ae-2	+	MOH(n-1)	=	Ha_aeMOH(n-3)	;	log_k	(valeur)	Ha_acdy-3	+	MOH(n-1)	=	Ha_acdyMOH(n-4)	;	log_k	(valeur)	;
Ha_bf-2	+	MOH(n-1)	=	Ha_bfMOH(n-3)	;	log_k	(valeur)	Ha_bcdy-3	+	MOH(n-1)	=	Ha_bcdyMOH(n-4)	;	log_k	(valeur)	;
Ha_cg-2	+	MOH(n-1)	=	Ha_cgMOH(n-3)	;	log_k	(valeur)	Ha_abey-3	+	MOH(n-1)	=	Ha_abeyMOH(n-4)	;	log_k	(valeur)	;
Ha_dh-2	+	MOH(n-1)	=	Ha_dhMOH(n-3)	;	log_k	(valeur)	Ha_cdfy-3	+	MOH(n-1)	=	Ha_cdfyMOH(n-4)	;	log_k	(valeur)	;
Ha_ef-2	+	MOH(n-1)	=	Ha_efMOH(n-3)	;	log_k	(valeur)	Ha_acgy-3	+	MOH(n-1)	=	Ha_acgyMOH(n-4)	;	log_k	(valeur)	;
Ha_gh-2	+	MOH(n-1)	=	Ha_ghMOH(n-3)	;	log_k	(valeur)	Ha_bdhy-3	+	MOH(n-1)	=	Ha_bdhyMOH(n-4)	;	log_k	(valeur)	;
Ha_abx-2	+	MOH(n-1)	=	Ha_abxMOH(n-3)	;	log_k	(valeur)	Ha_aefy-3	+	MOH(n-1)	=	Ha_aefyMOH(n-4)	;	log_k	(valeur)	;
Ha_cdx-2	+	MOH(n-1)	=	Ha_cdxMOH(n-3)	;	log_k	(valeur)	Ha_bghy-3	+	MOH(n-1)	=	Ha_bghyMOH(n-4)	;	log_k	(valeur)	;
Ha_aex-2	+	MOH(n-1)	=	Ha_aexMOH(n-3)	;	log_k	(valeur)	Ha_cegy-3	+	MOH(n-1)	=	Ha_cegyMOH(n-4)	;	log_k	(valeur)	;
Ha_bfx-2	+	MOH(n-1)	=	Ha_bfxMOH(n-3)	;	log_k	(valeur)	Ha_dfhy-3	+	MOH(n-1)	=	Ha_dfhyMOH(n-4)	;	log_k	(valeur)	;
Ha_cgx-2	+	MOH(n-1)	=	Ha_cgxMOH(n-3)	;	log_k	(valeur)	Ha_efgy-3	+	MOH(n-1)	=	Ha_efgyMOH(n-4)	;	log_k	(valeur)	;
Ha_dhx-2	+	MOH(n-1)	=	Ha_dhxMOH(n-3)	;	log_k	(valeur)	Ha_efhy-3	+	MOH(n-1)	=	Ha_efhyMOH(n-4)	;	log_k	(valeur)	;
Ha_efx-2	+	MOH(n-1)	=	Ha_efxMOH(n-3)	;	log_k	(valeur)	Ha_eghy-3	+	MOH(n-1)	=	Ha_eghyMOH(n-4)	;	log_k	(valeur)	;
Ha_ghx-2	+	MOH(n-1)	=	Ha_ghxMOH(n-3)	;	log_k	(valeur)	Ha_fghy-3	+	MOH(n-1)	=	Ha_fghyMOH(n-4)	;	log_k	(valeur)	;
Ha_abxx-2	+	MOH(n-1)	=	Ha_abxxMOH(n-3)	;	log_k	(valeur)	Ha_abcyy-3	+	MOH(n-1)	=	Ha_abcyyMOH(n-4)	;	log_k	(valeur)	;
Ha_cdxx-2	+	MOH(n-1)	=	Ha_cdxxMOH(n-3)	;	log_k	(valeur)	Ha_abdyy-3	+	MOH(n-1)	=	Ha_abdyyMOH(n-4)	;	log_k	(valeur)	;
Ha_aexx-2	+	MOH(n-1)	=	Ha_aexxMOH(n-3)	;	log_k	(valeur)	Ha_acdyy-3	+	MOH(n-1)	=	Ha_acdyyMOH(n-4)	;	log_k	(valeur)	;
Ha_bfxx-2	+	MOH(n-1)	=	Ha_bfxxMOH(n-3)	;	log_k	(valeur)	Ha_bcdyy-3	+	MOH(n-1)	=	Ha_bcdyyMOH(n-4)	;	log_k	(valeur)	;
Ha_cgxx-2	+	MOH(n-1)	=	Ha_cgxxMOH(n-3)	;	log_k	(valeur)	Ha_abeyy-3	+	MOH(n-1)	=	Ha_abeyyMOH(n-4)	;	log_k	(valeur)	;
Ha_dhxx-2	+	MOH(n-1)	=	Ha_dhxxMOH(n-3)	;	log_k	(valeur)	Ha_cdfyy-3	+	MOH(n-1)	=	Ha_cdfyyMOH(n-4)	;	log_k	(valeur)	;
Ha_efxx-2	+	MOH(n-1)	=	Ha_efxxMOH(n-3)	;	log_k	(valeur)	Ha_acgyy-3	+	MOH(n-1)	=	Ha_acgyyMOH(n-4)	;	log_k	(valeur)	;
Ha_ghxx-2	+	MOH(n-1)	=	Ha_ghxxMOH(n-3)	;	log_k	(valeur)	Ha_bdhyy-3	+	MOH(n-1)	=	Ha_bdhyyMOH(n-4)	;	log_k	(valeur)	;
Ha_abc-3	+	MOH(n-1)	=	Ha_abcMOH(n-4)	;	log_k	(valeur)	Ha_aefyy-3	+	MOH(n-1)	=	Ha_aefyyMOH(n-4)	;	log_k	(valeur)	;
Ha_abd-3	+	MOH(n-1)	=	Ha_abdMOH(n-4)	;	log_k	(valeur)	Ha_bghyy-3	+	MOH(n-1)	=	Ha_bghyyMOH(n-4)	;	log_k	(valeur)	;
Ha_acd-3	+	MOH(n-1)	=	Ha_acdMOH(n-4)	;	log_k	(valeur)	Ha_cegyy-3	+	MOH(n-1)	=	Ha_cegyyMOH(n-4)	;	log_k	(valeur)	;
Ha_bcd-3	+	MOH(n-1)	=	Ha_bcdMOH(n-4)	;	log_k	(valeur)	Ha_dfhyy-3	+	MOH(n-1)	=	Ha_dfhyyMOH(n-4)	;	log_k	(valeur)	;
Ha_abe-3	+	MOH(n-1)	=	Ha_abeMOH(n-4)	;	log_k	(valeur)	Ha_efgyy-3	+	MOH(n-1)	=	Ha_efgyyMOH(n-4)	;	log_k	(valeur)	;
Ha_cdf-3	+	MOH(n-1)	=	Ha_cdfMOH(n-4)	;	log_k	(valeur)	Ha_efhyy-3	+	MOH(n-1)	=	Ha_efhyyMOH(n-4)	;	log_k	(valeur)	;
Ha_acg-3	+	MOH(n-1)	=	Ha_acgMOH(n-4)	;	log_k	(valeur)	Ha_eghyy-3	+	MOH(n-1)	=	Ha_eghyyMOH(n-4)	;	log_k	(valeur)	;
Ha_bdh-3	+	MOH(n-1)	=	Ha_bdhMOH(n-4)	;	log_k	(valeur)	Ha_fghyy-3	+	MOH(n-1)	=	Ha_fghyyMOH(n-4)	;	log_k	(valeur)	;

Eléments à définir dans le fichier d'entrée de PHREEQC :

"EQUILIBRIUM_PHASES" :

Ha 0 (concentration en HA en g/L)

"SURFACE" :

-donnan (paramètre de Debye-Huckel)

-only_coutrer_ions

Ha_aH	Ha	eq	3.59E-04	(valeur SA)
Ha_bH	Ha	eq	3.59E-04	
Ha_cH	Ha	eq	3.59E-04	
Ha_dH	Ha	eq	3.59E-04	
Ha_eH	Ha	eq	1.79E-04	
Ha_fH	Ha	eq	1.79E-04	
Ha_gH	Ha	eq	1.79E-04	
Ha_hH	Ha	eq	1.79E-04	
Ha_abH2	Ha	eq	2.48E-04	
Ha_cdH2	Ha	eq	2.48E-04	
Ha_aeH2	Ha	eq	1.24E-04	
Ha_bfH2	Ha	eq	1.24E-04	
Ha_cgH2	Ha	eq	1.24E-04	
Ha_dhH2	Ha	eq	1.24E-04	
Ha_efH2	Ha	eq	6.19E-05	
Ha_ghH2	Ha	eq	6.19E-05	
Ha_abxH2	Ha	eq	2.48E-05	
Ha_cdxH2	Ha	eq	2.48E-05	
Ha_aexH2	Ha	eq	1.24E-05	
Ha_bfxH2	Ha	eq	1.24E-05	
Ha_cgxH2	Ha	eq	1.24E-05	
Ha_dhxH2	Ha	eq	1.24E-05	
Ha_efxH2	Ha	eq	6.19E-06	
Ha_ghxH2	Ha	eq	6.19E-06	
Ha_abxxH2	Ha	eq	2.48E-06	
Ha_cdxxH2	Ha	eq	2.48E-06	
Ha_aexxH2	Ha	eq	1.24E-06	
Ha_bfxxH2	Ha	eq	1.24E-06	
Ha_cgxxH2	Ha	eq	1.24E-06	
Ha_dhxxH2	Ha	eq	1.24E-06	
Ha_efxxH2	Ha	eq	6.19E-07	
Ha_ghxxH2	Ha	eq	6.19E-07	
Ha_abcH3	Ha	eq	7.16E-06	
Ha_abdH3	Ha	eq	7.16E-06	
Ha_acdH3	Ha	eq	7.16E-06	
Ha_bcdH3	Ha	eq	7.16E-06	
Ha_abeH3	Ha	eq	1.07E-05	
Ha_cdfH3	Ha	eq	1.07E-05	
Ha_acgH3	Ha	eq	1.07E-05	
Ha_bdhH3	Ha	eq	1.07E-05	

Ha_aefH3	Ha	eq	5.37E-06
Ha_bghH3	Ha	eq	5.37E-06
Ha_cegH3	Ha	eq	5.37E-06
Ha_dfhH3	Ha	eq	5.37E-06
Ha_efgH3	Ha	eq	8.95E-07
Ha_efhH3	Ha	eq	8.95E-07
Ha_eghH3	Ha	eq	8.95E-07
Ha_fghH3	Ha	eq	8.95E-07
Ha_abcyH3	Ha	eq	7.15E-07
Ha_abdyH3	Ha	eq	7.15E-07
Ha_acdyH3	Ha	eq	7.15E-07
Ha_bcdyH3	Ha	eq	7.15E-07
Ha_abeyH3	Ha	eq	1.07E-06
Ha_cdfyH3	Ha	eq	1.07E-06
Ha_acgyH3	Ha	eq	1.07E-06
Ha_bdhyH3	Ha	eq	1.07E-06
Ha_aefyH3	Ha	eq	5.36E-07
Ha_bghyH3	Ha	eq	5.36E-07
Ha_cegyH3	Ha	eq	5.36E-07
Ha_dfhyH3	Ha	eq	5.36E-07
Ha_efgyH3	Ha	eq	8.94E-08
Ha_efhyH3	Ha	eq	8.94E-08
Ha_eghyH3	Ha	eq	8.94E-08
Ha_fghyH3	Ha	eq	8.94E-08
Ha_abcyyH3	Ha	eq	7.15E-08
Ha_abdyyH3	Ha	eq	7.15E-08
Ha_acdyyH3	Ha	eq	7.15E-08
Ha_bcdyyH3	Ha	eq	7.15E-08
Ha_abeyyH3	Ha	eq	1.07E-07
Ha_cdfyyH3	Ha	eq	1.07E-07
Ha_acgyyH3	Ha	eq	1.07E-07
Ha_bdhyyH3	Ha	eq	1.07E-07
Ha_aefyyH3	Ha	eq	5.36E-08
Ha_bghyyH3	Ha	eq	5.36E-08
Ha_cegyyH3	Ha	eq	5.36E-08
Ha_dfhyyH3	Ha	eq	5.36E-08
Ha_efgyyH3	Ha	eq	8.94E-09
Ha_efhyyH3	Ha	eq	8.94E-09
Ha_eghyyH3	Ha	eq	8.94E-09
Ha_fghyyH3	Ha	eq	8.94E-09

Annexe 3 : Supporting information : Chapitre III

Pourcentage de REE complexées aux acides humiques en l'absence de Al pour des pH variants de 3 à 6, Σ[REE] = 10µM, [DOC] = 6,7 mg L^{-1} et IS = 0.01 M (NaCl).

pH	2.99	3	2.99	3.46	3.47	3.47	3.99	3.98	4.00
La	23.16	25.19	19.97	34.96	35.55	36.42	52.11	49.38	53.50
Ce	28.01	27.32	23.28	40.74	40.95	40.53	58.90	56.23	59.33
Pr	31.11	27.86	25.27	43.81	44.01	42.38	62.16	59.52	61.89
Nd	32.21	28.95	26.53	45.42	45.49	43.72	63.42	61.14	63.21
Sm	35.82	29.51	28.42	48.26	48.42	46.23	66.97	64.66	66.76
Eu	34.93	28.12	26.67	46.50	46.62	44.95	65.95	63.39	65.61
Gd	31.26	25.39	22.27	40.77	40.92	40.22	60.19	57.57	60.75
Tb	31.14	22.72	19.70	38.23	38.58	37.61	57.92	55.08	58.86
Dy	29.50	22.01	18.35	36.03	36.37	36.35	55.73	52.88	57.19
Ho	28.91	20.92	16.43	33.24	33.13	34.27	52.29	49.37	54.45
Er	28.02	19.23	15.45	31.81	31.65	32.29	50.74	47.69	52.61
Tm	29.08	20.20	15.24	31.40	31.29	33.21	50.11	47.20	53.01
Yb	28.38	20.38	15.49	32.01	31.85	33.55	51.11	48.10	53.80
Lu	28.61	19.00	14.23	30.71	30.43	31.60	49.23	46.13	51.74

pH	4.46	4.47	4.49	4.95	4.95	4.98	5.47	5.47	5.47
La	61.19	72.39	74.48	78.17	79.72	81.27	88.78	88.74	86.28
Ce	67.10	77.99	79.75	82.81	84.21	85.46	91.47	91.49	89.62
Pr	69.79	80.38	82.00	84.78	86.17	87.22	92.60	92.58	91.02
Nd	71.22	81.22	82.87	85.63	86.81	87.83	92.93	92.95	91.58
Sm	74.71	83.85	85.28	88.07	88.86	89.65	94.08	94.08	93.26
Eu	73.99	83.03	84.47	87.68	88.36	89.20	93.74	93.70	93.04
Gd	69.56	79.41	81.05	84.98	85.68	86.74	92.24	92.25	91.38
Tb	68.04	78.05	79.87	84.35	84.71	85.77	91.75	91.75	91.09
Dy	66.75	76.28	78.21	83.55	83.49	84.68	91.11	91.12	90.71
Ho	64.19	73.60	75.80	81.75	81.44	82.79	89.93	89.89	89.51
Er	62.53	72.18	74.46	80.72	80.39	81.79	89.31	89.22	88.91
Tm	63.03	71.87	74.15	81.14	80.31	81.60	89.19	89.16	89.29
Yb	64.04	72.45	74.65	82.01	80.91	82.23	89.58	89.50	89.94
Lu	62.14	70.87	73.42	80.80	79.61	80.98	88.86	88.81	89.21

pH	5.99	5.97	5.97
La	96.01	94.80	93.49
Ce	96.86	96.23	95.04
Pr	97.14	96.78	95.61
Nd	97.25	96.98	95.79
Sm	97.49	97.63	96.33
Eu	97.36	97.54	96.15
Gd	96.87	96.92	95.37
Tb	96.68	96.85	95.16
Dy	96.44	96.69	94.84
Ho	96.03	96.26	94.19
Er	95.79	96.07	93.83
Tm	95.70	96.23	93.81
Yb	95.80	96.51	94.06
Lu	95.51	96.23	93.62

Pourcentage de REE et de Al présents dans la fraction > 5kDa lors de la compétition entre REE et Al pour la complexation par les acides humiques pour des pH variants de 3 à 6, Σ[REE] = [Al] = 10µM, [DOC] = 6,7 mg L^{-1} et IS = 0.01 M (NaCl).

pH	3.00	3.00	2.98	3.48	3.50	3.48	4.02	4.00	4.03
Al	13.15	26.67	12.74	22.43	31.17	22.98	40.15	39.20	45.59
La	17.74	17.63	12.77	26.17	29.84	28.60	38.51	35.51	39.02
Ce	20.94	20.81	16.16	31.16	31.97	33.71	45.30	42.09	43.67
Pr	22.89	22.78	18.19	34.02	32.20	36.60	48.71	45.37	45.49
Nd	24.13	24.01	19.43	35.71	32.80	38.86	50.40	46.97	46.39
Sm	25.59	25.48	21.43	38.15	33.93	41.11	54.21	50.81	49.56
Eu	24.24	24.11	19.74	36.34	32.75	39.32	53.04	49.80	48.29
Gd	19.64	19.52	14.88	31.18	30.55	33.70	46.66	43.07	43.79
Tb	17.65	17.53	13.05	29.08	28.72	31.40	44.52	40.64	41.71
Dy	16.75	16.64	12.00	27.04	27.58	29.55	42.33	38.66	39.84
Ho	15.20	15.07	10.24	24.32	26.09	26.85	38.98	35.40	37.38
Er	14.00	13.88	9.36	22.88	24.60	25.66	37.46	34.00	35.52
Tm	14.01	13.90	9.52	23.05	25.59	25.51	36.91	33.67	36.39
Yb	14.50	14.37	9.59	23.77	25.90	25.73	38.20	34.55	37.16
Lu	13.66	13.54	8.41	22.35	24.53	24.60	36.53	32.79	35.57

pH	4.48	4.47	4.50	4.98	4.95	4.98	5.50	5.45	5.48
Al	54.17	52.33	63.98	80.99	77.43	80.82	92.55	95.02	96.23
La	38.67	37.40	46.68	48.44	42.49	46.20	53.85	65.08	54.87
Ce	46.43	44.84	52.47	56.35	50.23	52.25	62.67	72.81	62.10
Pr	50.23	48.63	54.83	60.71	54.63	54.88	66.90	76.23	65.56
Nd	51.97	50.15	56.08	62.34	56.34	56.45	68.67	77.60	67.14
Sm	56.58	55.09	60.16	67.33	61.81	61.14	74.25	81.99	72.45
Eu	55.13	53.56	59.01	66.40	60.64	60.07	73.43	81.40	71.97
Gd	48.54	47.12	53.97	60.34	54.25	54.96	68.04	77.10	67.36
Tb	46.51	45.11	52.38	58.78	52.57	54.06	67.44	76.70	67.31
Dy	44.28	42.96	50.77	56.92	50.58	52.70	66.28	75.79	66.56
Ho	40.69	39.39	47.91	53.59	46.94	49.88	63.15	73.28	64.03
Er	39.19	37.98	46.15	52.14	45.52	48.26	62.28	72.59	63.17
Tm	39.15	37.87	47.01	52.84	46.07	49.42	63.42	73.49	65.09
Yb	39.83	38.74	48.08	54.64	47.76	51.00	65.73	75.36	67.38
Lu	38.21	36.91	46.28	52.59	45.69	49.05	64.19	74.17	65.84

pH	6.00	5.99	5.99
Al	98.44	99.67	98.09
La	74.88	75.66	77.10
Ce	81.79	81.72	83.26
Pr	84.72	84.23	85.92
Nd	85.98	85.36	86.96
Sm	89.51	89.05	90.08
Eu	89.21	88.87	89.79
Gd	86.37	86.34	87.17
Tb	86.55	86.84	87.31
Dy	86.25	86.70	86.99
Ho	84.76	85.49	85.61
Er	84.71	85.47	85.50
Tm	85.90	86.90	86.52
Yb	87.65	88.59	88.05
Lu	87.04	88.00	87.49

Logarithme des concentrations en REE et Al libres (mol) à pH = 3 pour une solution initiale avec Σ[REE] = 1µM, [Al] variant de 0 à 20µM, [DOC] = 9 $mg L^{-1}$ et IS = 0.01 M (NaCl).

pH	3.02	2.98	3.00	3.03	3.03	2.98	3.02	3.00	3.02
Al				-6.22	-6.23	-6.48	-5.78	-5.74	-5.79
La	-8.48	-8.65	-8.70	-8.45	-8.28	-8.37	-8.05	-8.07	-8.04
Ce	-8.61	-8.81	-8.85	-8.57	-8.42	-8.54	-8.18	-8.20	-8.18
Pr	-8.91	-8.89	-8.93	-8.63	-8.47	-8.59	-8.24	-8.26	-8.23
Nd	-8.92	-8.92	-8.96	-8.64	-8.48	-8.61	-8.27	-8.29	-8.26
Sm	-9.00	-9.03	-9.07	-8.71	-8.56	-8.66	-8.33	-8.35	-8.32
Eu	-9.00	-9.02	-9.06	-8.67	-8.52	-8.63	-8.29	-8.32	-8.28
Gd	-8.89	-8.92	-9.00	-8.58	-8.42	-8.54	-8.20	-8.23	-8.19
Tb	-8.90	-8.90	-9.01	-8.51	-8.36	-8.48	-8.14	-8.16	-8.13
Dy	-8.87	-8.90	-9.02	-8.50	-8.35	-8.46	-8.13	-8.15	-8.12
Ho	-8.85	-8.89	-9.01	-8.47	-8.31	-8.43	-8.10	-8.11	-8.08
Er	-8.86	-8.94	-9.06	-8.46	-8.31	-8.43	-8.09	-8.11	-8.07
Tm	-8.91	-9.06	-9.19	-8.47	-8.31	-8.44	-8.10	-8.12	-8.08
Yb	-9.01	-9.26	-9.39	-8.50	-8.34	-8.47	-8.13	-8.14	-8.10
Lu	-9.03	-9.33	-9.46	-8.50	-8.34	-8.46	-8.13	-8.14	-8.10

pH	3.00	2.98	2.98	3.00	3.00	3.00
Al	-5.28	-5.27	-5.26	-4.86	-4.87	-4.88
La	-7.79	-7.79	-7.79	-7.62	-7.64	-7.60
Ce	-7.92	-7.92	-7.91	-7.74	-7.76	-7.71
Pr	-7.97	-7.97	-7.97	-7.79	-7.81	-7.76
Nd	-8.00	-8.01	-8.00	-7.82	-7.84	-7.79
Sm	-8.06	-8.06	-8.05	-7.88	-7.90	-7.85
Eu	-8.03	-8.03	-8.02	-7.85	-7.87	-7.83
Gd	-7.94	-7.94	-7.93	-7.77	-7.79	-7.74
Tb	-7.88	-7.88	-7.88	-7.71	-7.74	-7.69
Dy	-7.87	-7.87	-7.87	-7.71	-7.73	-7.69
Ho	-7.84	-7.84	-7.83	-7.67	-7.70	-7.65
Er	-7.83	-7.83	-7.83	-7.67	-7.69	-7.65
Tm	-7.84	-7.84	-7.83	-7.67	-7.70	-7.66
Yb	-7.86	-7.86	-7.86	-7.70	-7.72	-7.68
Lu	-7.86	-7.86	-7.85	-7.70	-7.72	-7.68

Logarithme des concentrations en REE et Al complexés aux acides humiques (mol/kg) à pH = 3 pour une solution initiale avec Σ[REE] = 1µM, [Al] variant de 0 à 20µM, [DOC] = 9 $mg\,L^{-1}$ et IS = 0.01 M (NaCl).

pH	3.02	2.98	3.00	3.03	3.03	2.98	3.02	3.00	3.02
Al				-1.05	-0.74	-0.85	-0.56	-0.55	-0.54
La	-2.12	-2.24	-2.22	-2.10	-2.11	-2.11	-2.14	-2.15	-2.14
Ce	-2.10	-2.24	-2.22	-2.11	-2.11	-2.12	-2.14	-2.16	-2.14
Pr	-2.30	-2.26	-2.23	-2.10	-2.11	-2.11	-2.14	-2.15	-2.13
Nd	-2.29	-2.26	-2.24	-2.11	-2.12	-2.11	-2.14	-2.15	-2.14
Sm	-2.32	-2.28	-2.26	-2.13	-2.14	-2.14	-2.16	-2.17	-2.16
Eu	-2.33	-2.28	-2.26	-2.15	-2.15	-2.16	-2.18	-2.19	-2.18
Gd	-2.34	-2.30	-2.27	-2.16	-2.17	-2.18	-2.20	-2.21	-2.20
Tb	-2.35	-2.31	-2.28	-2.15	-2.16	-2.17	-2.20	-2.21	-2.20
Dy	-2.34	-2.31	-2.29	-2.18	-2.19	-2.19	-2.22	-2.23	-2.22
Ho	-2.36	-2.32	-2.29	-2.19	-2.19	-2.19	-2.23	-2.24	-2.23
Er	-2.36	-2.32	-2.30	-2.19	-2.20	-2.20	-2.23	-2.25	-2.23
Tm	-2.37	-2.33	-2.30	-2.20	-2.20	-2.21	-2.24	-2.25	-2.24
Yb	-2.37	-2.33	-2.31	-2.20	-2.21	-2.21	-2.25	-2.25	-2.25
Lu	-2.38	-2.34	-2.31	-2.21	-2.22	-2.23	-2.26	-2.27	-2.27

pH	3.00	2.98	2.98	3.00	3.00	3.00
Al	-0.36	-0.37	-0.37	-0.31	-0.22	-0.20
La	-2.21	-2.21	-2.22	-2.28	-2.32	-2.25
Ce	-2.19	-2.20	-2.21	-2.25	-2.29	-2.22
Pr	-2.18	-2.18	-2.20	-2.23	-2.27	-2.20
Nd	-2.20	-2.19	-2.20	-2.24	-2.28	-2.21
Sm	-2.20	-2.20	-2.22	-2.24	-2.29	-2.23
Eu	-2.22	-2.23	-2.24	-2.27	-2.31	-2.24
Gd	-2.26	-2.27	-2.28	-2.32	-2.36	-2.29
Tb	-2.25	-2.25	-2.27	-2.32	-2.35	-2.29
Dy	-2.29	-2.29	-2.30	-2.35	-2.40	-2.33
Ho	-2.30	-2.30	-2.32	-2.38	-2.42	-2.35
Er	-2.31	-2.32	-2.33	-2.39	-2.43	-2.37
Tm	-2.31	-2.31	-2.33	-2.39	-2.43	-2.37
Yb	-2.32	-2.31	-2.33	-2.39	-2.42	-2.36
Lu	-2.33	-2.33	-2.34	-2.40	-2.45	-2.38

Annexe 4 : Supporting information : Chapitre IV

Pourcentage de REE et de Fe présents dans la fraction > 5kDa lors de la compétition entre REE et Fe pour la complexation par les acides humiques pour des pH variants de 3 à 6, Σ[REE] = [Fe] = 10µM, [DOC] = 6,7 mg L^{-1} et IS = 0.01 M (NaCl).

pH	3.02	3.02	3.00	3.52	3.49	3.50	4.00	4.00	4.02
Fe	50.56	54.83	49.20	69.70	72.95	67.16	77.76	77.82	84.28
La	7.41	7.69	3.26	16.29	21.90	13.26	25.10	22.18	27.46
Ce	7.78	8.96	4.06	18.12	22.59	14.80	30.24	26.19	29.36
Pr	8.06	9.43	4.31	19.35	21.85	15.65	32.82	28.07	29.32
Nd	9.02	10.19	4.45	20.64	22.08	17.11	34.17	29.47	29.93
Sm	9.02	10.34	5.15	20.45	21.55	17.21	36.88	31.88	30.87
Eu	8.12	8.39	4.57	20.05	20.70	16.66	35.90	30.98	29.55
Gd	6.26	7.17	2.77	17.05	20.02	13.99	31.04	26.30	27.47
Tb	5.37	5.60	1.83	15.32	17.45	12.46	28.22	24.12	24.71
Dy	5.37	5.68	1.88	13.96	16.57	11.53	26.79	22.62	23.52
Ho	5.10	4.30	1.22	12.88	16.40	10.46	24.35	20.73	22.47
Er	4.69	4.33	0.70	12.45	14.72	9.76	23.27	19.74	20.73
Tm	5.04	4.06	1.39	12.43	16.24	9.92	22.90	19.75	22.24
Yb	4.53	4.10	1.91	12.49	16.01	10.39	23.63	19.91	21.93
Lu	4.11	3.68	1.01	11.63	14.94	9.36	22.23	18.86	20.56

pH	4.47	4.47	4.50	4.98	4.95	4.98	5.45	5.47	5.50
Fe	86.00	87.55	89.89	96.45	91.74	93.49	92.69	94.15	97.12
La	32.38	35.58	39.95	49.49	49.43	58.33	64.01	67.96	67.10
Ce	38.61	42.12	44.35	57.22	57.17	64.00	71.72	75.06	73.93
Pr	41.54	45.19	45.74	60.83	61.04	66.18	75.07	78.15	76.49
Nd	43.19	46.63	46.98	62.38	62.78	67.34	76.51	79.48	77.75
Sm	47.30	50.97	49.88	66.97	67.46	70.82	80.73	83.13	81.42
Eu	45.67	49.24	48.42	65.93	66.19	69.83	79.96	82.47	80.88
Gd	40.14	43.41	44.43	60.31	60.30	65.68	75.41	78.36	77.22
Tb	38.14	41.28	41.94	58.21	58.54	64.12	74.59	77.37	76.66
Dy	35.78	39.01	40.35	56.27	56.37	62.68	73.25	76.06	75.67
Ho	32.80	36.17	38.33	52.83	53.08	60.35	70.29	73.37	73.46
Er	31.44	34.77	36.45	51.38	51.50	58.70	69.13	72.20	72.33
Tm	31.48	34.61	37.50	51.63	51.63	59.46	69.43	72.48	73.23
Yb	31.85	35.04	37.91	52.91	52.95	60.29	70.67	73.63	74.44
Lu	30.34	33.36	36.22	50.68	50.73	58.61	69.05	72.09	72.80

pH	5.97	5.96	9.96
Fe	97.68	98.74	97.69
La	86.81	86.47	85.61
Ce	90.63	90.22	89.79
Pr	92.08	91.49	91.33
Nd	92.67	92.06	91.94
Sm	94.26	93.78	93.71
Eu	93.98	93.61	93.42
Gd	92.24	92.02	91.55
Tb	92.10	91.98	91.35
Dy	91.61	91.60	90.85
Ho	90.44	90.64	89.57
Er	89.98	90.20	89.07
Tm	90.20	90.74	89.34
Yb	90.84	91.40	90.05
Lu	90.08	90.72	89.29

Bibliographie

Abate G. and Masini J.C. (2002) Complexation of Cd(II) and Pb(II) with humic acids studied by anodic stripping voltammetry using differential equilibrium functions and discrete site models. *Org. Geochem.* **33**, 1171–1182.

Allard T., Menguy N., J. Salomon J., Calligaro T., Weber T., Calas G. and Benedetti M. F. (2004) Revealing forms of iron in river-borne material from major tropical rivers of the Amazon Basin (Brazil). *Geochim. Cosmochim. Acta* **68**, 3079-3094.

Andersson K., Dahlqvist R., Turner D., Stolpe B., Larsson T., Ingri J., and Andersson P. (2006) Colloidal rare earth elements in boreal river: Changing sources and distributions during the spring flood. *Geochim. Cosmochim. Acta.* **70**, 3261–3274.

Appelo C. and Postma D. (2005) *Geochemistry, groundwater and pollution* (2nd edition). Taylor & Francis, p. 595.

Aubert D., Stille P., and Probst A. (2001) REE fractionation during granite weathering and removal by waters and suspended loads: Sr and Nd isotopic evidence. *Geochim. Cosmochim. Acta* **65**, 387-406.

Auterives C. (2007) Influence des flux d'eau souterraine entre une zone humide superficielle et un aquifère profond sur le fonctionnement hydrochimique des tourbières: exemple des marais du Cotentin, Basse-Normandie. Ph.D. thesis, University of Rennes I, France. Mémoires du CAREN 17, ISBN 2-914375-46-8, p. 261.

Bau M. and Dulski P. (1996) Anthropogenic origin of positive gadolinium anomalies in river waters. *Earth Planet. Sci. Lett.* **143**, 245-255.

Bau M., Möller P., and Dulski P. (1997) Yttrium and lanthanides in eastern Mediterranean seawater and their fractionation during redox-cycling. *Mar. Chem.* **56**, 123-131.

Benedetti M. F., Milne C. J., Kinniburgh D. G., van Riemsdijk W. H., and Koopal L. K. (1995) Metal-ion binding to humic substances: application of the nonideal competitive adsorption model. *Environ. Sci. Technol.* **29**, 446–457.

Bidoglio G., Grenthe I., Qi P., Robouch P. and Omentto N. (1991) Complexation of Eu and Tb with fulvic acids as studied by time-resolved laser-induced fluorescence. *Talanta* **38** (9), 999–1008.

Braun J. J., Viers J., Dupré B., Polvé M., Ndam J., and Muller J. P. (1998) Solid/liquid REE fractionation in the lateritic system of Goyoum, East Cameroon: the implication for the present dynamics of the soil covers of the humid tropical regions. *Geochim. Cosmochim. Acta* **62**, 273-299.

Browne B.A. and Discoll C.T. (1993) pH-dependent binding of aluminum by a fulvic acid. *Environ. Sci. Technol.* **27**, 915-922.

Buschmann J. and Sigg L. (2006) Arsenite and arsenate binding to dissolved humic acids: Influence of pH, type of humic acid, and aluminum. *Environ. Sci. Technol.* **40** (19), 6015-6020.

Buschmann J., Kappeler A., Lindauer U., Kistler D., Berg M. and Sigg L. (2004) Antimony(III) binding to humic substances: Influence of pH and type of humic acid. *Environ. Sci. Technol.* **38** (17), 4535−4541.

Byrne R. H. and Kim K.-H. (1990) Rare earth element scavenging in seawater. *Geochim. Cosmochim. Acta* **54**, 2645-2656.

Byrne R. H. and Li B. (1995) Comparative complexation behaviour of the rare earth elements. *Geochim. Cosmochim. Acta* 59, 4575-4589.

Byrne R.H. and Sholkovitz E.R. (1996) Marine chemistry and geochemistry of the lanthanides. *Handbook on the Physics and Chemistry of Rare Earths* **23**. Elsevier, Amsterdam, 497–593.

Casey W. H., Phillips B. L. and Furres G. (2001) Aqueous aluminum polynuclear complexes and nanoclusters: a review. In *Nanoparticle and the Environment. Reviews in Mineralogy & Geochemistry*, vol. 44 (eds. J. F. Banfield and A. Navrotsky). The Geochemical & Mineralogical Society of America, Washington, DC, pp. 167–190.

Coppin F., Berger G., Bauer A., Castet S., and Loubet M. (2002) Sorption of lanthanides on smectite and kaolinite. *Chem. Geol.* **182**, 57-68.

Davranche M., Pourret O., Gruau G., and Dia A. (2004) Impact of humate complexation on the adsorption of REE onto Fe oxyhydroxide. *J. Colloid Interface Sci.* **277**, 271-279.

Davranche M., Pourret O., Gruau G., Dia A., and Le Coz-Bouhnik M. (2005) Adsorption of REE(III)-humate complexes onto MnO_2: Experimental evidence for cerium anomaly and lanthanide tetrad effect suppression. *Geochim. Cosmochim. Acta* **69**, 4825-4835.

Davranche M., Pourret O., Gruau G., Dia A., Jin D. and Gaertner D. (2008) Competitive binding of REE to humic acid and manganese oxide: impact of reaction kinetics on Ce anomaly development and REE adsorption. *Chem. Geol*. **247**, 154-170.

De Baar H. J. W., Bacon M. P., and Brewer P. G. (1983) Rare-earth distributions with a positive Ce anomaly in the Western North Atlantic Ocean. *Nature* **301**, 324-327.

De Baar H. J. W., Bacon M. P., Brewer P. G., and Bruland K. W. (1985) Rare earth elements in the Pacific and Atlantic Oceans. *Geochim. Cosmochim. Acta* **49**, 1943-1959.

De Baar H. J. W., German C. R., Elderfield H., and van Gaans P. (1988) Rare earth element distributions in anoxic waters of the Cariaco Trench. *Geochim. Cosmochim. Acta* **52**, 1203-1219.

De Carlo E. H. and Green W. J. (2002) Rare earth elements in the water column of Lake Vanda, McMurdo Dry Valleys, Antarctica. *Geochim. Cosmochim. Acta* **66**, 1323-1333.

Deberdt S., Viers J., and Dupré B. (2002) New insights about the rare earth elements (REE) mobility in river waters. *Bull. Soc. Geol. Fr.* **173**, 147-160.

Dia A., Gruau G., Olivié-Lauquet G., Riou C., Molénat J. and Curmi P. (2000) The distribution of rare-earths in groundwater: assessing the role of source-rock composition, redox changes and colloidal particles. *Geochim. Cosmochim. Acta* **64**, 4131–4151.

Duncan T. and Shaw T. J. (2004) The mobility of rare earth elements and redox sensitive elements in the groundwater/seawater mixing zone of a shallow coastal aquifer. *Aquat. Geochem.* **9**, 223-255.

Dupré B., Gaillardet J., Rousseau D., and Allègre C. J. (1996) Major and trace elements of river-borne material: The Congo Basin. *Geochim. Cosmochim. Acta* **60**, 1301-1321.

Dupré L., Viers J., Dandurand J.-L., Polvé M., Bénézeth P., Vervier P. and Braun J.-J. (1999) Major and trace elements associated with colloids in organic-rich river waters: Ultrafiltration of natural and spiked solutions. *Chem. Geol.* **160**, 63–80.

Elbaz-Poulichet F. and Dupuy C. (1999) Behaviour of rare earth elements at the freshwater-seawater interface of two acid mine rivers: the Tinto and Odiel (Andalucia, Spain). *Appl. Geochem.* **14**, 1063-1072.

Elderfield H. (1988) The oceanic chemistry of the rare earth elements in seawater. *Phil. Trans. R. Soc. Lond.* **A 325**, 105-126.

Elderfield H. and Greaves M. J. (1982) The rare earth elements in seawater. *Nature* **296**, 214-219.

Elderfield H., Upstill-Goddard R. and Sholkovitz E.R. (1990) The rare earth elements in rivers, estuaries, and coastal seas and their significance to the composition of ocean waters. *Geochim. Cosmochim. Acta* **54**, 971–991.

Fee J. A., Gaudette H. E., Lyons W. B., and Long D. T. (1992) Rare-earth element distribution in Lake Tyrrell groundwaters, Victoria, Australia. *Chem. Geol.* **96**, 67-93.

Frenkel A.I., Korshin G.V. and Ankudinov A.L. (2000) XANES study of Cu^{2+}-binding sites in aquatic humic substances. *Environ. Sci. Technol.* **34**, 2138-2142.

Gaillardet J., Dupré B., Allègre C. J., and Négrel P. (1997) Chemical and physical denudation in the Amazon River Basin. *Chem. Geol.* **142**, 141-173.

Gaillardet J., Viers J. and Dupré B. (2004) Elements in river waters. *In Treatise on Geochemistry*, vol. 5 (ed. E. D. Holland and K. K. Turekian). Elsevier-Pergamonm, pp. 225–263.

Gammons C. H., Wood S. A., Ponas J. P. and Madison J. P. (2003) Geochemistry of the rare-eath elements and uranium in the acidic Berkeley Pit Lake, Butte, Montana. *Chem. Geol.* **198**, 269-288.

Gerard M., Seyler P., Benedetti M. F., Alves V. P., Boaventura G. R. and Sondag F. (2003) Rare earth elements in the Amazon basin. *Hydrol. Proc.* **17**, 1379-1392.

German C. R., Holiday B. P. and Elderfield H. (1991) Redox cycling of rare earth elements in the suboxic zone of the Black Sea. *Geochim. Cosmochim. Acta* **55**, 3553-3558.

German C. R., Masuzawa T., Greaves M. J., Elderfield H., and Edmond J. M. (1995) Dissolved rare earth elements in the Southern Ocean: Cerium oxidation and the influence of hydrography. *Geochim. Cosmochim. Acta* **59**, 1551-1558.

Glaus M. A., Hummel W. and Van Loon L. R. (1995) Stability of mixed-ligand complexes of metal ions with humic substances and low molecular weight ligands. *Environ. Sci. Technol.* **29**, 2150-2153

Glaus M.A., Hummel W. and Van Loon L.R. (2000) Trace metal-humate interactions I. Experimental determination of conditional stability constants. *Appl. Geochem.* **15,** 953–973.

Goldberg E. D., Koide M., Schmitt R. A., and Smith R. H. (1963) Rare earth distribution in the marine environment. *J. Geophys. Res.* **68**, 4209-4217.

Goldstein S. J. and Jacobsen S. B. (1988) Rare earth elements in river waters. *Earth Planet. Sci. Lett.* **89**, 35-47.

Gruau G., Dia A., Olivié-Lauquet G., Davranche M. and Pinay G. (2004) Controls on the distribution of rare earth elements in shallow groundwaters. *Wat. Res.* **38**, 3576-3586.

Gustafsson J. P., Persson I., Kleja D. B. and van Schaik J. W. J. (2007) Binding of iron(III) to organic soils: EXAFS spectroscopy and chemical equilibrium modeling. *Environ. Sci. Technol.* **41**, 1232–1237.

Haskin L. A., Haskin M. A., Frey F. A., and Wilderman T. R. (1968) Relative and absolute terrestrial abundances of the rare earths. In *Origin and distribution of the elements*, Vol. 30 (ed. A. L.H.), pp. 889-912.

Hiradate S. and Yamaguchi N.U. (2003) Chemical species of Al reacting with soil humic acids. *Journal of Inorganic Biogeochemistry* **97**, 26-31.

Hoyle J., Elderfield H., Gledhill A., and Greaves M. (1984) The behaviour of rare earth elements during mixing of river and sea waters. *Geochim. Cosmochim. Acta* **48**, 143-149.

Ingri J., Widerlund A., Land M., Gustafsson O., Andersson P., and Ohlander B. (2000) Temporal variations in the fractionation of the rare earth elements in a boreal river; the role of colloidal particles. *Chem. Geol.* **166**, 23-45.

IUPAC (2001) *IUPAC Stability Constants Database.* Version 5.4, IUPAC and Academic Software (acadsoft@bcs.org.uk).

Janssen R. P. T. and Verweij W. (2003) Geochemistry of some rare earth elements in groundwater, Vierlingsbeek, The Netherlands. *Wat. Res.* **37**, 1320-1350.

Johannesson K. H. and Hendry M. J. (2000) Rare earth element geochemistry of groundwaters from a thick till and clay-rich aquitard sequence, Saskatchewan, Canada. *Geochim. Cosmochim. Acta* **64**, 1493-1509.

Johannesson K. H. and Lyons W. B. (1994) The rare earth element geochemistry of Mono Lake water and the importance of carbonate complexing. *Limn. Oceanogr.* **39**, 1141-1154.

Johannesson K. H. and Lyons W. B. (1995) Rare-earth element geochemistry of Colour Lake, an acidic freshwater lake on Axel Heiberg Island, Northwest Territories, Canada. *Chem. Geol.* **119**, 209-223.

Johannesson K. H. and Zhou X. (1999) Origin of middle rare earth element enrichments in acid waters of a Canadian High Arctic lake. *Geochim. Cosmochim. Acta* **63**, 153-165.

Johannesson K. H., Farnham I. M., Guo C., and Stetzenbach K. J. (1999) Rare earth element fractionation and concentration variations along a groundwater flow path within a shallow, basin-fill aquifer, southern Nevada, USA. *Geochim. Cosmochim. Acta* **63**, 2697-2708.

Johannesson K. H., Lyons W. B., Yelken M. A., Gaudette H. E., and Stetzenbach K. J. (1996a) Geochemistry of the rare earth elements in hypersaline and dilute acidic natural terrestrial waters: complexation behavior and middle rare-earth element enrichments. *Chem. Geol.* **133**, 125-144.

Johannesson K. H., Stetzenbach K. J., and Hodge V. F. (1995) Speciation of the rare earth element neodymium in groundwaters of the Nevada Test Site and Yucca Mountain and implications for actinide solubility. *Appl. Geochem.* **10**, 565-572.

Johannesson K. H., Stetzenbach K. J., and Hodge V. F. (1997) Rare earth elements as geochemical tracers of regional groundwater mixing. *Geochim. Cosmochim. Acta* **61**, 3605-3618.

Johannesson K. H., Stetzenbach K. J., Hodge V. F., and Lyons W. B. (1996b) Rare earth element complexation behavior in circumneutral pH groundwaters: Assessing the role of carbonate and phosphate ions. *Earth Planet. Sci. Lett.* **139**, 305-319.

Johannesson K. H., Zhou X., Guo C., Stetzenbach K. J., and Hodge V. F. (2000) Origin of rare earth element signatures in groundwaters of circumneutral pH from southern Nevada and eastern California. *Chem. Geol.* **164**, 239-257.

Johannesson K.H., Tang J., Daniels J.M., Bounds W.J. and Burdige D.J. (2004) Rare earth element concentrations and speciation in organic rich blackwaters of the Great Dismal Swamp, Virginia, USA. *Chem. Geol.* **209**, 271–294.

Karlsson T. and Persson P. (2010) Coordination chemistry and hydrolysis of Fe(III) in a peat humic acid studies by X-ray absorption spectroscopy. *Geochim. Cosmochim. Acta* **74**, 30-40.

Kim J.I. and Czerwinski K.R. (1996) Complexation of metal ions with humic acid: metal ion charge neutralisation model. *Radiochim. Acta* **73**, 5-10.

Kinniburgh D. G., van Riemsdijk W. H., Koopal L. K., Borkovec M., Benedetti M. F. and Avena M. J. (1999) Ion binding to natural organic matter: competition, heterogeneity, stoichiometry and thermodynamic consistency. *Colloid Surf. A* **151**, 147–166.

Kinniburgh D.G., Milne C.J., Benedetti M.F., Pinheiro J.P., Filius J., Koopal L. and Van Riemsdijk W.H. (1996) Metal ion binding by humic acid: application of the NICA-Donnan model. *Environ. Sci. Technol.* **30**, 1687-1698.

Koopal L.K., van Riemsdijk W.H., de Wit J.C.M and Benedetti M.F. (1994) Analytical isotherm equations for multicomponent adsorption to heterogeneous surfaces. *J. Coll. Int. Sci.* **166**, 51-60.

Lawrence M. G. and Kamber B. S. (2006) The behaviour of the rare earth elements during estuarine mixing - revisited. *Mar. Chem.* **100**, 147-161.

Lead J. R., Hamilton-Taylor J., Peters A., Reiner S., and Tipping E. (1998) Europium binding by fulvic acids. *Anal. Chim. Acta* **369**, 171-180.

Lippold H., Evans N.D.M., Warwick P. and Kupsch H. (2007) Competitive effect of iron(III) on metal complexation by humic substances: Characterization of ageing processes. *Chemosphere* **67**, 1050-1056.

Lippold H., Mansel A. and Kupsch H. (2005) Influence of trivalent electrolytes on the humic colloid-borne transport of contaminant metals: competition and flocculation effects. *J. Contam. Hydro.* **76**, 337-352.

Liu D.J, Bruggeman C. and Maes N. (2008) The influence of natural organic matter on the speciation and solubility of Eu in Boom Clay porewater. *Radiochim. Acta* **96**, 711-720.

Liu X. and Millero F. J. (1999) The solubility of iron hydroxide in sodium chloride solutions. *Geochim. Cosmochim. Acta* **63**, 3487-3497.

Lofts S., Tipping E. and Hamilton-Taylor J. (2008) The Chemical Speciation of Fe(III) in Freshwaters. *Aquat. Geochem.* **14**, 337-358.

Luo Y.-R. and Byrne R. H. (2004) Carbonate complexation of yttrium and the rare earth elements in natural rivers. *Geochim. Cosmochim. Acta* **68**, 691-699.

Mandal R., Sekaly A.L.R, Murimboh J., Hassan N.M., Chakrabarti C.L., Back M.H., Grégoire D.C. and Schroeder W.H. (1999) Effect of the competition of copper and cobalt on the lability of Ni(II)-organic ligand complexes, Part II: in freshwaters (Rideau River surface waters). *Anal. Chim. Acta* **395**, 323-334.

Marang L., Reiller P.E., Eidner S., Kumke M.U. and Benedetti M.F. (2008) Combining Spectroscopic and Potentiometric Approaches to Characterize Competitive Binding to Humic Substances. *Environ. Sci. Technol.* **42**, 5094-5098.

Marinsky J.A. and Ephraim J. (1986) A unified physicochemical description of the protonation and metal ion complexation equilibria of natural organic acids (humic and fulvic acids). 1. Analysis of the influence of polyelectrolyte properties on protonation equilibria in ionic media: fundamental concept. *Environ. Sci. Technol.* **20**, 349-354.

Marsac R., Davranche M., Gruau G. and Dia A. (2010) Metal loading effect on rare earth element binding to humic acid: Experimental and modelling evidence. *Geochim. Cosmochim. Acta* **74**, 1749-1761.

Marsac R., Davranche M., Gruau G., Bouhnik-Le Coz M and Dia A. (2011a) An improved description of the interactions between rare earth elements and humic acids by modelling. *Geochim. Cosmochim. Acta* (in press).

Marsac R., Davranche M., Gruau G., Dia A. and Bouhnik-Le Coz M. (2011b) Aluminium competitive impact on Rare Earth Elements binding to humic acid. *Geochim. Cosmochim. Acta* (submitted).

Martell A.E. and Hancock R.D. (1996) Metal Complexes in Aqueous Solutions. New York: Kluwer.

Martin J.-M., Hogdahl O., and Philippot J. C. (1976) Rare earth element supply to the ocean. *J. Geophys. Res.* **81**, 3119-3124.

Masion A., Thomas a F., Bottero J.-Y., Tchoubar D. and Tekely P. (1994) Formation of amorphous precipitates from aluminum-organic ligands solutions: macroscopic and molecular study. *Journal of Non-Crystalline Solids* **171**, 191-200.

McLennan S. M. (1989) Rare earth element geochemistry in sedimentary rocks: influence of provenance and sedimentary processe. In *Geochemistry and mineralogy of rare earth elements*, Vol. 21 (ed. Lipin B.R. and Mc Kay G.A.), pp. 169-200.

Milne C.J, Kinniburgh D.G., van Riemsdijk W.H. and Tipping E. (2003) Generic NICA-Donnan model parameters for metal-ion binding by humic substances. *Environ. Sci. Technol.* **37**, 958-971.

Möller P. and Bau M. (1993) Rare-earth patterns with positive cerium anomaly in alkaline waters from Lake Van, Turkey. *Earth Planet. Sci. Lett.* **117**, 671-676.

Mota A.M., Rato A., Brazia C. and Simoes Gonçalves M.L. (1996) Competition of Al^{3+} in complexation of humic matter with Pb^{2+}: a comparative study with other ions. *Environ. Sci. Technol.* **30**, 1970-1974.

Naber A., Plaschke M., Rothe J., Hofmann H. and Fanghänel T. (2006) S Scanning transmission X-ray and laser scanning luminescence microscopy of the carboxyl group and Eu(III) distribution in humic acid aggregates. *J. Electron Spectrosc. Relat. Phenom.* **153**, 71-74.

Nelson B. J., Wood S. A., and Osiensky J. L. (2004) Rare earth element geochemistry of groundwater in the Palouse Basin, northern Idaho-eastern Washington. *Geochem. Explor. Environ. Anal.* **4**, 227-241.

Ohta A. and Kawabe I. (2000) Rare earth element partitioning between Fe oxyhydroxide precipitates in aqueous NaCl solutions doped with $NaHCO_3$: Determinations of rare earth element complexation constants with carbonate ions. *Geochem. J.* **34**, 439-454.

Ohta A. and Kawabe I. (2001) REE(III) adsorption onto Mn dioxide and Fe oxyhydroxide: Ce(III) oxidation by Mn dioxide. *Geochim. Cosmochim. Acta* **65**, 695-703.

Olivié-Lauquet G., Allard T., Benedetti M. and Muller J.-P. (1999) Chemical distribution of trivalent iron in riverine material from a tropical ecosystem: a quantitative EPR study. *Wat. Res.* **33**, 2726-2734.

Parkhurst D.L. and Appelo C.A.J. (1999) User's guide to PHREEQC (Version 2) - a computer program for speciation, batch reaction, one-dimensional transport and inverse

geochemical calculation. Water-resources Investigation Report 99-4259, USGS, Denver, Colorado, p. 312.

Pédrot M., Dia A., Davranche M., Bouhnik-Le Coz M., Henin O. and Gruau G. (2008) Insights into colloid-mediated trace element release at soil/water interface. *J. Colloid Interface Sci.* **325**, 187-197.

Pédrot M., Le Boudec A., Davranche M., Dia A. and Henin O. (2011) How does organic matter constrain Fe nano-particles nature, size and availability to biological reduction ?. *J. Colloid Interface Sci.* **359**, 75-85.

Peters A., Hamilton-Taylor J. and Tipping E. (2001) Americium binding to humic acid. *Environ. Sci. Technol.* **35**, 3495–3500.

Pinheiro J.P., Mota A.M. and Benedetti M.F. (2000) Effect of aluminum competition on lead and cadmium binding to humic acids at variable ionic strength. *Environ. Sci. Technol.* **34**, 5137-5143.

Plaschke M., Rothe J., Denecke M. A. and Fanghänel T. (2004) Soft X-ray spectromicroscopy of humic acid europium(III) complexation by comparison to model substances. *J. Electron Spectrosc. Relat. Phenom.* **135**, 53-65.

Pokrovsky O.S., Dupré B. and Schott J. (2005) Fe-Al-organic Colloids Control of Trace Elements in Peat Soil Solution: Results of Ultrafiltration and Dialysis. *Aquat. Geochem*. **11**, 241-278.

Pokrovsky O.S., Schott J. and Dupré B. (2006) Trace element fractionation and transport in boreal rivers and soil porewaters of permafrost-dominated basaltic terrain in Central Siberia. *Geochim. Cosmochim. Acta* **70**, 3239–3260.

Pourret O. and Martinez R. E. (2009) Modelling lanthanide series binding on humic acid. *J. Colloid Interface Sci.* **330**, 45-50.

Pourret O., Davranche M., Gruau G. and Dia A. (2007a) Organic complexation of rare earth elements in natural waters: evaluating model calculations from ultrafiltration data. *Geochim. Cosmochim. Acta* **71**, 2718–2735.

Pourret O., Davranche M., Gruau G. and Dia A. (2007b) Rare earth complexation by humic acid. *Chem. Geol.* **243**, 128-141.

Quinn K. A., Byrne R. H., and Schijf J. (2004) Comparative scavenging of yttrium and the rare earth elements in seawater: competitive influences of solution and surface chemistry. *Aquat. Geochem.* **10**, 59-80.

Quinn K. A., Byrne R. H., and Schijf J. (2006) Sorption of yttrium and rare earth elements by amorphous ferric hydroxide: Influence of pH and ionic strength. *Mar. Chem.* **99**, 128-150.

Ritchie J.D. and Perdue E.M. (2003) Proton-binding study of standard and reference fulvic acids, humic acids, and natural organic matter. *Geochim. Cosmochim. Acta* **67,** 85-96.

Sasaki T., Kobayashi T., Tagagi I. and Moriyama H. (2008) Discrete fragment model for complex formation of europium(III) with humic acid. *J. Nucl. Sci. Technol.* **45**(8), 718-724.

Schijf J. and Byrne R.H. (2001) Stability constants for mono-and dioxalato-complexes of Y and the REE, potentially important species in groundwaters and surface freshwaters. *Geochim. Cosmochim. Acta* **65**, 1037–1046.

Shacat J. A., Green W. J., De Carlo E. H., and Newell S. (2004) The geochemistry of Lake Joyce, McMurdo Dry Valleys, Antarctica. *Aquat. Geochem.* **10**, 325-352.

Shiller A. M. (2002) Seasonality of dissolved rare earth elements in the Lower Mississippi River. *Geochem. Geophys. Geosyst.* **3**, 1068.

Sholkovitz E. R. (1993) The geochemistry of rare earth elements in the Amazon River estuary. *Geochim. Cosmochim. Acta* **57**, 2181-2190.

Sholkovitz E. R. (1995) The aquatic chemistry of rare earth elements in rivers and estuaries. *Aquat. Geochem.* **1**, 1-34.

Smedley P. L. (1991) The geochemistry of rare earth elements in groundwater from the Carnmenellis area, southwest England. *Geochim. Cosmochim. Acta* **55**, 2767-2779.

Sparks D.L. (1995) Environmental soil chemistry. Academic Press, London

Sonke J.E. (2006) Lanthanide–humic substances complexation. II. Calibration of humic ion-binding model V. *Environ. Sci. Technol.* **40**, 7481-7487.

Sonke J.E. and Salters V.J.M. (2006) Lanthanide–humic substances complexation. I. Experimental evidence for a lanthanide contraction effect. *Geochim. Cosmochim. Acta* **70**, 1495–1506.

Stern J. C., Sonke J. E. and Salters V. J. M. (2007) A capillary electrophoresis-ICP-MS study of rare earth elements complexation by humic acids. *Chem. Geol.* **246**, 170-180.

Sutheimer S.H. and Cabaniss S.E. (1997) Aluminum binding to humic substances determined by high performance cation exchange chromatography. *Geochim. Cosmochim. Acta* **61**, 1-9.

Takahashi Y. Yamamoto M., Yamamoto Y. and Tanaka K. (2010) EXAFS study on the cause of enrichment of heavy REEs on bacterial cell surfaces. *Geochim. Cosmochim. Acta* **74**, 5443-5462.

Takahashi Y., Châtellier X., Hattori K. H., Kato K., and Fortin D. (2005) Adsorption of rare earth elements onto bacterial cell walls and its implication for REE sorption onto natural microbial mats. *Chem. Geol.* **219**, 53-67.

Takahashi Y., Hirata T., Ozaki T. and Fortin D. (2007) A rare earth element signature of bacteria in natural waters? *Chem. Geol.* **244** (3–4), 569–583.

Takahashi Y., Minai Y., Ambe S., Makide Y., Ambe F. and Tominaga T. (1997) Simultaneous determination of stability constants of humate complexes with various metal ions using multitracer technique. *The Science of the Total Environment* **198**, 61–71.

Takahashi Y., Tada A., Kimura T. And Shimizu H. (2000) Formation of Outer- and Inner-Sphere Complexes of Lanthanide Elements at Montmorillonite-Water Interface. *Chem. Lett.* **6**, 700-701.

Takahashi Y., Yamamoto M., Ozaki T. and Fortin D. (2008) Characterisation of binding sites of metal ions at bacterial cell surface by REE distribution pattern and EXAFS analysis. 8th Annual V M Goldschmidt Conference. *Geochim. Cosmochim. Acta* **72,** A926-A926.

Tang J. and Johannesson K.H. (2003) Speciation of rare earth elements in natural terrestrial waters: assessing the role of dissolved organic matter from the modeling approach. *Geochim. Cosmochim. Acta* **67**, 2321–2339.

Tang J. and Johannesson K.H. (2010) Ligand extraction of rare earth elements from aquifer sediments: Implications for rare earth element complexation with organic matter in natural waters. *Geochim. Cosmochim. Acta* **74**, 6690-6705.

Tanizaki Y., Shimokawa T., and Nakamura M. (1992) Physicochemical speciation of trace elements in river waters by size fractionation. *Environ. Sci. Technol.* **26**, 1433-1444.

Taylor S. R. and McLennan S. M. (1985) The Continental Crust: Its composition and evolution, pp. 312. Blackwell.

Thurman E.M. (1985) Organic geochemistry of natural waters. In: Nijhoff/Junk (Ed.), Dordrechtthe, Netherlands.

Tipping E. (1998) Humic ion-binding model VI: an improved description of the interactions of protons and metal ions with humic substances. *Aquatic Geochemistry* **4**, 3–48.

Tipping E. (2002) Cation binding by humic substances. *Cambridge University Press* **12**, pp. 434.

Tipping E. (2005) Modeling Al competition for heavy metal binding by dissolved organic matter in soil and surface waters of acid and neutral pH. *Geoderma* **127**, 293–304.

Tipping E. (2007) Modelling the interactions of Hg(II) and methylmercury with humic substances using WHAM/Model VI. *Appl. Geochem.* **22,** 1624–1635.

Tipping E. and Hurley M.A. (1992) A unifying model of cation binding by humic substances. *Geochim. Cosmochim. Acta* **56**, 3627-3641.

Tipping E., Rey-Castro C., Bryan S.E. and Hamilton-Taylor J. (2002) Al(III) and Fe(III) binding by humic substances in freshwaters, and implications for trace metal speciation. *Geochim. Cosmochim. Acta* **66**, 3211–3224.

Tosiani T., Loubet M., Viers J., Yanes C., Dupré B. and Tapia J. (2004) Major and trace elements in river borne materials from the Cuyuni Basin (Southern Venezuela): evidence for organo-colloidal control on the dissolved load and element redistribution between the dissolved load and the suspended load, *Chem. Geol.* **211**, 305–334.

Tricca A., Stille P., Steinmann M., Kiefel B., Samuel J., and Eikenberg J. (1999) Rare earth elements and Sr and Nd isotopic compositions of dissolved and suspended loads from small river systems in the Vosges mountains (France), the river Rhine and groundwater. *Chem. Geol.* **160**, 139-158.

Vermeer A.W.P., Van Riemsdijk W.H. and Koopal L.K. (1998) Adsorption of humic acid to mineral particles. 1. Specific and electrostatic interactions. *Langmuir* **14**, 2810–2819.

Viers J., Dupré B., Deberdt S., Braun J. J., Angeletti B., Ndam Ngoupayou J. and Michard A. (2000) Major and traces elements abundances, and strontium isotopes in the Nyong basin rivers (Cameroon): constraints on chemical weathering processes and elements transport mechanisms in humid tropical environments. *Chem. Geol.* **169**, 211–241.

Viers J., Dupré B., Polvé M., Schott J., Dandurand J.-L. and Braun J.J. (1997) Chemical weathering in the drainage basin of a tropical watershed (Nsimi–Zoetele site, Cameroon): comparison between organic poor and organic-rich waters. *Chem. Geol.* **140**, 181–206.

Vilgé-Ritter A., Rose J., Masion A., Bottero J.-Y. and Lainé J.-M. (1999) Chemistry and structure of aggregates formed with Fe-salts and natural organic matter. *Colloids Surf. A: Physicochem. Eng. Aspects* **147**, 297–308.

Weber T., Allard T., Tipping E. and Benedetti M. (2006) Modelling Iron Binding to Organic Matter. *Environ. Sci. Technol.* **40**, 7488-7493.

Weng L., Temminghoff E.J.M. and Van Riemsdijk W.H. (2002) Aluminum speciation in natural waters: measurement using Donnan membrane technique and modeling using NICA-Donnan. *Water Research* **36**. 4215-4226.

Wu F. and Tanoue E. (2001) Geochemical characterization of organic ligands for copper (II) in different molecular size fractions in Lake Biwa. *Japan. Org. Geochem*. **32**, 1311–1318.

Yamamoto Y., Takahashi Y. and Shimizu H. (2005) Systematics of stability constants of fulvate complexes with rare earth ions. *Chem. Lett.* **34**, 880-881.

Yamamoto Y., Takahashi Y. and Shimizu H. (2006) Interpretation of REE patterns in natural water based on the stability constants. *Geochim. Cosmochim. Acta* **70**, A717-A717.

Yamamoto Y., Takahashi Y. and Shimizu H. (2009) Speciation of iron in humic substances by X-ray absorption fine structure and its effect on the complexation between humic substances and trace metal ions. *Chem. Lett.* **38**, 278-279.

Yamamoto Y., Takahashi Y. and Shimizu H. (2010) Systematic change in relative stabilities of REE-humic complexes at various metal loading levels. *Geochem. J.* **44**, 39-63.

Yoon S.J., Diener L. M., Bloom P. R., Nater E. A. and Bleam W. F. (2005) X-ray absorption studies of CH_3Hg^+-binding sites in humic substances. *Geochim. Cosmochim. Acta* **69**, 1111-1121.